Dissertation
zur Erlangung des Doktorgrades
der Fakultät für Chemie und Pharmazie
der Ludwig-Maximilians-Universität München

# Formulation studies, lyophilization and *in vivo* investigation of 1,2-dipalmitoyl-*sn*-glycero-3-phosphodiglycerol-based thermosensitive liposomes for the delivery of gemcitabine, irinotecan and SN-38


**Barbara Cornelia Kneidl**
aus
Weiden i.d. OPf., Deutschland

2017

Erklärung

Diese Dissertation wurde im Sinne von § 7 der Promotionsordnung vom 28. November 2011 von Herrn Prof. Dr. Lars Lindner betreut und von Herrn Prof. Dr. Gerhard Winter von der Fakultät für Chemie und Pharmazie vertreten.

Eidesstattliche Versicherung

Diese Dissertation wurde eigenständig und ohne unerlaubte Hilfe erarbeitet.

München, den 09.08.2017

Barbara Kneidl

| | |
|---|---|
| Dissertation eingereicht am | 10. August 2017 |
| 1. Gutachter: | Prof. Dr. Gerhard Winter |
| 2. Gutachter: | Prof. Dr. Lars Lindner |
| Mündliche Prüfung am | 05. Oktober 2017 |

# Table of Content


1. Introduction ..... 1
2. Background ..... 2
2.1 Liposomes ..... 2
2.1.1 Long-circulating liposomes ..... 3
2.1.2 Thermosensitive liposomes (TSL) ..... 3
2.1.3 Phase-transition temperature ($T_m$) and influence of lipid composition ..... 5
2.2 Hyperthermia ..... 7
2.3 Pancreatic cancer ..... 8
2.4 Used drugs ..... 9
2.4.1 Gemcitabine ..... 9
2.4.2 Irinotecan ..... 10
2.4.3 Onivyde® ..... 11
2.5 Lyophilization of liposomal dispersions ..... 12
2.5.1 Cryoprotectants during lyophilization ..... 12
2.5.2 Steps during lyophilization ..... 13
2.6 Objective of the thesis ..... 15
3. Material and methods ..... 17
3.1 Chemicals and drug formulations ..... 17
3.2 Liposome preparation ..... 17
3.3 Liposome preparation by dual asymmetric centrifugation (DAC) ..... 18
3.4 Drug loading ..... 18
3.4.1 Passive loading to pre-formed liposomes ..... 18
3.4.2 Active loading to pre-formed liposomes ..... 19
3.4.3 Film loading ..... 19
3.4.4 Passive loading of CF during formation of liposomes ..... 20
3.5 Liposomal characterization ..... 20
3.5.1 Dynamic light scattering ..... 20

3.5.2 Quantification of total lipid concentration ..... 20
3.5.3 Determination of lipid composition ..... 21
3.5.4 Quantification of drug concentration ..... 21
3.5.5 Temperature-dependent drug release ..... 22
3.5.6 Time-dependent CPT-11 release ..... 23
3.5.7 Osmolarity ..... 24
3.5.8 Differential scanning calorimetry ..... 24
3.5.9 Free fatty acid determination ..... 24
3.5.10 Cryo-TEM measurement ..... 25
3.6 HPLC ..... 25
3.6.1 dFdC determination in plasma- and aqueous samples ..... 25
3.6.2 CPT-11 and SN-38 determination in aqueous-, plasma- and cell lysate samples ..... 26
3.6.3 CPT-11 and SN-38 determination from tissue samples ..... 26
3.7 Lyophilization ..... 27
3.7.1 Freeze-dryer Epsilon 2-6D ..... 27
3.7.2 Freeze-dryer Epsilon 2-12D ..... 27
3.7.3 Residual moisture ..... 28
3.8 Storage stability study ..... 29
3.8.1 dFdC-TSL at 2-8°C ..... 29
3.8.2 CPT-11-TSL at 2-8°C ..... 29
3.8.3 Lyophilized CF-TSL at 2-8°C or RT ..... 29
3.9 Cell Culture ..... 29
3.9.1 Culture conditions ..... 29
3.9.2 Freezing and thawing of cells ..... 30
3.9.3 Cell counting in Neubauer counting chamber ..... 31
3.9.4 Conversion of CPT-11 to SN-38 ..... 31
3.10 Animal experiments ..... 31
3.10.1 In vivo experiments dFdC ..... 32
3.10.1.1 Pharmacokinetic study ..... 32

3.10.1.2 Therapeutic study....32
3.10.2 In vivo experiments CPT-11....33
3.10.2.1 Pharmacokinetic study....33
3.10.2.2 Biodistribution....33
3.10.2.3 Therapeutic study....33
4. Results....34
4.1 Thermosensitive liposomal gemcitabine....34
4.1.1 Establishment of an assay to quantify free fatty acids....34
4.1.2 Stabilization of liposomes....37
4.1.2.1 Influence of osmolarity....37
4.1.2.2 pH titration....37
4.1.2.3 Adjustment of loading strategy....39
4.1.2.4 Effect of phospholipid composition....41
4.1.2.5 Storage stability of dFdC-TSL....45
4.1.3 dFdC-TSL preparation with DAC....48
4.1.4 In vivo experiments....50
4.1.4.1 Pharmacokinetic study....50
4.1.4.2 Therapeutic study....52
4.2 Thermosensitive liposomal irinotecan....54
4.2.1 Analytical methods....54
4.2.1.1 Quantification of CPT-11 and SN-38 in complex matrices by HPLC....54
4.2.1.2 Quantification of CPT-11 in aqueous samples by fluorescence spectroscopy....57
4.2.2 Formulation development SN-38....57
4.2.2.1 Encapsulation of the active metabolite SN-38....57
4.2.2.2 Preparation of NTSL....62
4.2.3 Formulation development CPT-11....63
4.2.3.1 Encapsulation process development....63
4.2.3.2 Release properties of CPT-11-TSL with different intraliposomal excipients....64

4.2.3.3 Stability study ..... 66
4.2.3.4 Effect of drug/lipid ratio on temperature-dependent CPT-11 release ..... 69
4.2.3.5 Effect of $DPPG_2$-amount on biophysical properties ..... 70
4.2.4 In vitro characterization ..... 71
4.2.4.1 Characteristics of CPT-11-TSL ..... 71
4.2.4.2 Time-dependent CPT-11 release ..... 72
4.2.4.3 Release for up to 3 h at 37°C ..... 74
4.2.4.4 DSC-measurement (Effect of CPT-11) ..... 75
4.2.4.5 Cryo-TEM ..... 76
4.2.4.6 Onivyde® ..... 77
4.2.4.7 Conversion of CPT-11 to SN-38 in different cell types ..... 78
4.2.5 In vivo experiments ..... 79
4.2.5.1 Pharmacokinetic study ..... 79
4.2.5.2 Biodistribution study ..... 81
4.2.5.3 Therapeutic study ..... 83
4.3 Lyophilization of $DPPG_2$-based TSL ..... 85
4.3.1 Development of a lyophilization cycle ..... 85
4.3.1.1 Lyophilization of CF-TSL without cryoprotectant ..... 85
4.3.1.2 Lyophilization of CF-TSL with different cryoprotectants ..... 86
4.3.1.3 Evaluation of reconstitution media ..... 88
4.3.1.4 Evaluation of different freezing methods ..... 88
4.3.1.5 Lyophilization with CN ..... 90
4.3.2 Storage stability of lyophilized CF-TSL ..... 92
4.3.3 Lyophilization of liposomes containing cytostatic agents ..... 95
4.3.3.1 Adjustment of the lyophilization process for vials wrapped in sterile bags with CF-TSL ..... 95
4.3.3.2 Lyophilization TSL containing cytostatic agents ..... 100
5. Discussion ..... 104
5.1 dFdC-TSL ..... 104
5.1.1 Assay to determine FFA in liposomal formulations ..... 104

5.1.2 Improvement of dFdC-TSL ..... 105
5.1.3 In vivo experiments of dFdC-TSL ..... 108
5.1.3.1 PK-study ..... 108
5.1.3.2 Therapeutic effect ..... 110
5.1.4 Outlook ..... 111
5.2 CPT-11-TSL ..... 112
5.2.1 Encapsulation of the active metabolite ..... 112
5.2.2 In vitro conversion of CPT-11 to SN-38 ..... 114
5.2.3 In vitro characterization of CPT-11-TSL ..... 114
5.2.3.1 Preparation of CPT-11-TSL ..... 114
5.2.3.2 Storage stability ..... 115
5.2.3.3 Drug release from $DPPG_2$-TSL ..... 115
5.2.3.4 $T_m$ of CPT-11-TSL ..... 117
5.2.3.5 Cryo-TEM of CPT-11-TSL ..... 118
5.2.3.6 In vitro characterization Onivyde® ..... 118
5.2.4 In vivo characterization of CPT-11-TSL ..... 119
5.2.4.1 Pharmacokinetic study ..... 119
5.2.4.2 Biodistribution study ..... 120
5.2.4.3 Therapeutic study ..... 122
5.2.5 Outlook ..... 125
5.3 Lyophilization ..... 126
5.3.1 Process development ..... 126
5.3.2 Lyophilization of $DPPG_2$-based TSL containing dFdC, CPT-11 or Dox ..... 129
5.3.3 Outlook ..... 130
6. Summary and conclusion ..... 131
7. Appendix ..... 134
7.1 References ..... 134
7.2 List of abbreviations ..... 150
7.3 List of figures ..... 152
7.4 List of tables ..... 158

7.5 List of publications .....160

Acknowledgements .....162

# 1. Introduction

In Germany, since the beginning of the 1970s the number of new cases of cancer nearly doubled [1]. A reason for this is the aging population, which stands in contrast to the improvement in new therapeutical possibilities. In 2013 approximately 482500 people in Germany newly suffered from cancer [1].

For therapy of solid tumors, the therapy options are mainly surgery, radiotherapy and drug treatment. One drawback in the treatment of cancer with conventional chemotherapeutic drugs is the lack of specificity only for tumor tissue as the main mechanism is the inhibition of rapidly dividing cells. This leads to damage of healthy tissue resulting in several side effects which are often dose-limiting. The reduction of side effects is a topic which was investigated intensively in the last years.

One possibility is the use of nanocarriers for increased targeting efficacy towards tumor tissue. Liposomes were used as such nanocarriers and some liposomal drugs for cancer are already on the market [2]. The liposomal membrane protects the healthy tissue from the cytotoxic properties of the drugs to prevent side effects. The liposomes on the market, like Doxil®, act via the enhanced permeability effect (EPR) and showed only a minor improvement in antitumor effect, due to the way of action.

One class of liposomes investigated for the treatment of cancer are thermosensitive liposomes (TSL). The liposomal membrane of this class of liposomes is composed in a way that it releases the intraliposomal content at temperatures around 41-42°C locally, which is a temperature range used in regional or local mild hyperthermia (HT) treatment in clinic in combination with standard chemotherapeutic treatment. As results, the cytotoxic effect of the drug is developed mostly in the targeted tumor area. One TSL formulation, Thermodox®, encapsulating Doxorubicin (Dox), is currently under clinical investigation [3].

In 2004 the first *in vitro* and *in vivo* results for a TSL formulation based on novel synthetic phosphatidyloligoglycerol were described, which showed promising results [4]. TSL composed of this lipid encapsulating different drugs for the potential treatment of pancreatic cancer were investigated in context of this work *in vitro* and *in vivo*.

# 2. Background

## 2.1 Liposomes

Liposomes are spherical nanoparticles build up by a membrane bilayer consisting of phospholipids. The aqueous core formed by the membrane can encapsulate hydrophilic drugs and in the lipophilic membrane lipophilic molecules can be incorporated (cf. Figure 2-1) [4, 5]. The advantage of liposomes for therapeutic purposes are the biocompatibility, biodegradability and non-immunogenicity [6].

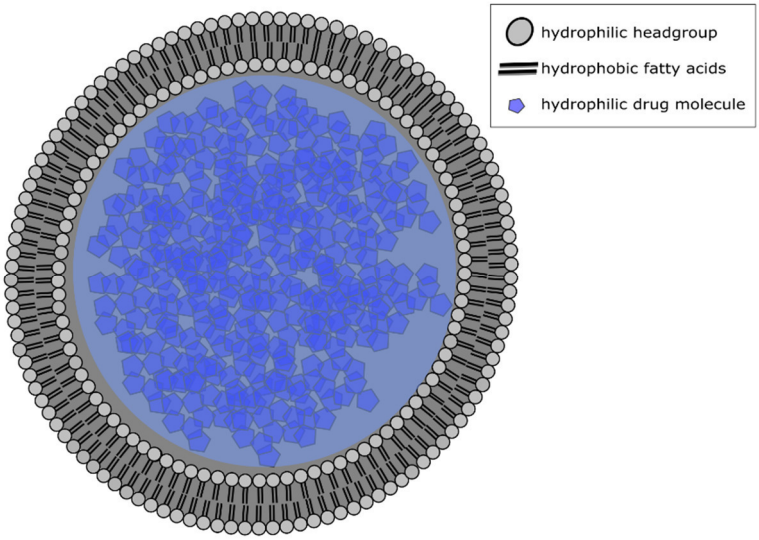


*Figure 2-1 Structure of a liposome*

The spontaneous formation of liposomes in aqueous solution containing phospholipids was described first in 1965 by Bangham et al [7]. The liposomes are formed because of the physicochemical properties of phospholipids. The fatty acid residues which form the hydrophobic tail are connected via a glycerol- or a sphingosine moiety with the hydrophilic headgroup (e.g. a phosphoglycerine or phosphocholine). This amphiphilic property combined with the three-dimensional structure is responsible for the formation of liposomes. In an aqueous environment, the hydrophobic tails align together and the hydrophilic head group is orientated to the hydrophilic environment forming lamellar structures like membrane bilayers. The vesicles formed during this spontaneous process are multilamellar. Unilamellar vesicles, with more defined biophysical characteristics are not formed spontaneously, they need further processing, e.g. by extrusion through filter membranes sonication, or freezing and thawing cycles.

The lipid composition and vesicle size of liposomes results in different biophysical and biochemical properties (e.g. phase-transition temperature $T_m$, zeta potential, surface tension) determining e.g. drug release, carrier stability and/ or *in vivo* behavior. These properties can be adjusted in various instances to yield particles with the needed characteristics.

Liposomes have been used as model membranes [8], in the field of cosmetics as well as non-viral vectors for better transfection efficacy [9]. A major field of importance for this project is the use of liposomes as nanocarriers for drugs. There are several liposomal drug formulations approved, e.g. Doxil®, a long-circulating formulation of doxorubicin (Dox), Onivyde®, a long circulation formulation of irinotecan (CPT-11) or Ambiosome®, using amphotericin B [2].

### 2.1.1 Long-circulating liposomes

Classical, long-circulating liposomes use PEGylation for the improvement of the circulation time. PEGylation is used to hinder opsonization of proteins resulting in less rapid uptake in the reticuloendothelial system (RES). The mechanism of action for long-circulating liposomes is the enhanced permeability and retention (EPR) effect, by passive accumulation inside the tumor tissue because of the leaky tumor vasculature [10]. However, increased clinical efficacy could not be achieved in the desired manner, due to several shortcomings. The accumulation of the liposomes depends on the specific structure of the tumor vasculature and could be increased by heating of the tissue [11, 12]. The rate-limiting step in this approach is the extravasation of the liposomes. The circulation half-lives of the vesicles have to be in the range of days to get a sufficiently high concentration accumulated in the tumor tissue [13]. In this time-span, uptake in liver and spleen of the nanoparticles is competing with the accumulation in the tumor tissue. In humans, it was shown with radioactively labeled long-circulating liposomes, that the accumulation efficacy is less than 5% of the injected dose [14]. The membrane of the accumulated liposomes still stays intact, resulting in release of only minor amounts of drug and therefore the bioavailability of the drug is limited [15, 16].

### 2.1.2 Thermosensitive liposomes (TSL)

An alternative to the passive targeting approach used for long-circulating liposomes is the external active targeting achieved by temperature-triggered, localized intravascular drug release from TSL through focused heating [17]. HT is used as tool to trigger the drug release.

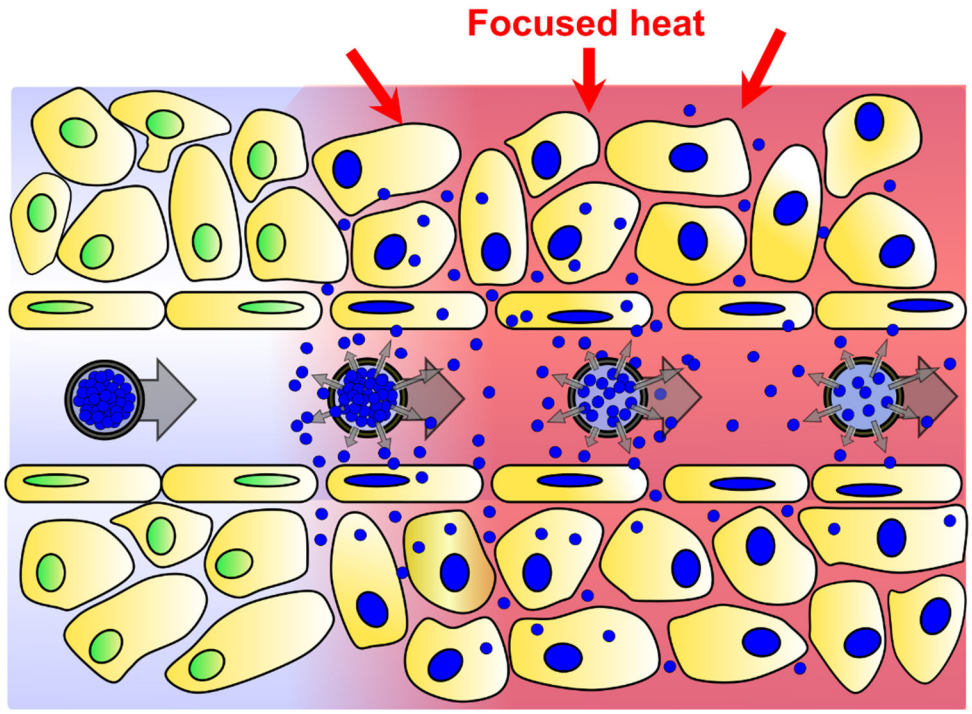


*Figure 2-2 Principle of external active targeting approach for TSL*

The basic principle of external active targeting for TSL is shown in Figure 2-2. After intravenous (i.v.) injection and reaching the heated tissue area the drug is rapidly released into the bloodstream, resulting in a high local drug concentration followed by a rapid redistribution in the tumor tissue. This approach is not dependent on the EPR effect [18]. For TSL formulations containing Dox it has been shown that the released drug is efficiently distributed from the tumor vasculature to the tumor cells and also the endothelial cells [19]. The high intravascular concentrations of the drug in the heated area increase the penetration depth and prevent washing out of the drug from the tissue [17]. Superiority of free drug to Doxil® has already been shown [17]. The approach of TSL in combination with HT decreases the systemic toxicity of the chemotherapeutic drug due to the liposomal encapsulation as well as the improved and triggered drug delivery and tumor sensitization by HT [20].

The first TSL formulation composed of 1,2-dipalmitoyl-*sn*-glycero-3-phosphocholine (DPPC)/ 1,2-distearoyl-*sn*-glycero-3-phosphocholine (DSPC) 3:1 (molar ratio) was described in 1978 by Yatvin et al [21]. Due to major shortcomings, like short circulation time and weak drug release upon heat-trigger, the formulation was changed in the last decades. The first TSL formulation which entered human clinical trials was described in 2000 by Needham et al (ThermoDox®) [11, 22-24].

### 2.1.3 Phase-transition temperature ($T_m$) and influence of lipid composition

The thermosensitive character of liposomes is achieved by the biophysical properties of the membrane forming phospholipids [5]. At temperatures around $T_m$ the structure of the lipid bilayer changes from a solid-gel phase ($L_\beta$) to a liquid-crystalline phase ($L_\alpha$) (cf. Figure 2-3), due to a conformation change of the C-C single bonds from trans to gauche conformation [25]. In the liquid-crystalline phase the membrane is more permeable for water and hydrophilic drugs compared to the solid-gel phase [26, 27]. At temperatures around $T_m$ the permeability for encapsulated hydrophilic drugs is maximal, due to the coexistence of both phases forming grain boundaries [28, 29]. The $T_m$ of a liposomal formulation is influenced by the $T_m$ of the single phospholipids [30, 31] as well as of the pH [32].

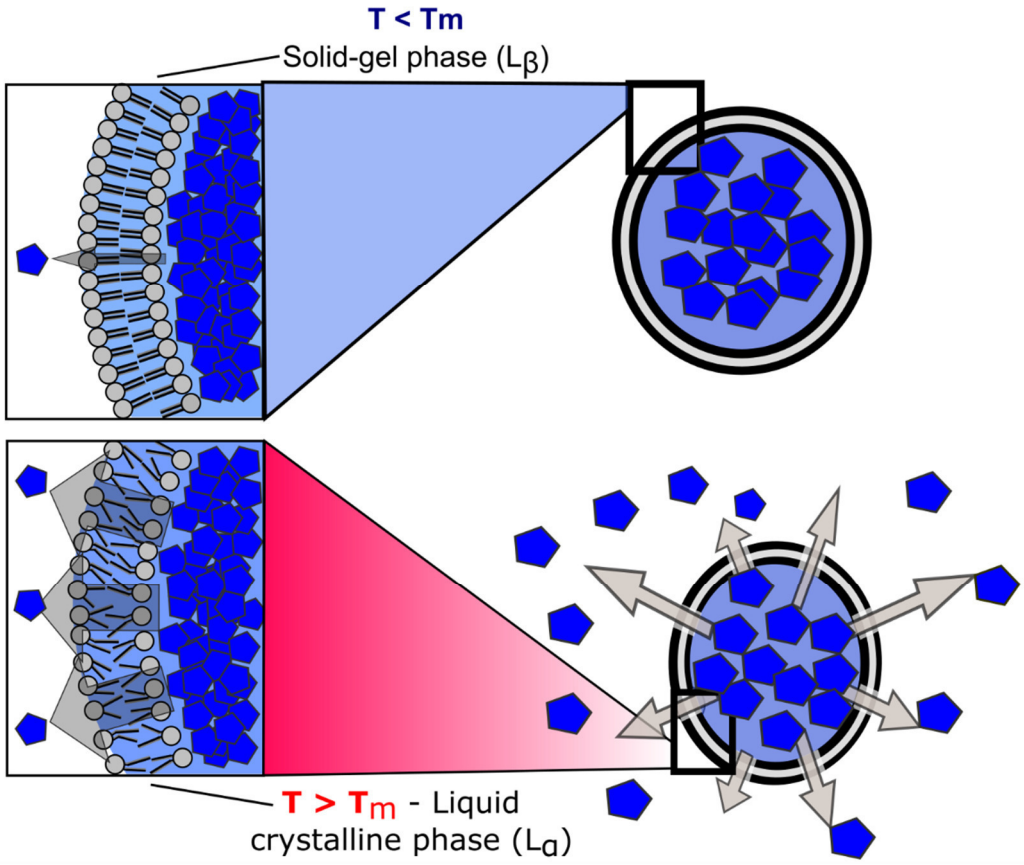


*Figure 2-3 Principle of phase-transition of TSL*

| | Membrane composition (molar ratio) | First publication | $T_m$ (encapsulated doxorubicin) |
|---|---|---|---|
| **First TSL** | DPPC/DSPC 3:1 | 1978 [21] | - |
| **LTSL** | DPPC/Lyso-PC/DSPE-$PEG_{2000}$ (90:10:4) | 2000 [22] | 40.8°C [3] |
| **$DPPG_2$-TSL** | DPPC/DSPC/$DPPG_2$ (50:20:30) | 2004 [4] | 41.9°C [5] |
| **HaT-TSL** | DPPC/Brij78 96:4 | 2011 [33] | 41.0°C [34] |

*Table 2-1 Overview of distinct TSL formulations*
*DPPC, 1,2-dipalmitoyl-*sn*-glycero-3-phosphocholine; DSPC, 1,2-distearoyl-*sn*-glycero-3-phosphocholine; Lyso-PC, Lyso-phosphatidylcholine; DSPE-$PEG_{2000}$, 1,2-distearoyl-*sn*-glycero-3-phosphoethanolamine-N-methoxy(polyethylenglycol)-2000; $DPPG_2$, 1,2-diplamitoyl-*sn*-glycero-3-phosphodiglycerol; Brij78, polyoxyethylene (20) stearyl ether.*

In most TSL formulations the phospholipid DPPC is used as major compound (cf. Table 2-1; red Figure 2-4), with a $T_m$ of 41.4°C, which is already within the temperature range suitable for drug release from TSL at mild hyperthermic temperatures [35-37]. To shift the $T_m$ to slightly higher temperatures and to stabilize the formulation low amounts of DSPC (grey Figure 2-4) can be incorporated in the formulation. 1,2-distearoyl-*sn*-glycero-3-phosphoethanolamine-N-methoxy(polyethylenglycol)-2000 (DSPE-$PEG_{2000}$; yellow Figure 2-4) is a polymer-modified phospholipid which hinders opsonization of proteins and this prevents rapid uptake in the reticuloendothelial system (RES) achieving longer circulation times [38-40]. In the LTSL formulation a 4 mol% of Lyso-PC (green Figure 2-4) was incorporated in the formulation to mediate the drug release around $T_m$ by formation of membrane pores [3, 41, 42]. Within the scope of this work the synthetic phospholipid 1,2-diplamitoyl-*sn*-glycero-3-phosphodiglycerol ($DPPG_2$) was used to prolong the circulation half-life in the same way as DSPE-$PEG_{2000}$ does. $DPPG_2$ has a $T_m$ of 39.7°C. Due to this low $T_m$ of $DPPG_2$, DSPC had to be incorporated to shift the $T_m$ of the overall formulation to temperatures >40°C. The incorporation of $DPPG_2$ in TSL formulations led to a prolonged circulation time and increased drug release rate [4, 43]. The standard phospholipid composition for $DPPG_2$-based TSL is DPPC/DSPC/$DPPG_2$ 50:20:30 (molar ratio) with a $T_m$ of 42.6°C [5]. *In vitro* it was shown that $DPPG_2$-based TSL show a higher stability in serum compared to LTSL [31]. Encapsulating gemcitabine in $DPPG_2$-based TSL results in an improved therapeutic efficacy in tumor-bearing rats compared to free drug [44]. In a rat study it was shown, that the formulation encapsulating Dox had a therapeutic advantage over non-liposomal Dox, Doxil® and LTSL [43]. $DPPG_2$-based Dox-loaded TSL were well tolerated by cats after i.v. application and showed Dox release in the heated area combined with therapeutic efficacy [45].

Most long-circulating liposomes consist of DSPC, Cholesterol (Chol) and DSPE-$PEG_{2000}$ and show no phase transition. Using Chol concentrations higher than 30% results in a loss of phase transition of liposomal formulations [46, 47] and thus in no temperature-dependent release of the encapsulated drug.

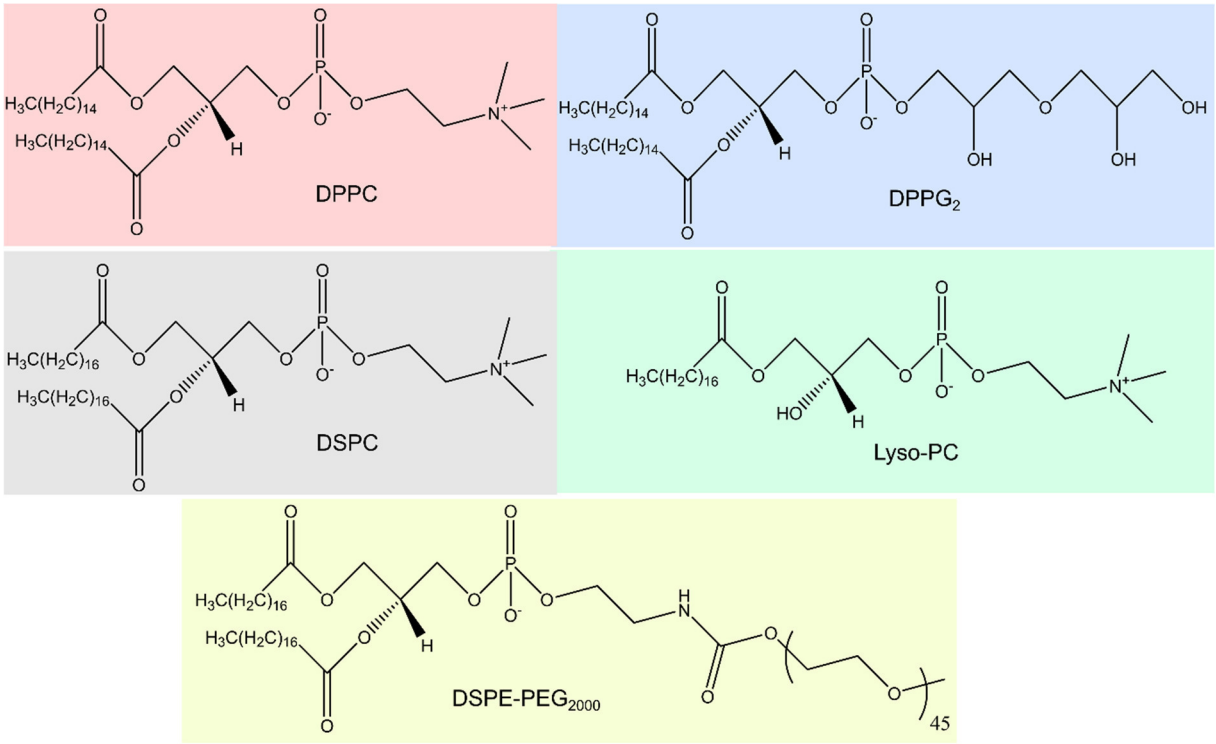


*Figure 2-4 Chemical structure of DPPC, DSPC, $DPPG_2$, Lyso-PC and DSPE-$PEG_{2000}$*

## 2.2 Hyperthermia

Regional mild hyperthermia (HT) describes the heating of tissue over a longer time-period to a few degrees above normal body-temperature (40-43°C, ~60 min), to achieve a change in the tissue- and cell physiology [48, 49]. In cancer treatment, HT is always used as a supportive therapy in combination with radiotherapy or chemotherapy [50, 51]. A result of the fast growth of tumor cells is a high vascularization of the tumor and so the tumor environment shows hypoxic areas or low pH values. These regions are more sensitive to increased heat in contrast to healthy tissue and are damaged during heating [52]. HT causes an increase of the membrane permeability, structural changes of the cytoskeleton, inhibition of the DNA repair mechanisms, improved perfusion and induction of apoptotic signaling cascades [53]. A significant advantage of the combination of chemotherapy and HT for the treatment of the soft tissue sarcoma was already shown in a multicenter phase III study [54]. Additionally, an improved efficacy when combining HT with several cytotoxic drugs was shown [52]. HT also plays a role to overcome tumor resistance against cytotoxic drugs [55].

In *in vivo* experiments, it was shown that HT, in combination with long-circulating non-TSL, was used as modulator of the enhanced permeability and retention (EPR) effect [56, 57]. The enhancement of tumor accumulation of non-TSL by local HT in preclinical studies in animals resulted in higher therapeutic efficacy [58-61]. The increased delivery of the non-TSL is based on a rise in vascular permeability [61-63] caused by accelerated blood flow [64-66] as well as an increase in intercellular gap size between vascular endothelial cells [56, 67].

## 2.3 Pancreatic cancer

Pancreatic cancer is one of the cancer types with highest mortality. Five-year survival in all stages is less than 5% [68]. A key factor for this bad outcome might be the early metastatic spread [68]. Until now no efficient method for the early diagnosis of pancreatic intraepithelial neoplasia, the precursor of pancreatic cancer, is known. For already developed tumors the low cancer cell amount as well as the pronounced desmoplasia (excessive proliferation of fibrotic tissue and intense production of extracellular matrix) hamper diagnosis by biopsy [68]. Another drawback is the poor response to chemotherapy and radiotherapy [69]. The stroma (build-up of extracellular matrix, activated fibroblasts, myofibroblasts, inflammatory cells, pancreatic stellate cells and blood- and lymph vessels) in pancreatic cancer is a barrier for chemotherapeutics resulting in bad response to the drug [68]. Higher local drug concentration could help to overcome this barrier achieving better response. The standard therapy used for adjuvant treatment is gemcitabine (dFdC) or fluorouracil. For palliative treatment, also dFdC is used based on a phase-III-study from 1997 of metastatic pancreatic cancer [70]. The widespread resistance to the drug may be caused by poor drug delivery and inherent chemoresistance [69]. Another treatment option is the FOLFIRINOX drug combination, with the drugs leucovorin, fluorouracil, irinotecan (CPT-11) and oxaliplatin. In a phase II-III study the FOLFIRINOX treatment showed an advantage over dFdC-treatment, but showed increased toxicity [71]. Abraxane® (albumin-bound paclitaxel) in combination with dFdC is approved for treatment of metastatic pancreatic cancer and might have effect on the stroma [68].

Despite this different treatment possibilities and ongoing research on this field, the therapeutic outcome is still unsatisfactory. Encapsulation of drugs against pancreatic cancer into TSL formulations could be a promising tool to improve drug delivery to tumors and increase therapeutic efficacy. In the next section, two drug candidates as well as commercially available formulation for pancreatic cancer relevant for the thesis are described.

## 2.4 Used drugs

### 2.4.1 Gemcitabine

dFdC is an analogue of the pyrimidine base cytidine. It differs from the natural occurring base in two fluorine atoms at the 2`-position of the furanose instead of a hydroxyl group and a hydrogen atom (cf. Figure 2-5) [72].

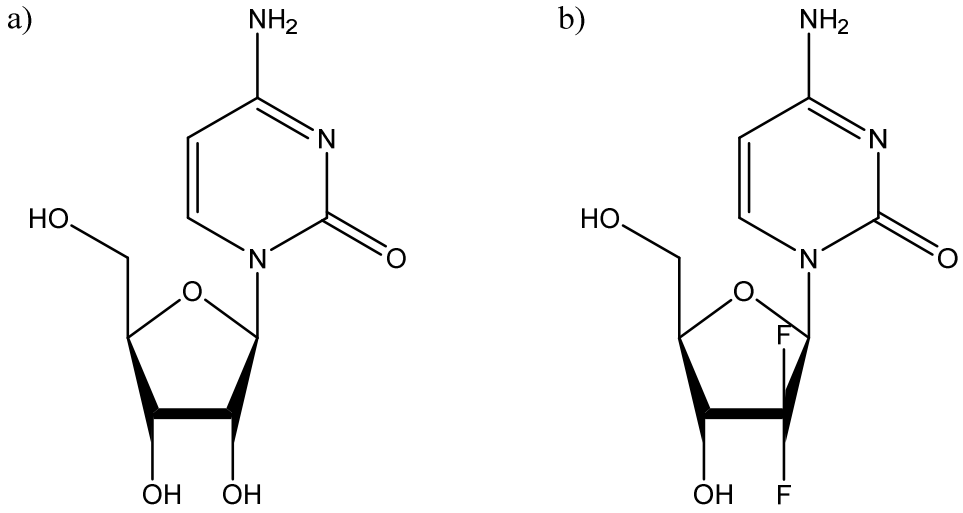


*Figure 2-5 Structure of a) cytidine and b) dFdC*

dFdC is transported in the cell via sodium-dependent concentration-controlled transporter or a sodium-independent equilibrium-controlled nucleoside transporter [73, 74]. Due to its hydrophilic character the presence of the nucleoside transporter is necessary for dFdC to cross the membrane and to inhibit cell growth [72].

As prodrug dFdC has to be converted to its active metabolites dFdC mono-, di- and triphosphate (dFdCMP, dFdCDP, dFdCTP) after entering the cell [72, 75, 76]. dFdCTP is the metabolite with the highest activity. The responsible enzymes for the intracellular phosphorylation are deoxycytidine kinase [77] and thymidine kinase II, where the thymidine kinase has a lower affinity to dFdC [78].

dFdCTP is inserted in the DNA instead of deoxycytidine triphosphate by the DNA-polymerase. This insertion leads to DNA polymerization termination [79], a single strand breakage [80], and modified the DNA seems to be resistant to DNA repair mechanisms of the cell [81].

The inactivation of dFdC to 2`,2`-difluorodeoxyuridine is catalyzed by the deoxycytidine deaminase, which is the main mechanism for metabolism of dFdC [72, 82]. Deamination of dFdCMP to 2`,2`-difluorodeoxyuridinemonophosphate and the reconversion of dFdCMP to dFdC by the 5`-nucleotidase are additional metabolism pathways of dFdC [72].

Side effects of a dFdC-treatment are myelosuppression and toxicities in the lung, liver, and kidneys. Clinically, dFdC is used as mono- or as combination treatment for mamma, urinary bladder, pancreatic, ovarian and non-small-cell lung carcinoma [83].

### 2.4.2 Irinotecan

Irinotecan (7-ethyl-10-[4-(1-piperidino)-1-piperidino]carbonyloxy-camptothecin; CPT-11) is a water-soluble semisynthetic analog of the naturally occurring alkaloid camptothecin (CPT). CPT-11 has two additional moieties compared to CPT, an ethyl group and a 4-piperidinopiperidine group (cf. Figure 2-6 a and b). The lactone ring in the molecule is important for the stabilization of the topoisomerase I-DNA adducts [84]. At high pH, the lactone ring is reversibly hydrolyzed to its carboxylate form (cf. Figure 2-6 b). The active form is the lactone, which is predominant at acidic pH [84].

The mechanism of action for CPT-analogs is binding to the topoisomerase I-DNA complex. This binding result in the prevention of re-ligation of the single-strand breaks of the DNA induced by topoisomerase I and thus in the formation of irreversible double strand breaks leading to cell death [85, 86].

Compared to other CPT analogs, CPT-11 is a prodrug that is converted to its more active metabolite 7-etyhl-10-hydroxycamptothecin (SN-38) by a carboxylesterase mediated cleavage of the carbamate bond between the CPT moiety and the dipiperidino group (cf. Figure 2-6 c) [85]. SN-38 is responsible for most of the biological activity of CPT-11 [87]. Carboxylesterase 2 is the enzyme with the highest affinity (in contrast to carboxylesterase 1 and 3) involved in the hydrolysis of CPT-11 to SN-38 [85]. However CPT-11 also shows antitumor activity without the conversion to SN-38 [84].

CPT-11 is metabolized in the liver to several degradation products by the cytochrome P 450 3A4 system. The main degradation product (7-etyhl-10-[4-*N*-(5-aminopentanoic acid)-1-piperidino]carbonyloxy-camptothecin), which results from oxidation of the terminal piperidine ring of CPT-11 [84], is inactive just as several other metabolites [88, 89].

CPT-11 is primarily used for treatment of colorectal cancer as well as treatment of for cervical, esophageal, gastric, lung and pancreatic cancer and glioma and mesothelioma [90].

Dose-limiting factor for the treatment with CPT-11 were side effects, mainly neutropenia and severe diarrhea [91].

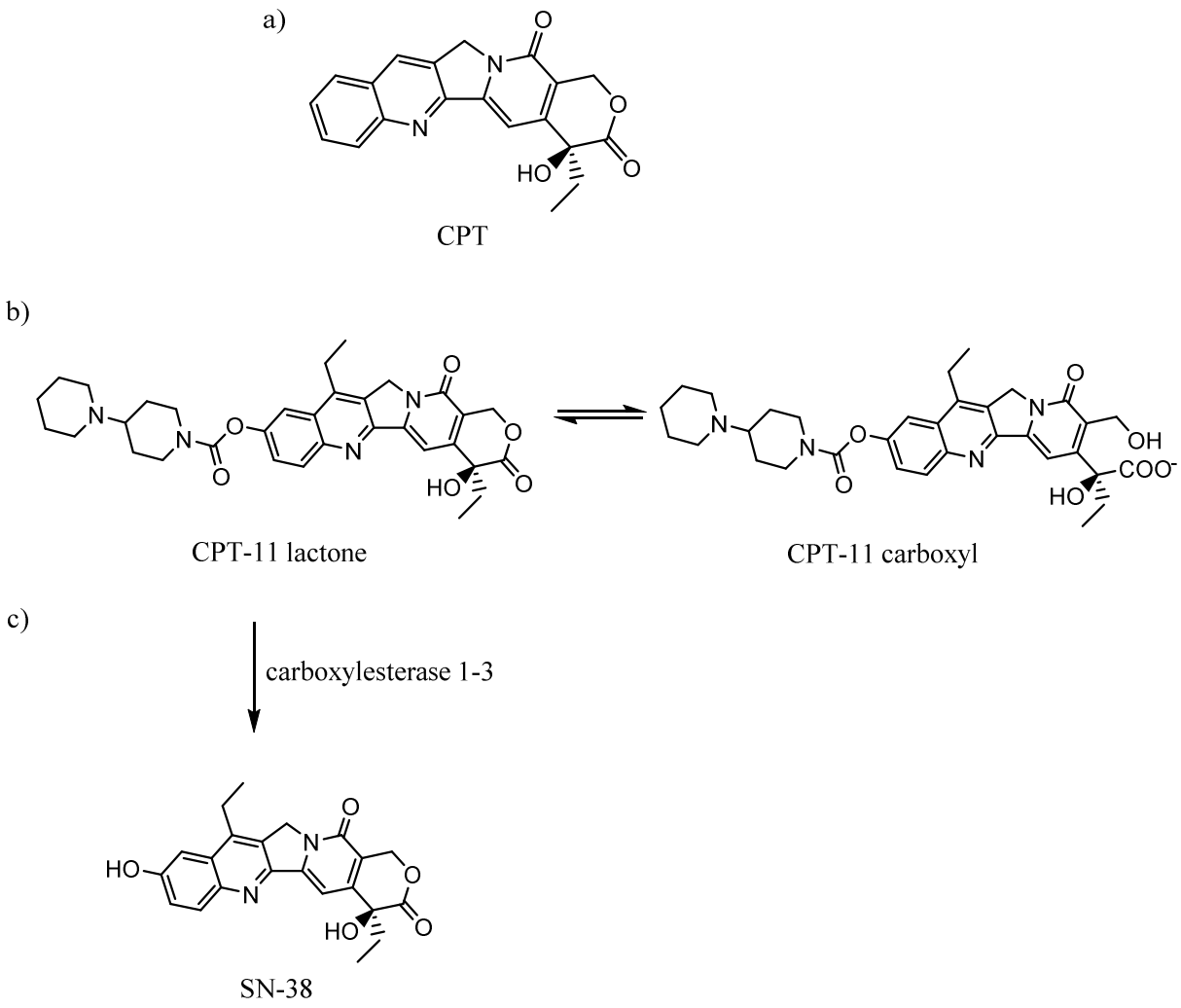


*Figure 2-6 a) structure of camptothecin (CPT), b) pH dependent reversible structure change of lactone to carboxyl form of CPT-11 c) enzymatic reaction of CPT-11 to SN-38 by carboxylesterase enzyme family.*

### 2.4.3 Onivyde®

Onivyde® a long-circulating, non-thermosensitive liposomal-based formulation of CPT-11, was developed to obtain a CPT-11 formulation with increased stability and decreased drug elimination. This leads to prolonged circulation time in the systemic circulation and an increase in accumulation in the target tissue resulting in an enhanced antitumor efficacy [92]. It was first described in 2006 by Drummond et al [93]. The lipid composition of this formulation is DSPC/Chol/DSPE-PEG2000 (60/39.7/0.3 molar ratio). The CPT-11 is stably encapsulated in the aqueous core by forming a complex with sucrose octasulfate [93]. With this loading method, a high drug loading capacity, a stable encapsulation and a strong protection of the CPT-11 against premature activation and elimination was achieved [91]. Onivyde® showed a prolonged plasma half-life and circulation time in rats (10.7 h vs. 0.27 h), slower metabolic clearance as well as a more efficient conversion of CPT-11 in the tumor

tissue to its active metabolite SN-38, when compared to non-liposomal CPT-11 [93, 94]. The mechanism of action is the same as described for CPT-11, the targeting of the topoisomerase I-DNA complex.

The clinical approval by the FDA was achieved based on a randomized phase III trial (NAPOLI-I) in patients with gemcitabine-refractory metastatic pancreatic cancer [91]. In the trial it was shown, that a combination of Onivyde® with fluorouracil/folinic acid showed superior progression-free survival and response rate compared to monotherapy [91, 95, 96]. There are additional clinical trials with Onivyde® for pancreatic cancer and other cancer types conducted and ongoing (overview see [96]).

## 2.5 Lyophilization of liposomal dispersions

Storage of liposomes in aqueous dispersions is challenging due to chemical and physical degradation resulting in changed characteristics of a liposomal drug product over time (e.g. aggregation, drug leakage, chemical decomposition of phospholipids and/or drug). One major chemical degradation pathway is phospholipid hydrolysis to its lysolipid and corresponding free fatty acid [97]. One option to avoid hydrolysis during storage is to remove the water from the formulation by lyophilization. The second degradation pathway is oxidation of the phospholipids.

### 2.5.1 Cryoprotectants during lyophilization

In absence of cryoprotectants the dehydration of liposomes would lead to fusion of liposomes, formation of aggregates or the leakage of the encapsulated material during rehydration [98]. To overcome these effects cryoprotectants like sugars (e.g. trehalose, sucrose) are used. The stabilizing effect of disaccharides is based on the following three hypotheses:

1. Vitrification: The used disaccharides form a glassy matrix, surrounding the liposomes, which results in protection from ice crystal damage and avoidance of liposome fusion. This matrix reduces the mobility of the molecules and thus additionally reduces the reaction speed [99, 100].
2. Reduction of the phase transition: Disaccharides reduce the $T_m$ of the liposomes and keep them in the liquid-crystalline phase during freezing. This avoids a phase-transition during freezing [101, 102].
3. Water replacement theory: This theory is the oldest and most studied one until now [98]. The sugar molecules form hydrogen-bonds with the polar head groups of the

phospholipids, replacing the water molecules during dehydration and thus prevent the aggregation and fusion between the membranes (cf. Figure 2-7) [102-104].

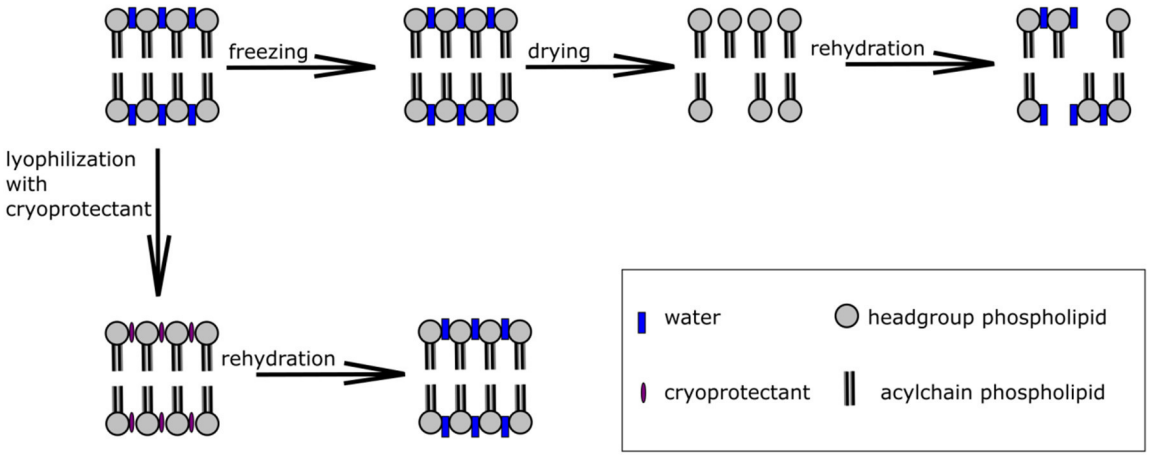


*Figure 2-7 Mechanism of water replacement during lyophilization. Adapted from [103].*

The mechanism of cryoprotection of liposomes is still under investigation and potentially all mentioned hypothesis contribute to the stabilizing effect.

### 2.5.2 Steps during lyophilization

A lyophilization process consists of three major steps. The first step is the freezing phase. Here, most of the solvent (e.g. water) is separated of the liposomes by formation of ice [98]. The freezing step is the most harmful and crucial step during lyophilization to yield a lyophilized product, with comparable characteristics to the product before lyophilization. The destruction of liposomes during freezing and thawing was already described in 1983 by Crommelin and van Bommel [105, 106]. Stress factors for liposomes during freezing can be an increase in liposome concentration resulting in aggregation or fusion of liposomes, disruption of the bilayer by the formation of ice crystals and segregation of liposomes and the cryoprotectant due to phase separation [98, 107]. During the development of a lyophilization process this step can be adjusted by e.g. changing the freezing rate. A fast freezing usually results in the formation of fine ice crystals and a homogenous distribution of the cryoprotectant, which might reduce the disruption of the bilayer [98]. In contrast a slower freezing rate might be beneficial concerning the drug leakage during the freezing step, since the osmotic pressure caused by the freeze-concentration could be reduced [108]. The freezing temperature might also have an influence on the quality of the liposomes after lyophilization. In combination with the freezing rate the freezing temperature has an influence on the ice nucleation rate, crystal growth and morphology of the freeze-dried material [98].

The freezing step could be adjusted by several techniques, like controlled nucleation and several other techniques [109]. The controlled ice nucleation leads to a nucleation of all vials at the same time and temperature, resulting in a more uniform product [110].
The second step after freezing of the liposomal dispersion is the primary drying. In this step, the chamber pressure is reduced and the shelf temperature is increased. This results in a sublimation of the ice crystals and so the formation of a porous cake structure of the freeze-concentrated matrix [107]. The primary drying should always be performed at temperatures lower than the glass transition temperature of the freeze-concentrated solution (Tg`) to minimize the degradation of the liposomes and to ensure the possibility of sublimation of the ice crystals without a collapse of the cake structure [107]. The primary drying is the freeze-drying step which takes most time and can last up to days.
The third and last step is the secondary drying, in which water is desorbed from the frozen product at elevated temperatures (20-40°C) and low pressure [103, 111]. This step is necessary to reduce the residual moisture to an acceptable value.

## 2.6 Objective of the thesis

Objective was the investigation, optimization and characterization of heat-inducible nanocarrier systems based on the $DPPG_2$ phospholipid for the targeted transport and release of active pharmaceutical ingredients known to be effective against pancreatic cancer. The thesis consists of three parts:

1. An existing $DPPG_2$-based dFdC-TSL formulation [44] should be optimized regarding stability during production process. The formulation suffered from significant lipid decomposition with a lysolipid content of already 1.1±1.2% (hydrolysis products of DPPC and DSPC) after preparation as well as unwanted initial drug leakage in fetal bovine serum (FBS) of 15.6±9.2% [44]. The lysolipid content could have influenced the release and circulation properties of the formulation and subsequently affected therapeutic efficacy *in vivo*. Ideally, lipid hydrolysis during production and initial drug leakage should be completely abolished. Moreover, the formulation was optimized to achieve long-term storage. The optimized dFdC-TSL formulations were tested *in vivo* (PK and therapeutic efficacy) and compared to the published formulation. The effect of production process and formulation changes on the *in vitro* characteristics and *in vivo* behavior of the nanocarrier had to be discussed.
2. A more potent drug candidate than dFdC should be encapsulated in $DPPG_2$-based TSL. The encapsulation of CPT-11 and its more active metabolite SN-38 in $DPPG_2$-based TSL had to be tested. After successful encapsulation, an in depth *in vitro* characterization of the best candidates should be performed and compared to the approved, long-circulating nanoliposomal CPT-11 formulation Onivyde®. The CPT-11-TSL candidate with the best *in vitro* characteristics (e.g. stability in FBS at temperatures < 39°C, fast release rates at temperatures > 40°C, short term stability) should be further evaluated *in vivo*. In the *in vivo* studies (PK, biodistribution and therapeutic study) the most suitable *in vitro* candidate should be compared to non-liposomal CPT-11 and Onivyde®. For PK & biodistribution studies a HPLC method for quantification of CPT-11 in complex matrices had to be developed. Results had to be discussed regarding the mechanistic difference between the clinically established formulations (e.g. Onivyde®) and the TSL formulation exploiting the novel intravascular drug release approach.
3. A lyophilization process for $DPPG_2$-based TSL should be developed, because for $DPPG_2$-based TSL the favored storage is as liquid or frozen dispersion due to lack of a lyophilization process. The storage as a dispersion could result either in freezing and thawing stress (storage at -20°C) or in hydrolysis of the phospholipids (storage at 2-8°C). The lyophilization process had to be developed with $DPPG_2$-based TSL encapsulating a non-toxic, fluorescing model drug like e.g. carboxyfluorescein (CF).

Different cryoprotectants as well as different freezing methods had to be tested and the characteristics (z-average, PDI, drug leakage) of the liposomes after lyophilization had to be compared to the characteristics before lyophilization, respectively. The quality of the lyophilized CF-TSL should be analyzed in a storage stability study at 2-8°C and RT to evaluate the advantage for storage of lyophilized TSL in contrast to storage as liposomal dispersion. The optimized lyophilization process for CF-TSL had to be further tested for lyophilization of dFdC-, CPT-11-, or Dox-containing $DPPG_2$-based TSL to evaluate the process for suitability for lyophilization of these TSL.

# 3. Material and methods

## 3.1 Chemicals and drug formulations

The synthetic phospholipid $DPPG_2$ was provided by Thermosome GmbH (Planegg, Germany). DSPE-$PEG_{2000}$ was obtained from Avanti Polar Lipids (Alabaster, Alabama, USA). All other phospholipids used as well as cholesterol were purchased from Corden Pharma Switzerland LLC (Liestal, Switzerland). Gemzar® (38 mg/ml dFdC) was obtained from Lilly Deutschland GmbH (Bad Homburg, Germany). Irinotecanhydrochlorid Hospira (20 mg/ml CPT-11) was obtained by Hospira Deutschland GmbH (München, Germany). Doxorubicin Aurobindo was purchased from Puren Pharma GmbH&Co. KG (München, Germany). SN-38 and CPT were purchased from TCI chemicals Deutschland (Eschborn, Germany). 5-fluorouridine (5-FU) was obtained from Sigma Aldrich (München, Germany). Onivyde® was purchased from Merrimack Pharmaceuticals (Cambridge, Massachusetts, USA). CF free acid (Sigma Aldrich GmbH, München, Germany) was transformed to its sodium salt with sodium hydroxide and additionally purified by crystallization. Fetal bovine serum (FBS) was from Biochrom AG (Berlin, Germany). All other chemicals were either purchased from Carl Roth GmbH (Karlsruhe, Germany), Sigma Aldrich GmbH (München, Germany) or Merck KGaA (Darmstadt, Germany). Aqueous solutions were prepared with deionized and purified water using an ultrapure water system (Milli Q Advantage, Merck Millipore, Darmstadt, Germany).

## 3.2 Liposome preparation

All liposomes were prepared with the lipid film hydration and extrusion method [31, 112]. Please refer to the results section for lipid composition and used buffer systems. The lipid components (e.g. DPPC, DSPC, $DPPG_2$, DSPE-$PEG_{2000}$, P-Lyso-PC, Chol) were dissolved in $CHCl_3$/MeOH 9:1 (v/v) in a round-bottom flask. Afterwards the solvents were removed by a rotary evaporator (Laborota 4001, Heidolph Instruments GmbH, Schwabach, Germany) to obtain a homogenous and dry lipid film. This lipid film was hydrated with an appropriate buffer for drug loading (refer to chapter 3.4) to produce multilamellar vesicles at 60°C for 7-15 min. The resulting lipid concentration was 50 mM. Thereafter the liposomes were extruded 10 times through two polycarbonate membranes with a pore size of 200 nm (Whatman® Nucleopore Tracked -Etched Membrane, Sigma Aldrich GmbH, München) in a high-pressure extruder (Lipex™ thermobarrel extruder, Northern Lipids Inc., Burnaby, Canada) at 60°C.

## 3.3 Liposome preparation by dual asymmetric centrifugation (DAC)

The preparation of liposomes with DAC was published 2008 by Massing et al [113]. For TSL preparation some adjustments were made. In brief, a lipid film with the lipid composition DPPC/DSPC/$DPPG_2$ 50:20:30 (molar ratio) was prepared as described in section 3.2. 40 mg of the lipid film or 40 mg of lipid powder (lipid composition the same as for lipid film) were weighed in 2 ml ZentriMix Vials (Andreas Hettich GmbH, Tuttlingen, Germany). Additionally, 60 mg of Gemzar®-solution with pH 3 or pH 6, CPT-11 solution (29.53 mmol), CPT-11 powder or SN-38 powder were added. For the batches with CPT-11 or SN-38 powder 60 µl of 0.9% NaCl was added to have an aqueous environment in the tube. 600 mg of zirconium oxide beads (1.5 mm) (Sigmund Lindner, Warmensteinach, Germany) were added to each vial. The vials were placed in the ZentriMix 380 R centrifuge (prototype, Andreas Hettich GmbH, Tuttlingen, Germany) and the preparation of the liposomes was performed for 30 min, 2350 rpm at 45°C. The obtained phospholipid gel was diluted by addition of 200 µl 0.9% NaCl and again centrifuged for 2 min at 1800 rpm.

## 3.4 Drug loading

### 3.4.1 Passive loading to pre-formed liposomes

The passive loading method was used for dFdC and SN-38. The feasibility of passive dFdC loading in preformed liposomes in HBS pH 7.4 was already shown for $DPPG_2$-TSL [44] and another liposomal formulation [114]. The extruded liposomal dispersion was diluted 1:1 (vol/vol) with the drug solution Gemzar® (38 mg/ml) or SN-38 (for concentration and pH refer to the results). For the passive loading process developed in this work the dispersion was centrifuged (Avanti-J26XP, Beckman Coulter, Krefeld, Germany) directly after extrusion at 75,600xg for 60 min at 15°C to achieve a higher lipid concentration. The resulting pellet was resuspended in Gemzar®-solution (< 38 mg/ml) adjusted to a pH 6-6.5 by addition of 600 mM $NaHCO_3$. The exact concentration of dFdC was not known after the adjustment of the pH. After addition of dFdC or SN-38 the dispersion was transferred in fresh tubes and incubated in a thermoshaker (Eppendorf AG, Hamburg, Germany) for 30 min at 60°C with constant shaking of 750 rpm. After cooling to 2-8°C the dispersion was transferred in centrifuge tubes and centrifuged (Avanti-J26XP, Beckman Coulter, Krefeld, Germany) at 75,600xg for 60 min at 15°C to concentrate the dispersion. After removal of the supernatant the resulting pellet was resuspended with HBS pH 7.4 (70% of initial TSL volume after extrusion). Unencapsulated traces of dFdC or SN-38 were removed by size exclusion chromatography (PD-10 columns, GE Healthcare, München, Germany) against HBS pH 7.4.

### 3.4.2 Active loading to pre-formed liposomes

For active loading of drugs a gradient method was used with some modifications [115]. A $H^+$- and/or $NH_4^+$- transmembrane gradient was achieved by performing a buffer exchange via an PD-10 column (GE Healthcare, München, Germany) or addition of 1 M $NaHCO_3$. The used extra- and intraliposomal buffer system for the different drugs are listed in Table 3-1.

| | **Intraliposomal buffer** | **Extraliposomal buffer** |
|---|---|---|
| **Dox** | DPPC/DSPC 3:1 | HBS pH 7.8 |
| **CPT-11** | 300 mM $(NH_4)_2SO_4$ pH 5.4<br>300 mM (NH4)2HPO4 pH 7.4<br>300 mM Citrate pH 4 | HBS pH 7.8<br>HBS pH 7.8<br>Titrated to pH 8 with 1 M $NaHCO_3$ |
| **SN-38** | 300 mM Citrate pH 4<br>Glycine pH 9 | 1 M $NaHCO_3$ pH 8<br>Histidine pH 6.4 |

*Table 3-1 Extra- and intraliposomal buffer systems used for active loading of Dox, CPT-11 or SN-38.*

The lipid concentration in the encapsulation volume was adjusted to 3 mM. The used drug concentration depended on the desired drug/lipid ratio in the final volume. The encapsulation was performed for 30-90 min at 36-37°C in a thermoshaker (Eppendorf GmbH, Hamburg, Germany). The encapsulation was monitored by taking samples and measuring the fluorescence intensity (Dox: Ex 470nm, Em 555nm; CPT-11: Ex 355nm, Em 515nm; SN-38: Ex 355nm, Em 553nm) (Cary Eclipse, Varian Inc., Palo Alto, California, USA). With increasing encapsulated drug concentration, the fluorescence intensity in the sample decreases, because of the self-quenching of the fluorescence intensity at higher drug concentration. After cooling to 2-8°C the dispersion was concentrated via centrifugation (Avanti-J26XP, Beckman Coulter, Krefeld, Germany) at 75,600xg for 60 min at 15°C. Afterwards the supernatant with unencapsulated drug was discarded and the pellet was resuspended in HBS pH 7.4.

### 3.4.3 Film loading

For SN-38 the film loading method published by Sadzuka et al was used with some changes [116]. In brief, liposomes were prepared as described above using a lipid concentration of 25 mM or 50 mM and with HBS pH 7.8. A SN-38-film was prepared by dissolving 5-10 mg in $CHCl_3$/MeOH 4:1 (v/v) and the solvents were removed with a rotary evaporator (Laborota 4001, Heidolph Instruments GmbH, Schwabach, Germany). The resulting SN-38 film was sonicated after addition of the liposomes for 10-12 min at 65°C to trap the SN-38 to the empty liposomes (Sonication bath Sonorex Super RK103H, Bandelin electronics GmbH&Co.

KG, Berlin, Germany). The cooled dispersion was centrifuged for 60 min at 15°C, 75,000xg (Avanti-J26XP, Beckman Coulter, Krefeld, Germany) and the pellet was resuspended in HBS pH 7.8. The remaining unencapsulated SN-38 was removed by size-exclusion chromatography.

### 3.4.4 Passive loading of CF during formation of liposomes

The lipid film was hydrated with 100 mM CF-solution pH 7.2 at 60°C for 10-15 min. After 10 subsequent steps of extrusion through two 200 nm polycarbonate filters the unencapsulated CF was removed by separation over a PD-10 column with 0.9% NaCl as eluent.

## 3.5 Liposomal characterization

### 3.5.1 Dynamic light scattering

The particle size (z-average), polydispersity index (PDI) and ζ-potential of the liposomes were analyzed by dynamic light scattering (Zetasizer Nano ZS, Malvern Instruments, Worcestershire, United Kingdom). The liposomal samples were diluted in 0.9% NaCl and measured at 25°C. The average diameter and width of the size distributions were evaluated by using a single exponential fit to the correlation function (cumulants fit) with the software provided by Malvern. Larger aggregates in the formulations were detected by analyzing the size distribution plots. For each sample, the device measured 12-14 times in a row for the size determination depending on the quality of the liposomal sample. For the ζ-potential for each sample three sets of 15 measurements were performed. The quality of the measurement was occasionally checked by a traceable size standard (125 nm, Nanosphere, Thermo Fisher Scientific, Waltham, Massachusetts, USA).

### 3.5.2 Quantification of total lipid concentration

The total lipid concentration was determined with a phosphate analysis analog to a published method [117]. This method is suitable for all lipids containing one phosphorus atom. In brief, by addition of sulfuric acid and perchloric acid to the samples and heating up to 300°C the phosphorus atom in the phospholipids is converted to phosphate. After addition of ammonium heptamolybdate a complex was formed. The samples were measured at 660 nm in a spectrophotometer (Beckmann DU 640, Beckman Coulter GmbH, Krefeld, Germany). A 1 g/l phosphate solution (Phosphate standard solution 1000 mg/ml, Merck KGaA, Darmstadt, Germany) was used for preparation of a standard curve. The quality of the method was checked occasionally by a traceable phosphate standard (Phosphorus ICP standard 1000 mg/ml Merck KGaA, Darmstadt, Germany).

### 3.5.3 Determination of lipid composition

TLC analysis was used for determination of the lipid composition and the appearance of degradation products of the phospholipids like lysolipids as described previously [31]. In brief, 1500 nmol TSL were transferred to a glass tube. 1 ml 0.9% NaCl and 2 ml of $CHCl_3$/MeOH 1:1 (v/v) was added and after mixing centrifuged to achieve a phase separation. The organic phase was transferred to a new tube and after evaporation of the solvent the residue in the tube was dissolved in 100 µl $CHCl_3$/MeOH 9:1 (v/v). 1.2 µl of this solution was applied to a HPTLC-plate (Silica 60, not modified, Merck KGaA, Darmstadt, Germany). The mobile phase consisted of $CHCl_3$/MeOH/$CH_3COOH$/$H_2O$ 100:60:10:5 (molar ratio) and allowed separation of lysolipids, phosphocholines, $DPPG_2$, and DSPE-$PEG_{2000}$. In each TLC run a lipid standard solution containing P-Lyso-PC, DPPC, $DPPG_2$ and DSPE-$PEG_{2000}$ was applied to check separation quality. The phospholipids were stained with a molybdenum spray [118]. Densitometric analysis of the spot intensity was performed with the software Gimp and ImageJ.

### 3.5.4 Quantification of drug concentration

*CPT-11*

CPT-11 content was quantified with fluorescence spectroscopy (Cary Eclipse, Varian Inc., Palo Alto, California, USA). The prepared reference standards in HBS pH 7.4 covered a concentration range form 0-1.14 µM and were prepared from a 2.953 mM standard solution of CPT-11 (dilution with $H_2O$ of standard solution with 29.53 mM provided by the pharmacy). The liposomes were diluted with HBS pH 7.4 to adjust the concentration to the range of the calibration curve. After addition of 200 µl 10% Triton X-100 to each prediluted sample (20 µl), they were incubated for 15 min at 45°C (Thermoshaker, Eppendorf AG, Hamburg, Germany). 20 µl of the incubated samples were diluted with 3 ml of HBS pH 7.4 and measured (Ex 355 nm, Em 515 nm).

*SN-38*

SN-38 was quantified in analogy to the CPT-11 determination with only changing the calibration range to 0-0.72 µM and the dilution medium (HBS pH 7.8), respectively. The settings for the spectrofluorometer were Ex 355 and Em 553 nm (Cary Eclipse, Varian Inc., Palo Alto, California, USA).

*dFdC*

For dFdC content determination, a HPLC method was used (cf. 3.6.1).

*Doxorubicin*

The encapsulated doxorubicin was determined with fluorescence spectroscopy. For this purpose, reference standards in the calibration range of 0-1.13 µM Dox were prepared by diluting a 2 mg/ml stock solution with $H_2O$. As control sample in each measurement the Dox concentration of Doxil® was measured. The liposomal samples were diluted to the calibration range by addition of HBS pH 7.4. 200 µl 10% Triton X-100 was added to all samples (20 µl) to destroy the liposomes and incubated for 15 min at 45°C (Thermoshaker, Eppendorf AG, Hamburg, Germany). Before measurement the samples were diluted with HBS pH 7.4 (20 µl samples and 3 ml HBS pH 7.4). The fluorescence of doxorubicin was measured at Ex of 470 nm and Em of 555 nm (Cary Eclipse, Varian Inc., Palo Alto, California, USA).

### 3.5.5 Temperature-dependent drug release

*CPT-11*

The CPT-11-content release was followed according to an already published method for doxorubicin with some minor changes [31]. CPT-11-TSL were diluted 1:12 (v/v) with HBS pH 7.4 or FBS, respectively. 20 µl of this sample were incubated for 5 min at a defined temperature (e.g. 37 to 45°C), or for 1 h (37 or 42°C) (Thermoshaker, Eppendorf AG, Hamburg, Germany). The reaction was stopped by addition of 1 ml cold HBS pH 7.4. For calculation of the release in %, additional samples were incubated for 1 h at 60°C, because at this temperature the whole CPT-11 is released. The fluorescence was measured at Ex 355 nm and Em 515 nm (Cary Eclipse, Varian Inc., Palo Alto, California, USA) and the %-release calculated with Equation 1.

$$R_T(\%) = \frac{c_T - c_{0\%}}{c_{100\%} - c_{0\%}} \times 100$$

$R_T$ temperature-dependent released CPT-11

$c_T$ non-liposomal CPT-11 after 5 min incubation at temperature T

$c_{0\%}$ non-liposomal CPT-11 without incubation

$c_{100\%}$ non-liposomal CPT-11 after incubation for 1 h at 60°C

*Equation 1*

*SN-38*

The SN-38 liposomes were diluted 1:4 (v/v) with HBS 7.8 for measurement of the temperature-dependent release profile. The diluted liposomes were further diluted 1:12 (v/v) with FBS and 20 µl of this sample was incubated for 5 min at a defined temperature in the range of 37-45°C (Thermoshaker, Eppendorf AG, Hamburg, Germany). The reaction was stopped by addition of 1 ml HBS pH 7.8. For the 100%-value, 20 µl of the prediluted liposomal solution was mixed with 20 µl of 10% Triton X-100 and incubated for 15 min at 45°C. The fluorescence of all samples was measured after dilution with HBS pH 7.8 in a

spectrofluorometer at Ex 355 nm and Em 553 nm (Cary Eclipse, Varian Inc., Palo Alto, California, USA). The %-release was calculated with equation 1.

For determination of SN-38 release in presence of acceptor-vesicles, the liposomes were also diluted 1:4 (v/v) with HBS pH 7.8. To 50 µl of diluted liposomes 100 µl acceptor vesicle (DSPC/Chol 55:40 (molar ratio)) and 100 µl of HBS pH 7.8 was added. The samples were incubated for 5 min at a defined temperature in the range between 37-45°C (Thermoshaker, Eppendorf AG, Hamburg, Germany) and cooled down in the fridge. The supernatant after centrifugation for 15 min at 16,000 g (Centrifuge 5451, Eppendorf AG, Hamburg, Germany) was removed and the pellet resuspended in 200 µl HBS pH 7.8. 20 µl of the resuspended solution was incubated with 20 µl of 10% Triton X-100 for 15 min at 45°C (Thermoshaker, Eppendorf AG, Hamburg, Germany). The reaction was stopped by adding 1 ml of HBS pH 7.8. The released SN-38 was measured in a spectrofluorometer at Ex 355 nm and Em 553 nm (Cary Eclipse, Varian Inc., Palo Alto, California, USA).

*dFdC*

Temperature-dependent dFdC release profiles were determined according to Limmer et al [44].

*CF*

The temperature-dependent release of the non-toxic artificial drug molecules was performed according to a published method with some minor changes [31].

The TSL were diluted 1:50 with 0.9% NaCl. 100 µl of the diluted liposomes were mixed with 100 µl 10% Triton X-100 and incubated for 15 min at 45°C (Thermoshaker, Eppendorf AG, Hamburg, Germany). To 20 µl of this incubated solution 1 ml NaCl/Tris-solution pH 8 was added. The measured fluorescence of this value was taken as 100%-release. For the temperature-dependent release 100 µl of the diluted TSL-solution were diluted with 1 ml of FBS or 0.9% NaCl. 20 µl of this solution were incubated at a defined temperature in the range between 37-45°C for 5 min or 37/42°C for 1 h. The fluorescence intensity of all samples was measured using a spectrofluorometer (Cary Eclipse, Varian Inc., Palo Alto, California, USA).

### 3.5.6 Time-dependent CPT-11 release

The time-dependent release of CPT-11 from TSL formulations was measured according to a published assay for doxorubicin release [31].

CPT-11 -TSL were diluted 1:21 (v/v) with HBS pH 7.4. For the 100%-value 40 µl liposomes were diluted with 100 µl HBS pH 7.4 and the sample was incubated for 1 h at 60°C

(Thermoshaker, Eppendorf AG, Hamburg, Germany). The reaction was stopped by addition of 700 µl HBS pH 7.4. For the measurement of the release kinetics, 3 ml of FBS or HBS pH 7.4 were preheated to the desired temperature in the range from 37-42°C in the spectrofluorometer (Cary Eclipse, Varian Inc., Palo Alto, California, USA). 20 µl of the 60°C/1 h-sample or 20 µl of the unheated sample were transferred in the preheated and stirred solution and the measurement started immediately. Fluorescence intensity was recorded every 20 s in the first 5 min of incubation and every 2 to 4 min thereafter. The percentage release over time was calculated with the Equation 1.
The release rate constant k at 37°C and 40°C was calculated for the first 300 s as described for Dox by Hossann et al [31].

### 3.5.7 Osmolarity

To analyze the osmolarity of liposomal formulations a vapor pressure osmometer (Vapro 5600, Wescor Inc., Logan, Utah, USA) was used. Before each measurement, the osmometer was calibrated with three standard solutions with osmolarities of 100 mmol/kg, 290 mmol/kg and 1000 mmol/kg (Optimole, Wescor Inc., Logan, Utah, USA) in triplicate. After the calibration 10 µl of sample were pipetted on the filter in the sample holder and the measurement was started.

### 3.5.8 Differential scanning calorimetry

The phase transition of TSL was measured with differential scanning calorimetry (DSC). The liposomal samples were concentrated via spin columns before measurement. 20 µl of the concentrated samples were transferred to 40 µl aluminum crucibles and sealed. The samples were scanned from 20°C to 60°C at an average heating rate of 1°C/min and cooled from 60°C to 20°C with a cooling rate of also 1°C/min in a Mettler Toledo DSC 821e (Mettler Toledo, Gießen, Germany). $T_m$ was determined at minimum of the phase transition curve.
$T_g$` was determined in a Netzsche DSC 204 (Netzsche GmbH, Selb, Germany) by cooling the sample from 20°C to -70°C and reheating to 20°C with a rate of 10°C/min. 20 µl of samples were transferred to aluminum crucibles and sealed before measurement.

### 3.5.9 Free fatty acid determination

To determine the non-esterified fatty acids (NEFA) in a liposomal dispersion a method based on the enzymatic endpoint method published by Trinder et al was established [119, 120]. The used kit was purchased from DiaSys Diagnostic Systems GmbH (Holzheim, Germany) and used according their standard protocol. The underlying reaction mechanism is shown in Scheme 1.

$$\text{Non-esterified fatty acids + coenzyme A + ATP} \rightarrow \text{Acyl-CoA + AMP + } PP_i$$

$$\text{Acyl-CoA + } O_2 \rightarrow \text{2,3-trans-Enoyl-CoA + } H_2O_2$$

$$2H_2O_2 + \text{Trinder-reagent} \rightarrow \text{Dye + } 4H_2O$$

*Scheme 1 Reaction mechanism underlying NEFA-determination*

In brief, 1000 µl of reagent 1 was added to 20 µl reference standard, water or sample, respectively. After 5 min incubation at 37°C in a thermoshaker. the absorbance at 546 nm was measured (=E1) (spectrophotometer Beckmann DU 640, Beckman Coulter GmbH, Krefeld, Germany). 250 µl of reagent 2 was added and the samples were incubated for 10 min at 37°C. The absorbance was measured again (=E2). The concentration of NEFA was calculated as shown Equation 2.

$$\Delta E = (E2 - E1)$$

$$NEFA\ [\frac{mg}{dl}] = \left(\frac{\Delta E(sample)}{\Delta E(standard)}\right) \times c(standard)$$

*Equation 2*

### 3.5.10 Cryo-TEM measurement

The cryo-transmission electron microscopy (Cryo-TEM) was performed by Mrs. Sabine Barnert (Pharmaceutical technology and biopharmaceutics, Albert-Ludwigs-University Freiburg, Germany) according to the method published by Holzer et al [121]. The liposomes were diluted with HBS to phospholipid concentrations between 10 and 15 mM. Approx. 3 µl of the sample were applied on a 400 x 100 mesh Quantifoil® S7/2 holey carbon film on copper grids. After removal of the excess of liquid with filter paper the grid was immediately shock-frozen by putting into liquid ethane (Kryogen, 90K). The frozen grid was fixed in the sample holder and transferred into the TEM (120 keV). Samples were analyzed and pictures taken with an image amplifier camera at magnifications from 6300x-12,500x.

## 3.6 HPLC

### 3.6.1 dFdC determination in plasma- and aqueous samples

A published method was applied to quantify the concentration of dFdC in aqueous- or plasma-samples with HPLC (515 HPLC pumps, 717 plus autosampler and 2489 UV/Vis detector, Waters corporation, Milford, Massachusetts, USA) [44, 75].

With a flow rate of 0.5 ml/min and 10 mM $KH_2PO_4$ pH 7 as mobile phase the samples were eluted from the column (C18, 3 mm x 100 mm, 2.6 µm, 100 Å, Kinetex, Phenomenex Inc., Torrance, California, USA). Column oven was set to 40°C. 5-FU was used as internal standard and Gemzar® was used as calibration standard. The analytes were detected with a UV-detector at λ=275 nm.

### 3.6.2 CPT-11 and SN-38 determination in aqueous-, plasma- and cell lysate samples

For simultaneous determination of CPT-11 and SN-38 the sample preparation was performed as described in Limmer et al with some minor changes [44]. In brief, 50 µl sample (plasma samples 1:25 diluted with 0.9% NaCl) were diluted with 25 µl internal standard camptothecin (CPT; 10 µg/ml in 25 mM $NaH_2PO_4$ pH 3.1/ACN 70:30) and 600 µl ACN. After vigorous mixing and subsequent centrifugation (6 min, 19,000xg) 600 µl of the supernatant was transferred to a fresh glass tube. Under $N_2$-flow at 40°C the solvent was removed. The dry residue was dissolved in 400 µl 25 mM $NaH_2PO_4$ pH 3.1/ACN 70:30. After vigorous mixing, the samples were centrifuged (10 min, 19,000xg), and the supernatants were transferred to HPLC-injection tubes. Runs were carried out on a Waters HPLC-system (515 HPLC pumps, 717 plus autosampler and 470 fluorescence detector, Waters corporation, Milford, Massachusetts, USA) using fluorescence detection (Ex 355 nm, Em 515 nm). A C18 column (5 µm, 125 Å, 250 mm x 4 mm, Phenomenex Inc., Torrance, California, USA) with 25 mM $NaH_2PO_4$ pH 3.1/ACN 70:30 as mobile phase was used. 50 µl of each sample was injected and eluted with an isocratic flow of 1 ml/min. The reference standard samples were prepared by spiking FBS, human plasma or HBS pH 7.4 with 25, 50 or 100 µl of SN-38 (100 µg/ml) and CPT-11 (100 µg/ml), respectively.

### 3.6.3 CPT-11 and SN-38 determination from tissue samples

CPT-11 and SN-38 concentration in tissue samples were quantified with the HPLC-method described above. Sample preparation was performed by a modified liquid extraction protocol from Galettis et al [122] as described by Willerding et al for Doxorubicin-TSL [123] with some adaptions. After addition of 350 µl $H_2O$, 950 µl MeOH and 300 µl of internal standard CPT (10 µg/ml in 25 mM $NaH_2PO_4$ pH 3.1/ACN 70:30) 100 mg of tissue were homogenized in a TissueLyser (30 Hz, 4x4 min) (Qiagen GmbH, Hilden, Germany). The CPT-11 and SN-38 were extracted in an organic phase consisting of 5 ml $CHCl_3$/2-propanol 2:1 (v/v). After mixing and centrifugation (2333xg, 10 min, RT) the organic phase was transferred to a fresh glass tube and the solvent was removed under $N_2$ at 40°C. The dry sediment was dissolved in 4 ml mobile phase, centrifuged (16 min, 19,000xg) and transferred to a HPLC injection tube.

## 3.7 Lyophilization

### 3.7.1 Freeze-dryer Epsilon 2-6D

The Epsilon 2-6D freeze-dryer (Martin Christ, Osterode, Germany) was used for liposomes containing CF to develop and investigate an appropriate lyophilization process for $DPPG_2$-TSL. For controlled nucleation of the vials the “ice-fog” method published by Geidobler et al was adjusted [124]. 1 ml CF-TSL were filled in 2R-vials, some vials were equipped with thermocouples and loaded in the freeze-dryer. The shelf of the freeze-dryer was cooled down to -5°C. After the vials also reached -5°C, a pressure of 4.020 mbar was applied. If the desired pressure was reached the drain valve, which ventilates via the cold condenser, of the freeze-dryer is immediately opened to reestablish atmospheric pressure in the chamber again. If nucleation was successful, the vials were frozen to -40°C at a freezing rate of 1°C/min. The temperature was held at this temperature for 1 h 25 min and then a pressure of 0.05 mbar was applied and the temperature increased to -30 °C with 0.5°C/min to the primary drying conditions. Primary drying was performed for around 40 h. Secondary drying was performed at 20°C for 6-10 h. A standard lyophilization cycle is shown in Figure 3-1.

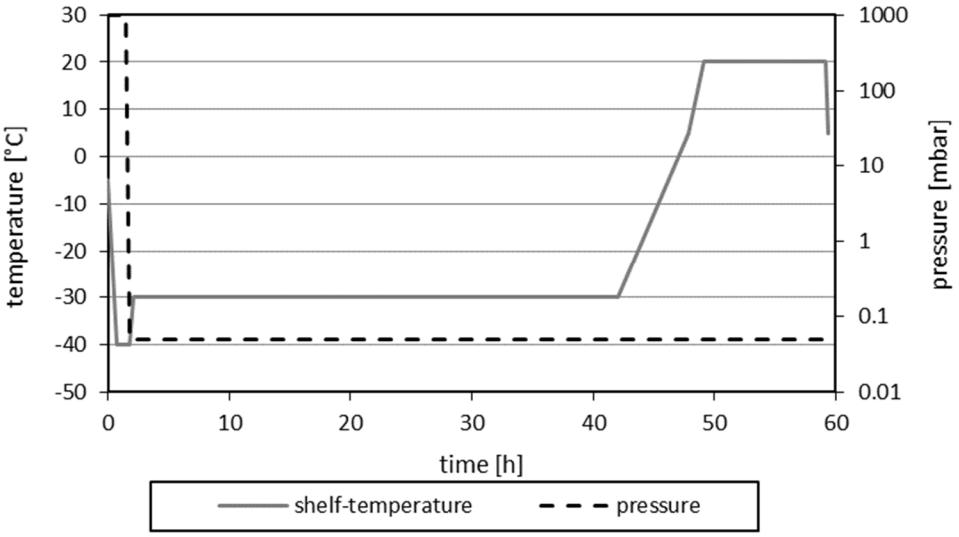


*Figure 3-1 Standard lyophilization cycle with controlled nucleation performed with the Epsilon 2-6D freeze-dryer*

### 3.7.2 Freeze-dryer Epsilon 2-12D

For TSL containing cytostatic drugs the freeze-dryer Epsilon 2-12D (Martin Christ, Osterode, Germany) was used. TSL were filled in vials and the vials were wrapped in sterile bags (cf. Figure 3-2) to avoid contamination of the freeze dryer in case of glass damage.

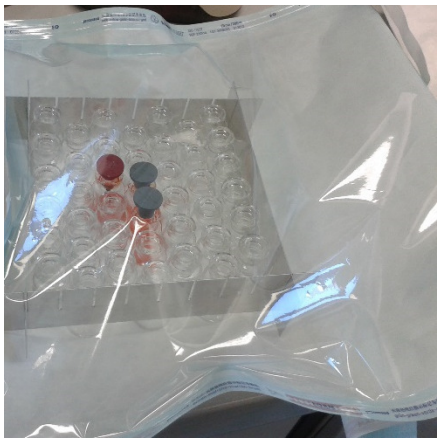

*Figure 3-2 Vials containing CF-liposomes wrapped in sterile bags prepared for lyophilization*

The vials wrapped in sterile bags were placed in the freeze-dryer. The process was again developed with CF-liposomes. Figure 3-3 shows the lyophilization cycle established with CF-liposomes and used for lyophilization of TSL loaded with doxorubicin, CPT-11 or dFdC, respectively.

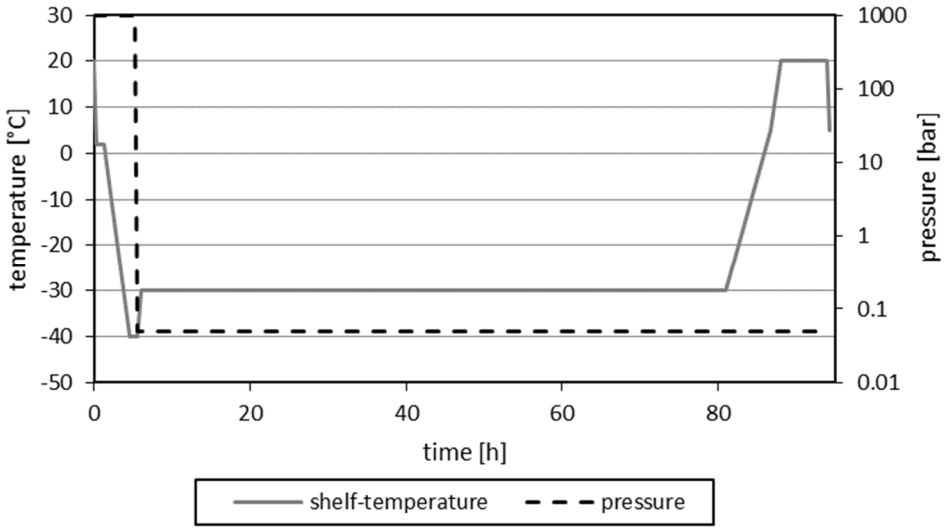


*Figure 3-3 Standard lyophilization cycle for vials wrapped in sterile bags to avoid contaminations with cytostatic agents performed with Epsilon 2-12 D freeze-dryer*

### 3.7.3 Residual moisture

The residual moisture in lyophilized samples was analyzed by a coulometric Karl Fischer titrator (Aqua 40.00, Elektrochemie Halle, Germany) with a head-space oven. Sealed dried samples (~10 mg) in 2R-vials were heated in the oven chamber to 80°C. Into a Karl-Fischer chamber the vaporized water from the samples was transported via needle-flexible tubing system.

## 3.8 Storage stability study

### 3.8.1 dFdC-TSL at 2-8°C

For a storage stability study at 2-8°C, different formulations of dFdC-TSL were prepared and directly stored in the fridge after preparation. At different time points z-average, PDI, NEFA-content, lysolipid-content and dFdC leakage were determined for 48-60 weeks.

### 3.8.2 CPT-11-TSL at 2-8°C

The CPT-11-TSL were stored at 2-8°C directly after preparation. After four weeks, the samples were stored at RT. After one, two and four weeks at 2-8°C and four weeks at 2-8°C plus additionally one and three weeks at RT, z-average, PDI, lysolipid-content and the temperature-dependent release was measured.

### 3.8.3 Lyophilized CF-TSL at 2-8°C or RT

The lyophilized vials were stored at 2-8°C or RT. After distinct time points, three vials per temperature were reconstituted by addition of Millipore water. One additional vial was used for residual moisture determination without reconstitution. The analyzed parameters were z-average, PDI, lysolipid-content, background fluorescence of CF and temperature-dependent CF-release of reconstituted samples and residual moisture of the lyophilized cake.

## 3.9 Cell Culture

All cell lines were incubated in an incubator (Binder, Tuttlingen, Germany) at 37°C in a humidified atmosphere of 95% air and 5% $CO_2$ in cell culture flasks. All working steps were performed under a laminar flow (Glaire BSB 4, ICN Flow, Eggenstein, Germany).

### 3.9.1 Culture conditions

All used cells were adherent growing. The culture medium was always supplemented with 10% FBS (v/v) and 100 U/ml penicillin and 100 U/ml streptomycin (all three Biochrom AG, Berlin, Germany). Table 3-2 shows culture medium, supplement in medium and trypsin/EDTA-concentration (purchased Biochrom AG, Berlin, Germany) for detachment used for every cell line.

| Cell line | Culture medium | Supplements for medium | Trypsin/EDTA concentration |
|---|---|---|---|
| BN175 (provided by Timo ten Hagen, Erasmus MC Rotterdam, Netherlands) | RPMI 1640 medium, $NaHCO_3$ buffered, w/+ stable glutamine (Biochrom AG, Berlin, Germany) | / | 0.05% |
| DSL-6A/C1 (provided by Holger Grüll, TU Eindhoven, Netherlands) | Waymouth`s MB 752/1 (Thermo Fisher Scientific Inc., Waltham, Massachusetts, USA) | / | 0.1% |
| HepG2 (provided by AG Denk, Klinikum der Universität München, Germany) | MEM, w/+ stable glutamine (Sigma Aldrich GmbH, München, Germany) | - 1x non-essential amino acids<br>- 1 mmol/l pyruvate<br>(both Merck KGaA, Darmstadt, Germany) | 0.05% |

*Table 3-2 Culture medium with additional supplements and trypsin/EDTA concentration used for each cell line*

The BN-175 and DSL-6A/C1 cells were passaged every 3-4 days and the HepG2-cells once per week by addition of trypsin/EDTA-solution for detachment. The detachment reaction was stopped by addition of fresh medium and parts of the cell suspension were seeded after centrifugation (HepG2 was not centrifuged) in a new flask with fresh medium.

### 3.9.2 Freezing and thawing of cells

For long-term storage cells were stored at -196°C in liquid $N_2$. For freezing, harvested cells were quickly resuspended in freezing medium consisting of FBS/DMSO 9:1 (v/v). In each cryo-tube 1.5 x $10^6$ cells in 1 ml freezing medium were frozen to -80°C and after 24 h transferred to liquid $N_2$.

For thawing, the cells in a cryo-tube were started to thaw in a water bath at 37°C and immediately afterwards mixed with warm medium to dilute the toxic DMSO. After centrifugation, the cell pellet was resuspended in fresh medium and the cells were seeded in a culture flask.

### 3.9.3 Cell counting in Neubauer counting chamber

To get a defined number of cells for cell experiments, freezing of cells and animal experiments, the cells were counted under a microscope in a “Neubauer improved” cell counting chamber.

### 3.9.4 Conversion of CPT-11 to SN-38

The conversion of CPT-11 to SN-38 in cells was analyzed in BN175, DSL-6A/C1 and HepG2 cells. The experimental setup was based on several publications [125-127].
Cells were seeded in different cell culture flask sizes (T25, T75, T175) and treated after 24 - 48 h incubation time with different concentrations of CPT-11 (5-20 µM). The incubation time with the drug was between 24 - 96 h. The medium was separated from the cells and the cells were lysed with ACN/MeOH 1:1 (v/v). The CPT-11 and SN-38 content of medium and cell lysates was determined with the HPLC-method described in section 3.6.

## 3.10 Animal experiments

All animal experiments were performed by Dr. Simone Limmer according to protocols approved by the responsible authority (Regierung of Oberbayern, Az. 55.2-1-54-2532-144-11). Brown Norway rats (Charles River GmbH, Sulzfeld, Germany) were housed in groups of three in cages with free access to chow (Ssniff Spezialdiäten GmbH, Soest, Germany) and water. The light/dark-cycle was 12 h at a room temperature of 21°C. After shipment, the animals had at least 14 days of setting-in period before starting the experiments. All experiments with the animals were performed under anesthesia with 2-5% isoflurane (Forene®, Abbott GmbH & Co. KG, Wiesbaden, Germany) and 1.5-2.0 l/min $O_2$. To stabilize the body temperature, animals were incubated on a heating pad (controlled with water bath at 37.5°C) and covered with a blanket during sedation. To avoid pain for the animals during and after the treatment, they received s.c. 100 mg/kg Metamizol (Vetalgin®, Intervet Deutschland GmbH, Unterschleißheim, Germany) and 0.5 mg/kg Meloxicam (Metacam®, Boehringer Ingelheim Pharma GmbH& Co. KG, Ingelheim am Rhein, Germany) before the experiment. Euthanasia at the end of the experiment or in case of early termination was done by injection of an overdose pentobarbital. For early termination of the experiment, human

endpoints were defined and stated in the animal protocol. In the therapeutic study the animals had to be sacrificed after the s.c. tumor reach a size of 3 $cm^3$.

## 3.10.1 *In vivo* experiments dFdC

The pharmacokinetic study and the therapeutic study for dFdC-TSL were performed as described by Limmer et al [44].

### *3.10.1.1 Pharmacokinetic study*

In brief for the pharmacokinetic study, different dFdC-TSL formulations were injected i.v. at a dose of 6 mg/kg dFdC in healthy Brown Norway rats. 2 min, 10 min, 30 min, 60 min, 90 min and 120 min after injection, 200 µl blood were collected in a lithium heparin microvette (Sarstedt, Nümbrecht, Germany) and centrifuged. The resulting plasma was stored at -20°C until analysis with HPLC.

The plasma concentration of dFdC was fitted with OriginPro 8.1.5 to a one compartment pharmacokinetic model:

$$c(t) = A_1 * e^{-k_1 * t}$$

$$t_{1/2} = \frac{\ln(0.5)}{k_1}$$

*Equation 3 Formulas used for calculation of plasma concentration. c(t)= dFdC-concentration at time t after i.v. application, $k_1$= rate constant for elimination. AUC calculated by integration of the first formula from t=0 to 120 min. The initial dFdC concentration at t=0 is given by c(0)=$A_1$.*

### *3.10.1.2 Therapeutic study*

Tumor fragments of soft tissue sarcoma BN175 were transplanted subcutaneously in the left hind leg of the rat. The tumor fragments were generated by injection of 1.5 x $10^6$ cells/ 50 µl medium s.c. in a leg of a rat to get a bulk tumor. After the bulk tumor reached a size of 1 $cm^3$, small pieces of 2 mm were frozen in liquid $N_2$ and implanted to the animals as first step of the experiment. If the tumor has a size of 0.5 cm in one diameter the treatment was started. The tumor was heated with a cold-light lamp (Photonic PI2000, Photonic Optics, Vienna, Austria) to a temperature of 41°C. Temperature was monitored with invasive temperature probes. When the tumor reached the desired temperature, the treatment started and the animals received intravenously 6 mg/kg dFdC-TSL and heating was continued for 60 minutes. The tumor growth was monitored every second day by caliper measurements.

## 3.10.2 *In vivo* experiments CPT-11

### *3.10.2.1 Pharmacokinetic study*

The circulation half-life of distinct CPT-11 formulations were determined in healthy Brown Norway rats using a dose of 20 mg CPT-11 per kg bodyweight. Free, non-liposomal CPT-11 and the TSL formulation were diluted with HBS pH 7.4 to CPT-11 concentration of Onivyde® (7.33 mM) to achieve comparable injection volumes for all formulations. ~200 µl blood were collected after 10 min, 30 min, 60 min, 120 min, 240 min, 360 min and 1440 min with a lithium heparin microvette (Sarstedt, Nümbrecht, Germany) and centrifuged. The plasma was collected and frozen at -20°C until HPLC measurement described in section 3.6. Plasma concentrations was fitted to a one compartment pharmacokinetic model analogous to Equation 3.

### *3.10.2.2 Biodistribution*

7-10 days before treatment, tumor fragments of a bulk tumor generated as described in section 3.10.1.2 were implanted in one hind leg. After the tumor reached a size of 0.45-1.36 $cm^3$ the tumor was heated up to 41°C. Temperature was controlled invasively with a probe in the center of the tumor. After the target temperature was reached, non-liposomal CPT-11, CPT-11-TSL or Onivyde® were injected at a dose of 20 mg/kg, respectively. The HT was continued for 60 min. Directly after the treatment the animals were sacrificed and blood samples were taken from the heart. A cardiac perfusion was performed with NaCl-solution and the tumor, heart, liver, spleen and kidney were removed. The generated plasma and tissue samples were stored at -20°C until CPT-11 and SN-38 quantification with HPLC.

### *3.10.2.3 Therapeutic study*

Tumor fragments of a bulk tumor were implanted 5-10 days before treatment in the left hind leg. Therapy was started when one diameter reached a size of 0.5 cm. Tumors were preheated to a temperature of 41°C, while controlling the temperature with a probe placed in the center of the tumor. The treatment started by i.v. injection of non-liposomal CPT-11, CPT-11-TSL or Onivyde® at a dose of 20 mg/kg after the target temperature of 41°C in the tumor was reached. Duration of HT treatment was 60 min at 41°C. Every second day the health and body weight of the animals was checked and a caliper measurement of the tumor was performed till termination of the experiment. The tumor volume was calculated with the ellipsoid formula:

$$V = a \times b \times c \times \frac{\pi}{6}$$

*Equation 4 Ellipsoid formula for calculation of tumor volume; a = length; b = width; c = height*

# 4. Results

## 4.1 Thermosensitive liposomal gemcitabine

Objective was the improvement of an existing dFdC-TSL formulation with the phospholipid composition DPPC/DSPC/$DPPG_2$ 50:20:30 (molar ratio) (=$dFdC_3$-$TSL_{5/2/3/0}$), which was developed in our group [44], regarding stability during production and long-term storage. The formulation had some drawbacks, like endogenously formed 1.1±1.2% lysolipids during preparation as well as unwanted initial drug leakage in FBS (15.6±9.2%) [44]. The formulation $dFdC_3$-$TSL_{5/2/3/0}$ used in this thesis was prepared analog to the published process. The aims for the improved formulation were to avoid the production of lysolipids and free fatty acids (FFA) during preparation, to yield a formulation with a defined lipid composition and no degradation product. Additionally, the improved formulation should be stable at temperatures < 40°C in serum with a high release rates at 41°C to avoid release at body temperature and get a high and fast release at temperatures in the temperature range of HT.

### 4.1.1 Establishment of an assay to quantify free fatty acids

For evaluation of changes in formulation and production process it is of importance to reliably quantify the main decomposition products of phospholipids. Therefore, an easy and fast assay to determine the FFA in a liposomal formulation was established, based on a clinically used kit for determination of non-esterified fatty acids (NEFA) in serum or plasma.

The method showed a linearity to ΔE (proportional to FFA concentration) < 0.65 a.U. at 546 nm (cf. Figure 4-1). For higher ΔE the linearity could not be shown, because of the low solubility of Na-palmitate in EtOH/$H_2O$ 1:1 (v/v). The highest measurable concentration in a sample was 7.08 mM.

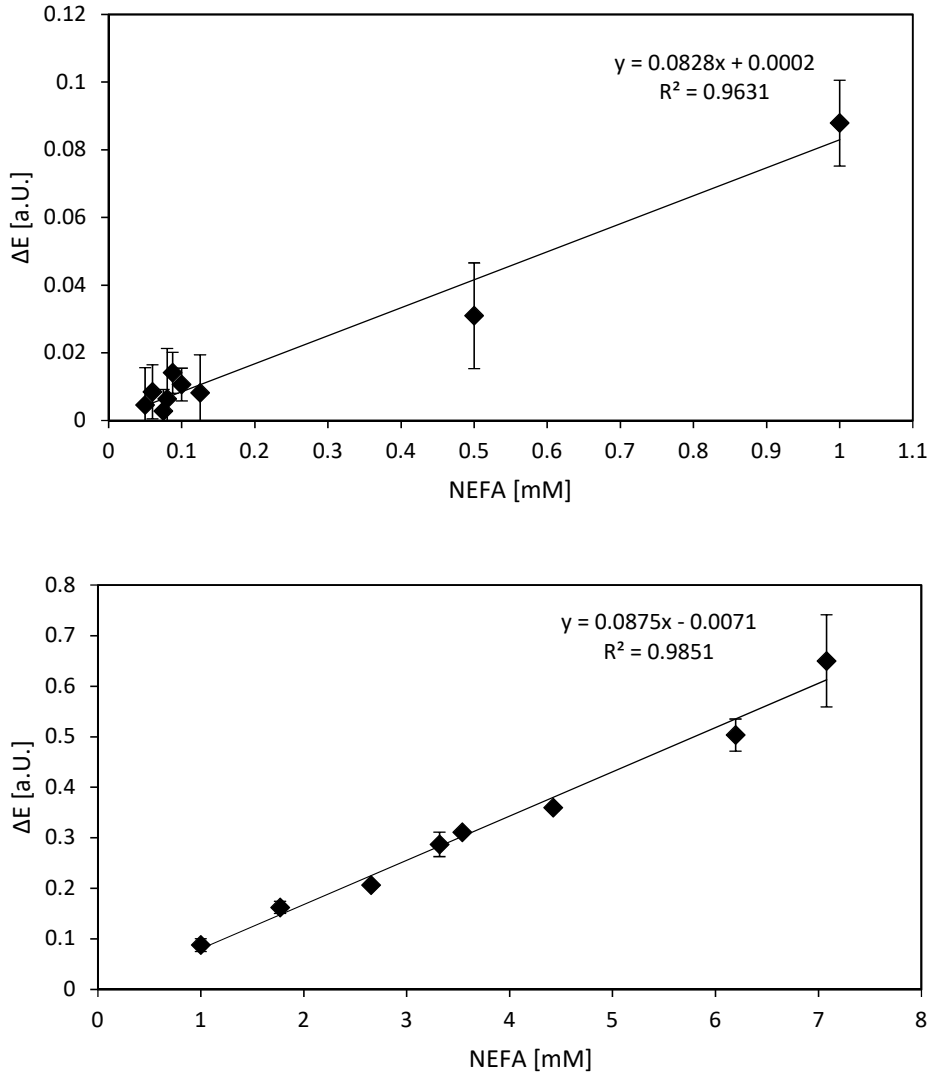


*Figure 4-1 Linearity of the NEFA-determination method. Values are given as mean value ± standard deviation (n=3).*

The influence of EtOH on the assay was analyzed because it was used for solubilization of sodium-palmitate for the standard curve. It was shown, that EtOH has no influence on the measurement by diluting the commercial FFA standard with EtOH 2:1 (v/v) (cf. Figure 4-2). The measured concentration of FFAs in the standard solution was 1 mM without EtOH und 0.99 mM with EtOH, respectively.

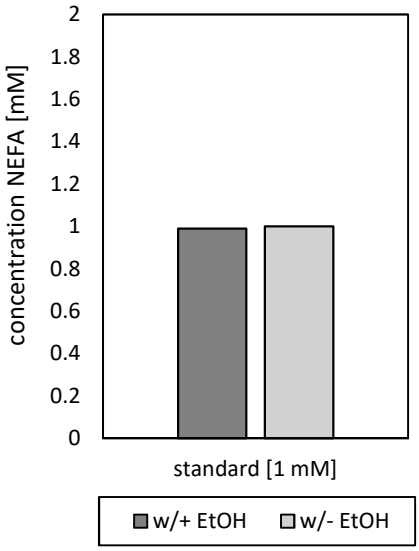


*Figure 4-2 Influence of EtOH on measured free fatty acid concentration of the commercial standard. The standard (1 mM) was diluted 2:1 (v/v) with EtOH.*

The limit of detection of the method, for liposomal samples with the used equipment, was 0.1 mM (= ΔE of 0.0106±0.0049) (see Figure 4-3). For liposomal samples with lipid concentration < 10 mM this limit of detection corresponded to a FFA content < 1% which is no longer detectable with this method.

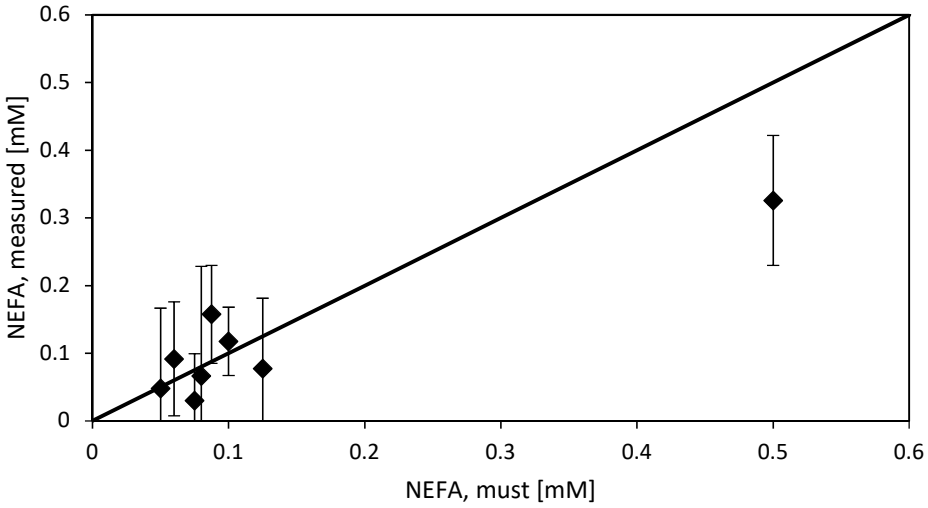


*Figure 4-3 Determination of the limit of detection of the method. The standard was diluted to concentrations between 0.05-0.5 mM with 0.9% NaCl. Values are given as mean value ± standard deviation (n=3).*

With some adjustments, the clinically used assay for determination of FFA could also be used for fast and easy determination of FFA in liposomal samples. The assay showed linearity in the range expected for liposomal samples and an acceptable limit of detection. The lysolipid content directly after preparation for the $dFdC_3$-$TSL_{5/2/3/0}$ prepared within the scope of this work was 4.3±3.5% and the FFA content was 4.5±1.4%, this means the assay

for detection of FFA gives reliable and similar results as the TLC for detection of lysolipids. For further experiments FFA assay was used for determination of FFA in liposomal samples.

## 4.1.2 Stabilization of liposomes

### *4.1.2.1 Influence of osmolarity*

Osmolarity of the dFdC$_3$-TSL$_{5/2/3/0}$ formulation as well as of dFdC-solution and HBS pH 7.4 was measured to investigate if initial drug leakage described for this formulation [44] was caused by osmotic pressure. Osmotic pressure is known to destabilize liposomal vesicles [128].

The osmolarity of dFdC$_3$-TSL$_{5/2/3/0}$ and a dFdC-solution used for the encapsulation was around the physiological osmolarity (290 mmol/kg; red line in Figure 4-4). For the dFdC-solution the measured osmolarity was 316.0±7.1 mmol/kg and for dFdC$_3$-TSL$_{5/2/3/0}$ 295.0±7.4 mmol/kg. Also, the used HBS pH 7.4 was in the physiological range (288.3±1.2 mmol/kg).

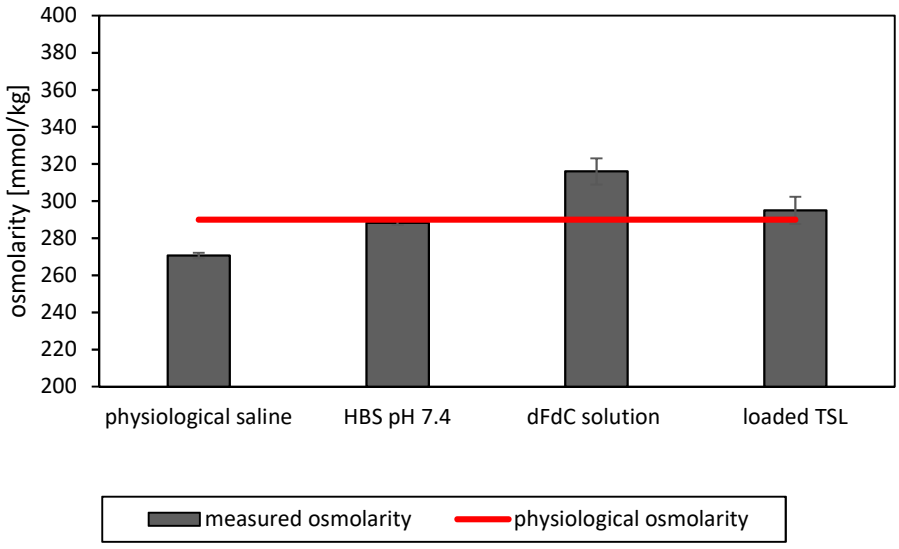


*Figure 4-4 Osmolarity of physiological saline, HBS pH 7.4, dFdC solution and loaded TSL dispersion. Values are given as mean value ± standard deviation (n=3).*

The instability observed for the dFdC-loaded DPPG$_2$-based formulation, which was published by Limmer et al [44], was not caused by osmotic pressure of the liposomes.

### *4.1.2.2 pH titration*

Next, it was investigated if the pH of the dFdC solution could be adjusted to more neutral pH-values. Low pH is known to cause hydrolysis of phospholipids [42, 97, 129, 130]. For this purpose, the Gemzar®-solution was titrated with $NaHCO_3$ from pH 2-7 and an UV-Vis

wavelength scan was performed to see if the pH change resulted in changes in the UV/Vis-spectrum due to degradation of dFdC or other effects.

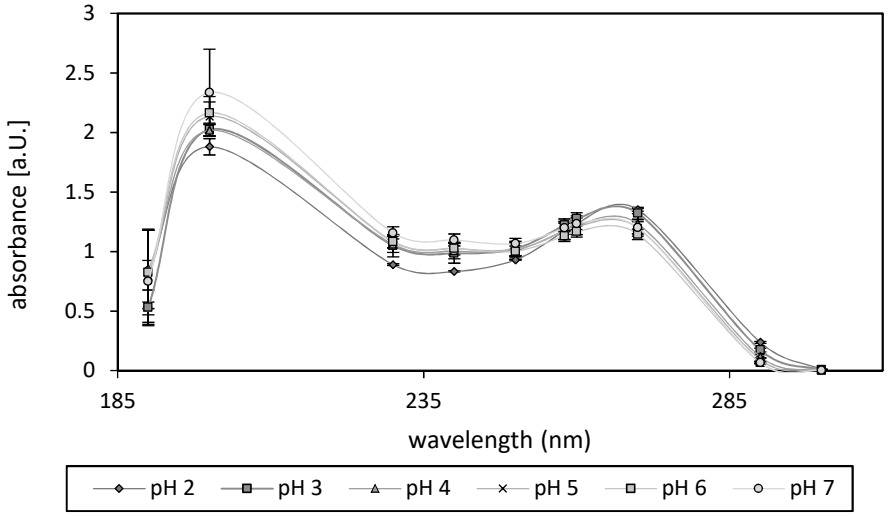


*Figure 4-5 Wavelength scan of Gemzar® solutions titrated to higher pH with $NaHCO_3$ solution. Values are given as mean value ± standard deviation (n=3).*

Increasing pH from 2 to 7 had no significant influence on the UV/Vis spectrum of dFdC (see Figure 4-5). To confirm that there was no change in dFdC concentration during addition of $NaHCO_3$ the concentration of the Gemzar®-solutions at different pH was measured with HPLC. Also in the HPLC there was no major concentration difference visible for the solution at different pH values (see Figure 4-6). The measured dFdC-concentration at pH 2 was 37.2±1.5 mM and at pH 7 it was 40.1±0.3 mM.

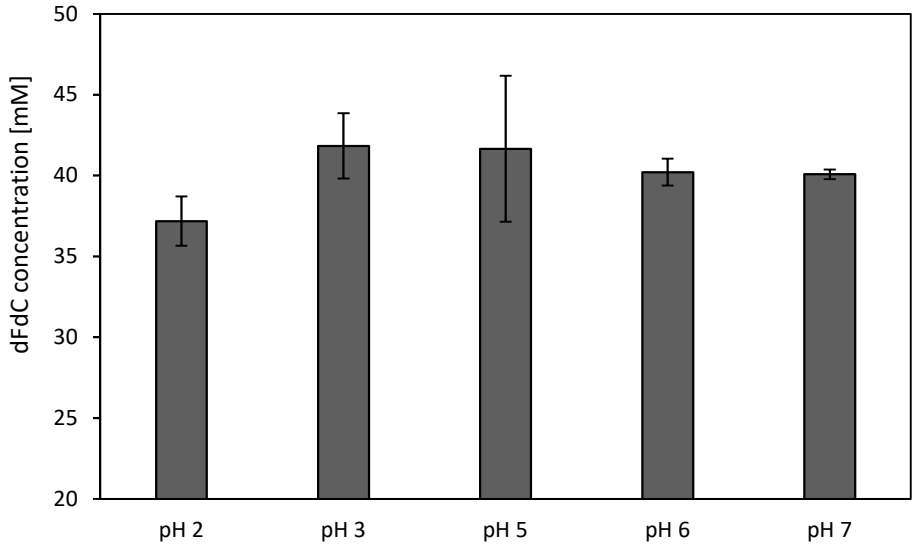


*Figure 4-6 dFdC-concentration determination with HPLC of Gemzar®-solution at different pH values. Values are given as mean value ± standard deviation (n=3).*

### *4.1.2.3 Adjustment of loading strategy*

TSL have been prepared with a Gemzar®-solution at a pH of 6-6.5 instead of pH 2-3. The loading procedure was also adjusted compared to the loading strategy of the published formulation [44] (cf. Figure 4-7).

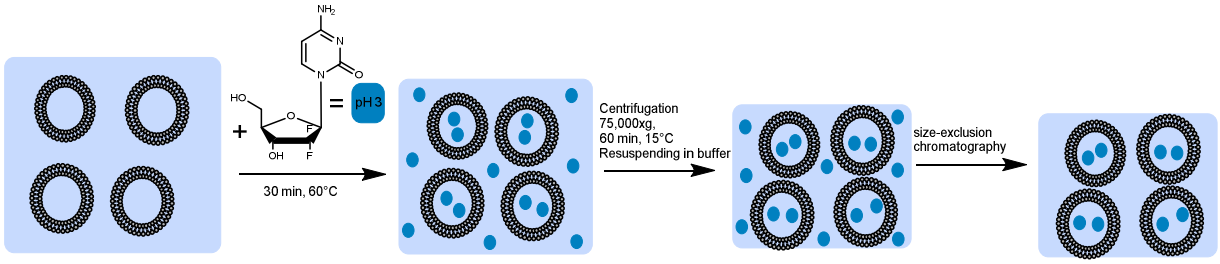


*Figure 4-7 Steps of the passive loading strategy used for the published formulation by Limmer et al [44].*

For improvement of the loading strategy two additional steps for concentration of the liposomes by a centrifugation and a resuspending step were added to achieve a comparable encapsulation efficacy as for liposomes prepared with the published method. This became necessary, since adjustment of the pH the dFdC solution by addition of a solution of 600 mM $NaHCO_3$ lowered drug concentration. After centrifugation and removal of supernatant, the pellet that contained the liposomes was directly resuspended with the dFdC solution (pH 6-6.5). The encapsulation efficacy (=EE) for the published loading process was 2.9 ±1.6% and for the new loading process 2.8±0.7%. The new loading process is shown in Figure 4-8.

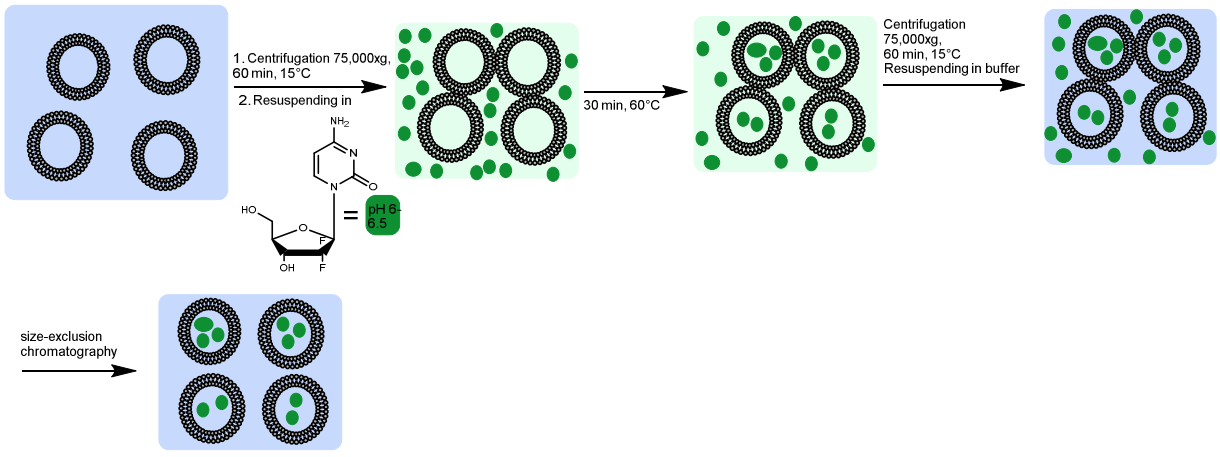


*Figure 4-8 Steps of improved passive loading of dFdC-solution with pH 6-6.5 to preformed $DPPG_2$-based TSL with lipid composition DPPC/DSPC/$DPPG_2$ 50:20:30 (molar ratio).*

| | z-average (nm) | PDI | ζ-potential (mV) | EE (%) | Lipid (mM) | dFdC (mM) | drug/lipid ratio (m/m) | Lyso-lipid (mM) | FFA (%) |
|---|---|---|---|---|---|---|---|---|---|
| **dFdC$_3$-TSL$_{5/2/3/0}$** | 162.3 ±33.9 | 0.107 ±0.073 | -25.5 ±4.9 | 2.9 ±1.6 | 26.3 ±8.1 | 3.6 ±2.1 | 0.127 ±0.047 | 4.3 ±3.5 | 4.5 ±1.4 |
| **dFdC$_6$-TSL$_{5/2/3/0}$** | 142.5 ±16.7 | 0.059 ±0.022 | -25.5 ±3.6 | 2.8 ±0.7 | 21.2 ±3.6 | 3.5 ±0.9 | 0.170 ±0.042 | 0.0 ±0.0 | 0.0 ± 0.0 |

*Table 4-1 Characteristics of liposomes prepared with published method with Gemzar® pH 3 (n=10) and improved method with Gemzar® pH 6-6.5 (n=4).*
*Liposomes were composed of DPC/DSPC/DPPG$_2$ 50:20:30 (molar ratio). Values given as mean value ± standard deviation.*

Table 4-1 shows that the liposomes prepared with the improved method demonstrated comparable characteristics to the published formulation. The achieved drug/lipid ratio (mol/mol) was even higher. Most important, neither lysolipids nor free fatty acids were detectable (compared to 4.3±3.5% lysolipids and 4.5±1.4% FFA with the published method). For all dFdC-liposomes prepared with Gemzar®-solution pH 6-6.5 the new method was used. To evaluate a potential impact of the changed production process and intraliposomal pH value, the temperature-dependent release of dFdC in FBS and HBS pH 7.4 was analyzed.

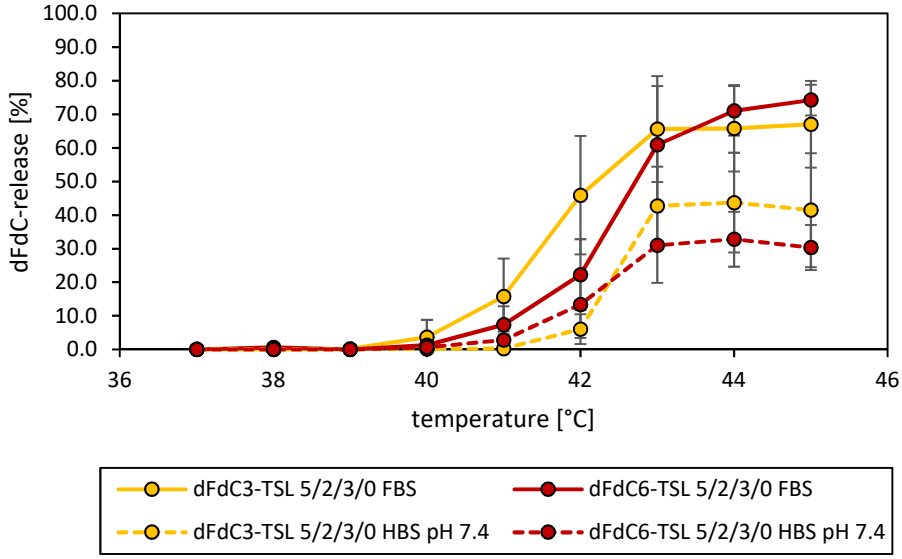


*Figure 4-9 In vitro temperature-dependent dFdC release from TSL prepared with two different preparation methods and different pH of the Gemzar®-solution.*
*In orange the formulation dFdC$_3$-TSL$_{5/2/3/0}$ is shown (n=8) and in red dFdC$_6$-TSL$_{5/2/3/0}$ (n=4). Temperature-dependent release profile was measured either in HBS pH 7.4 or FBS after 5 min incubation at different temperatures. Values are given as mean value ± standard deviation.*

The temperature-dependent dFdC release from dFdC$_6$-TSL$_{5/2/3/0}$ was shifted to higher temperatures (cf. Figure 4-9). The release in FBS at 41°C was 7.4±5.4% and at 42°C

22.3±10.5%, compared to 15.8±11.3% and 45.9±17.6% for $dFdC_3$-$TSL_{5/2/3/0}$, respectively. At temperatures < 40°C both formulations were stable.

### *4.1.2.4 Effect of phospholipid composition*

To obtain a similar or higher release at 41-42°C, formulations with different phospholipid compositions were prepared with Gemzar®-solution pH 6. The used phospholipids were DPPC/DSPC/$DPPG_2$/P-Lyso-PC in different molar ratios (cf. Table 4-2). P-Lyso-PC was added to produce a formulation with similar lipid composition as the formulation $dFdC_3$-$TSL_{5/2/3/0}$ in which the Lyso-PC was generated endogenously by lipid hydrolysis during preparation.

| | **z-average (nm)** | **PDI** | **ζ-potential (mV)** | **EE (%)** | **phosphate value (mM)** | **dFdC-content (mM)** | **drug/ lipid ratio (m/m)** |
|---|---|---|---|---|---|---|---|
| **$dFdC_3$-$TSL_{5/2/3/0}$** | 162.3±33.9 | 0.107± 0.073 | -25.5±4.9 | 2.9±1.6 | 26.3±8.1 | 3.6±2.1 | 0.127± 0.047 |
| **$dFdC_6$-$TSL_{5/2/3/0}$** | 142.5±16.7 | 0.059± 0.022 | -25.5±3.6 | 2.8±0.7 | 21.2±3.6 | 3.5±0.9 | 0.170± 0.042 |
| **$dFdC_6$-$TSL_{6/1/3/0}$** | 163.9±5.0 | 0.090± 0.046 | -26.5±2.8 | 3.3±0.8 | 26.2±3.2 | 4.1±1.1 | 0.157± 0.036 |
| **$dFdC_6$-$TSL_{7/0/3/0}$** | 164.0±4.7 | 0.094± 0.031 | -27.1±1.7 | 3.5±0.8 | 27.0±3.5 | 4.5±1.0 | 0.165± 0.027 |
| **$dFdC_6$-$TSL_{4.52/3/0.5}$** | 167.4±7.2 | 0.097± 0.045 | 25.7±4.4 | 3.5±0.9 | 21.4±3.7 | 4.4±1.1 | 0.203± 0.027 |
| **$dFdC_6$-$TSL_{5.5/1.5/3/0}$** | 162.5±3.5 | 0.067± 0.015 | -26.6±0.4 | 4.4±1.1 | 30.1±1.3 | 5.6±1.4 | 0.186± 0.038 |
| **$dFdC_6$-$TSL_{3/2/5/0}$** | 171 | 0.174 | -61.4 | 3.8 | 26.1 | 4.8 | 0.184 |
| **$dFdC_6$-$TSL_{7/1/2/0}$** | 163 | 0.05 | -24.4 | 3.0 | 30.9 | 3.8 | 0.123 |

*Table 4-2 Characteristics of dFdC-liposomes with varying lipid concentrations of DPPC, DSPC, $DPPG_2$ and P-Lyso-PC. Values given as mean value ± standard deviation.*

For all tested formulations the characteristics like z-average, PDI, ζ-potential, EE, lipid and dFdC content as well as the drug/lipid ratio were in the same range (cf. Table 4-2).

The temperature-dependent release of drugs from TSL is mostly influenced by the phase-transition temperature of the formulation. To evaluate the influence of the different phospholipid compositions and amounts, the improved preparation method on the phase transition and thus the temperature-dependent behavior, DSC measurement of the

formulations dFdC$_3$-TSL$_{5/2/3/0}$, dFdC$_6$-TSL$_{5/2/3/0}$, dFdC$_6$-TSL$_{6/1/3/0}$, dFdC$_6$-TSL$_{7/0/3/0}$ and dFdC$_6$-TSL$_{4.5/2/3/0.5}$ in comparison to liposomes without dFdC (HBS-TSL$_{5/2/3/0}$) were performed.

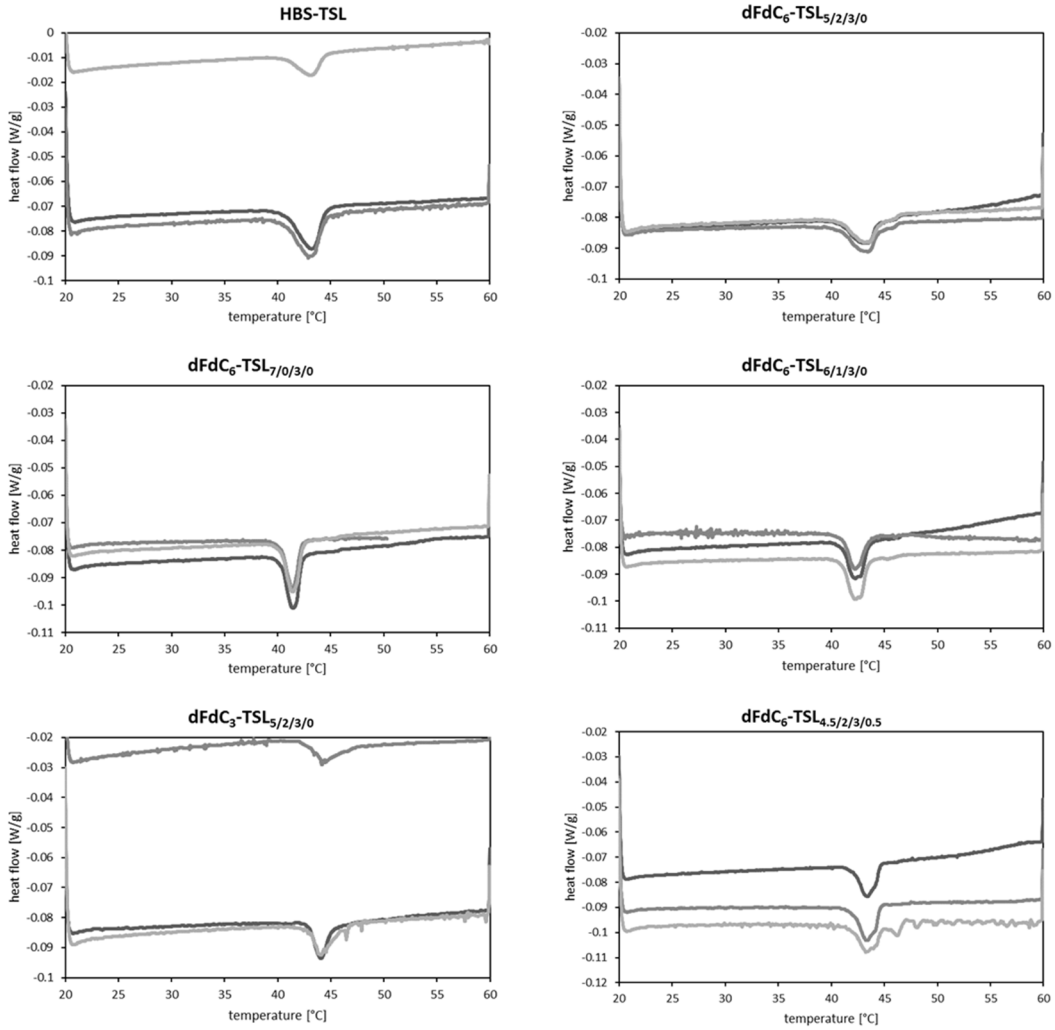


*Figure 4-10 Plots of the heating phase from 20-60°C with a heating rate of 1°C/min of different dFdC-TSL formulations.*

| | $T_m$ [°C] |
|---|---|
| **HBS-TSL$_{5/2/3/0}$** | 43.79±0.12 |
| **dFdC$_3$-TSL$_{5/2/3/0}$** | 43.73±0.42 |
| **dFdC$_6$-TSL$_{5/2/3/0}$** | 44.27±0.26 |
| **dFdC$_6$-TSL$_{6/1/3/0}$** | 42.59±0.60 |
| **dFdC$_6$-TSL$_{4.5/2/3/0}$** | 43.68±0.43 |
| **dFdC$_6$-TSL$_{7/0/3/0}$** | 41.88±0.06 |

*Table 4-3 Overview of $T_m$ values of different dFdC-TSL formulations determined with DSC. Values are given as mean value ± standard deviation of three independent measurements.*

The results of the DSC measurements are shown in Figure 4-10 and Table 4-3. With decreasing DSPC amount $T_m$ decreased (dFdC$_3$-TSL$_{5/2/3/0}$ 43.73±0.42°C compared to dFdC$_3$-TSL$_{7/0/3/0}$ 41.88±0.06°C). The encapsulation of dFdC pH 6-6.5 increased the $T_m$ (dFdC$_6$-

$TSL_{5/2/3/0}$ 44.27±0.26°C compared to $dFdC_3$-$TSL_{5/2/3/0}$ 43.73±0.42°C). Presence of DSPC in the formulation resulted in a peak broadening. A deviation between individual measurements was observed for some formulations (cf. Figure 4-10).

The temperature-dependent dFdC-release in FBS is shown in Figure 4-11 and in HBS pH 7.4 in Figure 4-12, respectively.

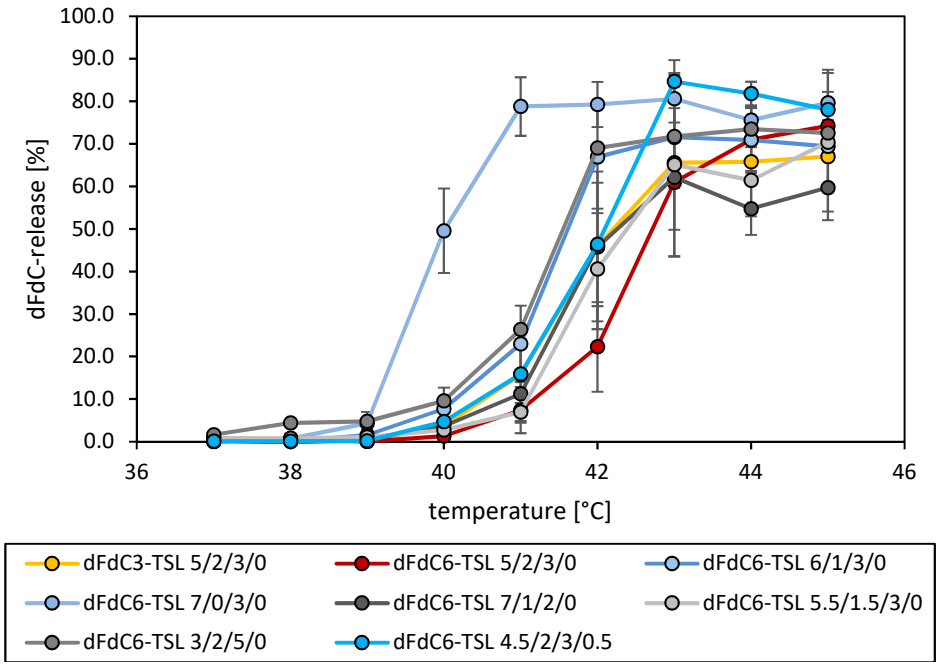


*Figure 4-11 In vitro temperature-dependent release profile of dFdC-formulations with different phospholipid ratios.*
*All TSL formulations, except for $dFdC_3$-$TSL_{5/2/3/0}$ (orange), were prepared with the improved preparation method and dFdC-solution with pH 6-6.5. The temperature dependent release was measured after incubation in FBS for 5 min at different temperatures. Values are given as mean value ± standard deviation.*

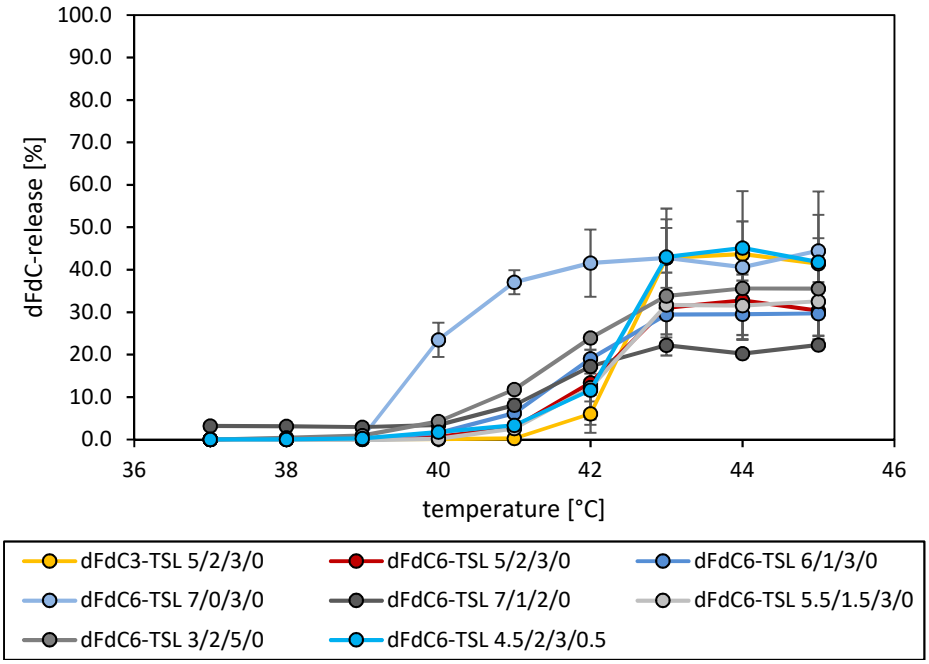


*Figure 4-12 In vitro temperature-dependent release profile of dFdC-formulations with different phospholipid ratios.*
*All TSL formulations, except for dFdC$_3$-TSL$_{5/2/3/0}$ (orange), were prepared with the improved preparation method and dFdC-solution with pH 6-6.5. The temperature dependent release was measured after incubation in HBS pH 7.4 for 5 min at different temperatures. Values are given as mean value ± standard deviation.*

For all tested formulations, the release in FBS at 41°C was higher compared to the formulation dFdC$_6$-TSL$_{5/2/3/0}$. The release profiles for formulations dFdC$_6$-TSL$_{6/1/3/0}$, dFdC$_6$-TSL$_{7/0/3/0}$, dFdC$_6$-TSL$_{4.5/2/3/0.5}$ were the most promising formulations (cf. Figure 4-11 and Figure 4-12 blue tones). They showed a similar or even higher release at 41°C than the formulation dFdC$_3$-TSL$_{5/2/3/0}$ and a high stability at lower temperatures. In more detail, the release at 41°C in FBS for formulation dFdC$_6$-TSL$_{6/1/3/0}$ was 22.95±8.99%, for formulation dFdC$_6$-TSL$_{4.5/2/3/0.5}$ 15.88±8.26% and for dFdC$_6$-TSL$_{7/0/3/0}$ 37.08±2.83% (formulation dFdC$_6$-TSL$_{5/2/3/0}$ 7.4±5.4%). The formulations dFdC$_6$-TSL$_{3/2/5/0}$, dFdC$_6$-TSL$_{5.5/1.5/3/0}$ and dFdC$_6$-TSL$_{7/1/2/0}$ (cf. Figure 4-11 and Figure 4-12 grey tones) were instable at temperatures around body temperature (dFdC$_6$-TSL$_{3/2/5/0}$ release at 38°C 4.35% in FBS) and showed less release at 41°C than the formulation dFdC$_3$-TSL$_{5/2/3/0}$ (dFdC$_6$-TSL$_{5.5/1.5/3/0}$ 6.97±2.14% in FBS) or less release at 43-45°C (dFdC$_6$-TSL$_{7/1/2/0}$ 54.70% in FBS at 44°C compared to 70.94±7.71% in FBS for formulation dFdC$_6$-TSL$_{6/1/3/0}$). The subsequent experiments were performed with the formulations dFdC$_6$-TSL$_{6/1/3/0}$, dFdC$_6$-TSL$_{7/0/3/0}$, dFdC$_6$-TSL$_{4.5/2/3/0.5}$ (cf. Figure 4-11 and Figure 4-12 blue tones).

The *in vitro* stability at 37°C, 38°C, 41°C and 42°C for 1 h was investigated next (cf. Figure 4-13), because 1 h is the time span of a HT treatment in humans [51]. Formulations dFdC$_6$-TSL$_{3/2/5/0}$, dFdC$_3$-TSL$_{5.5/1.5/3/0}$ and dFdC$_6$-TSL$_{7/1/2/0}$ have been excluded, because of

inappropriate stability at <40° ($dFdC_6$-$TSL_{3/2/5/0}$) or low dFdC release at 41-43°C ($dFdC_6$-$TSL_{5.5/1.5/3/0}$ and $dFdC_6$-$TSL_{7/1/2/}$) compared to the other formulations.

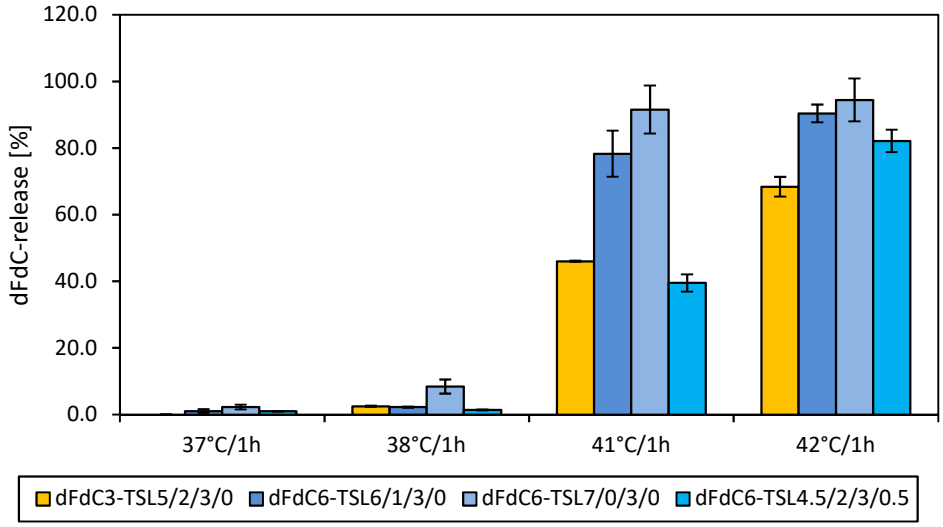


*Figure 4-13 In vitro temperature-dependent release profile of dFdC-formulations with different phospholipid amounts after 1 h incubation in FBS.*
*All TSL formulation, except for the orange one, were prepared with the improved preparation method and dFdC-solution with pH 6-6.5. Values are given as mean value ± standard deviation (n=3).*

The formulations $dFdC_3$-$TSL_{5/2/3/0}$, $dFdC_6$-$TSL_{6/1/3/0}$, $dFdC_6$-$TSL_{7/0/3/0}$ and $dFdC_6$-$TSL_{4.5/2/3/0.5}$ were stable formulations at 37°C and 38°C. Only the formulation $dFdC_6$-$TSL_{7/0/3/0}$ showed a minor release at 38°C (8.4±2.1%), but this was still in an acceptable range. The stability at 37-38°C is important to avoid drug release at body temperature *in vivo*. At 41°C, $dFdC_6$-$TSL_{6/1/3/0}$ and $dFdC_6$-$TSL_{7/0/3/0}$ showed a marked release (78.3±6.9% and 91.5±7.2%, respectively). The formulations $dFdC_3$-$TSL_{5/2/3/0}$ and $dFdC_6$-$TSL_{4.5/2/3/0.5}$ showed less release, but still in a range acceptable for a 1 h HT treatment (46.0±0.2% or 39.5±2.6%).

### *4.1.2.5 Storage stability of dFdC-TSL*

$dFdC_3$-$TSL_{5/2/3/0}$ were generally stored under frozen conditions (-20°C) to avoid further decomposition during long-term storage [44]. Therefore, a freezing and thawing study was performed with $dFdC_6$-$TSL_{6/1/3/0}$ to investigate if the formulation could be stored under frozen conditions and thawed without changes in the biophysical parameters.

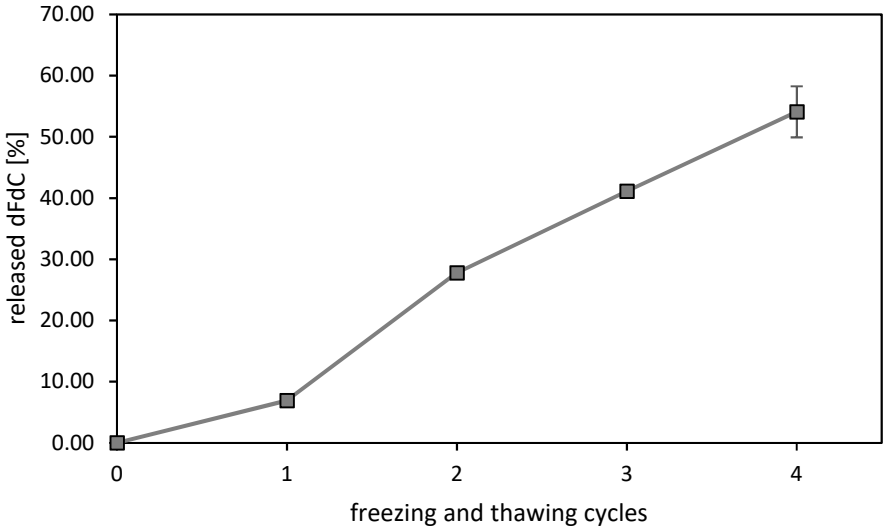


*Figure 4-14 Free dFdC after 0-4 freezing and thawing cycles of dFdC$_6$-TSL$_{6/1/3/0}$.*
*Values are given as mean value ± standard deviation of three independent measurement.*

Figure 4-14 shows that with each freezing and thawing cycle of dFdC$_6$-TSL$_{6/1/3/0}$ the amount of unwanted released dFdC was rising. Directly after preparation 0% of the encapsulated dFdC were released, but already after 4 cycles 54.09±4.17% of free dFdC could be measured. Due to this freezing and thawing effect, the storage of dFdC-TSL at -20°C should be avoided. To find an alternative approach a stability study for dFdC$_3$-TSL$_{5/2/3/0}$, dFdC$_6$-TSL$_{5/2/3/0}$, dFdC$_6$-TSL$_{6/1/3/0}$, dFdC$_6$-TSL$_{7/0/3/0}$ and dFdC$_6$-TSL$_{4.5/2/3/0.5}$ at 2-8°C as liquid dispersion was started. Directly after preparation the liposomes were stored at 2-8°C and after different time points z-average, PDI, lysolipids, FFA and dFdC leakage was evaluated.

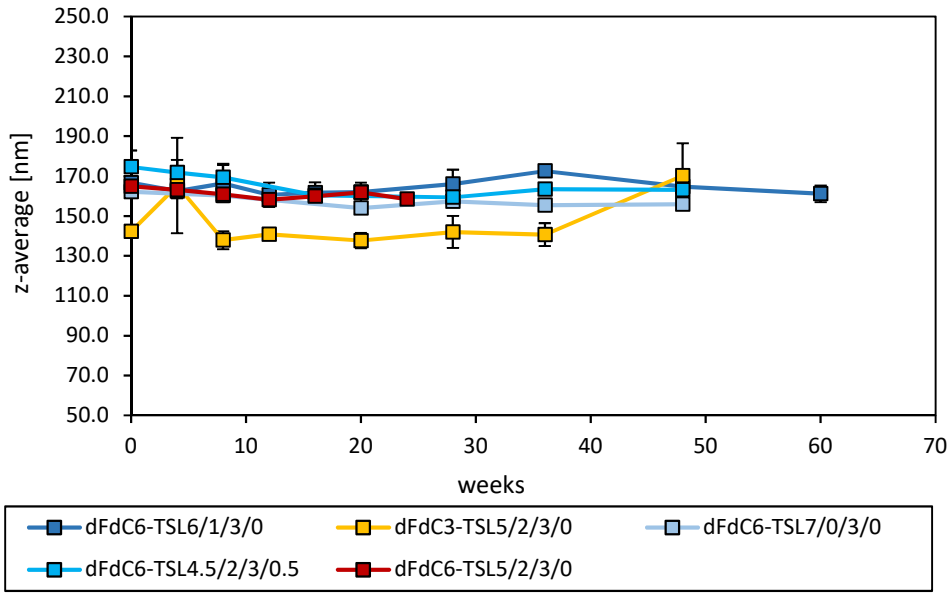

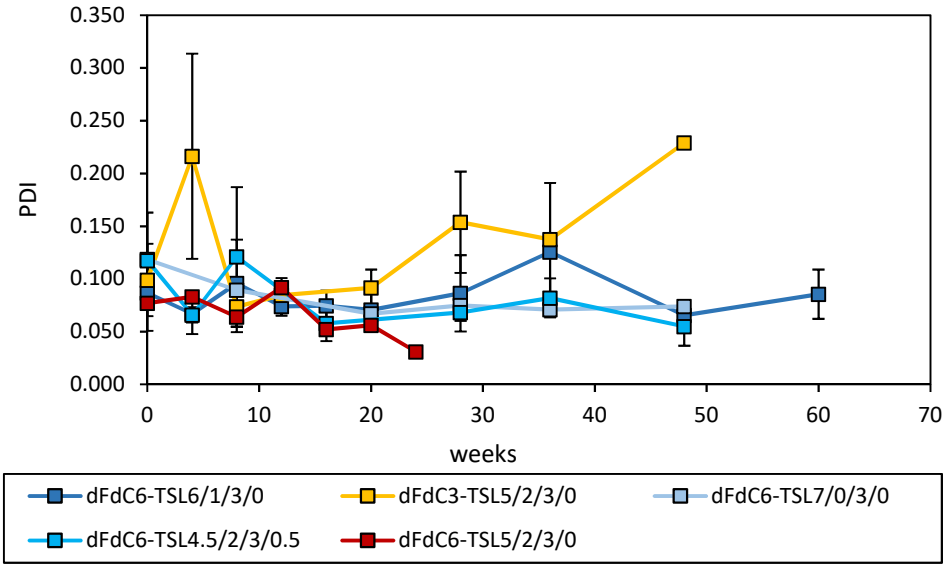
PDI
0.350
0.300
0.250
0.200
0.150
0.100
0.050
0.000
0
10
20
30
40
50
60
70
weeks
dFdC6-TSL6/1/3/0
dFdC3-TSL5/2/3/0
dFdC6-TSL7/0/3/0
dFdC6-TSL4.5/2/3/0.5
dFdC6-TSL5/2/3/0

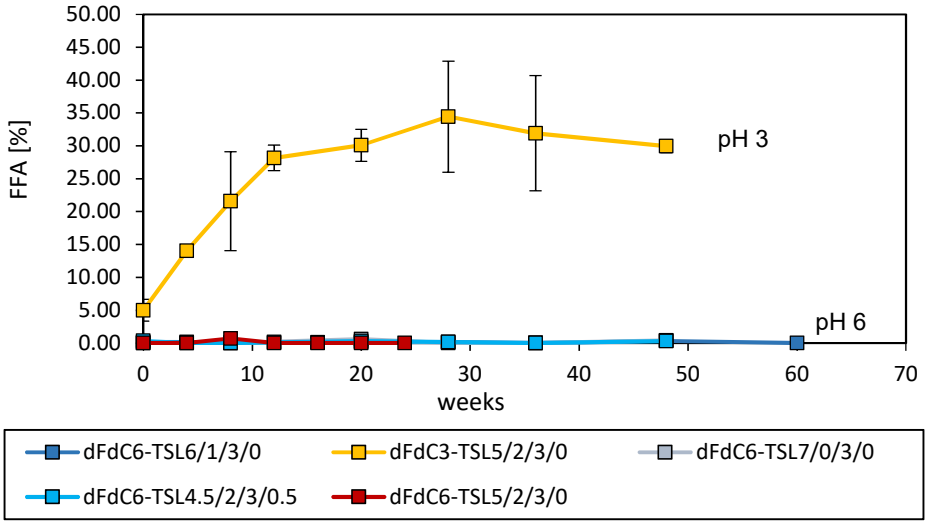
FFA [%]
50.00
45.00
40.00
35.00
30.00
25.00
20.00
15.00
10.00
5.00
0.00
pH 3
pH 6
0
10
20
30
40
50
60
70
weeks
dFdC6-TSL6/1/3/0
dFdC3-TSL5/2/3/0
dFdC6-TSL7/0/3/0
dFdC6-TSL4.5/2/3/0.5
dFdC6-TSL5/2/3/0

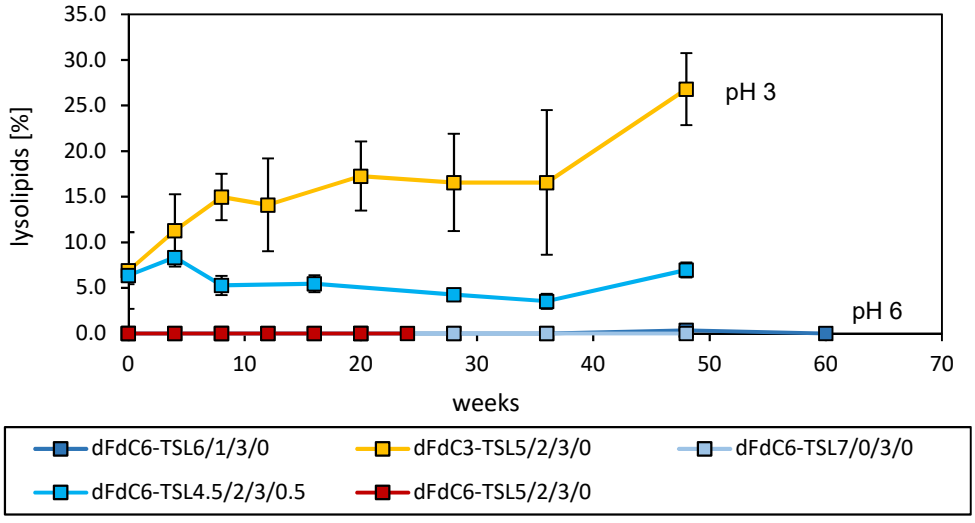
lysolipids [%]
35.0
30.0
25.0
20.0
15.0
10.0
5.0
0.0
pH 3
pH 6
0
10
20
30
40
50
60
70
weeks
dFdC6-TSL6/1/3/0
dFdC3-TSL5/2/3/0
dFdC6-TSL7/0/3/0
dFdC6-TSL4.5/2/3/0.5
dFdC6-TSL5/2/3/0

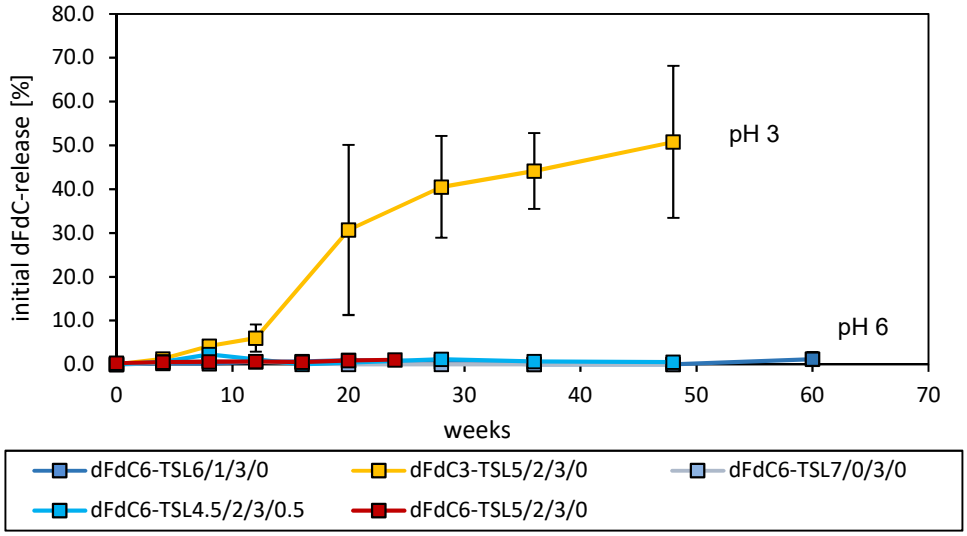


*Figure 4-15 dFdC-TSL with different formulations and pH 3 or 6 of dFdC were prepared and stored at 2-8°C for up to 60 weeks.*
*At different time points of storage z-average, PDI, FFA, lysolipid, and dFdC leakage in FBS were analyzed. Values are given as mean value ± standard deviation of at least three independent prepared batches except for dFdC$_6$-TSL$_{7/0/3/0}$ (n=2) and dFdC$_6$-TSL$_{5/2/3/0}$ (n=1).*

All formulations prepared with dFdC pH 6 (dFdC$_6$-TSL$_{5/2/3/0}$, dFdC$_6$-TSL$_{6/1/3/0}$, dFdC$_6$-TSL$_{7/0/3/0}$ and dFdC$_6$-TSL$_{4.5/2/3/0.5}$) were stable up to 48 weeks storage at 2-8°C. The liposomes showed neither change in size, PDI, FFA-, lysolipid-content nor dFdC leakage (Figure 4-15). For the formulation Gem$_6$-TSL$_{6/1/3/0}$ the storage stability could be proven even after 60 weeks. The lysolipids in the formulation Gem$_6$-TSL$_{4.5/2/3/0.5}$ were no degradation products caused by storage, but intendent present in the formulation from preparation of the lipid film.
The formulation dFdC$_3$-TSL$_{5/2/3/0}$ prepared with pH 3 (yellow line in Figure 4-15) already showed degradation products (free fatty acids and lysolipids) directly after the preparation, which increased after 4 weeks. The initial release increased also during storage and after 8 weeks of storage is already 4.2±0.2%.

### 4.1.3 dFdC-TSL preparation with DAC

Liposomal preparation with DAC was tested to evaluate if this preparation method is feasible for dFdC-TSL and if higher encapsulation efficacy could be achieved.
Two different ways were tested, on the one hand preparation of TSL with an already prepared lipid film and on the other hand with lipid powder in the wanted amounts. Additionally, two different pH ranges, pH 3 and pH 6 were tested. The phospholipid composition for all DAC experiments was DPPC/DSPC/DPPG$_2$ 50:20:30 (molar ratio).

| | form of used lipids | z-average [nm] | PDI | lipid content | lysolipid [%] | dFdC [mM] | EE [%] |
|---|---|---|---|---|---|---|---|
| **$dFdC_3$-$TSL_{5/2/3/0}$-DAC** | lipid film | 108.0 ±6.5 | 0.200± 0.015 | 42.9± 11.8 | 2.35±0.21 | 2.81± 0.36 | 10.0±1.32 |
| **$dFdC_6$-$TSL_{5/2/3/0}$-DAC** | lipid film | 105.6 ±3.5 | 0.200± 0.037 | 58.3 | 0 | 3.01± 0.22 | 14.4±1.19 |
| **$dFdC_6$-$TSL_{5/2/3/0}$-DAC-powder** | lipid powder | 134.3 | 0.326 | / | / | / | / |

*Table 4-4 Characteristics of dFdC-TSL prepared with DAC. Values given as mean value ± standard deviation.*

Both formulations prepared with a lipid film showed characteristics in the same range as achieved for dFdC-TSL prepared with lipid film hydration and extrusion method and passive encapsulation of dFdC. Only the PDI was higher, but still in an acceptable range. One major advantage of the DAC-TSL was the encapsulation efficacy. It was 3.4-fold higher for $dFdC_3$ and 4.1-fold higher for $dFdC_6$ compared to $dFdC_3$-$TSL_{5/2/3/0}$ (cf. Table 4-1 and Table 4-4). The TSL prepared with a lipid powder mixture in the same ratio as in the lipid film were not further analyzed after measurement of z-average and PDI, because these two values were not in an acceptable range.

To see if the DAC-prepared TSL show the same temperature dependence as TSL prepared by the standard method, a temperature-dependent release in FBS was performed (cf. Figure 4-16).

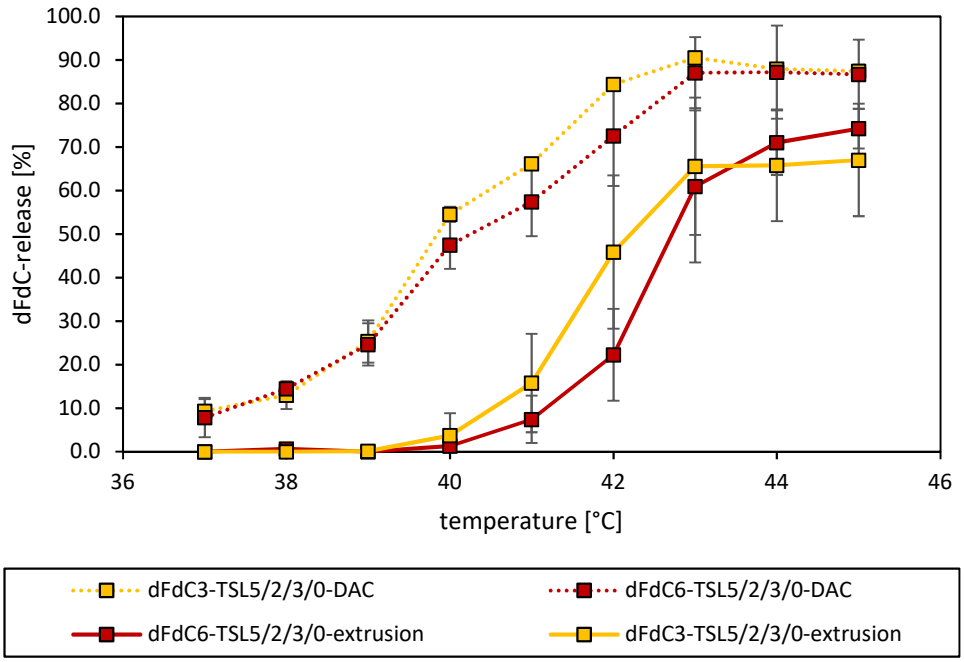


*Figure 4-16 Temperature-dependent dFdC release after 5 min in FBS of TSL prepared with DAC (dashed lines; n=2) in comparison with TSL prepared with lipid film hydration and extrusion method (solid line; n≥4).*
*For both methods, TSL were prepared with dFdC pH 3 (orange) or pH 6 (red). Values given as mean value ± standard deviation.*

All dFdC-TSL prepared with DAC showed a notably different temperature-dependent release profile in comparison to TSL prepared with lipid film hydration and extrusion method. The DAC-prepared TSL showed increased released already at 37°C (8.6±3.2% compared to 0%). The DAC-prepared TSL were unstable at all analyzed temperatures (37-45°C). In contrast, TSL prepared by the lipid film hydration and extrusion method showed a temperature release profile with a sharp transition ~1-2°C between temperatures where hardly any drug release occurs (≤ 41°C) and temperatures with notable drug release (≥ 42°C).

## 4.1.4 *In vivo* experiments

The *in vivo* experiments were conducted with the three improved formulations ($dFdC_6$-$TSL_{6/1/3/0}$, $dFdC_6$-$TSL_{7/0/3/0}$ and $dFdC_6$-$TSL_{4.5/2/3/0.5}$) and $dFdC_3$-$TSL_{5/2/3/0}$ as control.

### *4.1.4.1 Pharmacokinetic study*

The blood circulation stability was investigated in a pharmacokinetic study in healthy male Brown Norway rats for all four formulations. Theoretical $c_{max}$ was calculated, assuming 4% of the bodyweight of a rat is plasma volume [131]. For an injected dose of 6 mg/kg dFdC, the $c_{max}$ is 150 µg/ml.

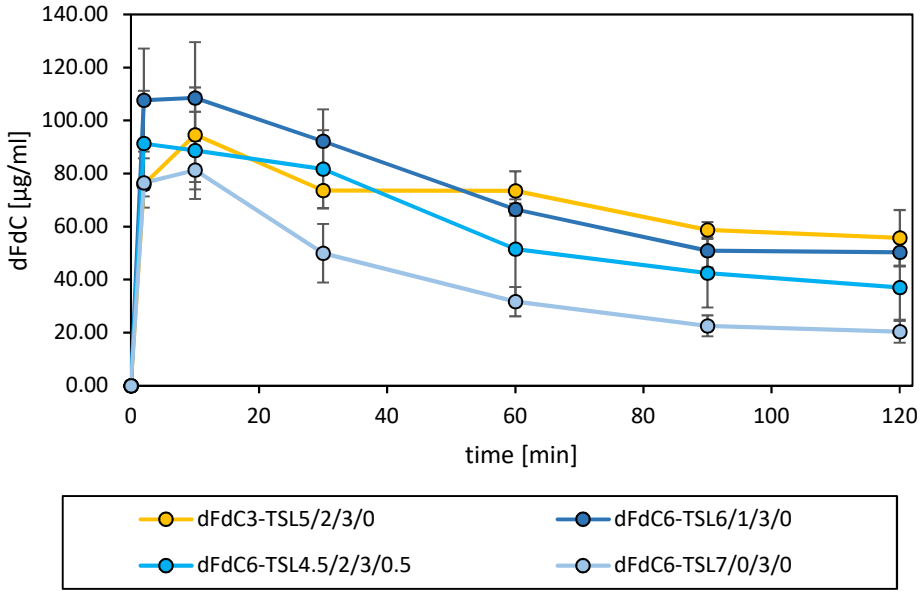


*Figure 4-17 Pharmacokinetic study of dFdC$_3$-TSL$_{5/2/3/0}$ (n=2), dFdC$_6$-TSL$_{6/1/3/0}$ (n=6), dFdC$_6$-TSL$_{7/0/3/0}$ (n=6) and dFdC$_6$-TSL$_{4.5/2/3/0.5}$ (n=3).*
*Liposomes were injected i.v. at a dose of 6 mg/kg in healthy BN rats. Blood samples were taken at certain time points and dFdC-concentration was measured with HPLC. Animal handling was performed by Dr. Simone Limmer.*

| | number of animals | $C_0$ (µg/ml) | $C_0$ % of calculated $c_{max}$ | $t_{1/2}$ (h) | $R^2$ | $AUC_{0\text{-}120\ min}$ (µg*min/ml) |
|---|---|---|---|---|---|---|
| **dFdC$_3$-TSL$_{5/2/3/0}$** | 2 | 88.40 | 58.9 | 2.63 | 0.8194 | 7379 |
| **dFdC$_6$-TSL$_{6/1/3/0}$** | 6 | 100.23 | 66.8 | 1.74 | 0.8368 | 7666 |
| **dFdC$_6$-TSL$_{7/0/3/0}$** | 6 | 118.17 | 78.8 | 0.83 | 0.8942 | 5803 |
| **dFdC$_6$-TSL$_{4.5/2/3/0.5}$** | 3 | 99.02 | 66.0 | 1.31 | 0.9559 | 6384 |

*Table 4-5 dFdC-plasma concentration after i.v. application of 6 mg/kg different dFdC-TSL.*
*$c_0$= calculated plasma concentration of dFdC at t=0 min; $t_{1/2}$=plasma half-life; $R^2$= coefficient of determination; $AUC_{0\text{-}120\ min}$=area under the curve 0-120 min. Values given as mean value ± standard deviation.*

The AUC was the highest for dFdC$_6$-TSL$_{6/1/3/0}$ (7666 µg*min/ml) followed by the dFdC$_3$-TSL$_{5/2/3/0}$ (7379 µg*min/ml). The $c_0$ for the formulation dFdC$_6$-TSL$_{6/1/3/0}$ was 66.8%, for dFdC$_6$-TSL$_{7/0/3/0}$ 78.8% and dFdC$_6$-TSL$_{4.5/2/3/0.5}$ 66.0% of calculated theoretical $c_{max}$. For the control formulation dFdC$_3$-TSL$_{5/2/3/0}$ only 58.9% was achieved. dFdC$_3$-TSL$_{5/2/3/0}$ showed the longest circulation half-life in blood with 2.63 h (cf. Figure 4-17 and Table 4-5). Formulation dFdC$_6$-TSL$_{7/0/3/0}$ was cleared form the blood stream with a plasma half-life of 0.83 h. The plasma

half-life of dFdC$_6$-TSL$_{6/1/3/0}$ and dFdC$_6$-TSL$_{4.5/2/3/0.5}$ was in-between the already mentioned formulations with 1.74 h and 1.31 h, respectively.

### *4.1.4.2 Therapeutic study*

The therapeutic efficacy was determined for dFdC$_6$-TSL$_{6/1/3/0}$ and dFdC$_6$-TSL$_{7/0/3/0}$ in comparison to dFdC$_3$-TSL$_{5/2/3/0}$ in the BN175 soft tissue sarcoma model [44]. The change in tumor size was monitored up to 16 days. The injected dose for each formulation was 6 mg/kg and the HT-treatment was performed by heating with a lamp for 1 h.

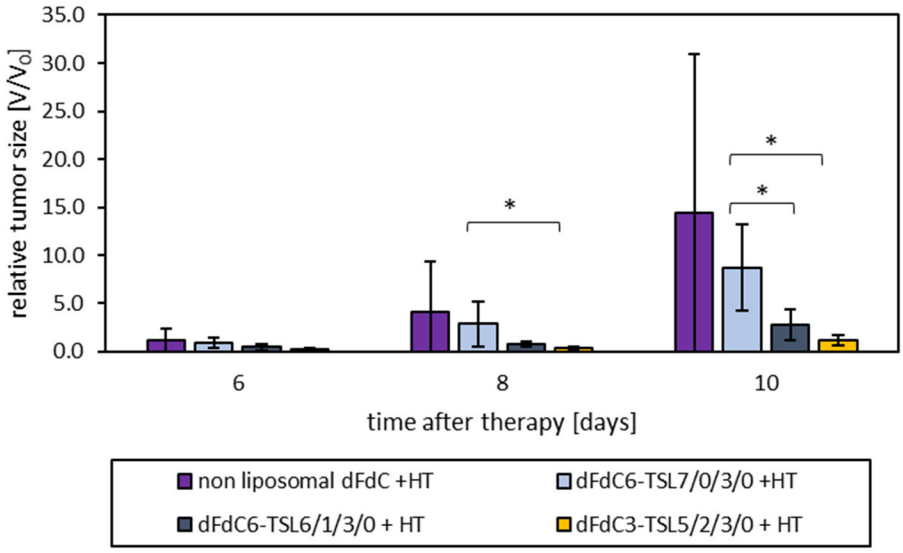


*Figure 4-18 Therapeutic efficacy 6, 8 and 10 days after therapy (HT treatment at 41°C for 60 min after injection of 6 mg/kg dFdC) of improved dFdC$_6$-TSL$_{6/1/3/0}$ (n=6) and dFdC$_6$-TSL$_{7/0/3/0}$ (n=6) in comparison with non-liposomal dFdC (n=12) and published formulation dFdC$_3$-TSL$_{5/2/3/0}$ (n=6) in the BN175 soft tissue sarcoma model [44].*
*Animal handling was performed by Dr. Simone Limmer. Values given as mean value ± standard deviation.*

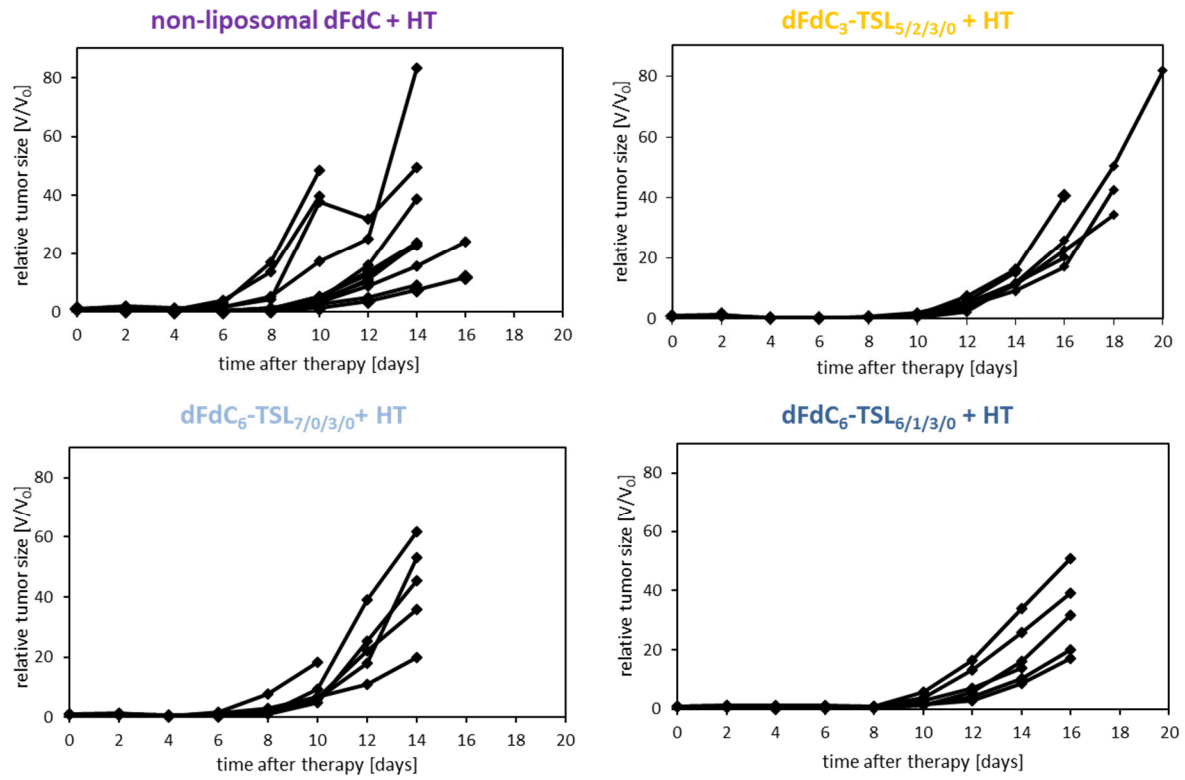


*Figure 4-19 Therapeutic efficacy of single animals of improved dFdC$_6$-TSL$_{6/1/3/0}$ and dFdC$_6$-TSL$_{7/0/3/0}$ (n=6) in comparison with non-liposomal dFdC (n=12) and published formulation dFdC$_3$-TSL$_{5/2/3/0}$ (n=6) with HT-treatment for 60 min at 41°C after injection of 6 mg/kg dFdC in the BN175 soft tissue sarcoma model [44].*
*Tumor growth was monitored for up to 10 days. Animal handling was performed by Dr. Simone Limmer.*

Tumor growth delay of dFdC$_3$-TSL$_{5/2/3/0}$ and dFdC$_6$-TSL$_{6/1/3/0}$ was comparable. Both formulations showed a significant tumor growth delay compared to formulation dFdC$_6$-TSL$_{7/0/3/0}$ after 10 days ($p<0.01$ resp. $p<0.05$) (cf. Figure 4-18). No significant improvement after 10 days was achieved compared to non-liposomal dFdC ($p=0.081$ resp. $p=0.121$), because of the deviation in therapeutic efficacy for non-liposomal dFdC. For the group treated with non-liposomal dFdC the deviation in tumor growth delay between single animals is high compared to the other groups (cf. Figure 4-19). After ten days, two animals of this group had to be sacrificed because of too large tumor sizes in contrast to two other animals which had tumor sizes quite small even after 16 days.

The formulation dFdC$_6$-TSL$_{6/1/3/0}$ showed no advantage over the formulation dFdC$_3$-TSL$_{5/2/3/0}$ in therapeutic efficacy, but a comparable efficacy with improved stability properties.

## 4.2 Thermosensitive liposomal irinotecan

### 4.2.1 Analytical methods

#### *4.2.1.1 Quantification of CPT-11 and SN-38 in complex matrices by HPLC*

To establish an assay for CPT-11 and SN-38 quantification in complex media like plasma or tissue a HPLC method based on fluorescence detection was developed. The excitation wavelength (Ex) was set to 355 nm and the emission wavelength (Em) was set to 515 nm based on a publication of Rivory et al, who tested different Ex and Em for the analytes CPT-11, SN-38 and CPT. CPT was used as internal standard [132]. For the first runs the mobile phase $NaH_2PO_4$ (25 mM pH 3.1)/ACN (50:50) described in literature was used [133].

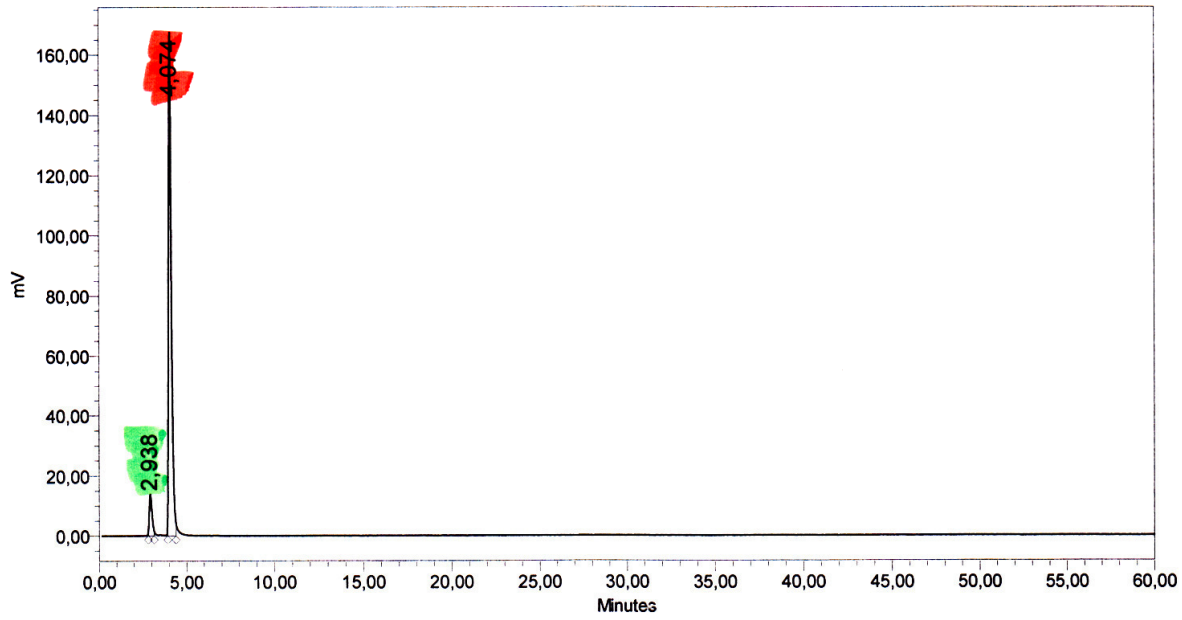


| | RT | Area | % Area | Height |
|---|---|---|---|---|
| 1 | 2,938 | 151336 | 7,34 | 13861 |
| 2 | 4,074 | 1909528 | 92,66 | 167602 |

*Figure 4-20 HPLC-profile of a solution containing CPT-11 and SN-38 with eluent 25 mM $NaH_2PO_4$ pH 3.1/ACN 50:50 (v/v) and fluorescence detection at Ex 355 nm and Em 515 nm (isocratic flow 1 ml/min).*
*A C18 column (5 µm, 125 Å, 250 mm x 4 mm) was used. Retention time 2.938 min CPT-11 and 4.074 min SN-38.*

The peak separation with the mobile phase 25 mM $NaH_2PO_4$ pH 3.1/ACN 50:50 (v/v) was not satisfactory and the retention times of CPT-11 (2.938 min) and SN-38 (4.074 min) were too close to the injection (cf. Figure 4-20). By lowering the amount of the organic solvent, a better separation was achieved and CPT was included as internal standard (cf. Figure 4-21).

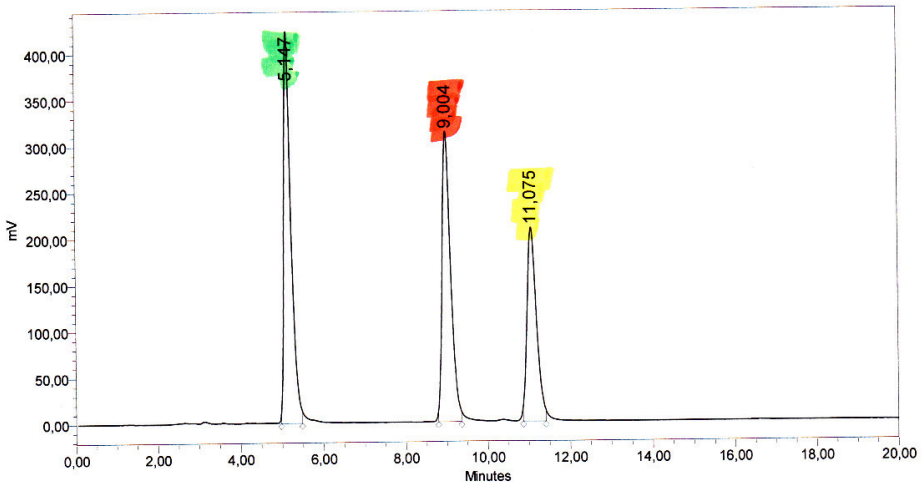


| | RT | Area | % Area | Height |
|---|---|---|---|---|
| 1 | 5,147 | 5082590 | 39,30 | 423466 |
| 2 | 9,004 | 4532525 | 35,05 | 314072 |
| 3 | 11,075 | 3316992 | 25,65 | 209379 |

*Figure 4-21 HPLC-profile of a solution containing CPT, CPT-11 and SN-38 with eluent 25 mM $NaH_2PO_4$ pH 3.1/ACN 70:30 (v/v) and fluorescence detection at Ex 355 nm and Em 515 nm (isocratic flow 1 ml/min).*
*A C18 column (5 µm, 125 Å, 250 mm x 4 mm) was used. Retention time 5.147 min CPT-11, 9.004 min SN-38 and 11.075 min CPT.*

The retention time of CPT-11 was shifted to 5.147 min and SN-38 to 9.004 min, respectively. The injection of the internal standard CPT resulted in a third separate peak at a retention time of 11.075 min.

Next, the HPLC method was validated concerning the recovery of the analytes in FBS, linearity, limit of quantification as well as the recovery of CPT-11 and SN-38 in liver spiked with both components. The recovery of CPT-11, SN-38 and CPT in samples spiked with FBS was 97.9±1.9%, 75.6±19.1% and 96.9±2.8% respectively. For liver samples spiked with CPT-11 and SN-38 the recovery was 101.2±0.8% (CPT-11) and 103.0±1.7% (SN-38).

For determination of the limit of quantification CPT-11 and SN-38 solutions with concentrations between 5 and 50 ng/ml were injected. The limit of quantification was determined to be 35 ng/ml (SN-38 89.3 nM and CPT-11 59.7 nM) for both analytes.

The linearity of the method in serum was analyzed for CPT-11 and SN-38, by diluting a stock solution of the analyte in FBS.

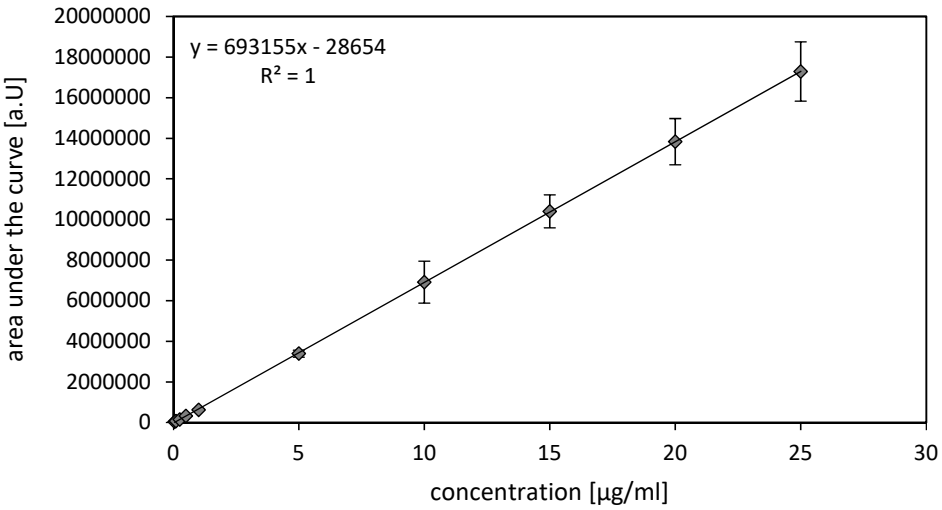


*Figure 4-22 Linearity of the CPT-11 signal in serum measured with HPLC in the concentration range from 0.05 to 25 µg/ml.*
*Values given as mean value ± standard deviation of three independent measurements.*

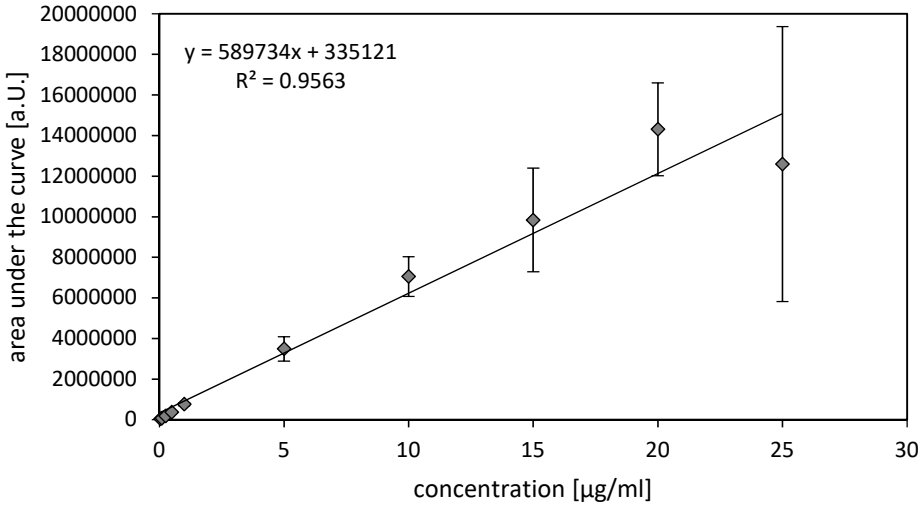


*Figure 4-23 Linearity of the SN-38 signal in serum measured with HPLC in the concentration range from 0.05 to 25 µg/ml.*
*Values given as mean value ± standard deviation of three independent measurements.*

The linearity for CPT-11 and SN-38 of the HPLC method was shown in the range from 0.05-25 µg/ml for CPT-11 (cf. Figure 4-22 CPT-11) and 0.05-20 µg/ml for SN-38 (Figure 4-23 SN-38). Nearly the whole detection range of the HPLC method for CPT-11 and SN-38 was covered, meaning, that quite small amounts of the analytes in PK samples as well as higher concentrated samples can be measured.

#### *4.2.1.2 Quantification of CPT-11 in aqueous samples by fluorescence spectroscopy*

A fluorescence spectroscopy method was additionally developed for a faster and more cost-efficient quantification of CPT-11 from aqueous samples like TSL batches. For four liposomal batches with different drug/lipid ratios a comparison of results obtained with both methods was performed (cf. Figure 4-24)

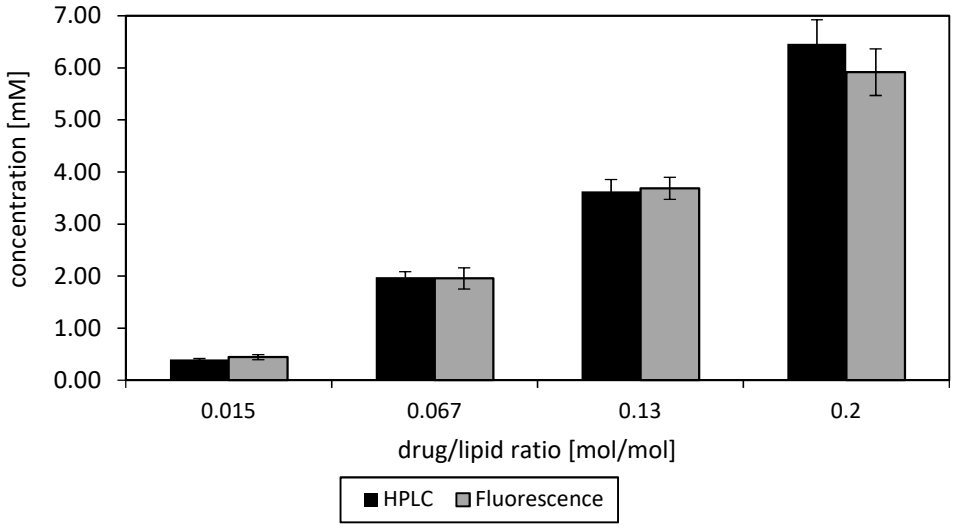


*Figure 4-24 Comparison of the determination of encapsulated CPT-11 in TSL with different drug/lipid ratios with HPLC and fluorescence spectroscopy.*
*Values given as mean value ± standard deviation of three independent measurements.*

Fluorescence spectroscopy showed similar results to the HPLC method (cf. Figure 4-24). The mean deviation for both methods was < 1%. Therefore, the fluorescence method was applied for measurement of the temperature-dependent release as well as for determination of encapsulated CPT-11 concentration in liposomal formulations.

### 4.2.2 Formulation development SN-38

#### *4.2.2.1 Encapsulation of the active metabolite SN-38*

To investigate if it is possible to encapsulate the more active metabolite of CPT-11, SN-38, in $DPPG_2$-TSL, different preparation methods were tested and the EE was analyzed (cf. Table 4-6). The active loading method with intraliposomal pH 4 and extraliposomal pH 8 was used based on the active loading method described for weak bases (SN-38 showed like CPT-11 a pH-dependent ring opening) like doxorubicin with minor changes [31]. The active loading with intraliposomal pH 9 and extraliposomal pH 6 was chosen to obtain reverse pH conditions, to facilitate drug loading for weak acids. Harsher pH conditions (pH < 4 or > 9) were not used to avoid phospholipid hydrolysis. The passive encapsulation method based on a published method for dFdC [44] allowed safe handling of cytotoxic drugs without contaminating the

equipment like the high-pressure extruder. Increasing concentrations of NaOH were used to solubilize higher SN-38 concentrations (higher pH more SN-38 solubilized. The loading of Dox via an $Mn^{2+}$-gradient was published by Chiu et al [134] and modified for test-loading of SN-38. The film-loading method was described for SN-38 loading in non-thermosensitive liposomes by Sadzuka et al [116] and also tested for loading of SN-38 in $DPPG_2$-based TSL.

| **encapsulation method** | | **encapsulated SN-38 (mM)** | **EE (%)** | **comments** |
|---|---|---|---|---|
| **active** | intraliposomal pH 4<br>extraliposmal pH 8 | 0.062 | 0.48 | / |
| **active** | intraliposmal pH 9<br>extraliposmal pH 6 | 0.08 | 0.58 | / |
| **passive** | 2.05 mg/ml SN-38 in 0.01 M NaOH | 0.06 | 1.14 | / |
| **passive** | 5.03 mg/ml SN-38 in 0.1 M NaOH | 0.27 | 2.1 | 6% lysolipids directly after preparation |
| **$Mn^{2+}$-gradient** | intraliposomal $MnSO_4$ pH 3.5<br>extraliposomal pH 7.8 | 0.0055 | 0.04 | / |
| **film loading** | HBS pH 7.8 for hydratisation; SN-38 film with ~10 mg | 0.53±0.24 | ~ 9% | aggregates due to preparation process |

*Table 4-6 Different SN-38 encapsulation methods tested and resulting encapsulation efficacy.*

The active loading via a Mn-gradient or a pH gradient was not successful, shown by EE of 0.04-0.58%. For active loading method, an EE of around 90% is usually achieved, but both applied methods resulted in values below 1%, respectively. Therefore, active loading was not suitable for SN-38. With passive loading, an EE of 1.14% for 0.01M NaOH (0.06 mM SN-38) or 2.1% for 0.1M NaOH (0.27 mM SN-38) was achieved. These EE were lower than expected for passive loading (5-10%), but in an acceptable range. Nevertheless, to achieve a higher EE, higher concentrations of NaOH were needed and resulted in notable lysolipid formation during preparation of already 6%. This encapsulation method was therefore not investigated further, because as shown with dFdC-TSL (section 4.1), lysolipid concentrations of more than 5% destabilize $DPPG_2$-TSL formulations. The film loading method with HBS pH 7.8 resulted in formulations with a SN-38 content of 0.53±0.24 mM (EE ~9%), which is still low, but in a range which can be used for further experiments. One drawback of this preparation method was the formation of aggregates during preparation, shown by DLS

measurements. The film loaded SN-38-TSL were further investigated by analyzing the temperature-dependent release.

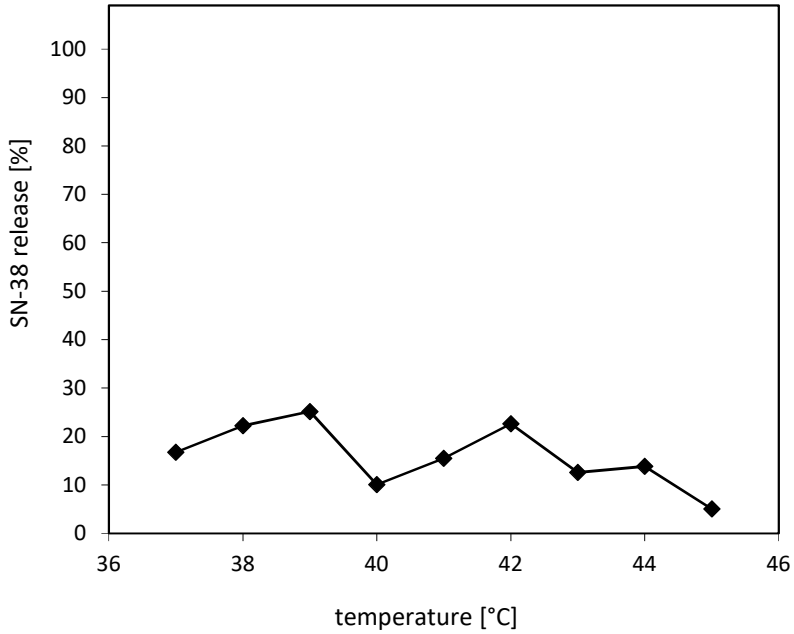


*Figure 4-25 Temperature-dependent SN-38 release of film loaded SN-38-TSL in FBS after 5 min incubation at temperatures between 37-45°C.*
*Values given as mean value of two independent measurements.*

Release of SN-38 from the TSL formulation showed no temperature dependency in the measured range from 37 to 45°C (cf. Figure 4-25). One explanation might be that SN-38 is too lipophilic and was therefore incorporated in the membrane during the film loading and not in the intraliposomal space. To analyze if the SN-38 was released when acceptor vesicles are present in a temperature-dependent manner, SN-38-TSL were incubated together with acceptor-vesicle liposomes consisting of DSPC/Chol 55:45 (molar ratio) at different temperatures. The amount of SN-38 in the acceptor-vesicles was measured after destroying these vesicles.

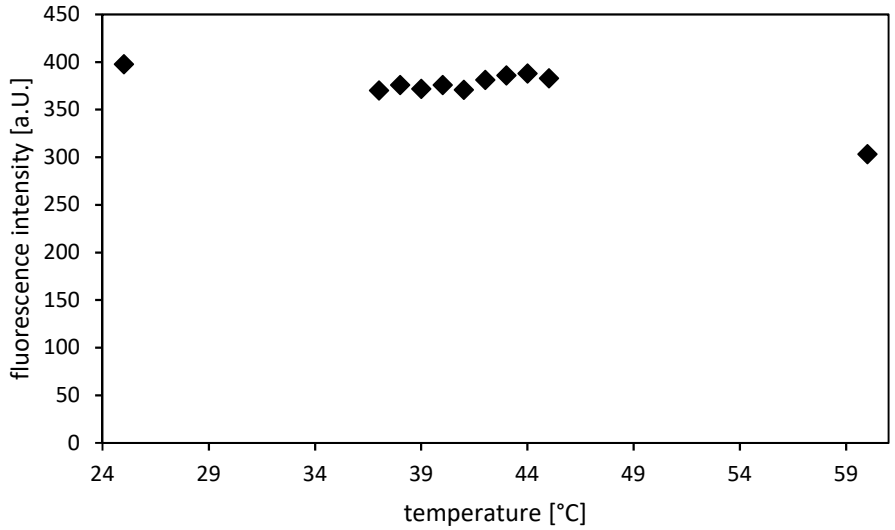


*Figure 4-26 Change of fluorescence of SN-38-TSL in presence of acceptor-vesicle liposomes DSPC/Chol 55:45 (molar ratio) in HBS pH 7.4 after 5 min incubation at different temperatures. Values given as mean value of two independent measurements.*

The fluorescence of SN-38 in the acceptor-vesicle was at all tested temperatures similar, except for 60°C (cf. Figure 4-26). SN-38 was not released in a temperature-dependent manner regardless of the presence of acceptor-vesicles. The difference at 60°C could be explained by a change of the SN-38 molecule from lactone to carboxylate form, which could result in lower fluorescence.

A DSC-measurement was performed to investigate if SN-38 encapsulation with film loading influences the phase transition of the membrane, e.g. if incorporated in the membrane.

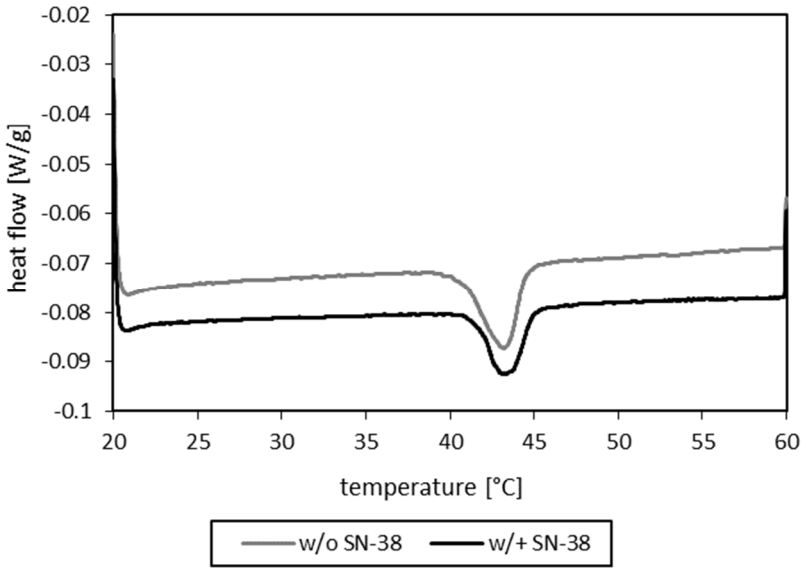


*Figure 4-27 Representative plots of the heating phase from 20-60°C with a heating rate of 1°C/min of TSL with or without SN-38 loaded with film loading. Values are mean values of three different measurements.*

| | $T_m$ [°C] |
|---|---|
| **w/o SN-38** | 43.79±0.12 |
| **w/+ SN-38** | 43.88±0.06 |

*Table 4-7 Overview of $T_m$ values of TSL formulations with or without SN-38 loaded with film loading determined with DSC.*
*Values are given as mean value ± standard deviation (n=3).*

Encapsulation of SN-38 with film loading in preformed TSL induced no change in phase transition compared to non-loaded TSL (cf. Table 4-7 and Figure 4-27). The peak shape was similar and there was neither an additional transition nor a broadening of the main transition peak visible for loaded TSL. For the loaded TSL, $T_m$ was 43.88±0.06°C compared to 43.79±0.12°C for TSL without SN-38.

Cryo-TEM measurements of TSL loaded with or without SN-38 were performed to obtain further insights into the structure of TSL prepared by film loading.

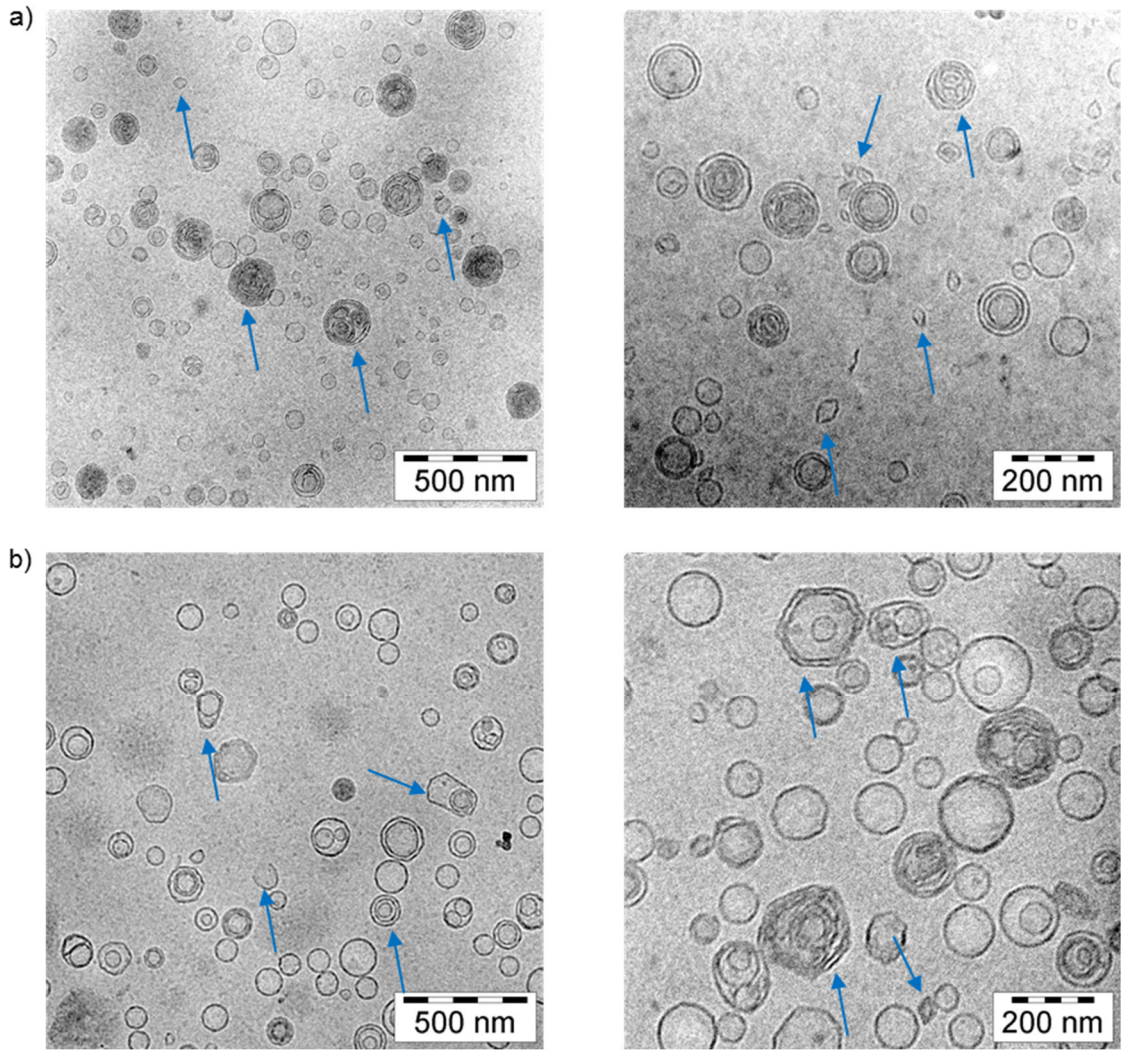


*Figure 4-28 Representative Cryo-TEM images of TSL prepared with film loading method a) without SN-38 and b) with SN-38.*

There was no difference visible in liposomal structure with (Figure 4-28 a) and without (Figure 4-28 b) SN-38. All structures which were not visible in "normal" liposomes (cf. Figure 4-44 a) may occur because of the film loading method. A detrimental step, which could cause fragmentation of liposomes and large, aggregated liposomes (cf. arrows, Figure 4-28), is the sonication step to encapsulate SN-38 in the extruded liposomes. The preparation method was destroying the liposomes to some extent. No specific structure which was only visible in the samples containing SN-38 was detected. This indicated that the encapsulated SN-38 might not form visible structures or crystals in Cryo-TEM images.

The encapsulation of SN-38 in $DPPG_2$-based TSL was tested with various encapsulation methods but only possible with the film loading method. With this method SN-38 was encapsulated in an acceptable concentration (0.53±0.24), but the resulting formulation showed no temperature-dependent release of the drug. Moreover, the preparation process resulted in formation of aggregates. Due to these findings, TSL with encapsulated SN-38 were not further investigated.

### *4.2.2.2 Preparation of NTSL*

To test if active loading of CPT-11, which is described in literature [135], is possible a non-thermosensitive formulation with the lipid composition DSPC/Chol/DSPE-$PEG_{2000}$ 55:40:5 (molar ratio) (CPT-11-NTSL) was chosen. The encapsulation was performed for 45 min at 36-37°C and as intraliposomal excipient $(NH_4)_2SO_4$ pH 5.4 was used. The characteristics of the prepared liposomes are shown in Table 4-8.

| | **z-average (nm)** | **PDI** | **ζ-potential (mV)** | **EE (%)** | **phosphate value (mM)** | **CPT-11 content (mM)** | **drug/ lipid ratio (m/m)** |
|---|---|---|---|---|---|---|---|
| **CPT-11-NTSL** | 163.3±21.9 | 0.091± 0.053 | -1.71±1.44 | 94.0±14.1 | 41.6±5.7 | 9.65±0.15 | 0.235± 0.035 |

*Table 4-8 Characteristics of CPT-11 NTSL (n=3). Values given as mean value ± standard deviation.*

Encapsulation of CPT-11 in NTSL in concentrations suitable for *in vivo* experiments was possible (9.65±0.15 mM). Also, all other parameters of the NTSL like z-average and PDI were like expected for NTSL. The next step was to encapsulate CPT-11 in $DPPG_2$-TSL.

## 4.2.3 Formulation development CPT-11

### *4.2.3.1 Encapsulation process development*

Encapsulation of CPT-11 in $DPPG_2$-based TSL was performed for TSL with the lipid composition DPPC/DSPC/$DPPG_2$ 50:20:30 (molar ratio), if not described otherwise. The intraliposomal buffer applied in the first loading experiment was 300 mM $(NH_4)_2SO_4$ at pH 5.4 and the encapsulation was performed for 45-60 min at 36-37°C, because this encapsulation procedure was successful for NTSL as described in 4.2.2.2.

To investigate if size-exclusion chromatography (SEC) after preparation of the liposomes is necessary to separate unencapsulated CPT-11 from the loaded-liposomes eight batches of liposomes were independently prepared and for half amount of the liposomes of each batch a SEC was performed and for the rest of the liposomes it was omitted. Subsequently the drug/lipid ratio of the differently treated liposomes was determined.

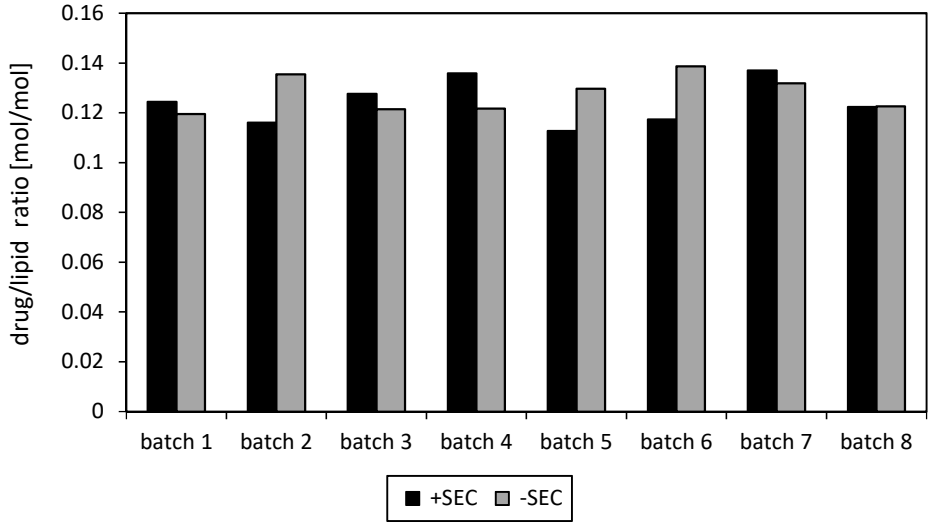


*Figure 4-29 Drug/lipid ratio (mol/mol) of different liposomal batches with and without SEC after centrifugation.*
*Lipid concentration was determined with phosphate assay and the encapsulated CPT-11 was measured with fluorescence spectroscopy.*

Figure 4-29 shows that SEC after centrifugation during preparation was not needed. The drug/lipid ratio was 0.121±0.009 (mol/mol) with SEC and 0.1276±0.0073 (mol/mol) without SEC, respectively.

The optimal incubation time needed for active loading was evaluated by preparing three batches of liposomes and stopping the encapsulation at 36-37°C for each batch after 10, 20, 30 or 45 min and subsequent determination of the reached drug/lipid ratio.

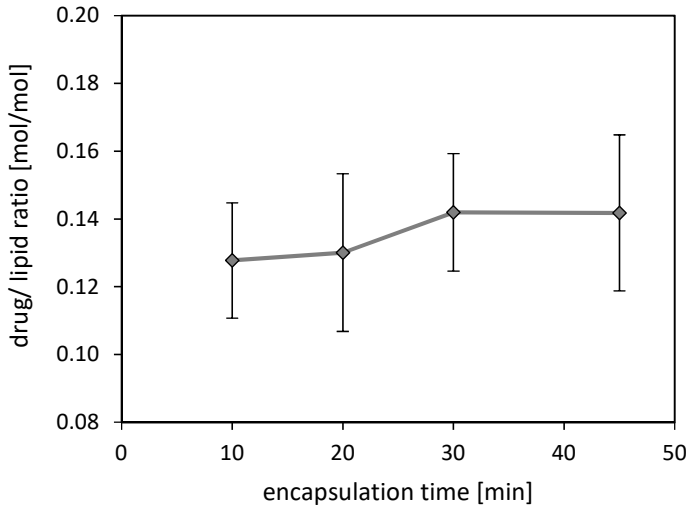


*Figure 4-30 Drug/lipid ratio (mol/mol) of CPT-11-TSL after active loading for 10, 20, 30 and 45 min at 36-37°C.*
*Lipid concentration was determined with phosphate assay and the encapsulated CPT-11 was measured with fluorescence spectroscopy. Values given as mean value ± standard deviation of three independent measurements.*

The encapsulation time for CPT-11 in $DPPG_2$-based TSL was set to 45 min for subsequently produced batches, since after 30 min the drug/lipid ratio of prepared liposomes reaches a plateau (cf. Figure 4-30). This means not more CPT-11 was encapsulated in the liposomes.

### *4.2.3.2 Release properties of CPT-11-TSL with different intraliposomal excipients*

To evaluate the effect of intraliposomal buffer for CPT-11 active loading on vesicle stability at temperatures < 39°C and heat-induced release at elevated temperatures, TSL with 300 mM citrate pH 4, 300 mM $(NH_4)_2HPO_4$ or 240 mM $(NH_4)_2SO_4$ were prepared and loaded with CPT-11. The temperature-dependent release in FBS for 5 min at 37-45°C was analyzed as well as the release after 1 h at 37°C or 42°C in FBS. Moreover, the effect of CPT-11 payload was investigated in the molar drug/lipid range from 0.015 to 0.245.

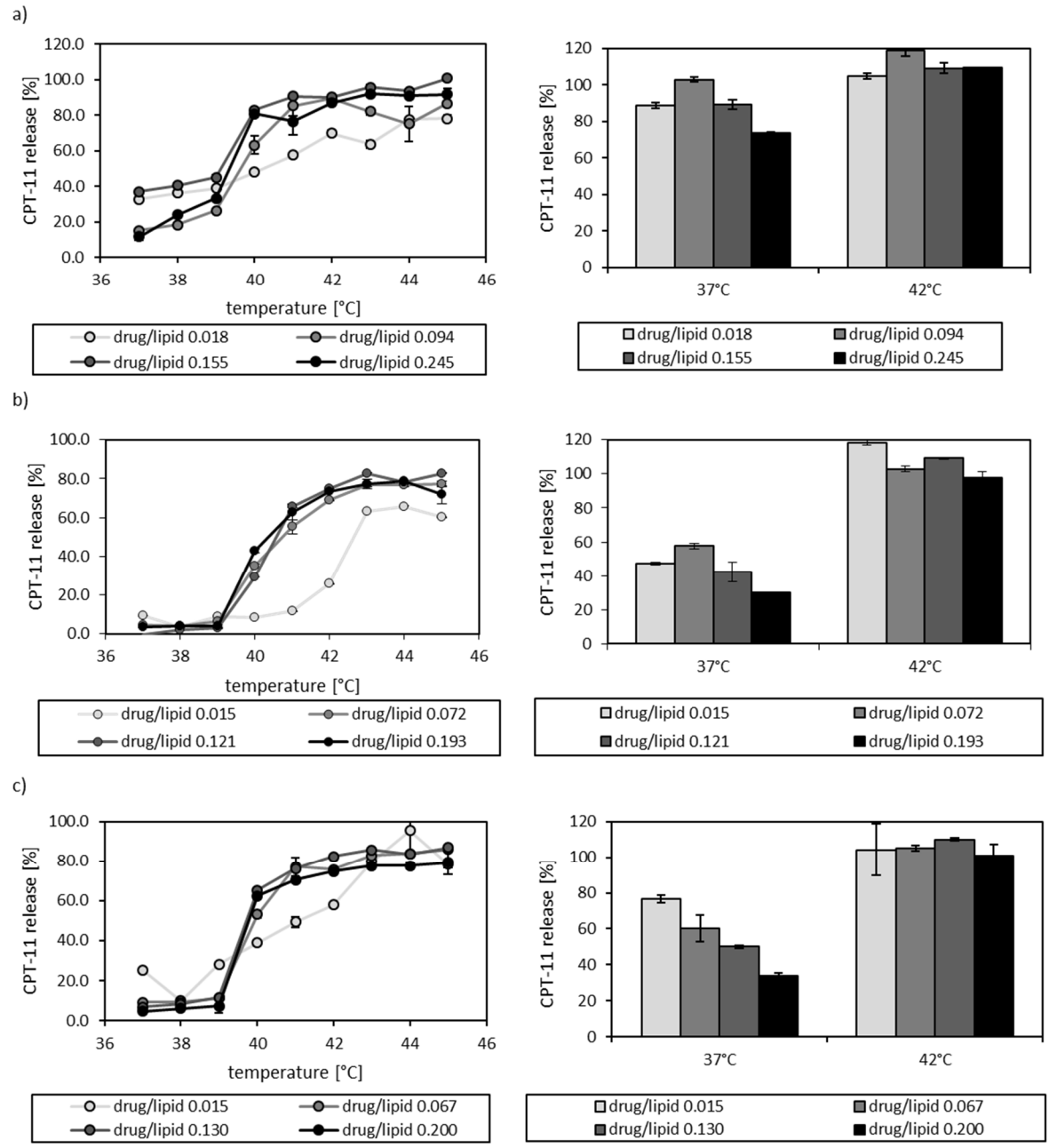


*Figure 4-31 Temperature-dependent release in FBS of CPT-11 from TSL with different drug/lipid ratios after 5 min incubation (left) or 1 h incubation (right) with intraliposomal a) 300 mM citrate pH 4, b) 300 mM $(NH_4)_2HPO_4$ pH 7.4 or c) 240 mM $(NH_4)_2SO_4$ pH 5.4 stored at -20°C.*

Independent of the intraliposomal excipient or drug/lipid ratio, all TSL formulations showed temperature-sensitive properties (cf. Figure 4-31). The TSL prepared with intraliposomal 300 mM citrate pH 4 showed the highest release already at 37°C after 5 min incubation (11.6±1.7%; drug/lipid 0.245 (mol/mol)) compared to TSL prepared with 300 mM $(NH_4)_2HPO_4$ (3.2±0.1%; drug/lipid 0.193 (mol/mol)) or 240 mM $(NH_4)_2SO_4$ (4.7±0.1%; drug/lipid 0.200 (mol/mol)), respectively. TSL with intraliposomal $(NH_4)_2HPO_4$ or $(NH_4)_2SO_4$ at higher drug/lipid ratios behave similarly. The release at 37°C after 1 h incubation was for the $(NH_4)_2HPO_4$-TSL 30.0±0.5% (drug/lipid ratio 0.193 (mol/mol)) and for the $(NH_4)_2SO_4$-TSL

33.8±1.6% (drug/lipid ratio 0.200 (mol/mol)). The release at 42°C 1 h was unaffected by intraliposomal excipient and drug/lipid ratios for all batches around 100%. With increasing drug/lipid ratio the amount of CPT-11 released during 1 h incubation at 37°C decreased, an observation that was independent from the used intraliposomal excipient for loading.

### *4.2.3.3 Stability study*

For dFdC-TSL an instability during freezing and thawing was shown in Figure 4-14. To investigate, if the CPT-11-TSL were also affected by freezing and thawing cycles, four batches with drug/lipid ratios between 0.016-0.215 (mol/mol) and $(NH_4)_2SO_4$ pH 5.4 as intraliposomal excipient were prepared and the fluorescence intensity at RT and the CPT-11 release after 1 h incubation at 37°C in FBS was analyzed directly after preparation and up to 3 freezing and thawing cycles.

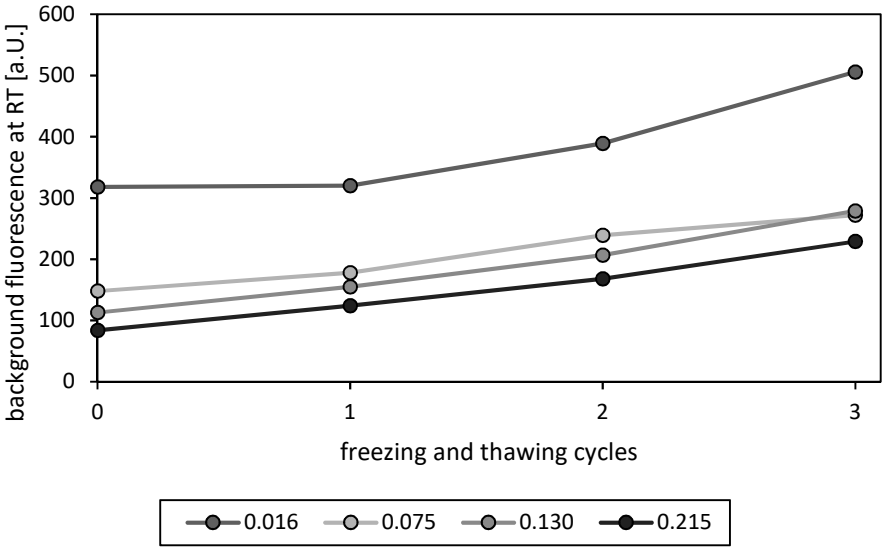


*Figure 4-32 Change in background fluorescence intensity in FBS at RT after up to 3 freezing and thawing cycles for four liposomal batches with different drug/lipid ratio.*
*Fluorescence was analyzed with fluorescence spectroscopy. Values given as mean value of two independent measurements.*

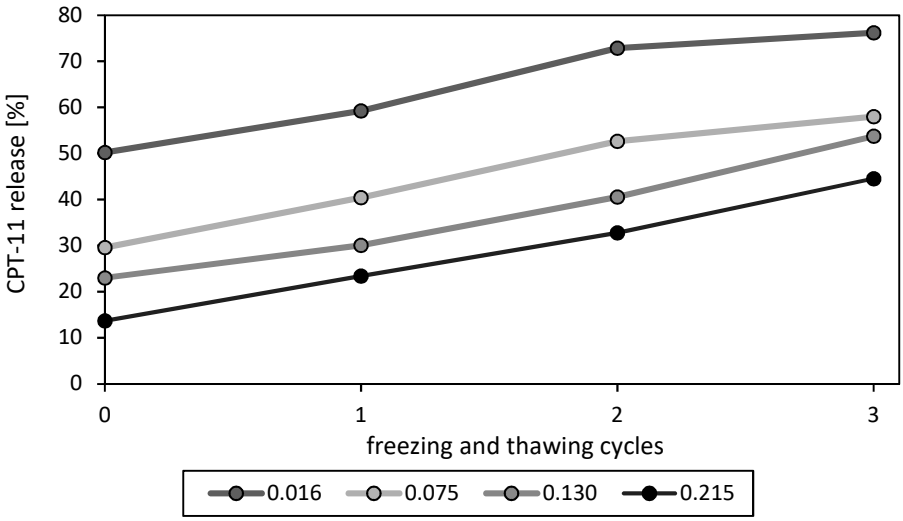


*Figure 4-33 Change in CPT-11 release after 1 h incubation at 37°C in FBS after up to 3 freezing and thawing cycles for four liposomal batches with different drug/lipid ratio.*
*Fluorescence was analyzed with fluorescence spectroscopy. Values given as mean of two independent measurements.*

With each freezing and thawing cycle, the fluorescence intensity at RT (cf. Figure 4-32) and the release at 37°C 1 h (cf. Figure 4-33) increased independently of the drug/lipid ratio of the investigated batches. For liposomes with a drug/lipid ratio of 0.215 the release at 37°C 1 h in FBS was 13.7±1.0% direct after preparation in comparison to 44.6±1.5% after three freezing and thawing cycles (3-fold increase).

Next, a short-term storage stability study at 2-8°C with TSL ($(NH_4)_2SO_4$ pH 5.4 as intraliposomal excipient) with different drug/lipid ratios was performed to investigate the storability of the formulation as liquid dispersion and to avoid detrimental freezing and thawing.

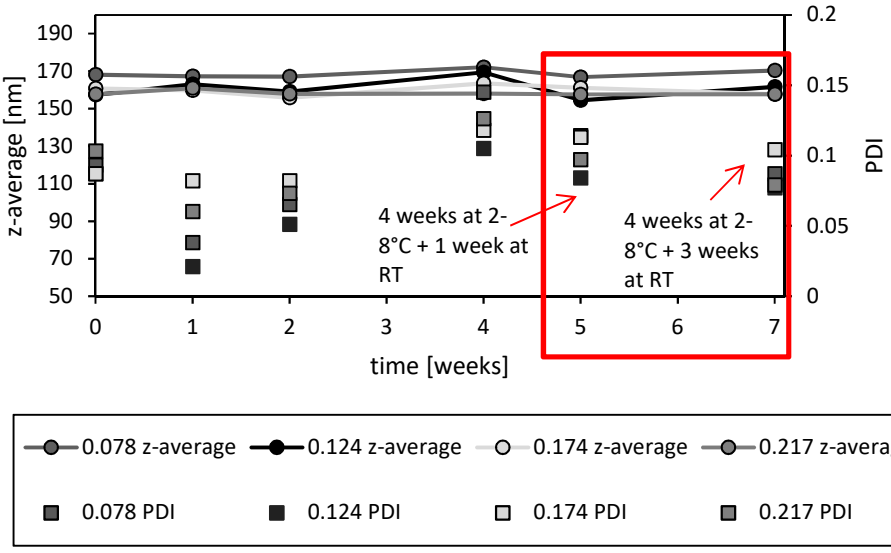


*Figure 4-34 Z-average and PDI of CPT-11-TSL with different drug/lipid ratios after storage for up to four weeks at 2-8°C and afterwards additional storage for up to three weeks at RT (values in red box) (n=1 for each time point).*

Z-average and PDI of CPT-11-TSL with different drug/lipid ratios showed no change during storage at 2-8°C for 4 weeks and additional storage at RT for up to three weeks (red box in Figure 4-34).

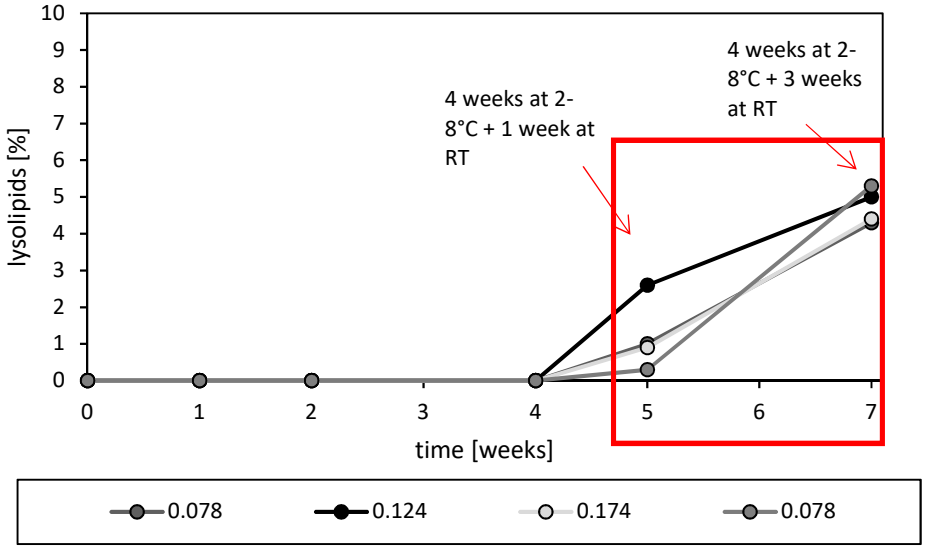


*Figure 4-35 Lysolipid content of CPT-11-TSL with different drug/lipid ratios after storage for up to four weeks at 2-8°C and afterwards additional storage for up to three weeks at RT (values in red box) (n=1 for each time point).*

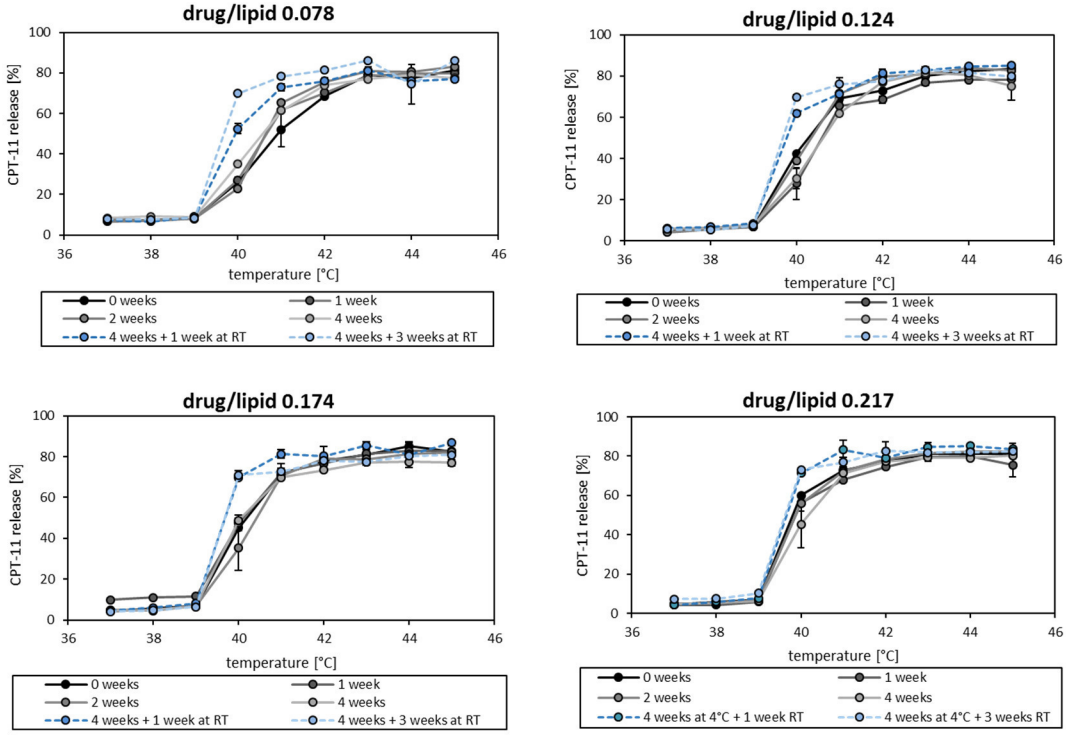


*Figure 4-36 Temperature-dependent CPT-11 release in FBS after 5 min of TSL with different drug/lipid ratios after storage for up to four weeks at 2-8°C and afterwards additional storage for up to three weeks at RT (blue dashed lines).*

During storage at 2-8°C no lysolipids were detected, after the first week of additional storage at RT between 0.3 and 2.6% have been measured. After additional 3 weeks at RT already 4.3-5.3% of lysolipids could be detected (cf. Figure 4-35). In the temperature-dependent

release assay no changes in the profile during the 4-week storage period at 2-8°C were observed, but the additional storage at RT increased the amount of CPT-11 released at 40°C (cf. Figure 4-36). For TSL with drug/lipid ratio 0.174 after four weeks' storage at 2-8°C the release at 40°C in FBS after 5 min was 48.9±2.5% and after one additional week storage at RT the release was 69.7±1.0%. No changes were detectable for the release after 1 h incubation at 37°C or 42°C during the overall storage period of 7 weeks (data not shown).
The study was also performed with TSL batches with intraliposomal buffer $(NH_4)_2HPO_4$ pH 7.4 and the same results were obtained (data not shown).

### *4.2.3.4 Effect of drug/lipid ratio on temperature-dependent CPT-11 release*

TSL with 240 mM intraliposomal $(NH_4)_2SO_4$ were prepared and stored at 2-8°C instead of -20°C to confirm the relationship increasing drug/lipid ratio resulting in decreasing amount of CPT-11 released after 1 h at 37°C (shown in 4.2.3.2).

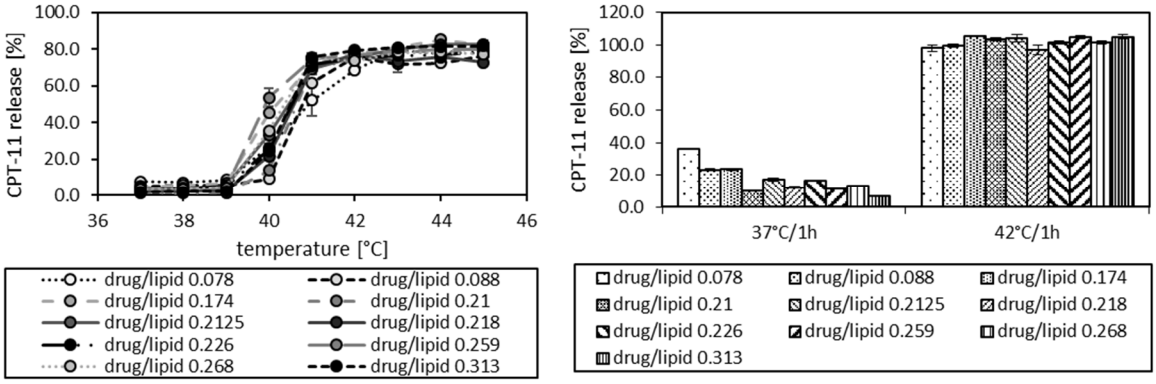


*Figure 4-37 Temperature-dependent release in FBS of CPT-11 from TSL with different drug/lipid ratios after 5 min incubation (left) or 1 h incubation (right) with intraliposomal 240/300 mM $(NH_4)_2SO_4$ buffer pH 5.4 stored at 2-8°C.*

With increasing drug/lipid ratio the amount of CPT-11 released 37°C 1 h incubation was decreased in relation to the complete encapsulated CPT-11 amount. This effect already described in 4.2.3.2 with different liposomal buffers was not caused by freezing and thawing, only the absolute values were higher for frozen TSL.
A threshold drug/lipid ratio for improved stability at 37°C was identified to be between 0.174 (mol/mol) (23.4±0.6% released CPT-11 during 1 h) and 0.21 (mol/mol) (10.2±0.2% released CPT-11 during 1 h). At drug/lipid ratios ≥ 0.21, CPT-11 release at 37°C during 1 h was fluctuating around 12.5±3.5%. When investigating CPT-11 release for 5 min at 37-45°C in FBS (cf. Figure 4-37) no major change in release behavior was observed. Only at 40°C the CPT-11 release was different between the formulations. Since no correlation between drug/lipid ratio and amount of drug released was observed, this is rather a measurement

artifact than formulation dependent, since 40°C is the temperature at which the formulations start to destabilize and therefore the variance of a single measurement was the highest.

### *4.2.3.5 Effect of $DPPG_2$-amount on biophysical properties*

To see if a change in formulation by lowering the $DPPG_2$ amount to 10 mol% instead of 30 mol% resulted in a higher stability at 37°C, TSL containing CPT-11 with the lipid composition DPPC/DSPC/$DPPG_2$ 70:20:10 (molar ratio) were prepared (=CPT-11-$TSL_{7/2/1}$).

| | **z-average (nm)** | **PDI** | **ζ-potential (mV)** | **EE (%)** | **phosphate value (mM)** | **CPT-11 content (mM)** | **drug/ lipid ratio (m/m)** |
|---|---|---|---|---|---|---|---|
| **CPT-11-$TSL_{7/2/1}$** | 160.3±4.0 | 0.088± 0.021 | -14.0±0.7 | 95.9±5.6 | 48.4±4.4 | 11.60±0.95 | 0.240± 0.014 |

*Table 4-9 Characteristics of CPT-11-$TSL_{7/2/1}$ (n=3). Values given as mean value ± standard deviation.*

The biophysical characteristics obtained for CPT-11-$TSL_{7/2/1}$ (cf. Table 4-9.) are comparable to the results obtained with CPT-11-TSL with 30 mol% $DPPG_2$ (cf. Table 4-10) (e.g. CPT-11 content for CPT-11-$TSL_{7/2/1}$ is 11.60±0.95 mM and 10.05±2.79 mM for the formulation with 30 mol% $DPPG_2$). Only the ζ-potential (-14.0±0.7 mV for CPT-11-$TSL_{7/2/1}$ vs. -28.9±2.4 mV for 30 mol% $DPPG_2$) was not comparable, but this is caused by the different $DPPG_2$-amounts.
The temperature-dependent CPT-11 release after 5 min or 1 h in comparison to the formulation with the lipid composition DPPC/DSPC/$DPPG_2$ 50:20:30 (molar ratio) (=CPT-11-TSL) were analyzed.

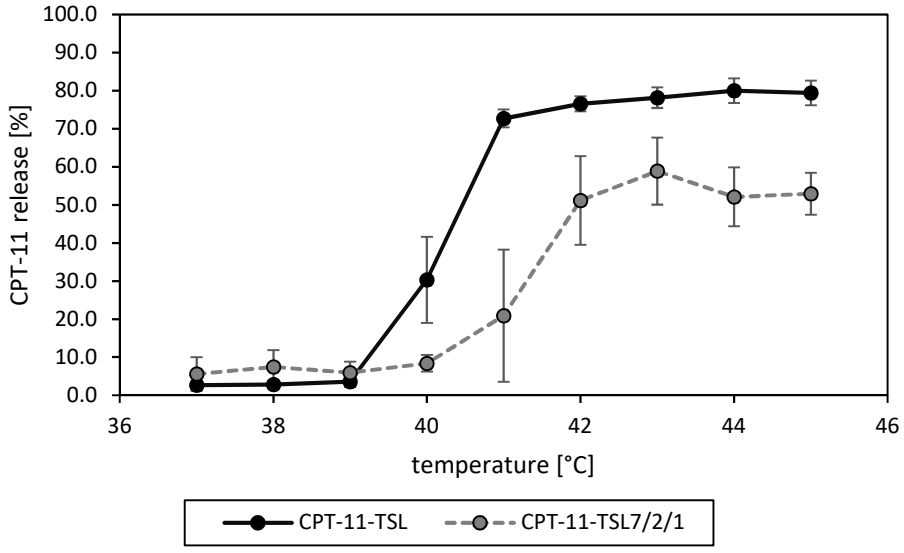


*Figure 4-38 Temperature-dependent CPT-11 release in FBS after 5 min incubation at different temperatures of CPT-11-TSL (drug/lipid 0.244±0.033 (mol/mol); black line; n=9) in comparison to CPT-11-$TSL_{7/2/1}$ (drug/lipid 0.240±0.014 (mol/mol); dashed grey line; n=3).*
*Values given as mean value ± standard deviation.*

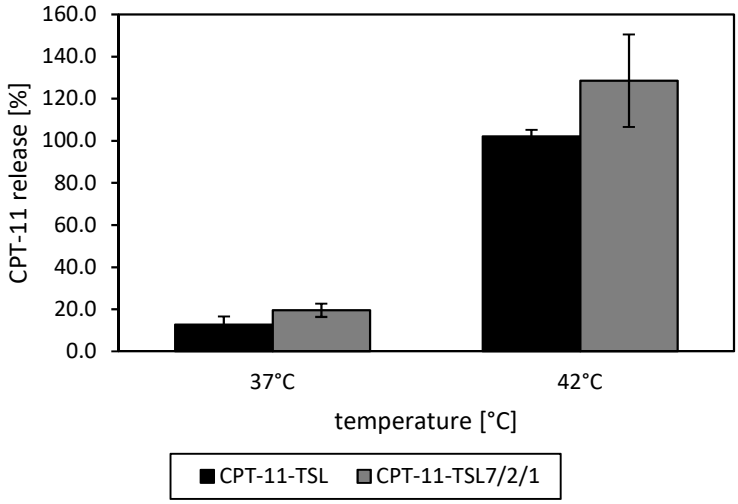


*Figure 4-39 Temperature-dependent CPT-11 release in FBS after 1 h incubation at 37°C or 42°C of CPT-11-TSL (drug/lipid 0.244±0.033 (mol/mol); black bar; n=9) in comparison to CPT-11-TSL$_{7/2/1}$ (drug/lipid 0.240±0.014 (mol/mol); grey bar; n=3).*
*Values given as mean value ± standard deviation.*

Formulation CPT-11-TSL showed only 12.8±3.8% release at 37°C after 1 h incubation compared to 19.5±3.2% for CPT-11-TSL$_{7/2/1}$ (cf. Figure 4-39). Additionally, after 5 min incubation the CPT-11-TSL reached higher CPT-11 release at 41°C (72.7±2.3%) in contrast to only 20.9±17.4% for CPT-11-TSL$_{7/2/1}$ (cf. Figure 4-38). The maximal release during 5 min of incubation for CPT-11-TSL$_{7/2/1}$ was also only 58.9±8.8% at 43°C (cf. maximal release for CPT-11-TSL 80.0±3.2% at 44°C).

## 4.2.4 *In vitro* characterization

Additional *in vitro* characterization of CPT-11 DPPG$_2$-based TSL was performed with the most promising candidate developed in section 4.2.3, the formulation CPT-11-TSL (DPPC/DSPC/DPPG$_2$ 50:20:30 (molar ratio)) with the intraliposomal excipient 300 mM $(NH_4)_2SO_4$ pH 5.4 and a drug/lipid ratio of ~0.23 (mol/mol) was prepared and stored at 2-8°C for a maximum of 4 weeks before usage. CPT-11-NTSL and CPT-11-TSL$_{7/2/1}$ were used as control in some experiments.

### *4.2.4.1 Characteristics of CPT-11-TSL*

Table 4-10 shows an overview of the characteristics of TSL performed for CPT-11-TSL which were used for the following experiments and the *in vivo* works. All analyzed parameters were in an acceptable range for TSL prepared with active loading via a pH gradient (cf. Table 4-10).

| | z-average (nm) | PDI | ζ-potential (mV) | EE (%) | phosphate value (mM) | CPT-11 content (mM) | drug/ lipid ratio (m/m) |
|---|---|---|---|---|---|---|---|
| **CPT-11-TSL** | 155.2±4.6 | 0.071± 0.025 | -28.9±2.4 | 88.2±9.2 | 43.3±5.7 | 10.05±2.79 | 0.230± 0.042 |

*Table 4-10 Characteristics of CPT-11-TSL (n=11). Values given as mean value ± standard deviation.*

For further characterization, osmolarity of different TSL formulations, CPT-11-TSL with different intraliposomal excipients and solutions used for preparation was measured.

| | osmolarity (mmol/kg) |
|---|---|
| **formulated CPT-11 (29.53 mM)** | 275±2 |
| **300 mM Citrate** | 614±1 |
| **300 mM $(NH_4)_2HPO_4$** | 618±13 |
| **300 mM $(NH_4)_2SO_4$** | 633±2 |
| **CPT-11-TSL intraliposomal citrate** | 276±6 |
| **CPT-11-TSL intraliposomal $(NH_4)_2HPO_4$** | 296±4 |
| **CPT-11-TSL intraliposomal $(NH_4)_2SO_4$** | 297±3 |
| **CPT-11-TSL$_{7/2/1}$** | 344±12 |
| **CPT-11-NTSL** | 328±4 |

*Table 4-11 Osmolarity measured for different CPT-11 liposomes and solutions used for CPT-11 encapsulation.*
*Values given as mean value ± standard deviation.*

Osmolarities of all three tested intraliposomal excipients used for encapsulation were similar (citrate 614±1 mmol/kg, $(NH_4)_2HPO_4$ 618±13 mmol/kg and $(NH_4)_2SO_4$ 633±2 mmol/kg). All tested formulations and formulated CPT-11 (29.53 mM) alone showed osmolarity around physiological osmolarity of 290 mmol/kg (cf. Table 4-11). In summary, the results of the following *in vitro* and *in vivo* experiments have not been biased by differences in osmotic pressure or osmolarity of the applied TSL formulations.

### *4.2.4.2 Time-dependent CPT-11 release*

The temperature-dependent release of CPT-11-TSL in comparison to CPT-11-TSL$_{7/2/1}$ was already shown in Figure 4-38 and Figure 4-39. To evaluate these results in more detail a measurement of the time-dependent release for 5 min and 1 h was performed.

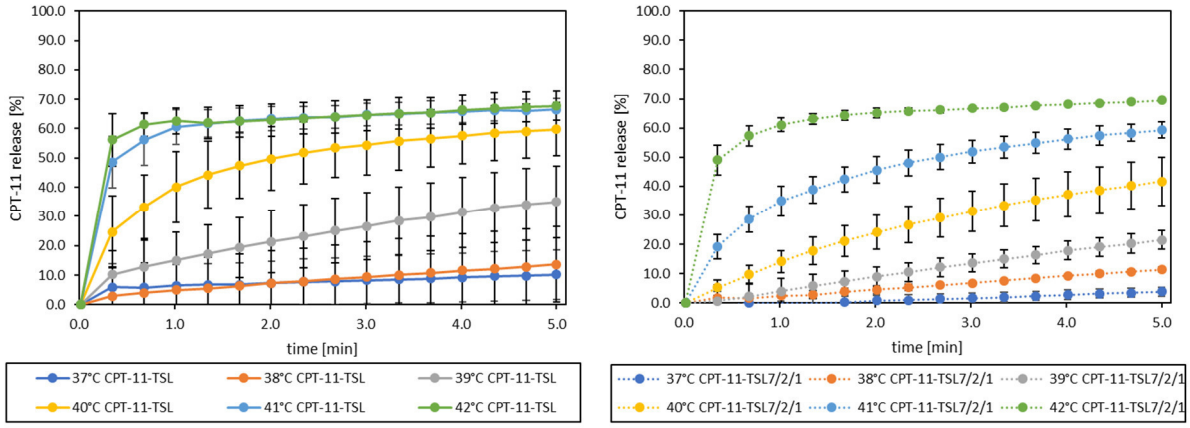


*Figure 4-40 Time-dependent CPT-11 release in FBS at 37-42°C for 5 min of CPT-11-TSL (drug/lipid 0.207±0.016 (mol/mol); left, solid lines) in comparison to CPT-11-TSL$_{7/2/1}$ (drug/lipid 0.240±0.014 (mol/mol); right, dashed lines).*
*Values given as mean value ± standard deviation of three independent measurements.*

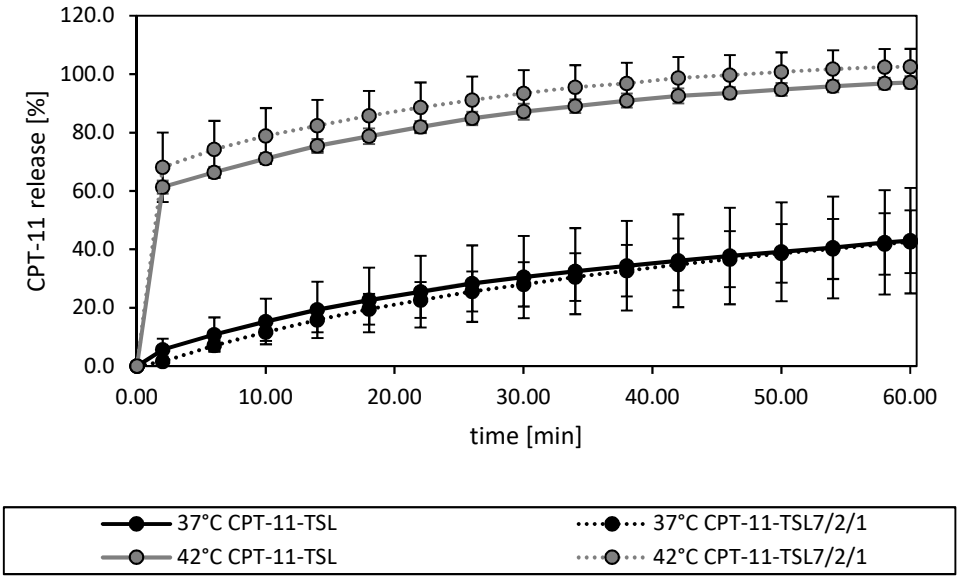


*Figure 4-41 Time-dependent CPT-11 release in FBS at 37 or 42°C for 1 h of CPT-11-TSL (drug/lipid 0.194±0.035 (mol/mol); solid lines) in comparison to CPT-11-TSL$_{7/2/1}$ (drug/lipid 0.240±0.014 (mol/mol); dashed lines).*
*Values given as mean value ± standard deviation of three independent measurements.*

| | **$k_{CPT-11}$ ($10^{-4}s^{-1}$) at 37°C** | **$R^2$ 37°C** | **$k_{CPT-11}$ ($10^{-4}s^{-1}$) at 40°C** | **$R^2$ 40°C** |
|---|---|---|---|---|
| **CPT-11-TSL** | 1.8±0.9 | 0.6424± 0.3027 | 20.2± 2.4 | 0.9623± 0.0248 |
| **CPT-11-TSL$_{7/2/1}$** | 1.7±0.6 | 0.6514± 0.3029 | 17.3± 5.1 | 0.9975± 0.0019 |

*Table 4-12 CPT-11 release rate constant k for CPT-11 at 37°C and 40°C for CPT-11-TSL and CPT-11-TSL$_{7/2/1}$.*
*The values were calculated from the release profile shown in Figure 4-40 for the first 300 s.*

Release at 37-39°C as well as the CPT-11 release rate constants at 37°C of both formulations calculated from the release kinetics shown in Figure 4-40 were comparable (cf. Table 4-12). At temperatures of 40-41°C the CPT-11-TSL showed higher CPT-11 release (e.g. 59.9±9.0%/5 min at 40°C in comparison to 41.7±8.3%/5 min). This was consistent with the CPT-11 release rate constants calculated from the release kinetics at 40°C (20.2±2.4 $10^{-4}$ $s^{-1}$ for CPT-11-TSL and 17.3±5.$110^{-4}s^{-1}$ for CPT-11-$TSL_{7/2/1}$). At 42°C in the time-dependent release the CPT-11 release also after 1 h incubation was again comparable between both formulations (CPT-11-TSL 97.2±2.1%; CPT-11-$TSL_{7/2/1}$ 102.6±6.1%) (cf. Figure 4-41).

### *4.2.4.3 Release for up to 3 h at 37°C*

To evaluate if the CPT-11 release from CPT-11-TSL after 1 h at 37°C in FBS (cf. Figure 4-39 and Figure 4-41) was constant also over longer period of time, TSL were incubated for up to 3 h at 37°C in FBS. The released CPT-11 was measured after several time points (5 min, 1 h, 2 h, 3 h).

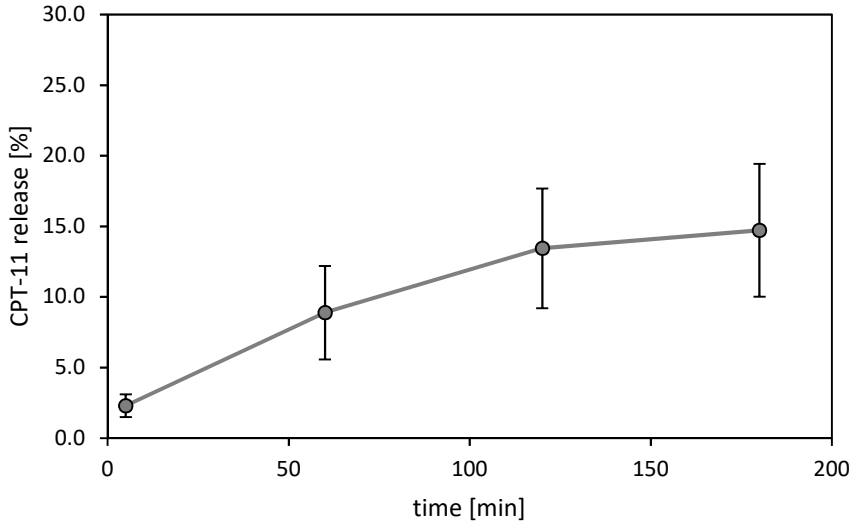


*Figure 4-42 Temperature-dependent CPT-11 release in FBS after 5-180 min of incubation at 37°C. Values given as mean value ± standard deviation of two independent measurements.*

Figure 4-42 shows, that the release was decreasing in a stepwise manner after incubation at 37°C. There was no linear release and after 2h a plateau was reached and nearly no additional CPT-11 was released at 37°C (13.4±4.2% after 2h and 14.7±4.7% after 3 h). The major part was released in the first 1 h (8.9±3.3%). It seems that parts of the CPT-11 were not stable encapsulated in the TSL.

### *4.2.4.4 DSC-measurement (Effect of CPT-11)*

To investigate if CPT-11 encapsulation in TSL influences the phase transition of the TSL membrane, DSC measurements of CPT-11-TSL, CPT-11-TSL$_{7/2/1}$, CPT-11-NTSL, CPT-11 alone, TSL with $(NH_4)_2SO_4$ buffer only and Onivyde® were performed.

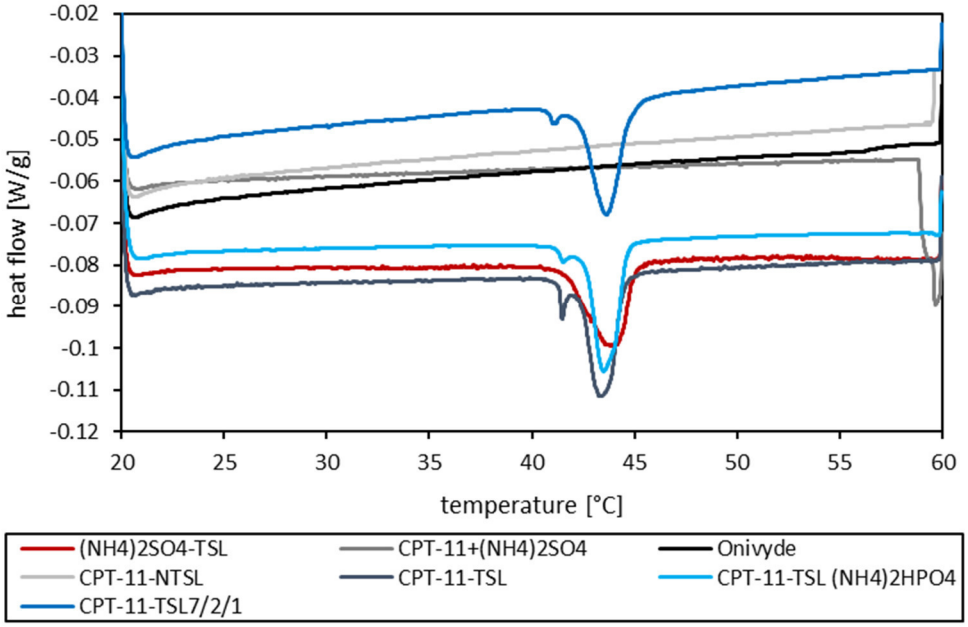


*Figure 4-43 Representing plots of the heating phase from 20-60°C with a heating rate of 1°C/min of $(NH_4)_2SO_4$-TSL, CPT-11+$(NH_4)_2SO_4$ (concentrations comparable to intraliposomal concentrations), Onivyde®, CPT-11-NTSL, CPT-11-TSL, CPT-11-TSL $(NH_4)_2HPO_4$, CPT-11-TSL$_{7/2/1}$.*
*Values are at least mean values of three independent measurements.*

| | **main transition $T_m$ [°C]** | **pre-transition [°C]** |
|---|---|---|
| **$(NH_4)_2SO_4$-TSL** | 44.40±0.17 | / |
| **CPT-11-TSL** | 43.88±0.12 | 41.24±0.17 |
| **CPT-11-TSL $(NH_4)_2HPO_4$** | 44.02±0.05 | 41.18±0.10 |
| **CPT-11-TSL$_{7/2/1}$** | 43.73±0.64 | 40.75±0.45 |

*Table 4-13 Overview of $T_m$ values of the main transition peak and the pre-transition peak of $(NH_4)_2SO_4$-TSL, CPT-11-TSL, CPT-11-TSL $(NH_4)_2HPO_4$, CPT-11-TSL$_{7/2/1}$ determined with DSC.*
*Values are given as mean value ± standard deviation of three independent measurements.*

Encapsulation of CPT-11 in TSL shifted the $T_m$ to lower temperatures. $T_m$ for unloaded $(NH_4)_2SO_4$-TSL was 44.40±0.17°C in contrast to 43.88±0.12°C for CPT-11-TSL (Table 4-13). The peak shape, however, was broader for $(NH_4)_2SO_4$-TSL compared to CPT-11 loaded TSL, which might explain the difference in $T_m$ (cf. Figure 4-43). For $DPPG_2$-based TSL loaded with CPT-11 a pre-transition around 41°C was visible, regardless of the intraliposomal excipient and the amount of $DPPG_2$. Onivyde® and NTSL showed no phase transition as well

as a solution of CPT-11 and $(NH_4)_2SO_4$ (concentrations of both compounds were like expected intraliposomal).

### *4.2.4.5 Cryo-TEM*

To investigate, if the encapsulated irinotecan forms an intraliposomal drug crystal, cryo-TEM measurements were performed at the group of Prof. Schubert at the University of Freiburg. For this purpose, CPT-11-TSL with a drug/lipid ratio of 0.226 (mol/mol) and unloaded TSL were analyzed, respectively. The unloaded TSL were prepared in the same way as the CPT-11-TSL with the only exception that no CPT-11 was added during the process.

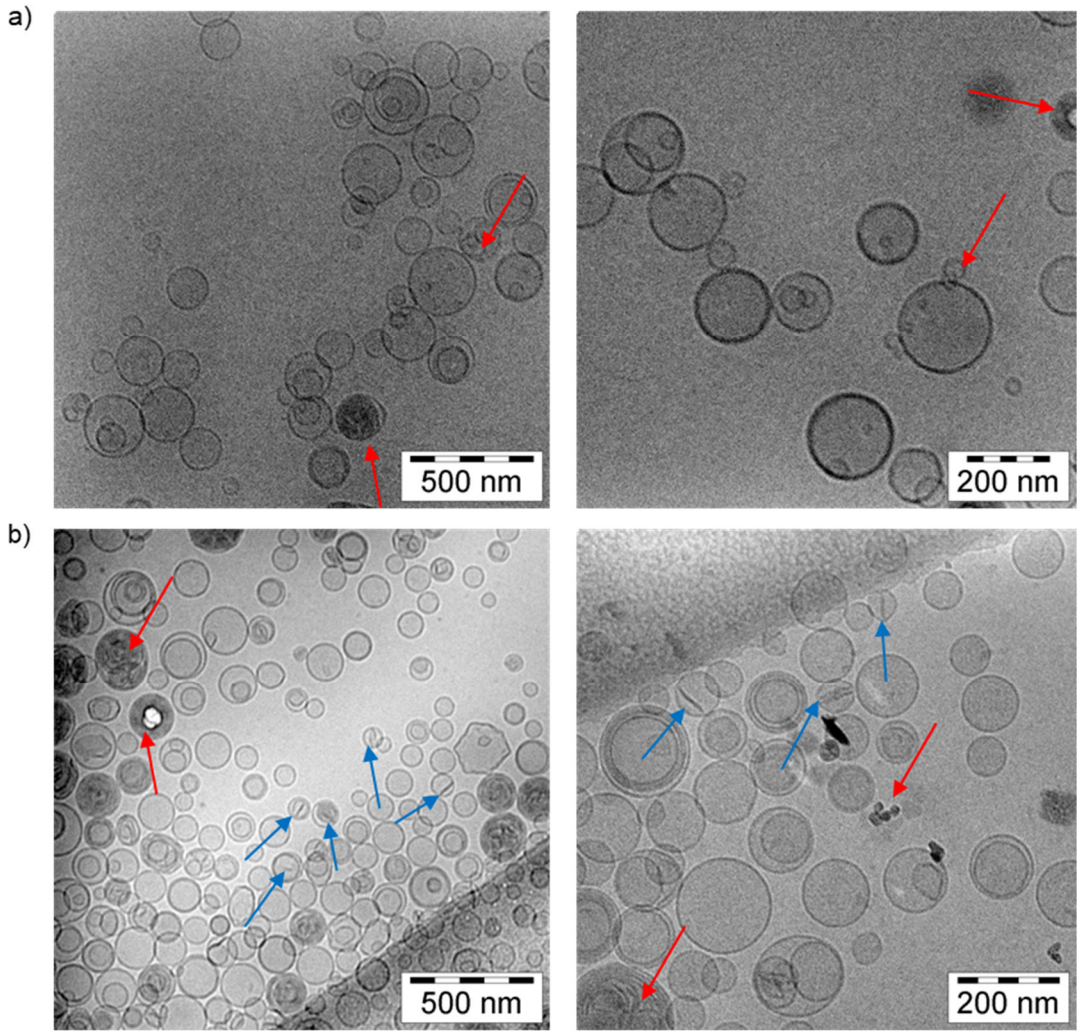


*Figure 4-44 Representative Cryo-TEM images of a) unloaded TSL and b) CPT-11-TSL. The drug/lipid ratio for CPT-11-TSL was 0.226 (mol/mol).*

The pictures in the bottom show the CPT-11-TSL. Some of the CPT-11-TSL contain rod-like structures (marked with blue arrows) in the liposomes. This rod-like structures could not be seen in the unloaded TSL (Figure 4-44 a). All other not well defined liposomal structures (marked with red arrows) were visible in CPT-11-TSL and unloaded TSL and were possibly generated during liposomal preparation.

### *4.2.4.6 Onivyde®*

For *in vivo* studies, the nanoliposomal long-circulating CPT-11 Onivyde® was used as control. Onivyde® was ordered from the manufacturer. To estimate the *in vivo* results more precisely Onivyde® was characterized with the same assays which were used to characterize CPT-11-TSL (cf. Table 4-14).

| | **Onivyde®** | **CPT-11-TSL** |
|---|---|---|
| **formulation (molar ratio)** | DSPC/Chol/DSPE-$PEG_{2000}$ 60/39.7/0.3 | DPPC/DSPC/$DPPG_2$ 50:20:30 |
| **z-average (nm)** | 106.6±1.1 | 155.2±4.6 |
| **PDI** | 0.049±0.017 | 0.071±0.025 |
| **ζ-potential (mV)** | -7.29±1.72 | -28.9±2.4 |
| **osmolarity (mmol/kg)** | 297±7 | 297±3 |
| **lysolipid-content (%)** | 7.4±0.6 | n.d. |
| **free fatty acids (%)** | 6.0±0.1 | n.d. |
| **lipid concentration determined by phosphate assay (mM)** | 8.8±0.2 (w/o Chol) 14.5±0.2 (w/Chol), assuming 39.7 mol% to be Chol | 43.3±5.7 |
| **CPT-11** | 7.37±0.22 | 10.05±2.79 |
| **drug/lipid ratio (mol/mol)** | 0.508 | 0.230±0.042 |

*Table 4-14 Characterization of commercial Onivyde® (three independent measurements) in comparison to CPT-11-TSL (11 independent prepared batches).*
*n.d.: not detectable. Values given as mean value ± standard deviation.*

Comparing Onivyde® and CPT-11-TSL, the differences which may influence the *in vivo* behavior were the vesicle size (z- average 106.6±1.1 nm or 155.2±4.6 nm, respectively), the ζ-potential and the difference in drug/lipid ratio (0.508 (mol/mol) compared to 0.230±0.042 (mol/mol)) as well as the lysolipid content. The lysolipid content and free fatty acids of Onivyde® was not expected in this amount (7.4±0.6% lysolipid, 6.0±0.1% FFA), because these components were not mentioned in the specification sheet of the drug product. All other characterization methods showed the expected values. After the expiry date, the lysolipid content and the free fatty acid was determined again. The lysolipid content increased to 13.5% and the free fatty acid content to 8.0±0.6%.

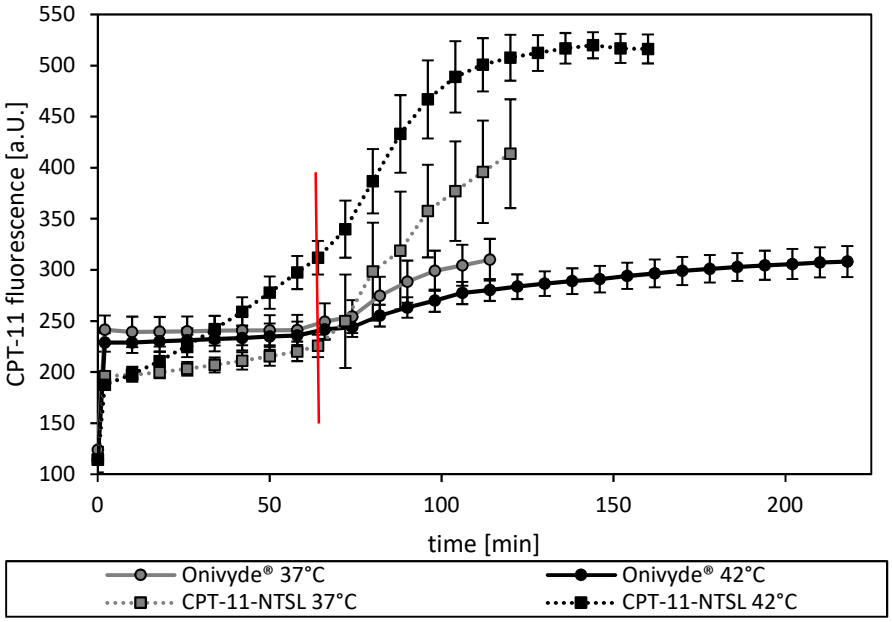


*Figure 4-45 Increase of fluorescence intensity of CPT-11 released from Onivyde® (solid lines) in comparison to CPT-11-NTSL (dashed line) in FBS at 37°C (grey lines) or 42°C (black lines). After the red line in serval steps (2x20 µl and 3-4x40 µl) 10% Triton X-100 was added to destroy the liposomes and achieve a maximum release. Values given as mean value ± standard deviation of two independent measurements.*

Comparing the fluorescence intensity change of CPT-11 of Onivyde® and CPT-11-NTSL during incubation at 37°C or 42°C, CPT-11-NTSL were less stable than Onivyde® (see Figure 4-45). CPT-11-NTSL showed a sustained release of CPT-11 in a small amount at 37°C and higher amount at 42°C. Onivyde® showed no change in fluorescence neither at 37°C nor at 42°C and so nearly no release of CPT-11 after 60 min incubation in FBS. Also, the addition of 10% Triton X-100 to Onivyde® samples had only a minor effect on the liposomes, whereas for CPT-11-NTSL the fluorescence intensity increased until a plateau was reached at 42°C, indicating complete release of encapsulated CPT-11 due to liposome destruction.

### *4.2.4.7 Conversion of CPT-11 to SN-38 in different cell types*

As pre-test for the *in vivo* experiment, the potential conversion of CPT-11 to its active metabolite SN-38 was investigated *in vitro* in different cell lines. The used cell lines were BN-175, a soft tissue sarcoma cell line, DSL-6A/C1 a pancreatic cancer cell line and HepG2, a human liver cancer cell line.

The cells were grown in different sizes of cell culture flasks (T-25, T-75, T-175), different times before treatment (24 h, 48 h), with different amounts of CPT-11 (5, 10, 20 µM) for several treatment times (24 h, 48 h, 96 h). The CPT-11 and SN-38 concentrations in the culture medium and in the cells were determined with HPLC.

For example, CPT-11 concentration in $HepG_2$-cells after treatment with 20 µM CPT-11 was < 1 µM. Most of the CPT-11 was still measurable in the culture medium (> 19 µM), indicating insufficient cellular uptake of CPT-11.

In all cell lines, the SN-38 concentration in the culture medium was under the limit of quantification but for cell lines DSL-6A/C1 and HepG2 over the limit of detection (very small peak measurable). In the cells, SN-38 was not detectable independent from cell line, cell amount, growth and treatment time.

## 4.2.5 *In vivo* experiments

The CPT-11-TSL with the lipid composition DPPC/DSPC/$DPPG_2$ (50:20:30 molar ratio) and $(NH_4)_2SO_4$ as loading excipient with a drug/lipid ratio of 0.275±0.033 (mol/mol) was further investigated *in vivo,* in a pharmacokinetic study, a biodistribution study as well as in a therapeutic study. As controls, Onivyde® and non-liposomal CPT-11 were tested in all experiments. For all experiments 20 mg/kg of CPT-11 was used as dosage and all drug solutions were adjusted to a concentration of 7.33 mM, to receive a comparable injection volume.

### *4.2.5.1 Pharmacokinetic study*

The blood circulation half-lives of non-liposomal CPT-11, Onivyde® and CPT-11-TSL were analyzed by measuring the CPT-11 and SN-38 concentration in plasma of healthy BN rats from 10 min to 1440 min. The theoretically calculated $c_{max}$ for an injected dose of 20 mg/kg CPT-11 was calculated to be 500 µg/ml (= ID) by assuming 4% of the body weight to be plasma.

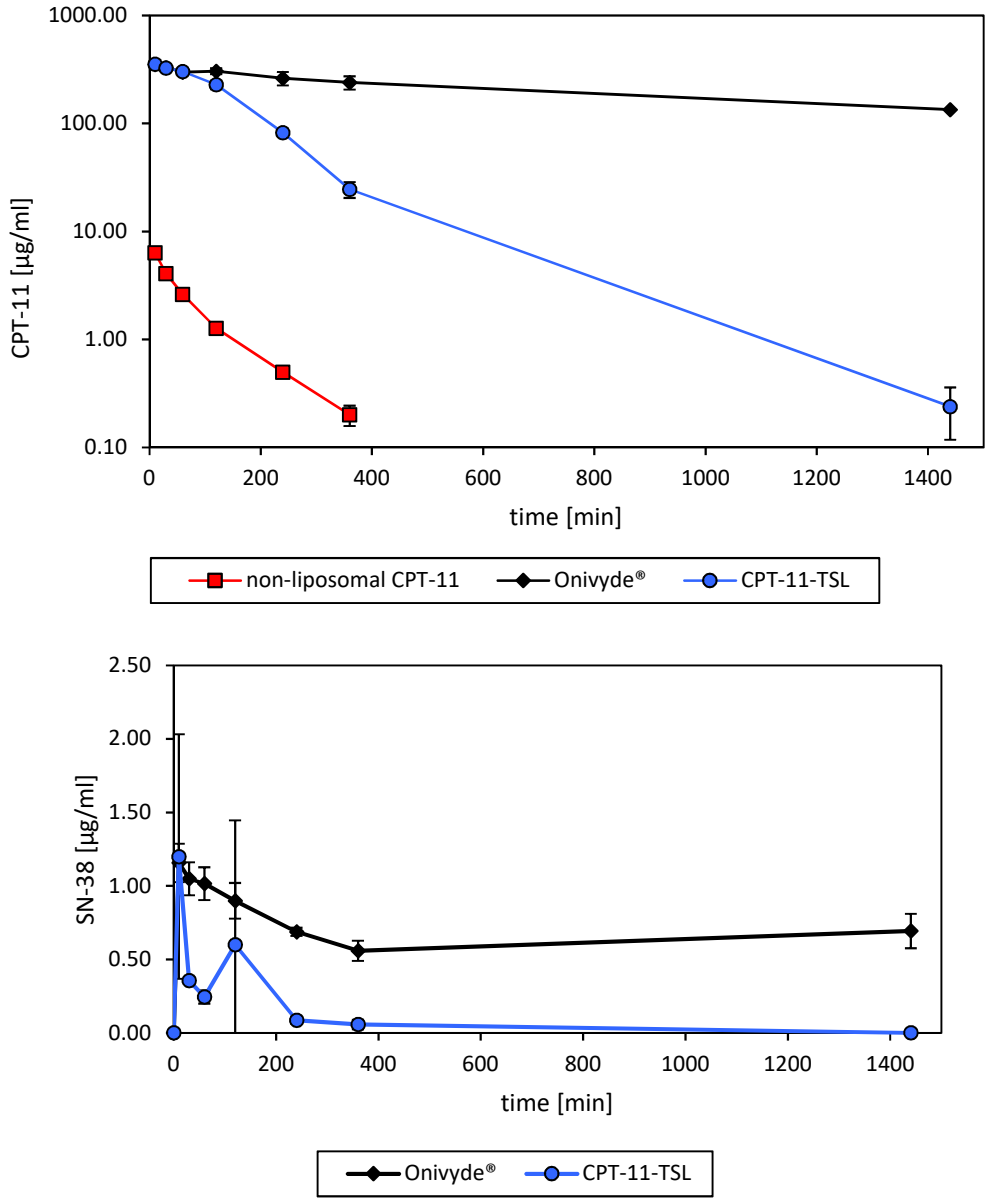


*Figure 4-46 Pharmacokinetic study of non-liposomal CPT-11, Onivyde® or CPT-11-TSL. Formulations and free drug were i.v. injected at a dose of 20 mg/kg CPT-11 in healthy BN rats (n=3). Blood samples were taken at certain time points and top) CPT-11 and bottom) SN-38 concentration were measured with HPLC. Animal handling was performed by Dr. Simone Limmer. Values given as mean value ± standard deviation.*

| | dosage (mg/kg) | $c_{10}$ CPT-11 (µg/ml) | $c_0$ CPT-11 (µg/ml) | $t_{1/2}$ (h) CPT-11 | $R^2$ | $AUC_{0\text{-}24h}$ (µg*h/ml) |
|---|---|---|---|---|---|---|
| **non-liposomal CPT-11** | 20 | 6.36±0.61 | 7.22 | 0.71 | 0.9856 | 6.25 |
| **Onivyde®** | 20 | 351.63±14.83 | 326.90 | 18.70 | 0.9890 | 5142.00 |
| **CPT-11-TSL** | 20 | 354.53±34.0 | 465.80 | 1.57 | 0.9954 | 978.80 |

*Table 4-15 CPT-11-plasma concentration after i.v. application of 20 mg/kg non-liposomal CPT-11, Onivyde® or CPT-11-TSL.*
*$c_0$= calculated initial plasma concentration at t=0 h based on monoexponential fit; $c_{10}$= measured plasma concentration at t=10 min; $t_{1/2}$=plasma half-life; $R^2$= coefficient of determination; $AUC_{0\text{-}24h}$=area under the curve 0-24 h.*

Non-liposomal CPT-11 showed the lowest plasma half-life with 0.71 h compared to 1.57 h (CPT-11-TSL) and 18.70 h (Onivyde®) (cf. Table 4-15). For non-liposomal CPT-11, only 1.3% of ID (6.36±0.61 µg/ml) was detectable 10 min after i.v. bolus injection. The $c_0$ achieved by a monoexponential fit of the data for CPT-11-TSL was higher compared to Onivyde® (465.80 µg/ml in contrast to 326.90 µg/ml). CPT-11 concentration of CPT-11-TSL and Onivyde® was comparable for the first 60 min. After 60 min, Onivyde® showed higher CPT-11 concentrations and the difference in CPT-11 concentration between CPT-11-TSL and Onivyde® increased. SN-38 concentration in plasma was only detectable for liposomal formulations (cf. Figure 4-46). After 10 min, the SN-38 concentrations for CPT-11-TSL and Onivyde® were similar (1.20±0.83 µg/ml resp. 1.16±0.13 µg/ml). For CPT-11-TSL, SN-38 plasma levels decreased much faster than for Onivyde®, after 6 h only 0.06±0.03 µg/ml were detectable and after 24 h no SN-38 could be detected. The SN-38 concentration for Onivyde® decreased in the first 4 h but then the SN-38 level stayed constant at concentrations between 0.56-0.69 µg/ml over 24 h.

### *4.2.5.2 Biodistribution study*

In this study, the accumulation of CPT-11 and its metabolite SN-38 in different organs and plasma was analyzed, when treating tumor-bearing BN rats with non-liposomal CPT-11, Onivyde® or CPT-11-TSL. The injection started after the tumor had reached the target temperature of 41°C, followed by a HT-treatment at this temperature for the next 60 min. After the HT-treatment, the animals were sacrificed and the tissue samples were taken.

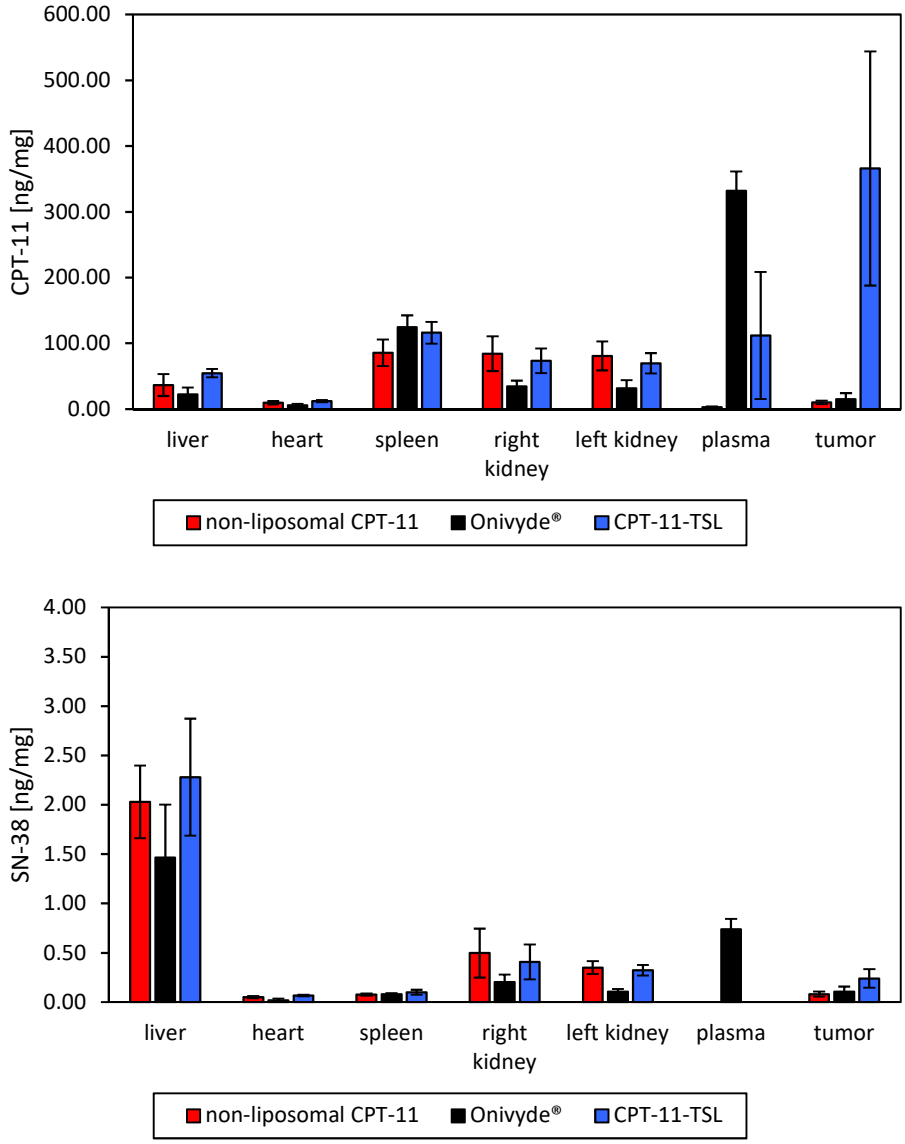


*Figure 4-47 Top) CPT-11 concentration and bottom) SN-38 concentration in different organs (heart, liver spleen, kidney) tumor and plasma after i.v. injection of non-liposomal CPT-11, Onivyde® or CPT-11-TSL at a dose of 20 mg/kg CPT-11 in tumor bearing BN-rats (n=4) and 1 h of HT-treatment of the tumor tissue.*
*CPT-11 and SN-38 concentration in all samples was measured with HPLC. Values given as mean value ± standard deviation.*

CPT-11 concentration in the tumor was 24-fold higher for CPT-11-TSL (365.75±177.95 ng/mg) compared to Onivyde® (15.23±9.06 ng/mg) and 36-fold higher in comparison to non-liposomal CPT-11 (10.22±2.79 ng/mg) (cf. Figure 4-47). The SN-38 concentration in the tumor for CPT-11-TSL was also higher compared to the other two groups (0.24±0.09 ng/mg for CPT-11-TSL, 0.11±0.05 ng/mg for Onivyde® and 0.08±0.03 ng/mg for non-liposomal CPT-11). In the kidneys, the CPT-11 concentration of Onivyde® (34.63±8.58 ng/mg and 31.76±12.25 ng/mg) was less than for non-liposomal CPT-11 (84.27±26.36 ng/mg and 80.85±21.97 ng/mg) and CPT-11-TSL (73.47±18.85 ng/mg and 69.91±15.49 ng/mg). The SN-38 concentration in this organ went in parallel, i.e. for Onivyde® less SN-38 was in the

kidneys compared to non-liposomal CPT-11 and CPT-11-TSL. In the liver tissue, the same trend was observed with lower CPT-11 and SN-38 concentration for Onivyde® compared to non-liposomal CPT-11 and CPT-11-TSL. In heart and spleen, the concentrations of CPT-11 were similar and the SN-38 concentrations were low for all three tested formulations. A major difference was measured in plasma after 60 mins, for Onivyde® (331.74±29.39 ng/mg) CPT-11 concentration was 3-fold higher compared to CPT-11-TSL (111.86±96.51 ng/mg) and for non-liposomal CPT-11 only 3.09±1.08 ng/mg were detected. SN-38 in plasma was only detectable for Onivyde® in a concentration of 0.74±0.11 ng/mg. For the other two treatment groups, no SN-38 could be detected.

### *4.2.5.3 Therapeutic study*

The therapeutic efficacy of CPT-11-TSL in comparison to non-liposomal CPT-11 and Onivyde® was evaluated in the BN175 soft tissue sarcoma model in BN rats. All animals were treated with a dose of 20 mg/kg CPT-11 directly after the tumor had reached the target temperature of 41°C. The HT-treatment was performed for 1 h at 41°C. The tumor growth was monitored for up to 18 days.

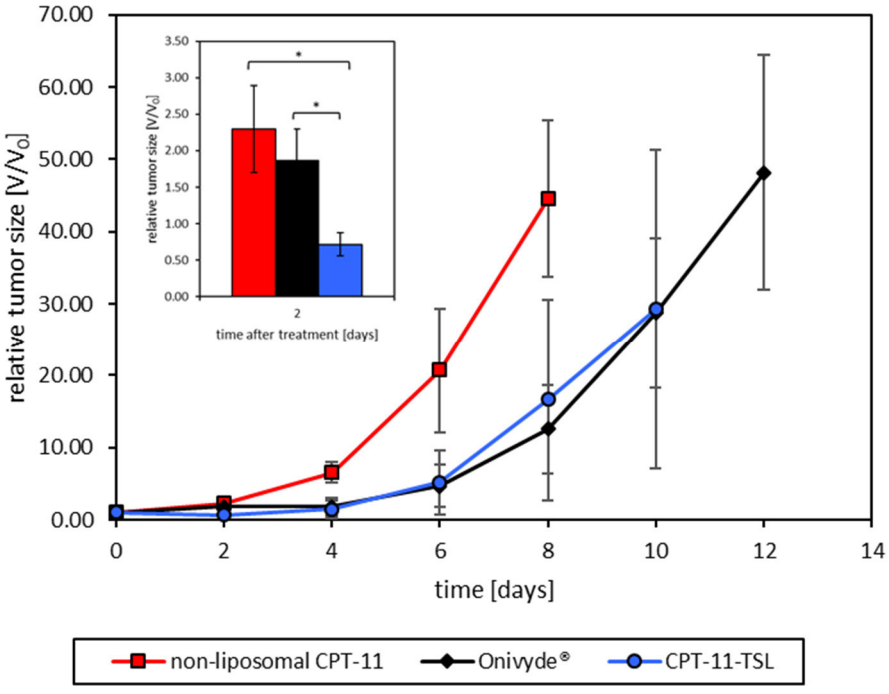


*Figure 4-48 Therapeutic efficacy of non-liposomal CPT-11, Onivyde® and CPT-11-TSL with HT-treatment for 60 min at 41° after injection of CPT-11 at dose of 20 mg/kg in the BN175 soft tissue sarcoma model (n=6 of non-liposomal CPT-11 and Onivyde®; n=7 for CPT-11-TSL).*
*Animal handling was performed by Dr. Simone Limmer. Values given as mean value ± standard deviation.*

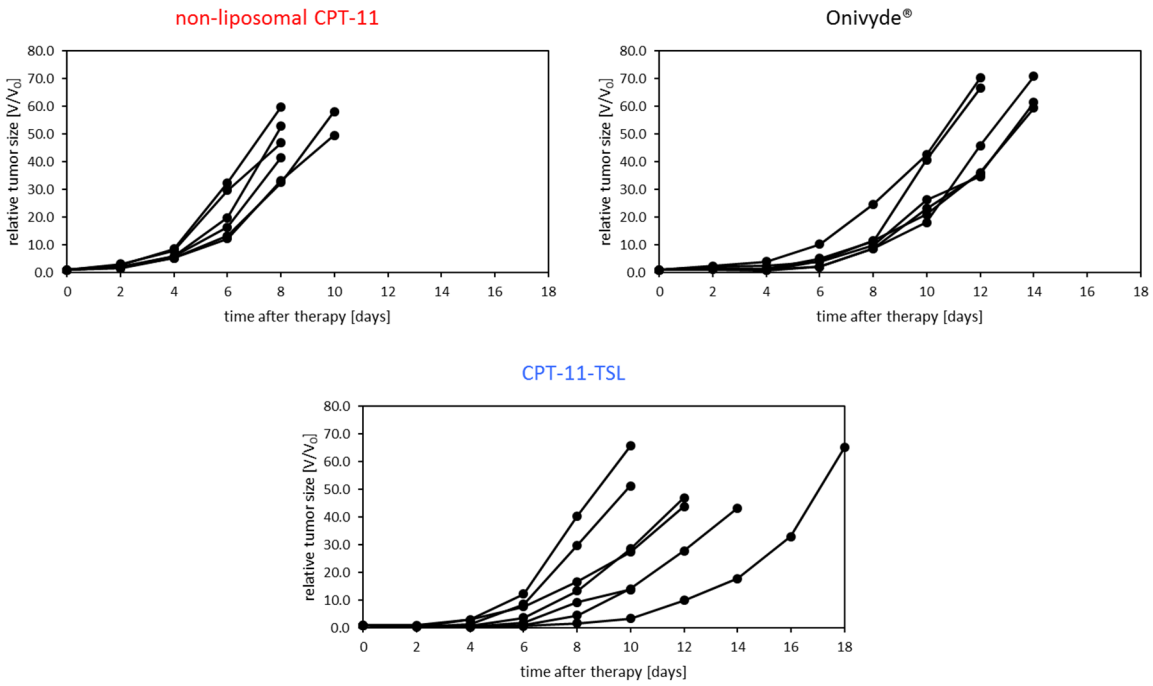


*Figure 4-49 Therapeutic efficacy in single animals of non-liposomal CPT-11, Onivyde® and CPT-11-TSL with HT-treatment for 60 min at 41° after injection of CPT-11 at dose of 20 mg/kg in the BN175 soft tissue sarcoma model (n=6 of non-liposomal CPT-11 and Onivyde®; n=7 for CPT-11-TSL). Tumor growth was monitored for up to 18 days. Animal handling was performed by Dr. Simone Limmer.*

CPT-11-TSL and Onivyde® showed tumor growth delay in rats when compared to non-liposomal CPT-11 (cf. Figure 4-48). For CPT-11-TSL, the tumor size was significantly reduced after 2 days of treatment compared to the other two treatment groups ($p < 0.00005$; insert Figure 4-48). The Onivyde® group shows a growth delay of 4 days. After 4 days in CPT-11-TSL- and Onivyde®-treated groups the tumor started again to grow. A significant difference for CPT-11-TSL and Onivyde® in comparison to non-liposomal CPT-11 was observed 8 days after treatment ($p<0.005$ and $p<0.0001$, resp.). Considering the results of the single animals of each group (cf. Figure 4-49) CPT-11-TSL treated animals showed a higher difference between the single animals in tumor growth compared to non-liposomal CPT-11 and Onivyde®.

## 4.3 Lyophilization of $DPPG_2$-based TSL

Storage of dFdC-TSL and CPT-11-TSL as liposomal dispersion at 2-8°C was possible (cf. 4.1.2.5 and 4.2.3.3). The lyophilization of $DPPG_2$-based TSL should be evaluated as next step to obtain an alternative storage possibility to store as liposomal dispersion. Lyophilized products have the advantage during storage that the lipid hydrolysis could be reduced, due to the lack of water.

### 4.3.1 Development of a lyophilization cycle

The development of a lyophilization cycle for $DPPG_2$-based TSL was performed with $DPPG_2$-TSL with encapsulated 100 mM CF with the phospholipid composition DPPC/DSPC/$DPPG_2$ 50:20:30 (molar ratio) (=CF-TSL). The liposomes were freshly prepared and fully characterized (z-average, PDI, ζ-potential, lipid and CF concentration, temperature-dependent CF-release, lipid composition) before lyophilization. CF was chosen as non-toxic surrogate molecule for encapsulation of drugs to avoid risk of contamination of facilities with cytotoxic drugs in the development phase.

#### *4.3.1.1 Lyophilization of CF-TSL without cryoprotectant*

CF-TSL without cryoprotectant were prepared and characterized with DLS, phosphate assay, TLC and temperature-dependent CF-release. 1 ml/vial of the formulation was aliquoted in six 2R-glass vials and placed on a shelf. The process graphic is shown in Figure 4-50.

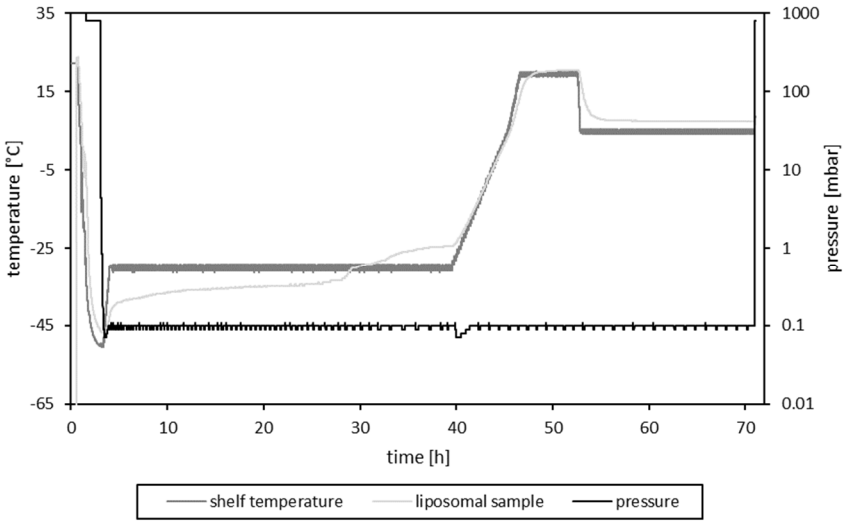


*Figure 4-50 Lyophilization process of CF-TSL without cryoprotectant.*
*A temperature-sensor was placed in one of the vials containing CF-TSL.*

After reconstitution of the lyophilized product with ultrapure water, z-average and PDI of the liposomal dispersion were measured with DLS. The liposomes showed a size of 412.1 nm and PDI of 0.451 (112.3 nm and 0.053 before lyophilization). The observed increase in size

and PDI were signs for the decomposition of the liposomes during lyophilization or reconstitution. The temperature-dependent release profile of these liposomes was not determined after lyophilization, because it was obvious that the liposomes were destroyed, as shown by the color change from orange to yellow of the dispersion due to notable CF leakage (cf. Figure 4-51).

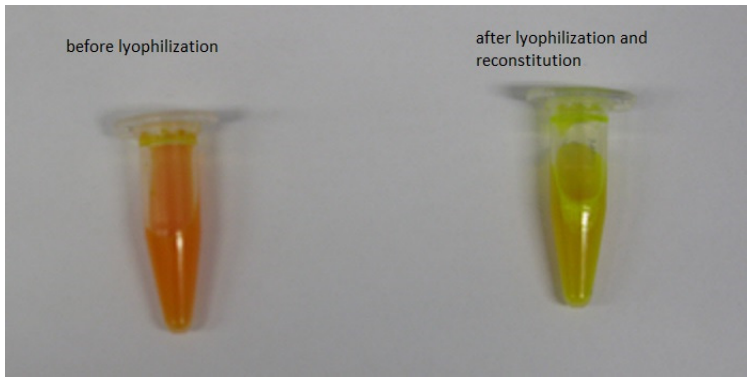


*Figure 4-51 Liposomal dispersion lyophilization (left) and after lyophilization and reconstitution (right).*

Amount of leakage of encapsulated compounds is a sign for the integrity of the liposomal dispersion during lyophilization and/or reconstitution. The leakage of CF, Dox or CPT-11 could be evaluated, comparing the background fluorescence intensity (BF) measured at RT of the dispersion before and after lyophilization. The increase in BF is proportional to the amount of leaked molecules [136]. Percentage BF is obtained by referring to fluorescence intensity of samples with completely released compounds by incubation with Triton X-100. Encapsulated CF, Dox, and CPT-11 are partly self-quenched due to the high intraliposomal concentration. After release and subsequent dilution into the extraliposomal buffer, fluorescence intensity increases. For evaluation of the success of a lyophilization cycle, the BF was determined as marker for CF-leakage additionally to the DLS measurements.

### *4.3.1.2 Lyophilization of CF-TSL with different cryoprotectants*

As next step liposomes with different intra- and extraliposomal cryoprotectants were prepared and characterized with DLS, phosphate assay, TLC and temperature-dependent CF-release (cf. Table 4-16). 1 ml/vial of the formulations was aliquoted in 2R-glass vials (number of vials cf. Table 4-16) and placed in the freeze-dryer.

| | **intraliposmal** | **extraliposomal** | **Vials lyophilized** |
|---|---|---|---|
| **formulation 1** | 100 mM CF in 5% trehalose | 5% trehalose + 0.45% NaCl | 2 |
| **formulation 2** | 100 mM CF in 0.9% NaCl | 5% sucrose + 0.4% NaCl | 7 |
| **formulation 3** | 100 mM CF in 5% trehalose | 10% trehalose | 2 |
| **formulation 4** | 100 mM CF in 5% sucrose | 5% sucrose + 0.4% NaCl | 2 |

*Table 4-16 Overview TSL formulations with intra- and extraliposmal different cryoprotectants used for lyophilization.*

Due to limited amounts of TSL (due to preparation process) only one vial per TSL formulation was analyzed after lyophilization. The freezing protocol was the same as shown in Figure 4-50 with some minor changes. The freezing temperature was set to -40°C instead of -50°C.

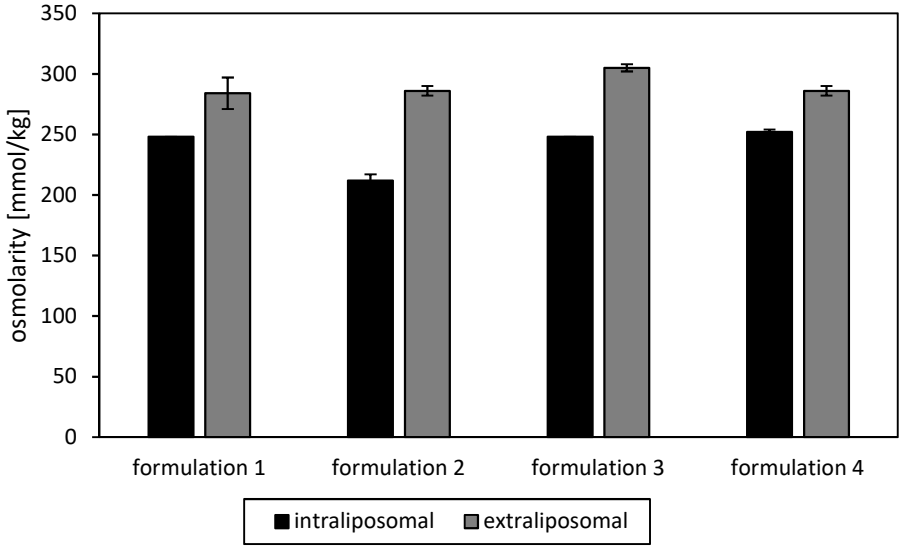


*Figure 4-52 Osmolarity of TSL with different intra- and extraliposomal cryoprotectants and cryoprotectant concentrations (refer to Table 4-16 for exact cryoprotectant and concentration). Values are given as mean value ± standard deviation of three independent measurements.*

The difference in osmolarity between extra- and intraliposomal space was similar for all used formulations (cf. Figure 4-52).

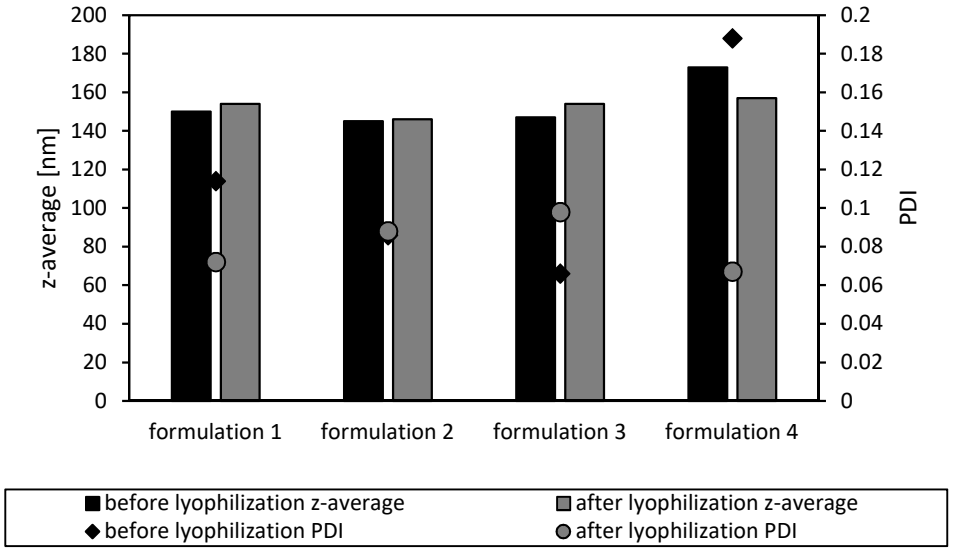


*Figure 4-53 z-average and PDI before and after lyophilization of CF-TSL with different intra- and extraliposomal cryoprotectants and cryoprotectant concentrations (refer to Table 4-16 for exact cryoprotectant and concentration).*

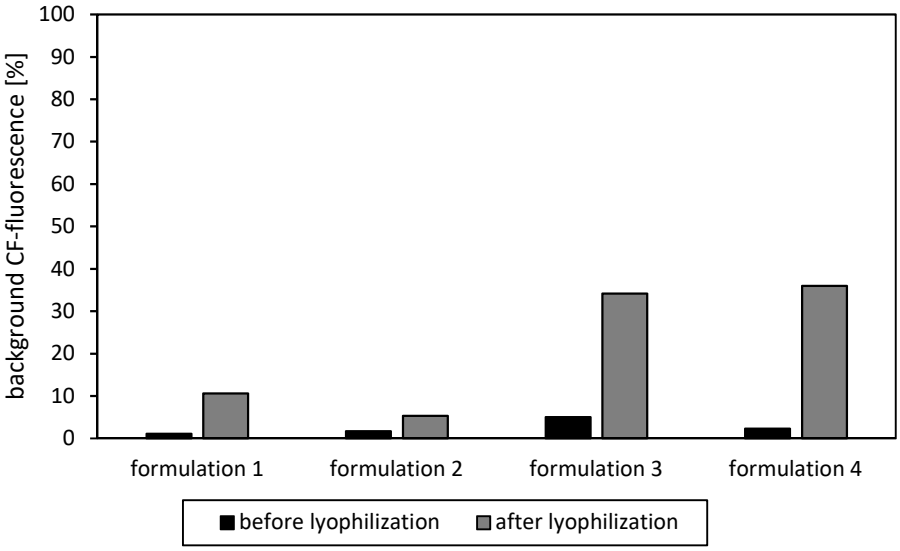


*Figure 4-54 BF before and after lyophilization of CF-TSL with different intra- and extraliposomal cryoprotectants and cryoprotectant concentrations (refer to Table 4-16 for exact cryoprotectant and concentration).*

No change in z-average and PDI was observed for the formulations before and after lyophilization (cf. Figure 4-53). CF-liposomes with intraliposomal 100 mM CF and extraliposomal 5% sucrose + 0.4% NaCl showed the lowest CF-leakage due to lyophilization (BF: 1.7% before drying; 5.3% after drying; cf. Figure 4-54). The NaCl was added to some extraliposomal solutions to adjust the osmolarity to physiological osmolarity when necessary. For trehalose the best result was achieved for CF-TSL with 5% intra- and extraliposomal trehalose (BF: 1.1% before drying; 10.6% after drying).

### *4.3.1.3 Evaluation of reconstitution media*

Next, different aqueous solutions were evaluated for reconstitution of CF-TSL after lyophilization. This experiment was performed with lyophilized CF-TSL with intraliposomal 100 mM CF and extraliposomal 5% sucrose + 0.4% NaCl.

Reconstitution of this CF-TSL in different media (ultrapure water; 0.9% NaCl; 5% dextrose), showed that the best result with regard to the CF-leakage was achieved by reconstitution with ultrapure water (7.1% compared to 17.7% for 0.9% NaCl and 11.1% for 5% dextrose).

### *4.3.1.4 Evaluation of different freezing methods*

In a subsequent step, the influence of freezing method was analyzed to find out which step in lyophilization is critical for integrity of CF-TSL. For this experiment CF-TSL shown in Table 4-17 were prepared and characterized with DLS, phosphate assay, TLC and temperature-dependent CF-release. 1 ml/vial of the formulations was aliquoted in 2R- glass vials (number of vials see Table 4-17) and three different freezing methods were tested. The tested

freezing methods were rapid freezing by using liquid $N_2$ or freezing after controlled nucleation (CN) at -5°C with a freezing rate of 1°C/min to -40°C. After freezing the vials were placed in the fridge to thaw again for evaluation of influence of freezing on the integrity of the liposomes.

| | intraliposmal | extraliposomal | Tested vials for each freezing method |
|---|---|---|---|
| **sucrose** | 100 mM CF in 0.9% NaCl | 5% sucrose + 0.4% NaCl | 2 |
| **gelatin** | 100 mM CF in 2% gelatin | 0.9% NaCl | 1 |
| **glycerol** | 100 mM CF in 0.9% NaCl | 2% glycerol | 2 |

*Table 4-17 Overview CF-TSL formulations used for evaluation of different freezing methods*

For CF-TSL with gelatin as cryoprotectant liposomal preparation and handling of the liposomes was difficult, due to gelling of the dispersion. Nevertheless, the results of the freezing study are shown, but for further experiments gelatin as cryoprotectant was not considered.

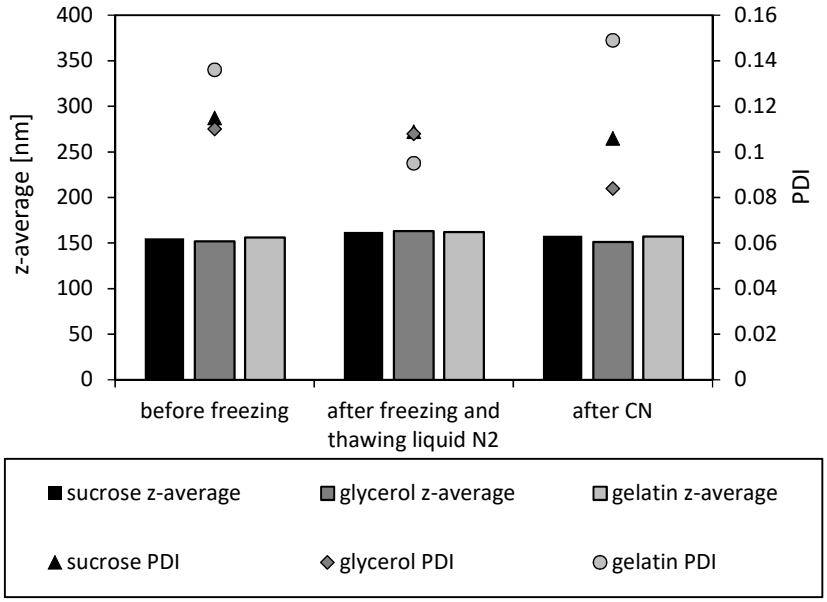


*Figure 4-55 Change in z-average and PDI after freezing either in liquid $N_2$ or with CN. Values are given as mean value of two analyzed vials for sucrose and glycerol TSL.*

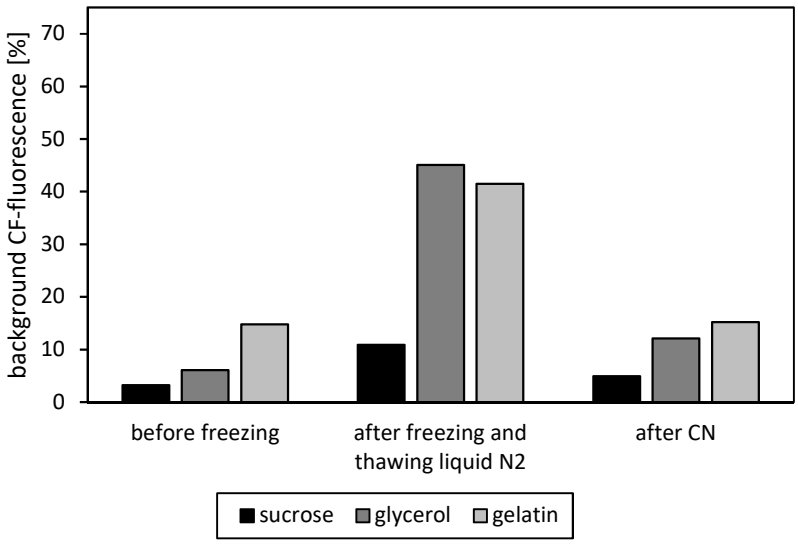


*Figure 4-56 Change in background CF-fluorescence after freezing either in liquid $N_2$ or with CN. Values are given as mean value of two analyzed vials for sucrose and glycerol.*

Necessity of cryoprotectants for lyophilization of $DPPG_2$-TSL was shown in 4.3.1.1 and 4.3.1.2, and therefore no TSL batch without cryoprotectants was used in the present experiment. The mode of freezing had no influence on z-average and PDI for all used cryoprotectants (cf. Figure 4-55), but influenced the leakage after different freezing methods. The best results were achieved with CN (cf. Figure 4-56). The sucrose CF-TSL showed the best results in both freezing experiments compared to CF-TSL with cryoprotectants gelatin or glycerol. The sucrose liposomes showed after CN and freezing to -40°C only a CF-leakage of 4.9±0.7% (before drying 3.2%) compared to 12.1±2.6% for glycerol and 15.2% for gelatin liposomes. The CF-leakage after fast freezing in liquid $N_2$ was higher for all tested formulations (10.9±0.9% for sucrose, 45.1±2% for glycerol and 41.2% for gelatin).
The leakage after freezing was in an acceptable range (< 10%) only for liposomes with sucrose as cryoprotectant and CN as freezing method.

### *4.3.1.5 Lyophilization with CN*

A complete lyophilization cycle with CN was performed to investigate if freezing or other process steps are critical to influence the quality of the liposomes. For this experiment two batches CF-TSL with 5% sucrose + 0.4% NaCl extraliposomal were prepared and characterized with DLS, phosphate assay, TLC and temperature-dependent CF-release. 1 ml/vial of the formulations was aliquoted in 2R- glass vials (3 vials batch 1, 10 vials batch 2) and lyophilized with the process shown in Figure 4-57.

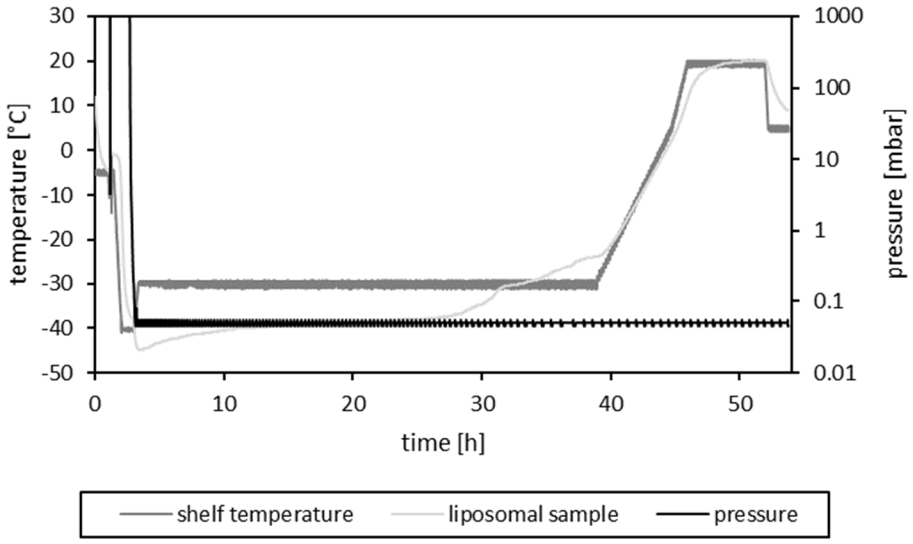


*Figure 4-57 Lyophilization process of CF-TSL (cryoprotectant extraliposomal 5% sucrose + 0.4% NaCl) with CN at -5°C and a freezing rate of 1°C/min.*
*A temperature-sensor was placed in one of the vials containing CF-TSL.*

Two independently prepared batches underwent the lyophilization process. For one batch Tg` was determined before drying (-29.8±1°C). After reconstitution of 3 vials of each batch, z-average, PDI and CF-release at RT were analyzed.

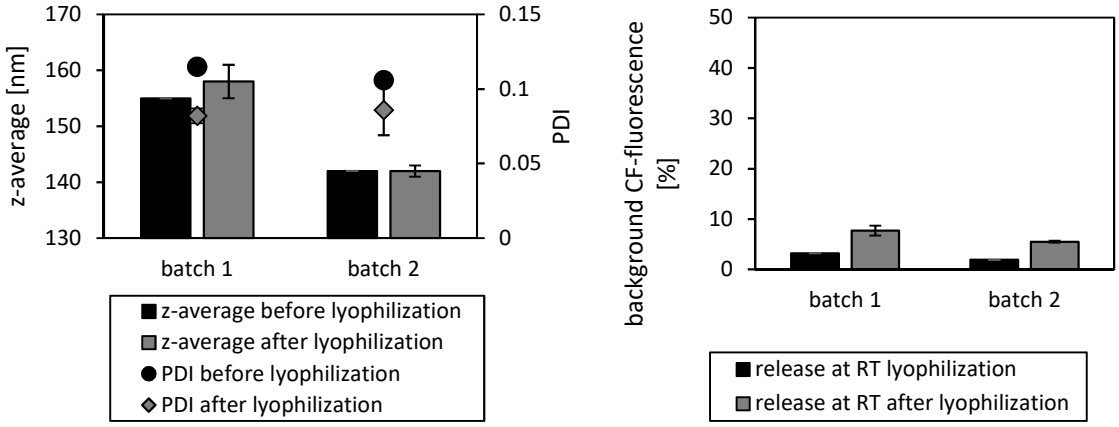


*Figure 4-58 left) z-average and PDI before and after lyophilization of CF-TSL. right) background CF-fluorescence before and after lyophilization of CF-TSL.*
*Values are given as mean value ± standard deviation of three analyzed vials.*

For both batches, PDI and z-average before and after lyophilization were similar (cf. Figure 4-58 left). The CF-leakage was increased but still in an acceptable range (< 10%). For one batch, the change was +4.5% and for the second batch it was +3.6%. The residual moisture was 2.69±0.39% (measured for one batch). The process shown in Figure 4-57 is suitable for CF-TSL with extraliposomal 5% sucrose + 0.4% NaCl. The regulatory authorities prefer a maximum water concentration of 3% [137] and so the residual moisture in these samples was close to this value.

## 4.3.2 Storage stability of lyophilized CF-TSL

Three vials of one batch prepared with controlled nucleation (cf. 4.3.1.5) were retested after 1.4 years' storage at 2-8°C. After reconstitution PDI, z-average, lysolipid content and CF-leakage in FBS were analyzed.

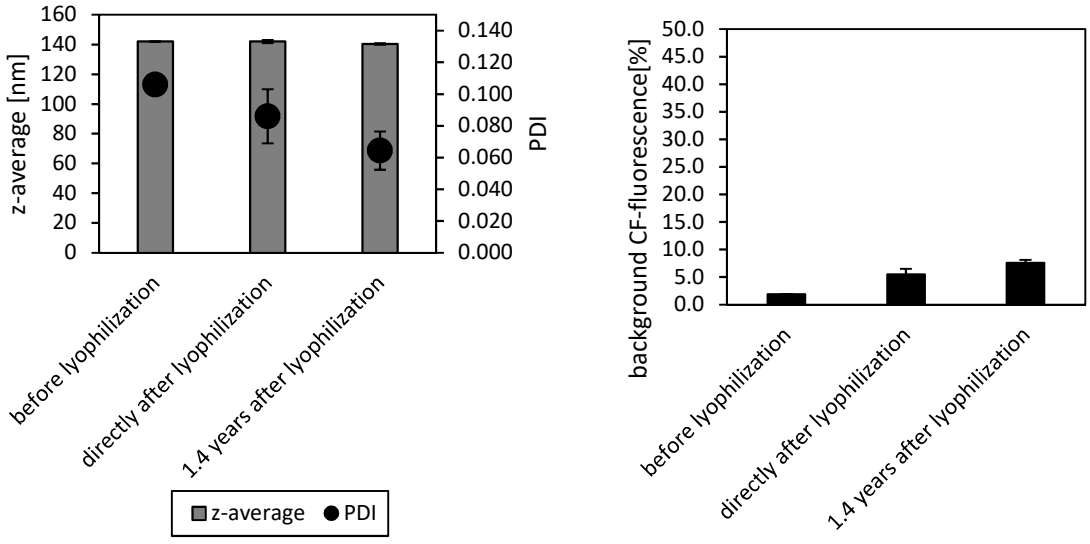


*Figure 4-59 left) Change in z-average and PDI of lyophilized CF-TSL after 1.4 years storage at 2-8°C right) Change in background CF-fluorescence of lyophilized CF-TSL after 1.4 years storage at 2-8°C. Values are given as mean value ± standard deviation of three analyzed vials.*

No change in z-average, PDI and CF-leakage in the reconstituted product could be detected compared to the results obtained directly after lyophilization (cf. Figure 4-59). The temperature-dependent release from 37-45°C was also unaffected by storage (data not shown). Also, no lysolipids, which are known to be generated during storage, were detectable (data not shown). These results indicate that lyophilized CF-TSL might be stable at 2-8°C during storage, but this has to be confirmed by a more formal stability study at 2-8°C. RT was chosen as second storage condition.

For the storage stability study CF-TSL with intraliposomal 100 mM CF and extraliposomal 5% sucrose + 0.4% NaCl as cryoprotectant were prepared and characterized with DLS, phosphate assay, TLC and temperature-dependent CF-release. 1 ml/vial of the formulations was aliquoted in 81 2R- glass vials. The lyophilization cycle of CF-TSL for the storage stability study is shown in Figure 4-60. Compared to the process depicted in Figure 4-57 the only change was the prolongation of the secondary drying time to 10 h instead of 6 h to reduce residual moisture in the lyophilized product (see section 4.3.1.5). The vials were stored at two storage conditions (2-8°C and RT) to investigate the effect of storage temperature on the stability. For each time point and conditions, 3 independent vials have been pulled and investigated with DLS, TLC, Karl-Fischer-titration and temperature-

dependent release, respectively. The time points were 0, 1, 3, 6 months and spare vials for additional time points up to 24 months were stored.

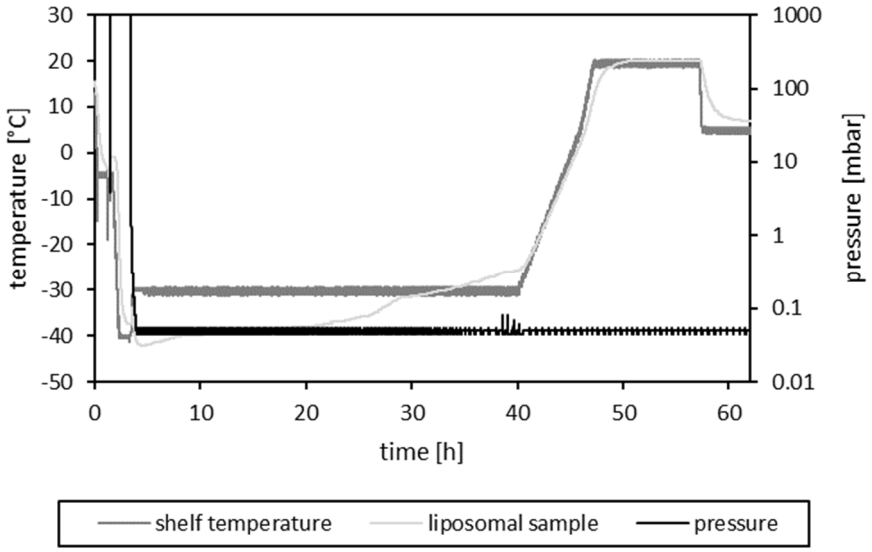


*Figure 4-60 Lyophilization process of CF-TSL (cryoprotectant extraliposomal 5% sucrose + 0.4% NaCl) with CN at -5°C and a freezing rate of 1°C/min for a storage stability study at 2-8°C and RT. A temperature-sensor was placed in one of the vials containing CF-TSL.*

After 0, 1, 3, and 6 months of storage, the temperature-dependent CF-release in FBS, CF-leakage, lysolipid content, z-average and PDI were analyzed after reconstitution of the product and residual moisture was determined of the lyophilized product.

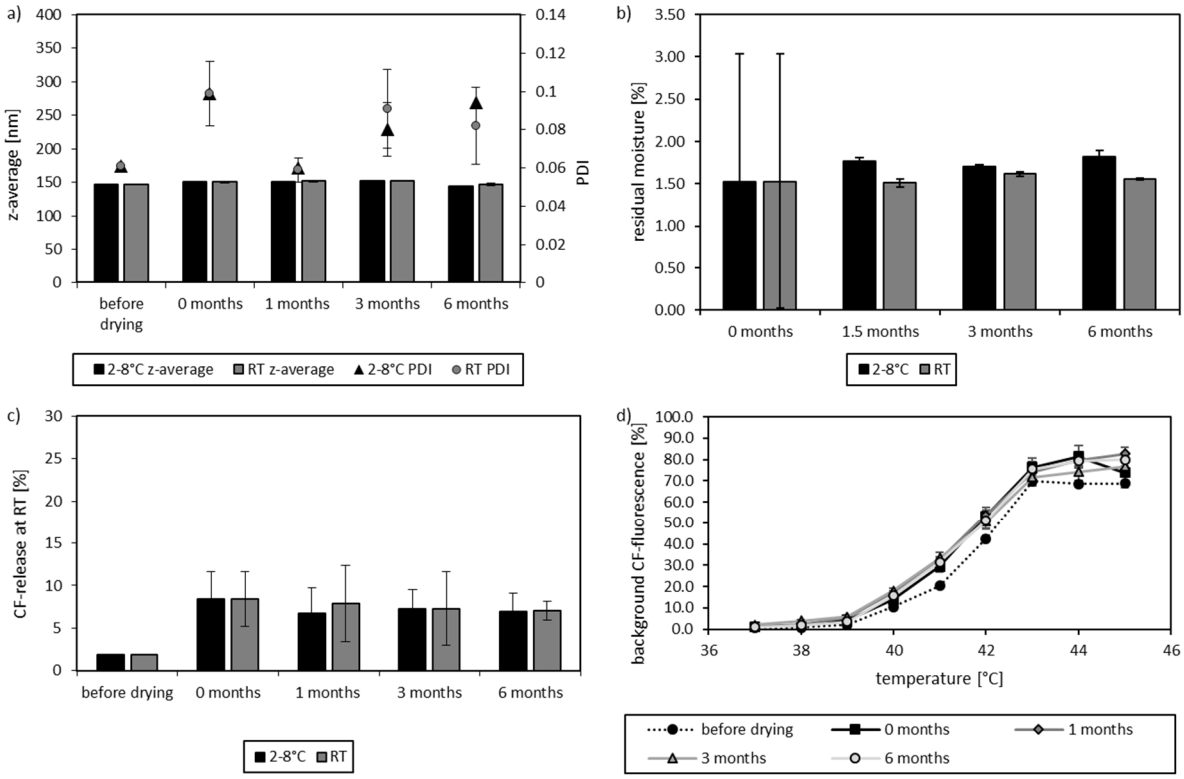


*Figure 4-61 Change in different parameters after storage of lyophilized CF-TSL at RT or 2-8°C. a) PDI and z-average; b) residual moisture; c) background CF-fluorescence; d) temperature-dependent CF-release after 5 min incubation at 37-45°C in FBS (data only shown for storage at 2-8°C). Values are given as mean value ± standard deviation of three analyzed vials.*

Figure 4-61 shows, that storage at 2-8°C and RT was possible for at least 6 months. No change in z-average, PDI, residual moisture, CF-leakage and CF-release at 37-45°C was detectable compared to the parameters directly after lyophilization. For the temperature-dependent CF-release at 37-45°C only the temperature profiles for the samples stored at 2-8°C were shown, because the profiles for the lyophilized samples stored at RT showed the same result. The standard deviation in the residual moisture for the measurement directly after lyophilization were high, due to a technical problem of the Karl-Fischer titrator. Because of the required repair work, the next measurement was only performed after 1.5 month. The samples stored at 2-8°C showed slightly higher residual moisture content compared to samples stored at RT already after 1.5 months (1.77±0.04% compared to 1.51±0.04%), but did not increase further during storage. A parameter which could be affected by residual moisture in the samples was the content of lysolipids, which might be formed due to phospholipid hydrolysis with water. However, in the first 6 months no lysolipids independent of storage temperature were detected. The visual inspection of the vials during storage also showed no visible change in cake appearance.

## 4.3.3 Lyophilization of liposomes containing cytostatic agents

### *4.3.3.1 Adjustment of the lyophilization process for vials wrapped in sterile bags with CF-TSL*

Since lyophilization of TSL containing cytostatic agents had to be performed with vials wrapped in sterile bags to avoid contaminations in case of breakage of the vials, the lyophilization cycle shown in 4.3.1 was changed, because CN with the ice-fog method is not possible through sterile bags. Two different changes to replace CN were tested, on the one hand an additional annealing step at -15°C for 4 h and on the other hand a reduced freezing rate of 0.2°C/min (instead of 1°C/min) (cf. Figure 4-62). Additionally, two different dispersion volumes (1 ml in a 2R-vial or 4 ml in a 10R-vial) were tested.

CF-TSL with intraliposomal 100 mM CF and extraliposomal 5% sucrose + 0.4% NaCl as cryoprotectant were prepared for these two experiments and characterized with DLS, lipid concentration, TLC and temperature-dependent CF-release.

The overall process time for the cycle with the freezing rate of 0.2°C/min was 14 h shorter compared to the process with the annealing step (72 h in comparison to 86 h) (cf. Figure 4-62).

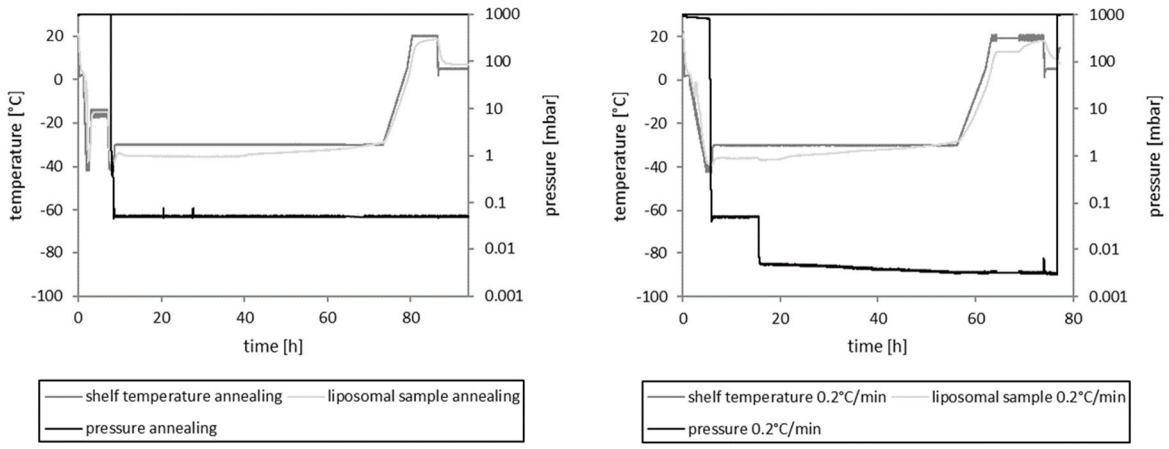


*Figure 4-62 Lyophilization process of CF-TSL (cryoprotectant extraliposomal 5% sucrose + 0.4% NaCl) with an annealing step at -15°C (left) or a freezing rate of 0.2°C/min (right).*
*A temperature-sensor was placed in one of the vials containing CF-TSL for each lyophilization cycle.*

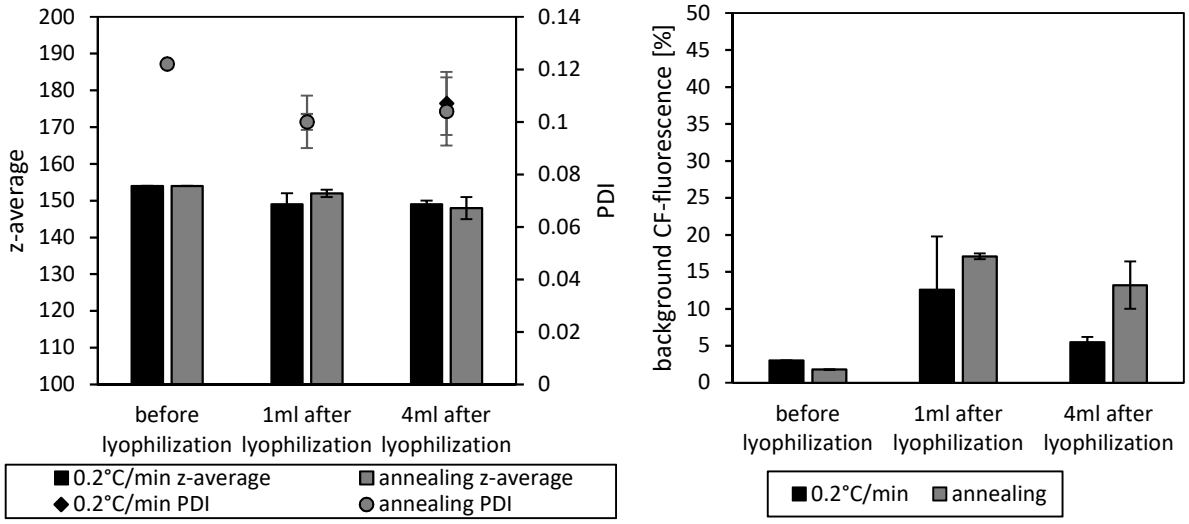


*Figure 4-63 left) Comparison of z-average and PDI of lyophilized CF-TSL after lyophilization with a freezing rate of 0.2°C/min (black) or an additional annealing step after freezing with a freezing rate of 1°C/min at -15°C for 4 h (grey) right) Comparison of background CF-fluorescence of lyophilized CF-TSL after lyophilization with a freezing rate of 0.2°C/min (black) or an additional annealing step after freezing with a freezing rate of 1°C/min at -15°C for 4 h (grey).*
*Two fill volumes 1 ml or 4 ml CF-TSL in 2R or 10R-vials were lyophilized. Values are given as mean value ± standard deviation of three analyzed vials.*

The PDI and z-average showed no change after lyophilization independent form the mode of freezing (annealing step or 0.2°C/min freezing rate) and different fill volumes (1 ml or 4 ml) (cf. Figure 4-63 left). But the CF-leakage was less for the low freezing rate of 0.2°C/min for the 1 ml (12.6±7.2%) and the 4 ml sample (5.5±0.7%) compared to the samples lyophilized with an annealing step (17.1±0.4% for 1 ml and 13.2±3.2% for 4 ml) (cf. Figure 4-63 right). Comparing the CF-leakage of the 4 ml fill volume lyophilized with 0.2°C/min freezing rate with CF-leakage of CF-TSL lyophilized with CN (1 ml sample) the leakage was similar (5.5±0.7% vs. 5.5±0.2%).

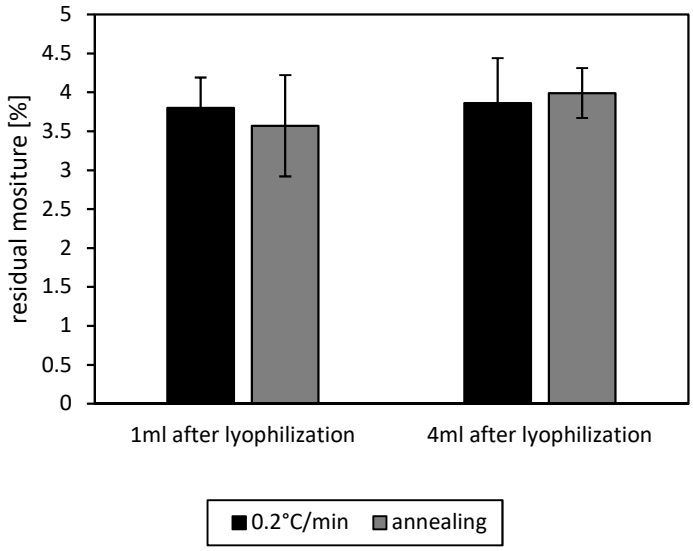


*Figure 4-64 Comparison of residual moisture of lyophilized CF-TSL after lyophilization with a freezing rate of 0.2°C/min (black) or an additional annealing step after freezing with a freezing rate of 1°C/min at -15°C for 4 h (grey).*
*Two fill volumes 1 ml or 4 ml CF-TSL in 2R or 10R-vials were lyophilized. Values are given as mean value ± standard deviation of three analyzed vials of each fill volume.*

The residual moisture was similar for all samples (cf. Figure 4-64), but one difficulty in handling the vials wrapped in sterile bags, was that the vials had to be stoppered by hand due to glass breakage, resulting when automatic stoppering of the vials was performed. This stoppering caused a higher residual moisture, but it is acceptable for further experiments with vials wrapped in sterile bags.

For shortening of the lyophilization process of vials wrapped in sterile bags, the freezing rate was again increased from 0.2°C/min to 1°C/min after the samples were nucleated. This experiment was performed in a fill volume of 4 ml of CF-TSL with intraliposomal 100 mM CF and extraliposomal 5% sucrose + 0.4% NaCl as cryoprotectant after characterization with DLS, lipid concentration, TLC and temperature-dependent CF-release.

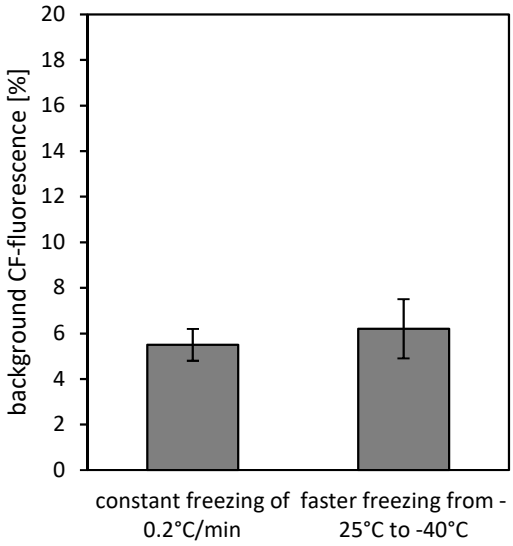


*Figure 4-65 Comparison of background CF-fluorescence of lyophilized CF-TSL with a constant freezing rate of 0.2°C/min to -40°C or a freezing rate of 0.2°C/min to -25°C with a subsequent freezing rate of 1°C/min to -40°C.*
*Values are given as mean value ± standard deviation of three analyzed vials.*

Figure 4-65 shows the faster freezing rate of 1°C/min (from -25°C to -40°C) after nucleation of the samples at a shelf temperature of -25°C instead of constant freezing rate of 0.2°C/min did not influence the CF-leakage. In z-average and PDI also no change was seen (data not shown).

Additionally, for optimization of the lyophilization of vials wrapped in sterile bags COP-plastic and glass vials (both 2R- and 10R-vials) were tested, to see if the vial material had an influence on the CF-leakage and z-average. For this experiment CF-TSL with intraliposomal 100 mM CF and extraliposomal 5% sucrose + 0.4% NaCl as cryoprotectant were prepared and characterized with DLS, lipid concentration, TLC and temperature-dependent CF-release.

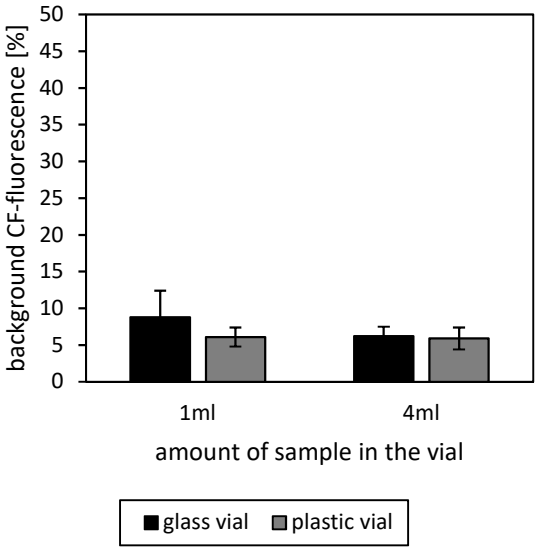


*Figure 4-66 Comparison of background CF-fluorescence after lyophilization of 1 ml or 4 ml CF-TSL in glass or plastic vials.*
*Values are given as mean value ± standard deviation of three analyzed vials, except for 4 ml plastic vials, for these only 2 vials were analyzed.*

For 4 ml liposomal sample in a 10R-vial the vial-material had no influence on the CF-leakage (cf. Figure 4-66). For glass vials the CF-leakage was 6.2±1.3% and for plastic vials 5.9±1.5%. For 1 ml of liposomal sample in 2R-vials the plastic vials showed slightly decreased CF-leakage (6.1±1.3%) compared to 1 ml liposomal sample in 2R- glass vials (8.8±3.6%). The z-average and PDI were not influenced by the used vial material (data not shown).

For vials wrapped in sterile bags (lyophilization with CN not possible) the dispersion volume had an influence on stability. With increasing dispersion volume, the CF-leakage decreased. The freezing rate also had an influence, with decreasing freezing rate (0.2°C/min instead of 1°C/min) the leakage also decreased. The slow freezing rate is only necessary until dispersion in all vials was nucleated, after this the freezing rate could be increased to shorten the lyophilization process. Due to better availability of glass vials, these vials were used for the following experiments, because for 4 ml fill volume no difference was seen between glass and plastic vials.
For lyophilization of TSL with cytostatic agents 4 ml fill volume as well as a freezing rate of 0.2°C/min should be used, because this process showed the best results for CT-TSL concerning the leakage.

### *4.3.3.2 Lyophilization TSL containing cytostatic agents*

For the lyophilization of TSL containing Dox, CPT-11 or dFdC the vials (4 vials per drug) containing 4 ml of liposomal sample were wrapped in sterile bags and the process established in 4.3.3.1 with a freezing rate of 0.2°C/min to -40°C was used. 5% sucrose + 0.4% NaCl were used extraliposomally as cryoprotectant for all TSL. As control, CF-TSL were also lyophilized for comparison of the process with former lyophilization cycles preformed during the process development. The vial material used was glass, due to better availability of these vials and no difference in CF-leakage between glass and plastic vials for 4 ml liposomal sample in a vial. The TSL encapsulating CF, Dox or CPT-11 had the phospholipid composition DPPC/DPSC/$DPPG_2$ 50:20:30 (molar ratio). The dFdC-TSL were composed of DPPC/DSPC/$DPPG_2$ 60:10:30 (molar ratio). The osmolarity of all four formulations was around physiological osmolarity (between 263-283 mmol/kg). The Tg` was for CF-TSL -29.8±1°C, for Dox-TSL -35.9±2.8°C and for dFdC-TSL -31.5±3.4°C.

The process graphic is shown in Figure 4-67. For each drug three vials were analyzed after lyophilization.

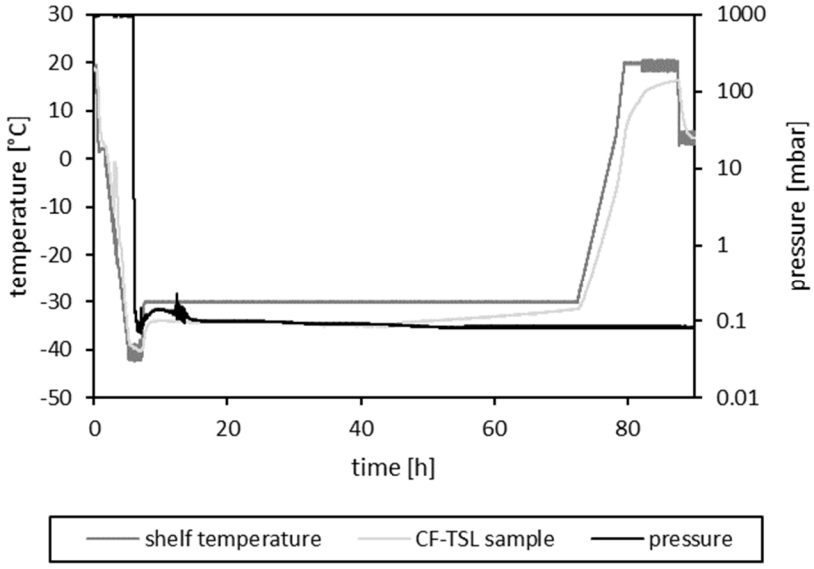


*Figure 4-67 Lyophilization process of CF-TSL, dFdC-TSL, Dox-TSL and CPT-11-TSL (cryoprotectant extraliposomal 5% sucrose + 0.4% NaCl) with a freezing rate of 0.2°C/min to -40°C.*
*A temperature-sensor was placed in one of the vials containing CF-TSL.*

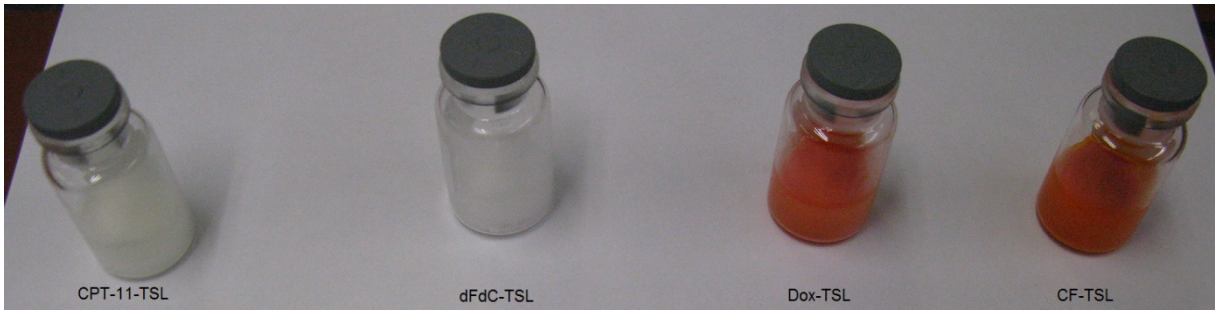


*Figure 4-68 Lyophilized samples of CPT-11-TSL, dFdC-TSL, Dox-TSL and CF-TSL.*

All TSL samples showed after lyophilization the same cake appearance independent from encapsulated compound (cf. Figure 4-68). The residual moisture was determined only for CF-TSL, due to safety issues by handling cytotoxic drugs in powder form. It was in an acceptable range for vials wrapped in sterile bags and stoppering of the vials per hand with 3.24±0.34%.

During reconstitution of CPT-11-TSL with ultrapure water the dispersion became very foamy and showed a gel-like behavior (cf. Figure 4-69). For all other formulations, the reconstitution step was unproblematic.

*Figure 4-69 CPT-11-TSL after reconstitution with ultrapure water.*

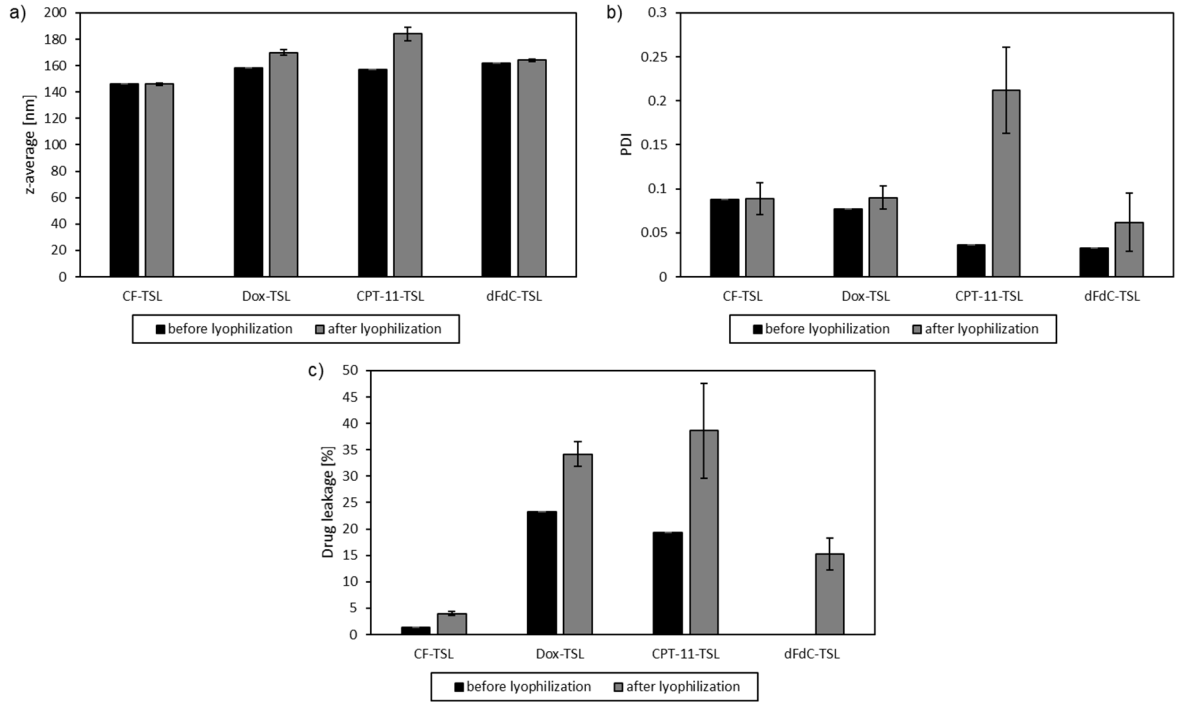


*Figure 4-70 a) z-average before and after lyophilization for CF-TSL, Dox-TSL, CPT-11-TSL and dFdC-TSL; b) PDI before and after lyophilization for CF-TSL, Dox-TSL, CPT-11-TSL and dFdC-TSL; c) drug-leakage before and after lyophilization for CF-TSL, Dox-TSL, CPT-11-TSL and dFdC-TSL.*
*Drug-leakage was calculated for dFdC-TSL by (free dFdC (µg/ml) at RT/ free dFdC (µg/ml) after triton treatment)x100. Values are given as mean value ± standard deviation of three analyzed vials.*

Z-average of CF-TSL and dFdC-TSL before and after lyophilization was not changed (cf. Figure 4-70 a, b). For Dox-TSL and CPT-11-TSL the z-average was increased after lyophilization (Dox-TSL 158±0nm before and 170±2nm after lyophilization; CPT-11-TSL 157±0nm before and 184±5nm after lyophilization). The PDI change for CF-TSL, Dox-TSL and dFdC-TSL was in an acceptable range, because for all three formulations after the lyophilization it was still < 0.1. For CPT-TSL the PDI increased to 0.212±0.049 after lyophilization (0.036 before lyophilization). For all three TSL formulations with cytostatic agents the drug-leakage was increased. For dFdC-TSL after lyophilization the dFdC-leakage was 15.3±3.0% in contrast to 0% before lyophilization (cf. Figure 4-70 c). The CPT-11-TSL showed an increase of BF to 38.6±9.0% compared to 19.3±0% BF before lyophilization and the Dox-TSL showed an increase of BF to 34.2±2.3% after lyophilization compared to 23.2±0% BF before lyophilization. The CF-TSL showed a similar CF-leakage after lyophilization as for freeze-drying cycles shown before (1.3±0% before and 4.0±0.4% after lyophilization).

The temperature-dependent drug release was measured for all three drug formulations to investigate the effect of lyophilization and reconstitution on the release behavior of the formulations (cf. Figure 4-71).

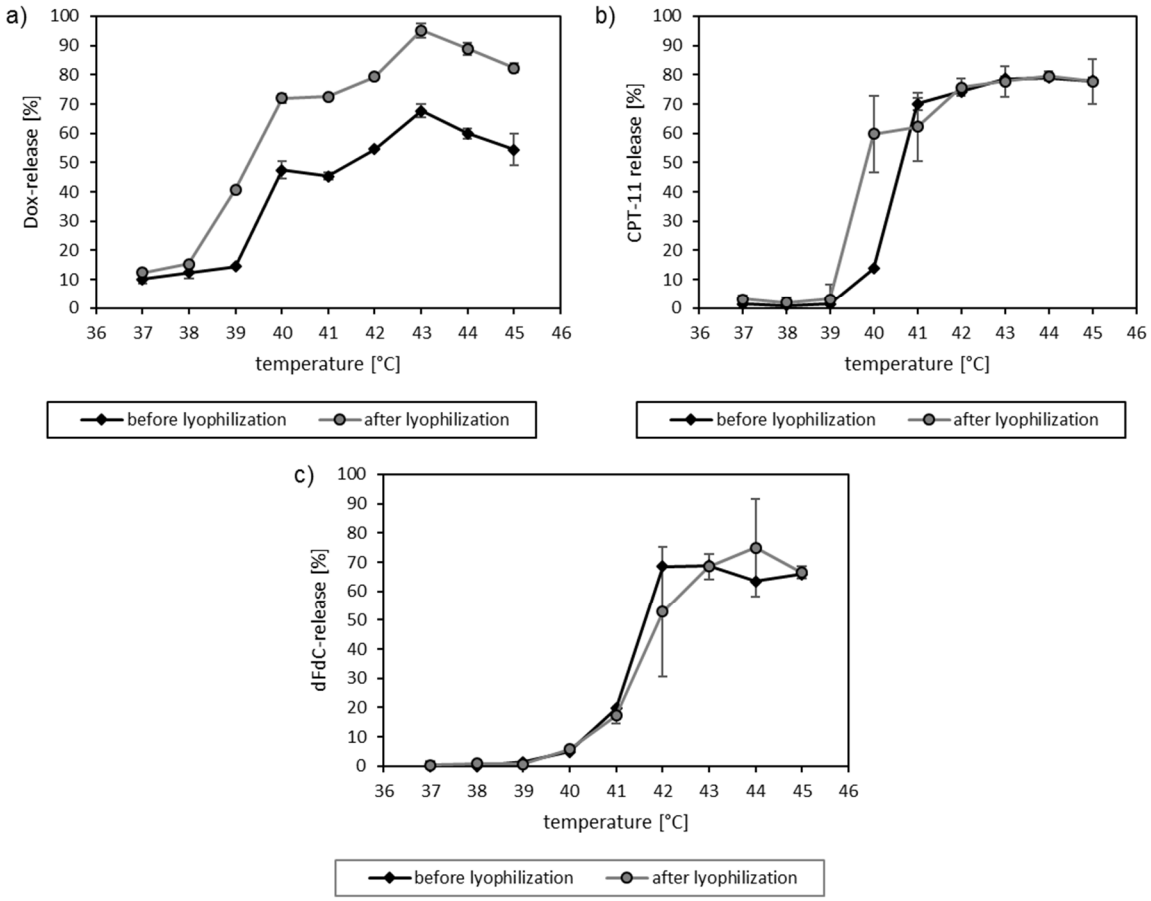


*Figure 4-71 Temperature-dependent a) Dox-, b) CPT-11- or c) dFdC-release after incubation for 5 min at temperatures between 37-45°C in FBS before and after lyophilization of the TSL.*
*Values are given as mean value ± standard deviation of three analyzed vials.*

The Dox-TSL were destabilized by lyophilization at temperatures > 38°C (cf. Figure 4-71 a). The release before lyophilization at 39°C was, e.g. 14.4±0.2% and after lyophilization 40.8±0.5%. The TSL with encapsulated CPT-11 showed also a less stable behavior at 40°C (13.7±0.3% before and 59.7±12.9% after lyophilization) after the lyophilization (cf. Figure 4-71b). For Dox-TSL and CPT-11-TSL no difference in release after incubation for 1 h at 37°C or 42°C was detectable comparing the values before and after lyophilization (data not shown). The dFdC-TSL showed a similar temperature-dependent behavior before and after lyophilization (cf. Figure 4-71c). The only difference was that the standard deviations of lyophilized samples was higher, especially at 42 and 44°C.

Success of lyophilization of $DPPG_2$-based TSL was influenced by the encapsulated drug. When using the same extraliposomal buffer (5% sucrose + 0.4% NaCl) and lyophilization process, the dispersion characteristic of $DPPG_2$-TSL with encapsulated dFdC were hardly affected, whereas the opposite was shown for $DPPG_2$-TSL with encapsulated CPT-11, respectively. Therefore, the lyophilization process developed for $DPPG_2$-TSL with encapsulated CF has to be individually adjusted to get an acceptable lyophilized product.

# 5. Discussion

## 5.1 dFdC-TSL

The objective was to improve a previously described TSL-formulation encapsulating dFdC ($dFdC_3$-$TSL_{5/2/3/0}$), which showed *in vitro* instability regarding phospholipid hydrolysis and unwanted initial drug leakage [44]. To ensure comparability of data, $dFdC_3$-$TSL_{5/2/3/0}$ was prepared in context of this work and used as control in the experiments instead of using already published data.

### 5.1.1 Assay to determine FFA in liposomal formulations

To analyze the degradation products of phospholipids in liposomal formulations during preparation an analytical method for determination of FFA was tested for usage for liposomal samples. As FFAs can be considered as markers of phospholipid hydrolysis, their determination (i.e. quantification) is crucial in the context of the characterization of liposomal formulations [97, 138]. FFA and endogenously generated lysolipids had been known to destabilize liposomal membranes [42, 97, 129, 130, 139, 140]. In literature, the determination of FFA for TSL formulations is no standard for *in vitro* characterization and therefore a method had to be established. Even the determination of lysolipids has been used only in a few publications [31, 44, 45] although the European Medicines Agency suggests the analysis of critical degradation in liposomal products [141].

The assay chosen for determination of FFA is based on a clinically used enzymatic kit, which uses the enzymatic endpoint method published by Trinder et al [119, 120]. This method was selected, because the relevance of quantification of formed FFAs prevailed over the relevance of the identification of individual FFA compounds. Only two different FFA were expected (palmitic and stearic acid). It could be shown that the method is linear in a range between 0.05 mM and 7.08 mM (Figure 4-1). Higher concentrations could not be measured due to limit of solubility of the reference standard sodium palmitate used. The limit of quantification was shown to be 0.1 mM (Figure 4-3). The standard liposomal formulation used within the scope of this work had a phospholipid concentration > 20 mM and so free fatty acids down to 0.5% in the formulation could be detected. For the TLC method used for lysolipid quantification the limit of detection was around 1% in a formulation as well. Other methods which were suitable to identify the FFA were HPLC methods with a CAD or MS detection as well as gas chromatography. Within the scope of this project the qualification was not necessary and the established method to quantify total FFA and lysolipid content was sufficient. One drawback of the method was the analysis of FFA in TSL when fluorescent molecules were encapsulated in the core, because the fluorescent compounds also showed an UV/Vis-absorption which interferes with the absorption of the analyte of the

enzymatic reaction (data not shown). For quantification of FFA from dFdC-TSL formulations, the enzymatic assay was feasible.

### 5.1.2 Improvement of dFdC-TSL

The $dFdC_3$-$TSL_{5/2/3/0}$ showed 1.3±1.1% Lyso-PC as well as an *in vitro* leakage upon rapid dilution of 15.6±9.2% [44], respectively. To reduce the degradation products as well as the leakage, the formulation was analyzed *in vitro* in more detail.

The pH of the Gemzar®-solution used for the passive encapsulation of $dFdC_3$-$TSL_{5/2/3/0}$ was measured to be 2-3. Since Grit and Crommelin showed in 1993 that the hydrolysis of phospholipids is pH dependent and has a minimum at a pH of 6.5 [97, 138], the acidic pH of the Gemzar® solution might be a driver behind the phospholipid hydrolysis during preparation and storage of the TSL formulation. To prevent lysolipid formation, the pH of Gemzar® had to be raised to more neutral conditions. It was demonstrated that it is possible to obtain a dFdC-solution with a pH of 6-6.5 by addition of $NaHCO_3$. The pH change did not result in precipitation of dFdC from the solution and thus to a lower concentration (cf. Figure 4-6). The adapted preparation method with two additional steps and a dFdC solution with pH 6-6.5 shown in Figure 4-8 resulted in dFdC-TSL with comparable characteristics like vesicle size, PDI, zeta potential, encapsulation efficacy, drug/lipid ratio as well as lipid and dFdC content but without detectable FFA and lysolipids (cf. Table 4-1). The two additional steps during preparation were necessary to achieve a comparable EE, because the adjustment of the pH to 6-6.5 resulted in a lower dFdC concentration due to dilution. The absence of lysolipids in the formulation ($dFdC_6$-$TSL_{5/2/3/0}$) resulted in a formulation with higher stability at 41-42°C in FBS. The release at 42°C after 5 min incubation was only 22.3±10.5% compared to 45.9±17.6% for $dFdC_3$-$TSL_{5/2/3/0}$ (cf. Figure 4-9). For *in vivo* experiments the amount of dFdC released within 5 min at 42°C was too low, because the tumor tissue could only be heated to 41°C by light exposure [44]. Insufficient amounts of dFdC would be released from TSL at this temperature. The release at 41°C after 5 min incubation was increased by changing the phospholipid composition by lowering the DSPC amount or the incorporation of 5% Lyso-PC in the formulation. Since $dFdC_3$-$TSL_{5/2/3/0}$ showed endogenously produced Lyso-PC levels due to phospholipid hydrolysis, a formulation with 5% P-Lyso-PC was produced with the improved method to obtain a formulation with a defined amount of Lyso-PC (Lyso-PC content for formulation $dFdC_3$-$TSL_{5/2/3/0}$ varied during batches), and no endogenously produced FFA, to investigate the effect of P-Lyso-PC on *in vitro* and *in vivo* behavior of dFdC-TSL. Lowering DSPC percentage shifted the $T_m$ to lower temperatures resulting in higher release at temperatures around 41-42°C with similar stability at 37-39°C (cf. Figure 4-11 and Table 4-3), because DSPC was the phospholipid with the highest $T_m$ (54.9°C) [26, 30, 37, 142, 143]. The temperature shift to lower temperatures by incorporation

of 5% Lyso-PC in the membrane could be explained by a model described by Banno et al, namely lysolipids tend to dissociate from the liposomal membrane at temperatures around $T_m$ [144]. Another explanation could be a shift of $T_m$ to lower temperatures by incorporation of Lyso-PC as seen for dFdC$_6$-TSL$_{4.5/2/3/0.5}$ in comparison to dFdC$_6$-TSL$_{5/2/3/0}$ (43.68±0.43°C vs. 44.27±0.26°C, cf. Table 4-3). This was also described by Needham (Patent application WO 1999/065466) for a formulation consisting of DPPC/P-Lyso-PC.

The change in phospholipid composition did not result in changes in the characteristics of the TSL like z-average, PDI, encapsulation efficacy and drug/lipid ratio (cf. Table 4-2). The formulations dFdC$_6$-TSL$_{6/1/3/0}$, dFdC$_6$-TSL$_{7/0/3/0}$ and dFdC$_6$-TSL$_{4.5/2/3/0.5}$ showed *in vitro* the most promising dFdC release, because of their stability at 37°C and an acceptably high release at 41°C. These formulations were evaluated in more detail. The 1 h stability at 37°C in FBS which was shown for all formulations (cf. Figure 4-13), was of particular importance, because 1 h is the standard HT-treatment time [51] and the TSL should circulate stably in the blood stream during this time in the non-heated body areas. In 2015 Affram et al published a dFdC-TSL formulation (phospholipid composition DPPC/MPPC/DSPE-PEG$_{2000}$ 90:10:4 molar ratio) which showed already 25% dFdC leakage after 10 min incubation at 37°C in PBS [145, 146], which might be notably higher in presence of FBS [30, 147]. For dFdC$_6$-TSL$_{6/1/3/0}$, dFdC$_6$-TSL$_{7/0/3/0}$ and dFdC$_6$-TSL$_{4.5/2/3/0.5}$ the release after 1 h incubation in FBS was less than 2.3% (cf. Figure 4-13). Measuring release of TSL in FBS was also more relevant with respect to *in vivo* conditions [147]. The release results shown by May et al for their HaT-dFdC formulation, which are composed of DPPC and Brij78, were performed in a mixture of FBS and saline (50:50) [148]. The HaT-formulation showed stability at body temperature with no observable release at 37°C for 30 min and marked release at temperatures >39°C already after 2 min (100% release at 41-42°C after < 2 min) [148]. This formulation should be more comparable in *in vivo* behavior to the improved formulations dFdC$_6$-TSL$_{6/1/3/0}$, dFdC$_6$-TSL$_{7/0/3/0}$ and dFdC$_6$-TSL$_{4.5/2/3/0.5}$.

By adjusting the pH of the dFdC-solution to pH 6-6.5 for encapsulation, the initial drug leakage observed for dFdC$_6$-TSL$_{5/2/3/0}$ and dFdC$_3$-TSL$_{5/2/3/0}$ was not solved [44]. First, it was shown that the leakage was not caused by osmotic pressure, which is known to destabilize vesicles [128]. Osmotic pressure is the result of differences between the intraliposomal and extraliposomal osmolarity. The osmolarity of all used solutions was around physiological range (cf. Figure 4-4). Moreover, it was shown for DPPG$_2$-TSL that the formulation is less sensitive to osmotic effects compared to other formulations, e.g. like LTSL, PEG-TSL or DPPG$_2$/PEG-TSL [147]. The leakage is rather caused by the storage of the liposomes directly after preparation at -20°C. It is known, that freezing could affect the drug retention of liposomes [105, 106]. For dFdC-TSL it was shown, that with increasing numbers of freezing

and thawing cycles the amount of leaked dFdC is increased (cf. Figure 4-14). To avoid freezing and thawing of dFdC-TSL a stability study at 2-8°C of formulations $dFdC_3$-$TSL_{5/2/3/0}$, $dFdC_6$-$TSL_{5/2/3/0}$, $dFdC_6$-$TSL_{6/1/3/0}$, $dFdC_6$-$TSL_{7/0/3/0}$ and $dFdC_6$-$TSL_{4.5/2/3/0.5}$ was performed. Storage at 2-8°C was feasible for $dFdC_6$-$TSL_{5/2/3/0}$, $dFdC_6$-$TSL_{6/1/3/0}$, $dFdC_6$-$TSL_{7/0/3/0}$ and $dFdC_6$-$TSL_{4.5/2/3/0.5}$ since hydrolysis of phospholipids has its minimum at a pH of 6.5 [97, 138]. Already approved liposomal formulations like Doxil® or Onivyde® were also stored at 2-8°C in liposomal dispersion.

All four formulations prepared with the improved preparation method and dFdC-solution with a pH of 6 can be stored at 2-8°C for at least 48 weeks. Parameters which are suitable for the evaluation of the storage stability are the quantification of FFA and lysolipids as degradation products of phospholipids as well as the leakage. There was no initial dFdC release detectable as well as no lysolipids and FFA (cf. Figure 4-15). In contrast, the formulation $dFdC_3$-$TSL_{5/2/3/0}$ showed already degradation products directly after preparation which increased during storage at 2-8°C after 4 weeks. The leakage after 8 weeks was already 4.2±0.2% and 50.8±17.3% after 48 weeks, respectively. This leakage could be caused by the instability of liposomal membrane due to hydrolysis of the phospholipids. Already 21.59±7.52% FFA and 15.0±2.5% lysolipids can be detected after 8 weeks storage at 2-8°C (cf. Figure 4-15), which are described in literature to have destabilizing effects on liposomal membranes [42, 97, 129, 130, 139, 140]. Storage of dFdC-TSL with an acidic intraliposomal pH of 2-3 is not possible at 2-8°C. The published dFdC-TSL formulation had to be used always directly after preparation, to avoid storage at 2-8°C or freezing and thawing stress when stored at -20°C.

The z-average and PDI were unaffected in all five analyzed formulations by storage at 2-8°C for at least 48 weeks (cf. Figure 4-15), even for $dFdC_3$-$TSL_{5/2/3/0}$ that showed notable lipid decomposition in the storage period. Therefore, DLS was not suitable to evaluate the storage stability of TSL formulations.

In literature, the storage stability of dFdC-liposomal formulations is hardly described. For a long-circulating pH sensitive dFdC-formulation a storage stability at 4°C for 3 months is described by Xu et al., but they only analyzed the particle size, PDI, zeta-potential and the total dFdC-amount and not potential lipid decomposition [149], which was shown to be a significant marker for stability in the present study. They stored their formulation as a pellet or as suspension and analyzed the described parameters after 0, 1, 2 or 3 months. After three months' particle size, PDI and dFdC-amount showed no change. Only the ζ-potential decreased by 5 mV [149]. Comparing this stability study with the stability study performed in this work, the chosen parameters of Xu et al. are not suitable for the evaluation of storage stability. The analysis of degradation products and leakage of drug are the parameters which allow to make a statement about the storage stability. It was shown in this work, that for the

long-circulating nanoliposomal CPT-11 formulation Onivyde®, one factor responsible for the storage term were lysolipids formed during storage (see section 4.2.4.6). These results obtained with Onivyde® showed, that the analysis of degradation products in liposomal formulations is very crucial in formulation development to evaluate storage stability. This is especially the case for TSL where a minor change (up to 5 mol%) in the phospholipid composition (e.g. by generation of lysolipids) can result in a changed release-profile (cf. Figure 4-9 and Figure 4-11). Therefore, TSL formulations should be stored in a lyophilized form to avoid hydrolysis of phospholipids in the presence of water. The European Medicine Agency also mentioned in their guidelines, that the stability of a liposomal product should be known, including the degradation products like lysolipids [141].

## 5.1.3 *In vivo* experiments of dFdC-TSL

To evaluate the *in vivo* behavior of $dFdC_6$-$TSL_{6/1/3/0}$, $dFdC_6$-$TSL_{7/0/3/0}$ and $dFdC_6$-$TSL_{4.5/2/3/0.5}$ a PK and therapeutic studies in BN-rats were performed and compared to $dFdC_3$-$TSL_{5/2/3/0}$. For the experiments, the TSL were prepared freshly and stored not more than two weeks at 2-8°C.

### *5.1.3.1 PK-study*

The plasma half-life of non-liposomal dFdC was described by Limmer et al as 0.07 h [44]. For all four $DPPG_2$-based dFdC-TSL the plasma half-life was longer as for free drug. The plasma half-life of $dFdC_3$-$TSL_{5/2/3/0}$ was similar to the published value (2.63 h vs. 2.59 h) [44]. This nicely demonstrates the reproducibility of the animal data obtained with $dFdC_3$-$TSL_{5/2/3/0}$. The area under the curve could not be compared, because for this project the plasma half-life was only monitored for 2 h and not for 6 h. Also, $c_0$ was lower for $dFdC_3$-$TSL_{5/2/3/0}$ prepared for this work (58.9% vs. 75.1%) [44]. This is potentially due to deviations during liposomal preparation of the $dFdC_3$-$TSL_{5/2/3/0}$, as the pH of the Gemzar®-solution provided by the pharmacy, used for preparation of this formulation, was pH 2, instead pH 3 [44]. With this low pH, it was not possible to prepare liposomes and so the pH had to be adjusted to pH 3 by addition of $NaHCO_3$. Whereas the phospholipid composition and the preparation method for both formulations (the published one and the one prepared for this project) were the same, the $dFdC_3$-$TSL_{5/2/3/0}$ after preparation were not completely identical and the minor differences observed *in vivo* could be caused by adjustment of the pH for the preparations in this work. Another difference was the injection method, where this formulation was injected in the tail vein of the rats compared to previous injection in the penis vein [44].

Comparing the plasma half-lives of $dFdC_6$-$TSL_{6/1/3/0}$, $dFdC_6$-$TSL_{7/0/3/0}$ and $dFdC_6$-$TSL_{4.5/2/3/0.5}$ to non-liposomal dFdC, all three formulations had a prolonged circulation half-life. The formulation $dFdC_3$-$TSL_{5/2/3/0}$ showed the longest circulation half-life (2.63 h), but the lowest $c_0$,

with only 58.9% compared to the improved formulations (cf. Table 4-5). This might be explained by the intrinsic instability (initial drug leakage) of $dFdC_3$-$TSL_{5/2/3/0}$ by rapid dilution and/or interaction with serum components after i.v. injection, as discussed in literature [44]. After stabilization of the formulation by altering the pH of the dFdC solution during preparation the risk to leak dFdC after i.v. injection was reduced (as shown by absence of the initial dFdC leakage *in vitro*, cf. 4.1.2). This fits nicely to the higher $c_0$ obtained for all three improved formulations, with 66.0%, 66.8%, and 78.8% for $dFdC_6$-$TSL_{4.5/2/3/0.5}$, $dFdC_6$-$TSL_{6/1/3/0}$, and $dFdC_6$-$TSL_{7/0/3/0}$, respectively.

The formulation $dFdC_6$-$TSL_{6/1/3/0}$ showed the longest circulation half-life of all improved formulations (1.74 h) compared to $dFdC_6$-$TSL_{7/0/3/0}$ and $dFdC_6$-$TSL_{4.5/2/3/0.5}$ (0.83 h and 1.31 h). The highest $AUC_{0\text{-}120\ min}$ was also calculated for $dFdC_6$-$TSL_{6/1/3/0}$. It was even higher than the $AUC_{0\text{-}120\ min}$ of $dFdC_3$-$TSL_{5/2/3/0}$, despite the shorter plasma half-life with 0.89 h, because of the notable higher $c_0$.

In absence of DSPC in the formulation the circulation half-life decreased. The decreasing stability with decreasing DSPC-amounts in a $DPPG_2$-based TSL formulation was already described by Lindner et al 2004 *in vitro* [4]. For a Dox-containing LTSL it was shown that with decreasing DSPC-amount (45 to 15 mol%) in a formulation the blood circulation half-life of the liposomal carrier was decreased from 8 to 4 h [150]. They ascribed this to decreasing membrane rigidity with decreasing DSPC, which leads to an increasing binding of serum opsonins and so an increased clearance rate [150-152]. This also might be the explanation for the reduced plasma half-life of formulation $dFdC_6$-$TSL_{7/0/3/0}$. The formulation $dFdC_6$-$TSL_{4.5/2/3/0.5}$ showed a 2-fold shorter plasma half-life compared to $dFdC_3$-$TSL_{5/2/3/0}$, although both formulations had a comparable amount of lysolipids. The formulation $dFdC_6$-$TSL_{4.5/2/3/0}$ contained 5% P-Lyso-PC added during preparation. For $dFdC_3$-$TSL_{5/2/3/0}$ ~4% endogenously formed lysolipids (S-Lyso-PC, P-Lyso-PC) were detected after preparation, but it also contained unquantified amounts of P-Lyso-$PG_2$, stearic acid and palmitic acid. *In vitro* the release profile was similar (cf. Figure 4-11). An explanation for the difference in plasma half-lives might be that the lysolipids generated during preparation were located in the inner leaflet of the membrane and the lysolipids of the formulation with 5% lysolipids in the lipid film might be equally distributed between inner- and outer leaflet of the membrane. The flip-flop of Lyso-PC between inner and outer leaflet doesn`t happen at RT [153]. The lysolipids in the outer leaflet might be easier dissociated after injection in the blood stream to interact with naturally occurring acceptor vesicles and so the formulation becomes more instable during circulation. Banno et al showed that more than 70% of lysolipids in a LTSL formulation were lost after 1 h circulation time in mice at 37°C [144]. The lysolipids generated during preparation due to the hydrolysis caused by the low pH of the dFdC-solution might be in the inner leaflet and thus protected from dissociation out of the bilayer.

Also, the difference in intraliposomal pH could explain the obtained PK parameters. Intraliposomal dFdC ($pK_a$ 3.5 [154]) could be deprotonated due to the higher pH (pH 6-6.5 compared to pH 3) and might be able to cross the membrane faster than the protonated form.

### *5.1.3.2 Therapeutic effect*

The therapeutic efficacies of $dFdC_6$-$TSL_{6/1/3/0}$ and $dFdC_6$-$TSL_{7/0/3/0}$ were compared to $dFdC_3$-$TSL_{5/2/3/0}$ in the s.c. BN175 soft tissue sarcoma model in rats. The improved formulation $dFdC_6$-$TSL_{6/1/3/0}$ showed a comparable tumor growth delay as the formulation $dFdC_3$-$TSL_{5/2/3/0}$ and an advantage over non-liposomal dFdC [44] (cf. Figure 4-18). In contrast, $dFdC_6$-$TSL_{7/0/3/0}$ however showed significant less tumor growth delay after 10 days compared to $dFdC_3$-$TSL_{5/2/3/0}$ and $dFdC_6$-$TSL_{6/1/3/0}$. This could be explained by its short plasma half-life (0.83 h). As a result, the number of liposomes passing the heated tumor in the treatment time of 60 min was lower compared to the other formulations and therefore, less dFdC could be released upon heat-activation. The therapeutic efficacy of the TSL in this tumor model was not optimal and should be adjusted. For the non-liposomal dFdC treated group the therapeutic efficacy between single animals was high compared to the other groups (cf. Figure 4-19), resulting from the aggressive growing tumor model. The first animals reached a relative tumor size of ~20 ($V/V_0$) after 8 days whereas other animals did not reach this tumor size even after 16 days. The difference is surprising, since all animals received the same treatment protocol. All animals were treated with same dose of dFdC (6 mg/kg) and the HT-treatment was also 1 h in all cases. The intratumoral temperature was also monitored to be around 41°C. For the TSL treated groups the difference between single animals was less. Due to limitations in the allowed injection volume for bolus injections to rats (5 ml/kg bodyweight), it was not possible to inject higher doses than 6 mg/kg, like it is done for other published dFdC-formulations (between 10 mg/kg-120 mg/kg) [146, 148, 155]. The allowed maximal injection volume was already used and higher intraliposomal encapsulation of dFdC was not possible, due to the passive encapsulation method and the concentration of the used Gemzar®-solution (38 mg/ml). Another drawback for the therapeutic outcome could be the only single treatment, e.g. Affram et al used a treatment every second day for two weeks [146].

The aggressively growing BN-175 tumor model in the treatment regime (single treatment with a low dose) used for dFdC-TSL was not the optimal choice and gives room for improvement. The therapeutic outcome could also be improved in another tumor model, like a pancreatic cancer model.

### 5.1.4 Outlook

To obtain a clinically relevant $DPPG_2$-based dFdC-TSL the improved formulation was a first promising step, since the pharmaceutical quality regarding stability was significantly improved and the *in vivo* results stayed similar to the already published data [44]. Further improvements of the formulation could be the preparation of TSL with higher dFdC content, by changing the loading strategy. A pH-gradient loading of dFdC in liposomes was described by Celano et al. The encapsulation efficacy was around 90% [156]. This was not tested within the scope of this thesis, because it is known, that this could be critical (personal communication Prof. Ulrich Massing). The change of the tumor model from the aggressive growing subcutaneous BN175 soft tissue sarcoma, to a more relevant pancreatic cancer model, should be the next step as well as the test of multiple injections. For Dox-loaded $DPPG_2$-TSL it was already shown in a former work in the group, that repeated injections of $DPPG_2$-TSL did not result in decrease of plasma half-life [157]. Meaning that the accelerated blood clearance effect after multiple injections which is described in literature intensively for PEGylated liposomes [158] does not exist for Dox-loaded $DPPG_2$-based TSL.

## 5.2 CPT-11-TSL

CPT-11 was chosen as second drug for pancreatic cancer treatment to be encapsulated in $DPPG_2$-based TSL within the scope of this work. Its active metabolite SN-38 was also tested for encapsulation. The developed CPT-11-TSL were analyzed *in vitro* as well as *in vivo* in detail.

### 5.2.1 Encapsulation of the active metabolite

CPT-11 acts as a prodrug and has to be converted to its more active metabolite SN-38 by carboxylesterase. SN-38 is up to 1000-fold more potent than CPT-11 [159]. A disadvantage of SN-38 for direct application in patients is the insolubility in most physiologically compatible solvents, because of its high lipophilicity in its active lactone form (log $P_a$=2.09 at pH 1.5) [160, 161]. Encapsulation of SN-38 in several liposomal formulations was achieved, but none of these showed temperature-sensitive characteristics [116, 162, 163].

To avoid the additional step of activation in cells after release of the drug from TSLs in the heated area as well as to overcome the insolubility problem the encapsulation of SN-38 in $DPPG_2$-TSL was evaluated.

Different encapsulation methods were tested, but neither active loading to preformed TSL via a pH gradient or a $Mn^{2+}$-gradient nor passive encapsulation showed promising results. For passive encapsulation, low amounts (0.27 mM) of SN-38 were encapsulated, but during the preparation lysolipids were generated due to the high pH of the applied SN-38 solution (pH 10-11). A high pH was needed, since SN-38 was hardly soluble at sufficiently high concentrations at lower pH in aqueous systems (data not shown). Another pitfall of a high pH is that the drug is in its inactive carboxylate form as well as the irreversible basic hydrolysis of phospholipids is favored [97, 138, 159, 164]. The low EE and the generation of lysolipids during preparation showed that passive encapsulation was not possible.

For active encapsulation, different forms of loading gradients were tested (cf. Table 4-6), but for all experiments the concentration of encapsulated SN-38 was too low (< 0.08 mM) to further evaluate these liposomes especially regarding *in vivo* experiments.

Encapsulation of SN-38 with DAC was also tested, but the PDI and the z-average of the resulting TSL were too high (0.508±0.072 and 198.9±45.5 nm) (data not shown). Further evaluation with DAC prepared SN-38-TSL was not performed, because the broad size distribution would not allow precise evaluation.

With the film loading method described by Sadzuka et al. loading of SN-38 into $DPPG_2$-based TSL was successful. SN-38 0.53±0.24 mM was encapsulated in the $DPPG_2$-TSL, with an EE of around 9% (cf. Table 4-6). This was quite low compared to the EE of 53.0% described for DSPC/Chol/DSPG (100:100:60 molar ratio) liposomes by Sadzuka et al [116]. The difference in encapsulation efficacy could also be caused by the difference in lipid

composition (e.g. presence of cholesterol to achieve a liquid disordered instead of a solid gel phase state), solubility of SN-38 in the membrane bilayer or differences in calculation of the EE.

For SN-38-loaded $DPPG_2$-TSL with film loading no temperature-dependency of drug release was found in FBS (cf. Figure 4-25). There was SN-38 released, but not in a temperature-dependent manner. The same results were achieved by performing a temperature-dependent release with acceptor-vesicle present, to facilitate release of lipophilic SN-38 to the membrane of acceptor vesicles, as e.g. shown for $C_6$- and $C_{16}$-ceramide by Shabbits et al [165].

This absence of temperature-dependent release might be caused by an encapsulation of SN-38 in the liposomal membrane or the encapsulation of small undissolved SN-38 particles during film loading. Due to the high lipophilicity of SN-38 an interaction with the lipophilic membrane appears to be the most likely explanation for the results. Peikov et al proposed some models for the localization of SN-38 in liposomal suspension at different pH conditions [160]. The hypothesis which fits nicely to the obtained results in this work was that SN-38 interacts with the lipids after rehydration at a low pH forming micro aggregates. This might be the reason why the SN-38 was not released in a temperature-dependent manner. The DSC-measurements shown in Figure 4-27 gave no hint that SN-38 was interacting with the lipids in the bilayer, because the phase transition was not influenced, when comparing the heating plots of TSL with and without SN-38. Since SN-38 concentration (0.53 mM) was low in comparison to lipid concentration (24.2 mM) (drug/lipid 0.022), an interaction could have been undetectable in the DSC measurement. The Cryo-TEM measurements also gave no information about the localization of SN-38 encapsulated with film loading in preformed TSL, but rather showed that the film loading disrupted the TSL. The film loading method created irregular, non-spherical particles, particle fragments as well as multilamellar vesicles independent if SN-38 was present or not (Figure 4-28). The sonication step during film loading might be the detrimental step.

In conclusion, further investigation of SN-38-TSL prepared by film loading as well as additional experiments for encapsulation of SN-38 in TSL were stopped. The failure to successfully encapsulate SN-38 with various active or passive encapsulation methods, and the low EE for the film method might be caused by the structure and lipophilicity of the drug, resulting also in low solubility in solid gel phase state membranes like the membrane of $DPPG_2$-TSL. Moreover, the lacking thermosensitivity of film loaded $DPPG_2$-TSL does not warrant the further evaluation of the formulation as candidate for heat-mediated drug delivery, therefore, the encapsulation of the prodrug CPT-11 was investigated.

## 5.2.2 *In vitro* conversion of CPT-11 to SN-38

One drawback of encapsulation of a prodrug like CPT-11 in TSL is the need of conversion to its active metabolite SN-38 after triggered release in the heated tumor tissue. For CPT-11 several groups showed, that in different tumor types the carboxylesterases are present and able to convert CPT-11 to SN-38 [125, 166, 167].

Evaluating the ability of a soft tissue sarcoma cell line (BN175), which is also used in the in vivo experiments in rats (see below), a pancreatic cancer cell line (DSL-6A/C1) and a liver cancer cell line (HepG2) for conversion of CPT-11 to SN-38, in the present study, was not possible. SN-38 was detected in the cell medium but the concentration could not be quantified, due to the high limit of quantification for SN-38 of the applied HPLC method (35 ng/ml; 89.3 nM). The SN-38 concentration in cells was not quantifiable and the CPT-11 concentration in the cells was quite low, < 1µM. In case of slow conversion to SN-38, the intracellular CPT-11 concentration might be too low to achieve quantifiable amounts of SN-38 in the cells. Other groups who successfully showed a conversion of CPT-11 to SN-38 in cells applied methods (fluorescence detection with MS) with limits of quantification of 0.5 ng/ml [126, 168]. Van Ark-Otte had a limit of quantification of 0.5 nM (= 0.2 ng/ml) (two fluorescence detectors) for SN-38 in cell lysates, and found SN-38 concentrations of around 2.8 nM after incubation of cells (human lung cancer cells) with CPT-11 [125].

## 5.2.3 *In vitro* characterization of CPT-11-TSL

### *5.2.3.1 Preparation of CPT-11-TSL*

CPT-11, which also shows notable cytotoxicity, was successfully encapsulated in $DPPG_2$-based TSL via a gradient. It was shown, that no SEC step was necessary after loading to separate potentially unencapsulated CPT-11, indicating a high EE with only traces of CPT-11 present. Moreover, 45 min loading time was sufficient to ensure encapsulation (cf. Figure 4-29 and Figure 4-30). Compared to $(NH_4)_2SO_4$- or $(NH_4)_2HPO_4$-gradient loading citrate gradient loading resulted in less stable liposomes *in vitro*. This was shown for Dox-loaded TSL with the formulation DPPC/DSPC/DSPE-$PEG_{2000}$ (50-80 mol%/ 15-45 mol%/ 5 mol%) by Lokerse et al [150]. The distinction in stability between the gradients was not caused by difference in osmolarity, because for all used solutions the osmolarity was in the same range (for the intraliposomal solution around 620 mmol/kg and for the ready prepared TSL around 290 mmol/kg) (cf. Table 4-11). The $(NH_4)_2SO_4$-gradient for preparation of CPT-11-TSL was used for the further experiments due to the fact, that experimental characterization (phosphate assay) was easier without additional phosphate in a formulation. The optimal drug to lipid ratio of CPT-11-TSL should be at least 0.2 (mol/mol), because at this drug/lipid ratio, the amount of CPT-11 not stably encapsulated (released after 1 h incubation at 37°C)

was less than 15% (cf. Figure 4-37). The encapsulation efficacy was 88.2±9.2% which was in a good range for an active loading process. For $DPPG_2$-based TSL encapsulating Dox an encapsulation efficacy of ~90% was achieved (data not published).

Major advantage of CPT-11-TSL compared to the improved dFdC-TSL was the possibility to load considerable higher amounts of drug in the TSL (10.1±2.8 mM in contrast to 4.1±1.1 mM for $dFdC_6$-$TSL_{6/1/3/0}$). The payload of CPT-11 might be increased further due to the active loading, but this was not tested anymore in the present thesis. However, for dFdC it will be a challenge to passively load more drug into the liposomes, since the solubility of dFdC is limited. An advantage of active loading in contrast to passive loading is the high encapsulation efficacy (around 90% for active loading, only 5-10% for passive loading). For industrial-scale manufacture the active loading is favorable, because most of the drug is encapsulated and the remaining not encapsulated drug had not to be separated. An additional separation step is quite expensive in industrial-scale manufacturing (personal communication, Dr. Martin Hossann, CTO, Thermosome GmbH). The other standard characteristics for CPT-11-TSL (cf. Table 4-10) were similar to Dox-loaded and dFdC-loaded $DPPG_2$-TSL [44, 112].

### *5.2.3.2 Storage stability*

As already shown for dFdC-TSL, storage at -20°C was also inappropriate for CPT-11-TSL, because each freezing and thawing cycle resulted in unwanted drug leakage at RT as well as release at 37°C after 1 h (cf. Figure 4-32 and Figure 4-33). In a stability study at 2-8°C (intended storage condition), the CPT-11-TSL were stable for at least 4 weeks (cf. Figure 4-34-Figure 4-36). For the planned animal experiments this time period was long enough, because it was possible to prepare and store the TSL in liquid dispersion. By storage of the CPT-11-TSL three additional weeks at RT (accelerated condition), 5.3% lysolipids were detected as well as an increased instability at 40°C. Vesicle size and PDI remained unchanged in this period of time. These results fit to the results shown for dFdC-TSL (section 4.1.2.5 and 5.1.2), which showed that z-average and PDI were unaffected by storage, but the lysolipid content as well as the drug leakage are feasible parameters to evaluate storage stability. The evaluation of degradation products of lipids is also suggested by the European Medicines Agency for analysis of the stabilization of liposomes [141].

### *5.2.3.3 Drug release from $DPPG_2$-TSL*

The phospholipid composition DPPC/DSPC/$DPPG_2$ 50:20:30 (molar ratio) showed an advantage over the formulation with 10% $DPPG_2$ (DPPC/DSPC/$DPPG_2$ 70:20:10 (molar ratio)) when comparing the stability at 37°C 1 h (12.8±3.8% to 19.5±3.2% CPT-11-release in FBS) and the release at 41°C after 5 min incubation (72.7±2.3% to 20.9±17.4% CPT-11

release in FBS). The decreased stability at 37°C 1 h was not expected, because Lindner et al showed for CF-loaded $DPPG_2$-based TSL, that with decreasing $DPPG_2$ amount the stability at temperatures < 41°C increased [4]. The decreased amount of drug released during 5 min at T≥41°C with decreasing $DPPG_2$ content was in accordance to the published results. Comparing the drug release of CPT-11-TSL to actively, citrate-gradient Dox-loaded $DPPG_2$-based TSL, the CPT-11-TSL were more stable at 39°C (3.6±1.4% compared to 38.3±2.3% in FBS), but for CPT-11-TSL at temperatures > 41 °C not more than 80% of CPT-11 were released after 5 min incubation (for Dox-loaded $DPPG_2$-based TSL more than 90%) [43]. This could be caused by a higher stability of the CPT-11-TSL at also higher temperatures or a slower CPT-11 release over the membrane compared to Dox-TSL.

Analyzing the time- and temperature-dependent CPT-11 release in FBS it could be shown that CPT-11-TSL showed weak release at temperatures < 40°C. The CPT-11-TSL showed a fast release in the first minute at 41-42°C (62.7±4.3%), but only 60-70% of encapsulated CPT-11 (cf. Figure 4-40) were released. The remaining CPT-11 was released over the subsequent 60 min (97.2±2.1% released CPT-11 after 60 min) (cf. Figure 4-41). Comparing these results with Dox-loaded $DPPG_2$-TSL, they showed a burst release of almost the complete encapsulated Dox. In the first 2 min of incubation at 41°C in FBS 97.3±1.4% Dox was released [31]. The release rate constant for CPT-11-TSL at 37°C was similar to the release rate constant of Dox-TSL at 38°C in FBS ($1.8±0.9*10^{-4}s^{-1}$ vs. $2±2*10^{-4}s^{-1}$) [31]. At 40°C the CPT-11-TSL formulation is more stable than the Dox-formulations (release constant CPT-11 $20.2±2.4*10^{-4}s^{-1}$ and for Dox-TSL $61±17*10^{-4}s^{-1}$) [31]. One difference in determination of release constants was, that for CPT-11-TSL it was determined for 300 s and for Dox-TSL only for 120 s. The incomplete release of encapsulated CPT-11 might be caused by the difference in the properties of the drugs, particularly the lipophilicity (as quantified by the log P-value) resulting in different behavior. The log P of Dox is described as 1.27 [169] and the log P of CPT-11 is 3.8 [170]. The higher the log P, the more lipophilic the drug. This means in the case of Dox and CPT-11 that CPT-11 is more lipophilic and so the tendency to interact with the lipophilic membrane is higher compared to Dox. Perhaps the CPT-11 interacts with the lipids around the $T_m$, resulting in a slower release and the occurrence of a pre-transition peak in the DSC measurements (cf. Figure 4-43). In a membrane mimetic model, it was shown that CPT-11 could interact with the membrane model without disturbing its structure [171]. This might be an explanation for the difference described above in time- and temperature-dependent release. CPT-11, which is not immediately released, could be ascribed to the CPT-11 interaction with the lipophilic membrane or proteins of the FBS sticking to the liposomal membrane and so it is released less rapidly than Dox.

Under physiological pH, the lactone form of CPT-11 is hydrolyzed to the inactive carboxylate form. Loos et al showed, that only the lactone form of a CPT analog could pass membranes [172]. The difference in release could be caused by the fact that most of the CPT-11 intraliposomal was in its lactone form (pH 5.4 intraliposomal) which was able to pass membranes and therefore it was rapidly released. At pH 5 most of CPT-11 was in its lactone form [173]. At the phase transition temperature, the pH gradient collapses and the remaining CPT-11 will be transferred in its carboxylate form (pH around 7.4). Fassberg et al described at pH >8 the ring was largely in its carboxylate form [173]. In its carboxylate form it was not able to pass the membrane, but because of being in a chemical equilibrium as soon as a lactone form was built, the lactone form of CPT-11 was released immediately. In this manner over the course of an hour, nearly the complete CPT-11 content could be released.
For the 5 min temperature-dependent release (cf. Figure 4-37) a maximum release of ~75% in FBS could be reached. This was around 10% more compared to the time- and temperature-dependent release, but the difference could be the amount of FBS used for dilution of the liposomes (20-fold more FBS) and so the protein concentration in contrast to the liposomes used for the experiment. Burke et al showed that CPT binds to HSA in its carboxylate form as well as in its lactone form [174-176]. This phenomenon might explain the difference after 5 min in both release experiments, because in one experiment more FBS was present, resulting also in higher HSA concentrations.

### *5.2.3.4 $T_m$ of CPT-11-TSL*

The incorporation of CPT-11 in $DPPG_2$-based TSL shifted the $T_m$ to slightly lower temperatures (empty $(NH_4)_2SO_4$-liposomes 44.40±0.17°C and 43.88±0.12°C) and generated a pre-transition peak at ~41°C (cf. Figure 4-43 and Table 4-13). The pre-transition peak was only measurable for liposomes containing $DPPG_2$ and CPT-11. This pre-transition peak might be attributed to the interaction of CPT-11 as positive charged molecule at pH around 7.4 ($pK_a$ of the terminal piperidine group 9.3 [170]) and the negative charged $DPPG_2$. Perhaps parts of the CPT-11 which were not completely stably encapsulated (release at 37°C in the first 2 to 3 h; Figure 4-42) might form a CPT-11 corona on the outer part of the liposomal membrane. This CPT-11 corona could be built up by the lipophilicity of the CPT-11 molecule interacting with the lipophilic parts of the liposomal membrane or by electrostatic interactions. The ζ-potential for CPT-11-TSL gave no hint for the formation of a CPT-11 corona, because it was similar to CF-TSL, empty TSL and FDG-TSL [136]. Nevertheless, sensitivity and precision of the DLS measurement might be too low to detect a change in ζ-potential by the low amounts of CPT-11 forming the corona. The amount of CPT-11 not stably encapsulated (CPT-11 released during 1 h incubation at 37°C) was limited (cf. 4.2.4.1).

### *5.2.3.5 Cryo-TEM of CPT-11-TSL*

To see if CPT-11 encapsulated via $(NH_4)_2SO_4$-gradient formed a crystal-like structure intraliposomally described for several Dox-formulations [177-180], Cryo-TEM measurements were performed. CPT-11 formed rod-like structures in some TSL (cf. Figure 4-44). This structure was described in literature for DOX-containing liposomes as crystal [180]. The CPT-11 crystal might be only formed at very high concentrations and in most liposomes the concentration was too low. The number of TSL containing the rod-like structures should increase when the intraliposomal CPT-11 increases as well. For $DPPG_2$-based TSL it was also shown that intraliposomal Dox formed crystal-like structures in nearly all liposomes (data not published). For DSPC/Chol liposomes encapsulating CPT-11 via an $CuSO_4$-gradient in Cryo-TEM measurements it was shown that with CPT-11 present intravesical spots were visible, which were attributed to complexes formed of CPT-11 and copper ions [181]. The rod-like structures seen for CPT-11-TSL seemed to be an intraliposomal precipitate of CPT-11.

### *5.2.3.6 In vitro characterization Onivyde®*

Analyzing the long-circulating liposomal CPT-11 formulation Onivyde® with the same methods used for characterization of CPT-11-TSL formulation the values were all as expected and described, only the FFA content and the lysolipid content (cf. Table 4-14) were higher. In the package insert lysolipids were not described, but measuring the lysolipid content of a fresh batch within the expiry date there was lysolipid content of more than 5% measurable. One month after the expiry date, the lysolipid content was already around 13%, leading us to the assumption, that one criterion for the definition of the expiry date was more than 10% of lysolipids (cf. 4.2.4.6). Grit and Crommelin described for a liposomal formulation (partially hydrogenated phosphatidylcholine/egg phosphatidylglycerol/Chol) that the lysolipid content has to be below 10% until it influences the stability of long-circulating liposomes [129].

In the temperature-dependent release assay at 37°C and 42°C it could be shown, that Onivyde® (with small amounts of lysolipid in the formulation ~7%) showed no release even after addition of a detergent solution (cf. Figure 4-45) as expected. A NTSL formulation encapsulating CPT-11 via a $(NH_4)_2SO_4$-gradient in contrast showed already minor CPT-11 release at 42°C. The higher stability of Onivyde® might be a result of the encapsulation via a sucrose octasulfat gradient and the lower DSPE-$PEG_{2000}$ amount in the formulation [93].

## 5.2.4 *In vivo* characterization of CPT-11-TSL

The *in vitro* characterization of CPT-11-TSL showed promising properties for further *in vivo* evaluation of the formulation. For the *in vivo* experiments, freshly prepared CPT-11-TSL were maximally stored as liquid dispersion at 2-8°C for up to 4 weeks before usage. The formulations had the phospholipid composition DPPC/DSPC/$DPPG_2$ 50:20:30 (molar ratio) and a drug/lipid ratio of 0.275±0.033 (mol/mol). All other *in vitro* characterizations showed comparable values as listed in Table 4-10.

### *5.2.4.1 Pharmacokinetic study*

In a pharmacokinetic study, the *in vivo* stability of CPT-11-TSL was analyzed in comparison to Onivyde® and non-liposomal CPT-11. The calculated $c_{max}$ after i.v. application of 20 mg/kg CPT-11 is 500 µg/ml. After 10 min 71% of $c_{max}$ was detected for CPT-11-TSL. For Onivyde® with 70.4% a similar amount was detectable, but for non-liposomal CPT-11 only 1.2% of the $c_{max}$ was found in blood. The plasma half-life for the TSL-formulation was 1.57 h in comparison to 0.71 h for non-liposomal CPT-11 and 18.71 h for Onivyde®. The CPT-11-TSL as well as Onivyde®, showed an advantage in plasma half-life over non-liposomal CPT-11.

Published plasma half-lives for non-liposomal CPT-11 and Onivyde® in female albino rats were 0.27 h and 10.7 h, respectively [93]. The differences in the plasma half-lives could arise from the different rat strains, injection methods, time spans (24 h in this experiment in contrast to 48 h for the published PK study) and CPT-11 concentrations (20 mg/kg for this study and 10 mg/kg for the published one). The effect of dose-dependent reduced degradation in mice for long-circulating liposomes containing Dox (Doxil®) was described in literature [182]. The mice received 2.5-20 mg/kg Doxil® and after 40 h at an 8-fold higher dose 15-fold higher Dox concentration in plasma was measured. For $DPPG_2$-based Dox-TSL a dose-dependent effect on PK profile was described as well in rats [157] as in cats [45]. Increasing the dosage from 2 mg/kg to 5 mg/kg (2.5-fold) the Dox concentration after 2 min in plasma was 3.6-fold higher. For cats, it was shown that the plasma half-life was also increased by infusion of a higher dose (22.5 min for 0.1 mg/kg Dox and 39.5 min for 0.4 mg/kg Dox) [45]. These effects might be the reason for the difference in plasma half-lives for Onivyde® and non-liposomal CPT-11 in this work and in the literature.

The plasma concentrations of CPT-11-TSL and Onivyde® were similar during the first 60 min (303.9±4.20 µg/ml and 299.58±8.98 µg/ml). The long-circulating advantage of Onivyde® was observable after 60 min, but this difference of the TSL and Onivyde® was expected. TSL formulations are designed to be less stable than a long-circulating formulation, to achieve a complete release of the drug in the 1 h HT treatment.

Measuring the SN-38 concentration in plasma for CPT-11-TSL and Onivyde® SN-38 was detectable with a maximum after 10 min (1.2±0.83 µg/ml and 1.16±0.13 µg/ml, respectively).

For non-liposomal CPT-11 no SN-38 could be detected over the whole time-frame. This is caused by the fast clearance of the CPT-11 after injection. The presence of SN-38 is quite important, because it is the active metabolite of CPT-11 and up to 1000-fold more active. The CPT-11-TSL and Onivyde® showed similar SN-38 concentrations after 10 min, but with progressing time after injection the difference in SN-38 content between the TSL and Onivyde® increased as well. For Onivyde® it nearly stayed constant after 4 h. The reason might be that the long-circulating Onivyde® showed a high stability over 24 h and after 24 h ¼ of the $c_{max}$ was still detectable. This means during this period of time there was always a high amount of CPT-11 present, which could be converted to SN-38. For TSL the CPT-11 amount after 4h was only 23% of the concentration after 10 min, with less CPT-11 present in the blood stream to be converted to SN-38.

For TSL and Onivyde® around 30% of the injected doses directly after injection were cleared from the blood stream. $c_0$ of CPT-11-TSL was 1.4-fold higher than for Onivyde®. This difference between $DPPG_2$-based TSL and long-circulating liposomes (Doxil®) concerning the $c_0$ was already described for Dox-loaded liposomes and might be caused by the absence of an initial fast distribution phase of TSL, which was mentioned for Doxil® in literature [43, 183].

### *5.2.4.2 Biodistribution study*

In a biodistribution study the accumulation of CPT-11 and SN-38 after 1 h HT-treatment of the tumor in different tissues was analyzed when CPT-11-TSL, Onivyde® or non-liposomal CPT-11 were injected. For CPT-11-TSL, the CPT-11 concentration in the tumor was 24-fold higher compared to Onivyde® and 36-fold higher compared to non-liposomal CPT-11 (cf. Figure 4-47). The SN-38 concentration in the tumor was 2-3-fold higher for CPT-11-TSL than non-liposomal CPT-11 or Onivyde®. The CPT-11-TSL released CPT-11 at 41°C in the tumor which was also measured *in vitro* and showed an advantage over the long-circulating Onivyde® in the targeting efficacy after 1 h HT treatment. The CPT-11-TSL released nearly the whole CPT-11 payload during the 1 h treatment resulting in a low plasma concentration (111.86±96.51 µg/ml) (see Figure 4-47). In the PK study without HT-treatment for Onivyde® and CPT-11-TSL similar amounts of CPT-11 were detectable after 1 h (299.58±8.98 µg/ml vs. 303.39±4.20 µg/ml). Onivyde® showed *in vitro* a very high stability over 60 min in FBS with nearly no released CPT-11 at 42°C (cf. Figure 4-45). This stability of Onivyde® was the reason for the high plasma concentration in the biodistribution study. The high CPT-11 concentration of Onivyde® in the plasma resulted also in a high SN-38 concentration in the plasma after 60 min. For CPT-11-TSL and non-liposomal CPT-11 no SN-38 could be detected after 60 min in the plasma. The high SN-38 concentration for Onivyde® in the

plasma could also be a disadvantage due to the high toxicity of the drug and resulting side effects on healthy tissue and organs.

Kang et al showed in a biodistribution study in tumor bearing nude mice, that elimination of CPT-11 and SN-38 was more rapid for non-liposomal CPT-11 compared to Onivyde® [184]. The CPT-11 and SN-38 concentrations in the tumor were slightly higher for Onivyde® compared to non-liposomal CPT-11 after 4 h. This was also observed in the study in rats performed in this work. However, the difference was that in the study performed in rats the tumor was heated for 1 h and the tissues were collected after 1 h. In another study in mice Kalra et al showed, that for non-liposomal CPT-11 a 5-fold higher dose of CPT-11 was required to achieve similar SN-38 concentrations in plasma and tumor tissue compared to Onivyde® [92].

Onivyde® and CPT-11-TSL were likely to be degraded in the spleen, because the CPT-11 tissue concentration in spleen was higher for the two liposomal formulations as for non-liposomal CPT-11 (cf. Figure 4-47). The reason for this might be the fast recognition of the liposomes by the reticuloendothelial system (RES) followed by a rapid clearance of the Kupffer cells in the liver and the fixed macrophages of the spleen [185]. The $PEG_{2000}$ amount in the Onivyde® formulation might not be enough to yield a fully hydrated liposome in the serum, which prevents the recognition of the liposomes from RES uptake, because the uptake of the spleen was higher than for the TSL formulation. In this work, it could also be shown, that CPT-11 was converted to SN-38 mostly in the liver. The enzyme family which is needed for the activation of CPT-11 is the carboxylesterase, which is primarily present in the liver and in plasma [186]. The CPT-11 concentration in the liver for CPT-11-TSL and non-liposomal CPT-11 was higher than for Onivyde®.

CPT-11 also was detectable in the kidneys, because CPT-11 is excreted via the renal and biliar excretion [186, 187]. The CPT-11 concentration in the kidneys of rats treated with Onivyde® was 2.2-2.5-fold lower compared to CPT-11-TSL and non-liposomal CPT-11. The SN-38 concentration of rats treated with Onivyde® was also lower (2.4-2.7-fold) in comparison to the other two groups. The reason for this might be, that parts of the non-liposomal CPT-11 were directly transferred to the kidneys to be metabolized or directly excreted. The same could be the case for the CPT-11-TSL which was released of the nanocarrier in the tumor and which was washed out of the tumor but was circulating as non-liposomal CPT-11 in the blood stream and excreted via the kidneys. For the Onivyde®, most liposomes were still intact as shown in the pharmacokinetic study after 1 h and therefore hardly any non-liposomal CPT-11 should be in the blood stream, which than could be further metabolized or excreted in the kidneys.

The concentration of CPT-11 in the tumor for Onivyde® might be this low compared to CPT-11-TSL because the mode of action is different. CPT-11-TSL were prepared with the aim to

have a formulation which shows a rapid release in an area heated to 41-42°C. Onivyde® in contrast was developed with the aim to have long-circulating properties and act via the EPR effect. The accumulation of the intact liposomes in the tumor tissue needed more time than only 1 h. If CPT-11 tumor concentration would have been measured after hours, it is reasonable to assume that CPT-11 concentration for Onivyde® would be notably higher and perhaps comparable to the CPT-11 concentration of CPT-11-TSL after 1 h incubation. This was shown, when Dox-loaded $DPPG_2$-based TSL were compared to long-circulating Doxil® in the same animal model [43]. Comparing the Dox accumulation in the heated tumor after 1 h the $DPPG_2$-based TSL show a 9.2-fold higher Dox concentration as Doxil®.

### *5.2.4.3 Therapeutic study*

For the novel CPT-11-TSL formulation the therapeutic efficacy in the rat s.c. soft tissue sarcoma model BN175 in rats was shown in comparison to free drug. In therapeutic studies in the same animal model the advantage of $DPPG_2$-based TSL encapsulating Dox or dFdC over free drug was already examined [43, 44].

CPT-11-TSL showed a significant advantage ($p>0.005$) in tumor growth delay compared to non-liposomal CPT-11 and a comparable efficacy as Onivyde® after single treatment with 20 mg/kg CPT-11 and 1 h HT treatment at 41°C (cf. Figure 4-48). The difference of CPT-11-TSL and non-liposomal CPT-11 in therapeutic efficacy could be explained by shorter plasma half-life (0.71 h in comparison to 1.57 h) and the decreased accumulation of CPT-11 in the tumor for non-liposomal CPT-11. Two days after treatment, CPT-11-TSL showed even a tumor size reduction, which was neither the case for Onivyde® nor non-liposomal CPT-11. For Onivyde® only a tumor growth inhibition was observed. After 4 days, the tumor volume was similar again for both liposomal formulations. There might be a difference in the mode of action of tumor growth inhibition between the two formulations. For Onivyde® the tumor growth might be inhibited by a constant delivery of CPT-11 and/or SN-38 to the tumor over a long time-period, because for Onivyde® a 3-fold higher plasma concentration of CPT-11 (in comparison to CPT-11-TSL) after 1 h HT in the biodistribution study was detectable as well as quite considerable amount of SN-38 which was not detectable for CPT-11-TSL. This might be a hint, that Onivyde® does not act mainly via the EPR effect, it rather acts via a sustained release of CPT-11 with subsequent conversion to SN-38 e.g. after decomposition of the liposomes in the liver and spleen. In the BD study in both organs CPT-11 and SN-38 were detectable. Only for Onivyde® SN-38 was detectable in the plasma after 1 h HT treatment, causing a constant delivery of SN-38 to the tumor. In the PK study, it was shown that after an initial decrease the SN-38 concentration in plasma stayed constant for at least 24 h and that the plasma half-life for CPT-11 was 18.7 h.

For CPT-11-TSL very high amounts of CPT-11 were detected in the tumor after 1 h HT treatment due to the local heat-triggered delivery, as well as lower amounts of SN-38 which might be responsible for the tumor shrinkage after 2 days. Compared to Onivyde® the tumor concentrations of CPT-11 were 24-fold higher and of SN-38 2.2-fold higher for CPT-11-TSL. The tumor volume reduction after 2 days in case of CPT-11-TSL might be caused by high CPT-11 concentrations directly after the HT-treatment, which resulted in a significant advantage over free drug and Onivyde®.

In the BD study it was shown, that in the tumor tissue SN-38 was also produced and that the carboxylesterase might be also present in tumor tissue as already shown by Kalra et al [92]. It was shown, that the SN-38 concentration in tumors was dependent on two factors, on the one hand the tumor CPT-11 concentration and on the other hand the activity of the carboxylesterase in the tumor [92].

For Onivyde® only ~3% of the $c_{max}$ (calculated from the measured plasma half-life of 18.7 h) of the liposomes circulate in the blood stream or remain accumulated in the tumor after 4 days. Therefore, the CPT-11 and SN-38 concentrations in tumor tissue might be also quite low, the tumor growth could be no longer inhibited.

As already mentioned for dFdC-TSL in chapter 5.1.3 the aggressive growing BN175 soft tissue sarcoma model showed a broad variance in therapeutic efficacy between single animals in the same treatment group. This effect was seen especially in the CPT-11-TSL treatment group but not in the group treated with the free drug as for dFdC. The reason could be differences in the tumor size at the start of the therapy, the viability of the used tumor piece for implantation or the positioning of the lamp for heating. For therapeutic efficacy of the CPT-11-TSL, a consistent heating of the whole tumor was needed. If the lamp was not in an optimal position, it could be that only the upper part of the tumor, where the temperature probe is located, reached the desired temperature and CPT-11 could be released of TSL. This could result in different therapeutic efficacies. For a first proof-of-concept of heat-induced CPT-11 delivery by new developed CPT-11-TSL the tumor model and treatment regimen was suitable. For further experiments a tumor model, e.g. a pancreatic cancer model, more sensitive for a CPT-11 treatment should be chosen.

The different tumor responses of an Onivyde®-like formulation and non-liposomal CPT-11 were shown by two separate groups in mice [92, 93]. Drummond et al tested non-liposomal CPT-11 and Onivyde® in a breast cancer model and a colon cancer model in mice. The efficacy in the breast cancer model was much better for both treatment groups compared to the colon cancer model at the same dose of 50 mg/kg and 4 repeated injections [93]. Kalra et al tested an Onivyde®-like formulation in three different tumor models in mice (colon cancer HT 29, Ewing`s sarcoma SK-ES-1, lung cancer A549) at a dose of 10 mg/kg and a weekly injection [92]. In the lung cancer model, there was no response for Onivyde® compared to the

saline treated control group. For the other two tumor-types the Onivyde®-treated group showed a significant tumor growth delay compared to the saline control group. The reason for the difference in tumor response was ascribed to the different SN-38 retention time (time-frame of SN-38 presence in the tumor cells) in the tumor cells. HT-29 and SK-ES-1 had an extended SN-38 retention time and A549 a shorter retention time, which corresponds to the therapeutic success [92].

For future *in vivo* experiments with CPT-11-TSL the treated tumor type plays a key role in the therapeutic efficacy.

In the therapeutic study performed within the scope of this work only a single-treatment was performed, whereas others who tested Onivyde® like formulations as well as CPT-11 loaded formulations used multiple injection regimes in mice. For example, 4 doses twice a week were used by Drummond et al and Noble et al [93, 188]. Kalra et al used a weekly injection [92]. Messerer et al could show that multiple injections (4 and 8 days after the first treatment) had an advantage over single injections for a long-circulating formulation [189]. For lipid-coated mesoporous silica particle encapsulating CPT-11 the therapeutic scheme was also a multiple injection every fourth day for up to 28 days and a maximum of 8 injections [190]. For further evaluation of the CPT-11-TSL in the therapeutic study a multiple treatment should be taken in consideration.

One further improvement for the next therapeutic study could be the usage of a higher dose of non-liposomal CPT-11, CPT-11-TSL and Onivyde®, because with 20 mg/kg the dose was quite low in comparison to literature. The commonly used dosages varied between 40 mg/kg to 100 mg/kg CPT-11 for Onivyde®-like formulations as well as for non-liposomal CPT-11 [92, 93, 188-190]. Administering higher doses of Onivyde® in the study performed in this work was not possible, because the commercially available Onivyde® had such a low lipid concentration that no higher CPT-11 levels could be injected due to the limitations of injection volume in a rat. The maximal injection volume was already reached with the 20 mg/kg CPT-11 injection. However, for non-liposomal CPT-11 as well as for CPT-11-TSL much higher concentrations can be injected. For reasons of comparison, the Onivyde® was the dose limiting factor and the maximal dose possible for Onivyde® was used as dose for all treatment groups.

Comparing the therapeutic efficacy in the BN175 soft tissue sarcoma model, the improved $dFdC_6$-$TSL_{6/1/3/0}$ and non-liposomal dFdC showed an advantage over CPT-11-TSL and non-liposomal CPT-11 (cf. Figure 5-1). After 10 days, the difference in tumor growth delay for CPT-11-TSL and $dFdC_6$-$TSL_{6/1/3/0}$ was significantly different ($p< 0.05$). After 4 days, the tumor size of animals treated with CPT-11-TSL was slightly higher and after 6 days the tumor growth of CPT-11-TSL was much faster. This might be caused by the above-mentioned reasons, e.g. the low dose of CPT-11, because the tumor growth inhibition for non-liposomal

CPT-11 was lower than for non-liposomal dFdC. The dose applied for dFdC-TSL and non-liposomal dFdC was probably closer to the maximally tolerated dose and the tumor model was more sensitive to dFdC than to CPT-11. Another reason might also be a difference in sensitivity of the BN175 tumors to the applied drugs.

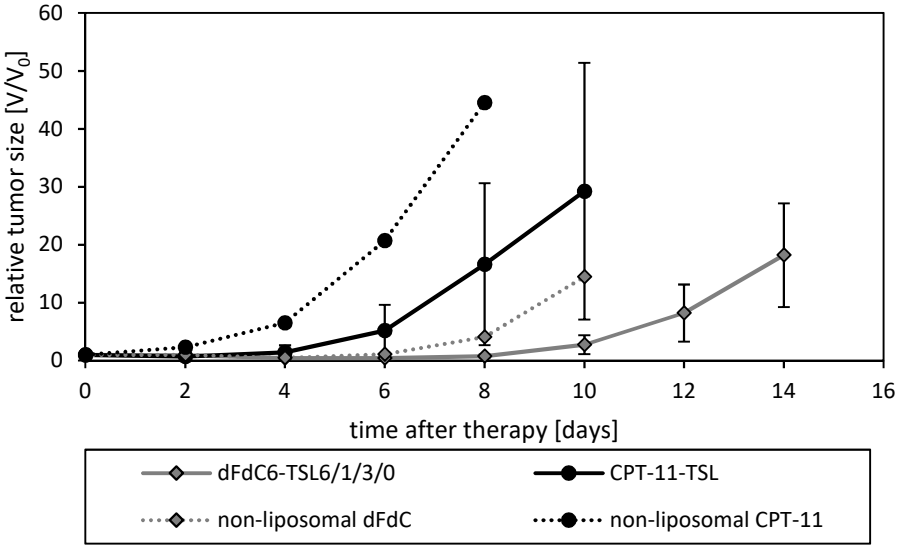


*Figure 5-1 Comparison of relative tumor size of improved dFdC-TSL formulation ($dFdC_6$-$TSL_{6/1/3/0}$), CPT-11-TSL and the non-liposomal drugs CPT-11 and dFdC in the soft tissue sarcoma model BN175 in rats.*
*Values are given as mean value ± standard deviation of 6 (dFdC-TSL, non-liposomal CPT-11), 7 (CPT-11-TSL) or 12 (non-liposomal dFdC) animals.*

In a different, more suitable tumor model and with adjusted dose of CPT-11-TSL the results could completely change. However, it is obvious that for both formulations there is still space for improvement especially in the *in vivo* part. As soon as a pancreatic cancer model in rats will be available both formulations will be tested in a more suitable model for these two drugs.

### 5.2.5 Outlook

The encapsulation of CPT-11 in $DPPG_2$-based TSL was successfully implemented with a high encapsulation efficacy, storage stability at 2-8°C, stability at 37°C in presence of serum and high release rates at temperatures > 40°C. *In vivo* the CPT-11-TSL formulation showed improved intravascular drug levels compared to non-liposomal CPT-11 and similar therapeutic efficacy as Onviyde®. The *in vivo* behavior of the formulation should be tested again in a more suitable tumor model as well as under application of higher doses and in a multiple treatment regime.

## 5.3 Lyophilization

Lyophilization of $DPPG_2$-based TSL was analyzed to obtain an alternative approach of storage for $DPPG_2$-TSL dispersions with extended storage stability. Advantage of lyophilized samples could be the lack of water resulting in less degradation products of lipids due to hydrolysis.

### 5.3.1 Process development

The development of the lyophilization process was performed with CF-loaded $DPPG_2$-based TSL with the formulation DPPC/DSPC/$DPPG_2$ 50:20:30 (molar ratio), due to the non-toxic and fluorescent characteristics of CF.

The lyophilization without cryoprotectant was performed to screen for parameters (z-average, PDI, temperature-dependent release, drug leakage were tested) potentially valid as indicators for the success of lyophilization. In this experiment it was shown, that lyophilization of $DPPG_2$-based TSL is not possible without cryoprotectants. The visual inspection after reconstitution showed already a degradation, because the color of the dispersion changed from orange to yellow. At high intraliposomal concentrations CF is orange. Due to the lyophilization most of the CF was released of the TSL and the CF was diluted in the external solution after rehydration of the lyophilized cake resulting in a yellow appearance, which is typical for CF at low concentrations. Additional parameters beside drug leakage, which changed after lyophilization were the z-average (112.3 nm before lyophilization and 412.1 nm after lyophilization) and the PDI (0.053 before lyophilization and 0.451 after lyophilization). The reason for this might be fusion of liposomes and the formation of aggregates as described by Ingvarsson et al [98]. Crowe et al also described that lyophilization of liposomes without cryoprotectant resulted in a complete leakage of the encapsulated material, as well as a quadrupling of the size [191]. After addition of small amounts of trehalose inside the liposomes (≤ 0.1 g trehalose/g phospholipid) and 3.2 g trehalose/g phospholipid extraliposomal, the drug retention, as well as the inhibition of fusion, could be increased [191]. Therefore, CF-leakage, z-average and PDI were the parameters used to evaluate the success of a lyophilization process for the present work.

Next, different cryoprotectants like sucrose and trehalose in different intra- and extraliposomal concentrations were tested, with 5% sucrose extraliposomally showing the best results for $DPPG_2$-TSL concerning the CF-leakage before and after lyophilization (cf. Figure 4-54). The cryoprotectants were chosen because trehalose was described as golden standard and sucrose was also used in many studies for lyophilization of liposomes [98] and was already approved in liposomal drug products (e.g. sucrose for Doxil®) [192]. For $DPPG_2$-based TSL sucrose showed superior results when analyzing the CF-leakage. Perhaps sucrose interacts in a more favorable manner with the components of the liposomal

membrane of $DPPG_2$-based TSL and result in a better protective effect, when water was replaced during lyophilization. Measuring the osmolarity of the different solutions intra- and extraliposomally for all tested formulations the difference between intra-and extraliposomal osmolarity was similar and the differences seen in the initial CF-release could not be caused by difference in osmotic pressure during liposomal preparation. For all tested formulations, the z-average and PDI did not change significantly (cf. Figure 4-53).

In literature, the freezing rate is described as important parameter during lyophilization for the quality of the resulting lyophilized samples [98, 107]. A fast freezing rate results in formation of fine ice-crystals and homogenous distribution of the cryoprotectant, resulting in a reduction of the disruption of the liposomal bilayer [98]. A slow freezing rate is ascribed to be beneficial for avoidance of drug leakage, because leakage caused by osmotic pressure during freeze-concentration is be reduced [108]. For the $DPPG_2$-based TSL, it was shown, that the freezing rate is the parameter influencing the CF-leakage during lyophilization. Fast freezing in liquid nitrogen resulted in 10.9±0.9% in BF (3.2% before freezing). After freezing with CN at -5°C the BF was only 4.9±0.7% (BF 3.2% before freezing). The slower freezing rate (1°C/min after CN) and the controlled ice crystal growth resulted in a better drug retention for the CF-TSL. This might be caused by lower osmotic pressure due to freeze-concentration during freezing and the reduction of stress for the rigid bilayer in the solid gel phase state. One disadvantage of a slower freezing rate was the formation of bigger ice crystals, which can be more detrimental to the membrane. The effect of the freezing-rate was also shown for vials wrapped in sterile bags. With a lower freezing rate (0.2°C instead of 1°C/min) the CF-leakage was decreased (cf. Figure 4-63).

The reproducibility of the CN lyophilization process was shown for two liposomal batches. An important advantage of CN is the increased reproducibility and decreased variance between the different vials in one process, because for all vials the nucleation takes place around the same temperature and not in a spontaneous manner. For the developed lyophilization process the temperature for CN was at -5°C and minimized the leakage. Fransen et al described that at -6 to -8°C in liposomes (composition hydrogenated soybean phosphatidylcholine and dicetylphosphate) the ice crystal formation started and a detectable leakage of CF was seen [193]. The CF loss increased when lower temperatures were reached. At temperatures when the samples are nearly completely frozen (-25 to -30°C) the CF leakage dropped to lower values again. In case of the CN the nucleation for all vials started at -5°C resulting in the CF loss seen in this work and then, after the first crystal growth no more CF might be released. If no CN or a high freezing rate was used, then the nucleation started at a different time point for each vial and a different temperature. Some vials could already nucleated around -10°C when a great amount of CF was already released due to osmotic pressure caused by freeze-concentration, compared to vials which nucleated

at -5°C. An additional aspect could be the fact that at this low freezing rate or after the controlled nucleation, the crystal formation is only in the extraliposomal space and not in the intraliposomal space resulting in no damage of the bilayer. Critical parameters influencing this phenomenon of internal ice formation were the water permeability of the bilayer and the potential of vesicle shrinkage to compensate for the increased salt concentration in the external phase during ice crystal formation [193].

The lyophilization of $DPPG_2$-based CF-TSL with CN showed acceptable drug retention during lyophilization when 5% sucrose was used as external cryoprotectant, with less than 10% CF-leakage. The steps made in this work resulted in acceptable lyophilization results for CF-TSL but there is further space for improvement. The residual moisture content was in an acceptable range, when the value of < 3% described in literature was taken as limit [137]. In literature, no single explanation for a protecting mechanism of liposomal formulations from freezing damage exist, because also each phospholipid has influence on the lyophilization behavior of a liposomal formulation as well as the phase of the liposomal membrane (solid-gel or liquid-crystalline phase).

The CF-TSL lyophilized with CN and 5% sucrose were investigated in a comprehensive storage stability study at two different storage conditions (RT and at 2-8°C) over 6 months. After up to 6 months the TSL were still stable with no visible change in PDI, z-average, CF-leakage and temperature-dependent release. Degradation products like lysolipids were also not detectable (cf. 4.3.2). A slightly higher residual moisture was visible for vials stored at 2-8°C compared to vials stored at RT after 1.5 months. This could be due to not completely leak-proof stoppers on the vials and the more humid environment in the fridge than at RT. The value did not increase over the storage time, perhaps after 1.5 months an equilibrium between the humidity inside and outside of the vial is reached. A pretest of CF-TSL stored for 1.4 years at 2-8°C showed, that the formulation was not affected during this time (cf. Figure 4-59). This result was a promising result for the proper stability study which is still ongoing and will last up to 24 months.

In a stability study performed with Dox-loaded liposomes (composition DPPC/DPPG/Chol) the stability for up to 6 months at temperatures up to 30°C was shown [194]. At higher temperatures Dox-degradation, Dox-leakage and increase in vesicle size was observed. For lyophilized samples with a higher residual moisture (2.3-3.5%) content at storage temperatures > 30°C a marked change in Dox-retention and vesicle size was detected, compared to samples with lower residual moisture (0.4-0.7%). A direct comparison of these results with the investigated CF-TSL in this thesis was not possible, due to the different drugs, the different liposomal formulation and the thermosensitive characteristics of TSL. Nevertheless, the results for CF-TSL are in a good agreement with the mentioned study, because after 6 months of storage at 2-8°C or RT no change was detectable.

### 5.3.2 Lyophilization of $DPPG_2$-based TSL containing dFdC, CPT-11 or Dox

For the lyophilization of TSL containing cytostatic agents (Dox, dFdC, CPT-11) the vials had to be wrapped in sterile bags to avoid the risk of contamination in case of breakage of vials. The process with CN was not possible, because the ice-crystals produced for CN with the ice-fog method were not able to reach the vials across the sterile bag. Due to this fact, the process was adjusted by replacing CN by use of bigger fill volume (4 ml instead of 1 ml) and a lower freezing rate (0.2°C instead of 1°C). The drug leakage after lyophilization for CF-TSL (5.5±0.7%) was comparable with samples produced with CN (5.5±0.2%). Drawbacks of the lyophilization were the longer process time (72 h vs. 57 h) and the higher residual moisture, due to the fact, that the vials had to be stoppered manually. The manual stoppering was needed, as safe automatic stoppering was not possible due to the use of sterile bags. Usage of sterile bags did not allow for upright positioning of the vials which is needed for avoidance of glass-breakage

For lyophilization of $DPPG_2$-based TSL encapsulating dFdC, CPT-11 or Dox the liposomes were prepared with extraliposomal 5% sucrose as cryoprotectant.

The lyophilization of CPT-11-TSL was possible, but the reconstitution of the cake failed due to a foamy and gel-like consistence of the resultant dispersion. This foamy and gel-like behavior of CPT-11-TSL in dispersion was also seen after preparing CPT-11-TSL with DAC (data not shown) after the redispersing step. Therefore, all obtained unfavorable results like the PDI and z-average increase as well as the increase in BF the instability at 40°C in the temperature-dependent release were rather an effect of the drug than of the lyophilization process. Onivyde®, the FDA approved nanoliposomal formulation, only was available in a liquid liposomal formulation and not as a lyophilized product. The reason might be that the developers encountered the same problem during establishment of a lyophilization process for their product, because storage of a liposomal drug product is always better in a lyophilized form than as dispersion due to the hydrolysis of the phospholipids.

The lyophilization of dFdC-TSL and Dox-TSL was more successful. The reconstitution for both showed no adverse observations and the z-average and the PDI were comparable for both before and after lyophilization.

For dFdC-TSL the leakage increased to 15.3±3.0% (before lyophilization 0%). The temperature-dependent release profile was comparable. The high standard deviation at 42°C and 44 °C might be caused by different temperatures for nucleation start between the single vials. This problem might be diminished, when CN could also be used for the lyophilization of TSL containing cytostatic agents.

For Dox-TSL, background fluorescence increased to 34.2±2.3% (23.0±0% before lyophilization; 1.4-fold) and the temperature-dependent release was also changed. The Dox-TSL were destabilized after lyophilization and reconstitution, because the release at 39-40°C was increased and more Dox was released at temperatures > 40°C (cf. Figure 4-71a).
Dox-TSL and dFdC-TSL showed a higher drug leakage after lyophilization, because the process was optimized for CF-TSL and not for the cytostatic drug.
One major difference between CF-TSL, Dox-TSL and dFdC-TSL was the difference in Tg` (CF-TSL -29.8±1°C, Dox-TSL -35.9±2.8°C, dFdC-TSL -31.5±3.4°C). Tg` of the cytotoxic containing TSL was lower and so the freezing step should probably be performed at lower temperatures than -40°C, e.g. -50°C, and the primary drying should be also at lower temperatures, e.g. -40°C. For integrity of the liposomes it is important that the samples were frozen at temperatures below their Tg` [107]. The difference in Tg` could be caused by the different molecules encapsulated in the intraliposomal space and the excipients used for the encapsulation ($(NH_4)_2HPO_4$ for Dox-loading and HBS pH 7.4 for dFdC-loading). Van Winden described that liposomes do not contribute to Tg` [107] and so the difference in the phospholipid composition of dFdC-TSL DPPC/DSPC/$DPPG_2$ 60:10:30 (molar ratio) in comparison to DPPC/DSPC/$DPPG_2$ 50:20:30 (molar ratio) for Dox-TSL and CF-TSL should not cause the difference in Tg`.

### 5.3.3 Outlook

For further development of a lyophilization process for dFdC-TSL and Dox-TSL other cryoprotectants than sucrose, as well as different concentrations of cryoprotectant intra- and extraliposomal should be tested. Trehalose used as golden standard for lyophilization might show better results regarding the drug leakage and the destabilization after lyophilization (seen for Dox-TSL) than for the TSL with 5% sucrose as cryoprotectant.
As additional improvement, CN needs to be tested for lyophilization of TSL containing cytotoxic drugs, because this could also result in a successfully freeze-dried product due to the higher vial reproducibility.
With some further improvements and changes in the lyophilization process, it should be possible to establish a lyophilization process for dFdC-TSL and Dox-TSL which results in a product with extended shelf-life and with acceptable and comparable characteristics compared to the characteristics before lyophilization.

# 6. Summary and conclusion

The objective of this work was the investigation, optimization and characterization of heat-inducible nanocarrier systems based on the $DPPG_2$ phospholipid for the targeted transport and release of active pharmaceutical ingredients effective against pancreatic cancer. The thesis consists of three parts:

In the first part, a previously investigated formulation $dFdC_3$-$TSL_{5/2/3/0}$ [44] was improved by solving the intrinsic instability of the formulation regarding initial drug leakage and decomposition of phospholipids during preparation. It was shown, that a clinically established assay for determination of FFA could also be used for measurement of FFA in liposomal samples. Improvement of the formulation was achieved by adjusting the pH of the dFdC-solution to pH 6-6.5, adding two additional steps in the preparation method and changing the phospholipid composition. The improved formulations $dFdC_6$-$TSL_{6/1/3/0}$, $dFdC_6$-$TSL_{7/0/3/0}$ and $dFdC_6$-$TSL_{4.5/2/3/0.5}$ showed no detectable lysolipids and FFA, a marked release at 41°C in FBS and were stable at 37-38°C in presence of serum. They were storable at 2-8°C for at least 60 weeks in contrast to $dFdC_3$-$TSL_{5/2/3/0}$ which already showed degradation products after 4 weeks. The stability study also showed that analysis of degradation products is important to evaluate (storage) stability of liposomal formulations. Such investigations are hardly performed in academia despite the fact that degradation products might bias the therapeutic outcome of liposomal formulations in animal models, as demonstrated here. Determination of z-average and PDI however is not sufficient to judge stability of a formulation. In the *in vivo* studies in rats, $dFdC_6$-$TSL_{6/1/3/0}$ showed a similar therapeutic efficacy as the formulation $dFdC_3$-$TSL_{5/2/3/0}$ with a higher $c_0$ and AUC, but a slightly lower plasma half-life. The improved formulation showed a notable increased circulation half-life and therapeutic effect compared to non-liposomal dFdC. Taking these findings together it was possible to obtain a dFdC-TSL formulation with improved *in vitro* behavior and the possibility for storage at 2-8°C with a similar *in vivo* behavior as the already described formulation $dFdC_3$-$TSL_{5/2/3/0}$ [44].

In the second part of the thesis, a thermosensitive liposomal formulation of CPT-11 based on $DPPG_2$-TSL was successfully developed. The formulation was stabilized by using $(NH_4)_2SO_4$ as loading excipient and higher drug/lipid ratios. The formulation showed less drug release at 37°C with increasing drug/lipid ratio. The resulting CPT-11-TSL showed acceptable stability at 37°C in presence of serum with a high heat-induced CPT-11 release at 41°C (72.7±2.3% after 5 min in FBS). The *in vitro* comparison with long-circulating nanoliposomal CPT-11 (Onivyde®) showed, that the established assays are suitable to analyze CPT-11 and to obtain reliable results for liposomal CPT-11 formulations. The aforementioned importance to

quantify lipid decomposition products was confirmed when measuring lysolipid and FFA content for Onivyde®. The obtained results indicated that the amount of lipid decomposition products is useful to determine the shelf life of the approved formulation. The established HPLC-method was suitable to detect CPT-11 as well as the more active metabolite SN-38 in one run. It was shown *in vivo*, that the CPT-11-TSL formulation had a notably prolonged circulation half-life in rats compared to non-liposomal CPT-11. The CPT-11 plasma concentration was comparable to Onivyde® in the first 60 min after injection, with a detectable amount of SN-38 in the blood stream. In the biodistribution study it was shown, that targeting of CPT-11-TSL to the tumor by focused local heating was possible by achieving notably higher intratumoral CPT-11 concentrations in comparison to non-liposomal CPT-11 and Onivyde®. The therapeutic efficacy (tumor growth delay) for CPT-11-TSL was improved compared to non-liposomal CPT-11 and in the same range as for Onivyde®. In contrast to Onivyde® and non-liposomal CPT-11, thermosensitive drug delivery of CPT-11 with TSL resulted as only formulation in a tumor size decrease after treatment. The animal studies also showed, that both liposomal formulations CPT-11-TSL and Onivyde® act in two different ways. CPT-11-TSL showed its therapeutic effect due to high intratumoral CPT-11 and SN-38 concentrations after the HT-treatment. In contrast, Onivyde® acted over its long-circulation time resulting in a constant CPT-11 and SN-38 delivery. Recapitulating this project together it was possible to load CPT-11 at high concentrations in $DPPG_2$-based TSL resulting in a formulation with high intratumoral CPT-11 and SN-38 concentration. The therapeutic effect in a first proof of concept study was similar to the approved formulation Onivyde®, in an animal model which was not optimal. The CPT-11-TSL showed a better local effect resulting in less systemic toxicity.

The last part was the development of a lyophilization process for $DPPG_2$-based TSL. For $DPPG_2$-based TSL encapsulating CF different cryoprotectants, as well as cryoprotectant concentrations were tested. The lyophilization with 5% sucrose extraliposomal as cryoprotectant showed the best result concerning drug leakage after lyophilization. Slow freezing (1°C/min) after CN was more favorable (less drug leakage) than fast freezing in liquid nitrogen. CN lyophilized CF-TSL (5% sucrose as cryoprotectant) showed a shelf life at both storage conditions (2-8°C and RT) for at least 6 months, but the study is still ongoing. It was also shown, that lyophilization of $DPPG_2$-based CF-TSL wrapped in sterile bags was possible. With an adjusted freezing rate of 0.2°C/min (in contrast to 1°C/min after CN) the drug leakage was similar to samples lyophilized with CN. Lyophilization of Dox-TSL and dFdC-TSL with the process developed for CF-TSL was possible, but some further improvements have to be made, to reduce the drug leakage after lyophilization and to overcome a destabilization of the formulation seen for Dox-TSL. Lyophilization of CPT-11-

TSL was possible, but the rehydration resulted in a foamy and gel-like formulation, leading higher z-average and PDI after lyophilization. Overall, it is feasible to lyophilize $DPPG_2$-based TSL, but for each drug the process has to be adjusted and developed.

# 7. Appendix

## 7.1 References

[1] Bericht zum Krebsgeschehen in Deutschland 2016, in, Zentrum für Krebsregisterdaten im Robert Koch-Institut, Berlin, 2016.

[2] B.S. Pattni, V.V. Chupin, V.P. Torchilin, New Developments in Liposomal Drug Delivery, Chem Rev, 115 (2015) 10938-10966.

[3] C.D. Landon, J.Y. Park, D. Needham, M.W. Dewhirst, Nanoscale Drug Delivery and Hyperthermia: The Materials Design and Preclinical and Clinical Testing of Low Temperature-Sensitive Liposomes Used in Combination with Mild Hyperthermia in the Treatment of Local Cancer, Open Nanomed J, 3 (2011) 38-64.

[4] L.H. Lindner, M.E. Eichhorn, H. Eibl, N. Teichert, M. Schmitt-Sody, R.D. Issels, M. Dellian, Novel temperature-sensitive liposomes with prolonged circulation time, Clin Cancer Res, 10 (2004) 2168-2178.

[5] B. Kneidl, M. Peller, G. Winter, L.H. Lindner, M. Hossann, Thermosensitive liposomal drug delivery systems: state of the art review, Int J Nanomedicine, 9 (2014) 4387-4398.

[6] L.H. Lindner, M. Hossann, Factors affecting drug release from liposomes, Curr Opin Drug Discov Devel, 13 (2010) 111-123.

[7] A.D. Bangham, M.M. Standish, J.C. Watkins, Diffusion of univalent ions across the lamellae of swollen phospholipids, J Mol Biol, 13 (1965) 238-252.

[8] G. Sessa, G. Weissmann, Phospholipid spherules (liposomes) as a model for biological membranes, J Lipid Res, 9 (1968) 310-318.

[9] P.L. Felgner, T.R. Gadek, M. Holm, R. Roman, H.W. Chan, M. Wenz, J.P. Northrop, G.M. Ringold, M. Danielsen, Lipofection: a highly efficient, lipid-mediated DNA-transfection procedure, Proc Natl Acad Sci U S A, 84 (1987) 7413-7417.

[10] H. Maeda, J. Wu, T. Sawa, Y. Matsumura, K. Hori, Tumor vascular permeability and the EPR effect in macromolecular therapeutics: a review, J Control Release, 65 (2000) 271-284.

[11] G. Kong, G. Anyarambhatla, W.P. Petros, R.D. Braun, O.M. Colvin, D. Needham, M.W. Dewhirst, Efficacy of liposomes and hyperthermia in a human tumor xenograft model: importance of triggered drug release, Cancer Res, 60 (2000) 6950-6957.

[12] L. Li, T.L. ten Hagen, M. Bolkestein, A. Gasselhuber, J. Yatvin, G.C. van Rhoon, A.M. Eggermont, D. Haemmerich, G.A. Koning, Improved intratumoral nanoparticle extravasation and penetration by mild hyperthermia, J Control Release, 167 (2013) 130-137.

[13] H. Maeda, The enhanced permeability and retention (EPR) effect in tumor vasculature: the key role of tumor-selective macromolecular drug targeting, Adv Enzyme Regul, 41 (2001) 189-207.

[14] K.J. Harrington, S. Mohammadtaghi, P.S. Uster, D. Glass, A.M. Peters, R.G. Vile, J.S. Stewart, Effective targeting of solid tumors in patients with locally advanced cancers by radiolabeled pegylated liposomes, Clin Cancer Res, 7 (2001) 243-254.

[15] K.M. Laginha, S. Verwoert, G.J. Charrois, T.M. Allen, Determination of doxorubicin levels in whole tumor and tumor nuclei in murine breast cancer tumors, Clin Cancer Res, 11 (2005) 6944-6949.

[16] A.L. Seynhaeve, B.M. Dicheva, S. Hoving, G.A. Koning, T.L. ten Hagen, Intact Doxil is taken up intracellularly and released doxorubicin sequesters in the lysosome: evaluated by in vitro/in vivo live cell imaging, J Control Release, 172 (2013) 330-340.

[17] A.A. Manzoor, L.H. Lindner, C.D. Landon, J.Y. Park, A.J. Simnick, M.R. Dreher, S. Das, G. Hanna, W. Park, A. Chilkoti, G.A. Koning, T.L. ten Hagen, D. Needham, M.W. Dewhirst, Overcoming limitations in nanoparticle drug delivery: triggered, intravascular release to improve drug penetration into tumors, Cancer Res, 72 (2012) 5566-5575.

[18] G.A. Koning, A.M. Eggermont, L.H. Lindner, T.L. ten Hagen, Hyperthermia and thermosensitive liposomes for improved delivery of chemotherapeutic drugs to solid tumors, Pharm Res, 27 (2010) 1750-1754.

[19] Q. Chen, S. Tong, M.W. Dewhirst, F. Yuan, Targeting tumor microvessels using doxorubicin encapsulated in a novel thermosensitive liposome, Mol Cancer Ther, 3 (2004) 1311-1317.

[20] G.A. Koning, L. Li, T.L. ten Hagen, Thermosensitive liposomes for the delivery of cancer therapeutics, Ther Deliv, 1 (2010) 707-711.

[21] M.B. Yatvin, J.N. Weinstein, W.H. Dennis, R. Blumenthal, Design of liposomes for enhanced local release of drugs by hyperthermia, Science, 202 (1978) 1290-1293.

[22] D. Needham, G. Anyarambhatla, G. Kong, M.W. Dewhirst, A new temperature-sensitive liposome for use with mild hyperthermia: characterization and testing in a human tumor xenograft model, Cancer Res, 60 (2000) 1197-1201.

[23] B.J. Wood, R.T. Poon, J.K. Locklin, M.R. Dreher, K.K. Ng, M. Eugeni, G. Seidel, S. Dromi, Z. Neeman, M. Kolf, C.D. Black, R. Prabhakar, S.K. Libutti, Phase I study of heat-deployed liposomal doxorubicin during radiofrequency ablation for hepatic malignancies, J Vasc Interv Radiol, 23 (2012) 248-255 e247.

[24] T.M. Zagar, Z. Vujaskovic, S. Formenti, H. Rugo, F. Muggia, B. O'Connor, R. Myerson, P. Stauffer, I.C. Hsu, C. Diederich, W. Straube, M.K. Boss, A. Boico, O. Craciunescu, P. Maccarini, D. Needham, N. Borys, K.L. Blackwell, M.W. Dewhirst, Two phase I dose-escalation/pharmacokinetics studies of low temperature liposomal doxorubicin (LTLD)

and mild local hyperthermia in heavily pretreated patients with local regionally recurrent breast cancer, Int J Hyperthermia, 30 (2014) 285-294.

[25] V.P. Torchilin, Liposomes: A Practical Approach, Oxford University Press, 2003.

[26] H. Grull, S. Langereis, Hyperthermia-triggered drug delivery from temperature-sensitive liposomes using MRI-guided high intensity focused ultrasound, J Control Release, 161 (2012) 317-327.

[27] E. Evans, D. Needham, Physical properties of surfactant bilayer membranes: thermal transitions, elasticity, rigidity, cohesion and colloidal interactions, J Phys Chem 91 (1987) 4219-4228.

[28] O.G. Mouritsen, M.J. Zuckermann, Model of interfacial melting, Phys Rev Lett, 58 (1987) 389-392.

[29] T. Kaasgaard, C. Leidy, J.H. Crowe, O.G. Mouritsen, K. Jorgensen, Temperature-controlled structure and kinetics of ripple phases in one- and two-component supported lipid bilayers, Biophys J, 85 (2003) 350-360.

[30] M.H. Gaber, K. Hong, S.K. Huang, D. Papahadjopoulos, Thermosensitive sterically stabilized liposomes: formulation and in vitro studies on mechanism of doxorubicin release by bovine serum and human plasma, Pharm Res, 12 (1995) 1407-1416.

[31] M. Hossann, M. Wiggenhorn, A. Schwerdt, K. Wachholz, N. Teichert, H. Eibl, R.D. Issels, L.H. Lindner, In vitro stability and content release properties of phosphatidylglyceroglycerol containing thermosensitive liposomes, Biochim Biophys Acta, 1768 (2007) 2491-2499.

[32] H. Trauble, H. Eibl, Electrostatic effects on lipid phase transitions: membrane structure and ionic environment, Proc Natl Acad Sci U S A, 71 (1974) 214-219.

[33] T. Tagami, M.J. Ernsting, S.D. Li, Efficient tumor regression by a single and low dose treatment with a novel and enhanced formulation of thermosensitive liposomal doxorubicin, J Control Release, 152 (2011) 303-309.

[34] T. Tagami, M.J. Ernsting, S.D. Li, Optimization of a novel and improved thermosensitive liposome formulated with DPPC and a Brij surfactant using a robust in vitro system, J Control Release, 154 (2011) 290-297.

[35] R.A. Demel, B. De Kruyff, The function of sterols in membranes, Biochim Biophys Acta, 457 (1976) 109-132.

[36] B.Z. Chowdhry, G. Lipka, A.W. Dalziel, J.M. Sturtevant, Effect of lanthanum ions on the phase transitions of lecithin bilayers, Biophys J, 45 (1984) 633-635.

[37] S. Mabrey, J.M. Sturtevant, Investigation of phase transitions of lipids and lipid mixtures by sensitivity differential scanning calorimetry, Proc Natl Acad Sci U S A, 73 (1976) 3862-3866.

[38] D. Papahadjopoulos, A. Gabizon, Liposomes designed to avoid the reticuloendothelial system, Prog Clin Biol Res, 343 (1990) 85-93.

[39] T.M. Allen, C.B. Hansen, D.E. Lopes de Menezes, Pharmacokineics of long-circulating liposomes, Adv Drug Deliv Rev, 16 (1995) 267-284.

[40] D. Needham, T.J. McIntosh, D.D. Lasic, Repulsive interactions and mechanical stability of polymer-grafted lipid membranes, Biochim Biophys Acta, 1108 (1992) 40-48.

[41] L.M. Ickenstein, M.C. Arfvidsson, D. Needham, L.D. Mayer, K. Edwards, Disc formation in cholesterol-free liposomes during phase transition, Biochim Biophys Acta, 1614 (2003) 135-138.

[42] J.K. Mills, D. Needham, Lysolipid incorporation in dipalmitoylphosphatidylcholine bilayer membranes enhances the ion permeability and drug release rates at the membrane phase transition, Biochim Biophys Acta, 1716 (2005) 77-96.

[43] R. Schmidt, Neuartige thermosensitive Liposomen zur zielgerichteten Therapie solider Tumoren - Charakterisierung in vitro und in vivo, Dissertation, (2011).

[44] S. Limmer, J. Hahn, R. Schmidt, K. Wachholz, A. Zengerle, K. Lechner, H. Eibl, R.D. Issels, M. Hossann, L.H. Lindner, Gemcitabine Treatment of Rat Soft Tissue Sarcoma with Phosphatidyldiglycerol-Based Thermosensitive Liposomes, Pharm Res, (2014).

[45] K. Zimmermann, M. Hossann, J. Hirschberger, K. Troedson, M. Peller, M. Schneider, A. Bruhschwein, A. Meyer-Lindenberg, G. Wess, M. Wergin, R. Dorfelt, T. Knosel, M. Schwaiger, C. Baumgartner, J. Brandl, S. Schwamberger, L.H. Lindner, A pilot trial of doxorubicin containing phosphatidyldiglycerol based thermosensitive liposomes in spontaneous feline soft tissue sarcoma, Int J Hyperthermia, 33 (2017) 178-190.

[46] D.A. Mannock, R.N. Lewis, R.N. McElhaney, A calorimetric and spectroscopic comparison of the effects of ergosterol and cholesterol on the thermotropic phase behavior and organization of dipalmitoylphosphatidylcholine bilayer membranes, Biochim Biophys Acta, 1798 (2010) 376-388.

[47] C. Demetzos, Differential Scanning Calorimetry (DSC): a tool to study the thermal behavior of lipid bilayers and liposomal stability, J Liposome Res, 18 (2008) 159-173.

[48] M.W. Dewhirst, Z. Vujaskovic, E. Jones, D. Thrall, Re-setting the biologic rationale for thermal therapy, Int J Hyperthermia, 21 (2005) 779-790.

[49] R. Issels, E. Kampmann, R. Kanaar, L.H. Lindner, Hallmarks of hyperthermia in driving the future of clinical hyperthermia as targeted therapy: translation into clinical application, Int J Hyperthermia, 32 (2016) 89-95.

[50] P. Wust, B. Hildebrandt, G. Sreenivasa, B. Rau, J. Gellermann, H. Riess, R. Felix, P.M. Schlag, Hyperthermia in combined treatment of cancer, The Lancet Oncology, 3 (2002) 487-497.

[51] R.D. Issels, Hyperthermia adds to chemotherapy, Eur J Cancer, 44 (2008) 2546-2554.

[52] L.H. Lindner, R.D. Issels, Hyperthermia in soft tissue sarcoma, Curr Treat Options Oncol, 12 (2011) 12-20.

[53] K. Ahmed, S.F. Zaidi, Treating cancer with heat: hyperthermia as promising strategy to enhance apoptosis, J Pak Med Assoc, 63 (2013) 504-508.

[54] R.D. Issels, L.H. Lindner, J. Verweij, P. Wust, P. Reichardt, B.C. Schem, S. Abdel-Rahman, S. Daugaard, C. Salat, C.M. Wendtner, Z. Vujaskovic, R. Wessalowski, K.W. Jauch, H.R. Durr, F. Ploner, A. Baur-Melnyk, U. Mansmann, W. Hiddemann, J.Y. Blay, P. Hohenberger, R. European Organisation for, T. Treatment of Cancer Soft, G. Bone Sarcoma, O. European Society for Hyperthermic, Neo-adjuvant chemotherapy alone or with regional hyperthermia for localised high-risk soft-tissue sarcoma: a randomised phase 3 multicentre study, Lancet Oncol, 11 (2010) 561-570.

[55] K.E. Tschoep-Lechner, V. Milani, F. Berger, N. Dieterle, S. Abdel-Rahman, C. Salat, R.D. Issels, Gemcitabine and cisplatin combined with regional hyperthermia as second-line treatment in patients with gemcitabine-refractory advanced pancreatic cancer, Int J Hyperthermia, 29 (2013) 8-16.

[56] Y. Dou, K. Hynynen, C. Allen, To heat or not to heat: Challenges with clinical translation of thermosensitive liposomes, J Control Release, 249 (2017) 63-73.

[57] J.P. May, S.D. Li, Hyperthermia-induced drug targeting, Expert Opin Drug Deliv, 10 (2013) 511-527.

[58] G. Kong, M.W. Dewhirst, Hyperthermia and liposomes, Int J Hyperthermia, 15 (1999) 345-370.

[59] S.K. Huang, P.R. Stauffer, K. Hong, J.W. Guo, T.L. Phillips, A. Huang, D. Papahadjopoulos, Liposomes and hyperthermia in mice: increased tumor uptake and therapeutic efficacy of doxorubicin in sterically stabilized liposomes, Cancer Res, 54 (1994) 2186-2191.

[60] C. van Bree, J.J. Krooshoop, R.C. Rietbroek, J.B. Kipp, P.J. Bakker, Hyperthermia enhances tumor uptake and antitumor efficacy of thermostable liposomal daunorubicin in a rat solid tumor, Cancer Res, 56 (1996) 563-568.

[61] G. Kong, R.D. Braun, M.W. Dewhirst, Hyperthermia enables tumor-specific nanoparticle delivery: effect of particle size, Cancer Res, 60 (2000) 4440-4445.

[62] M.H. Gaber, N.Z. Wu, K. Hong, S.K. Huang, M.W. Dewhirst, D. Papahadjopoulos, Thermosensitive liposomes: extravasation and release of contents in tumor microvascular networks, Int J Radiat Oncol Biol Phys, 36 (1996) 1177-1187.

[63] G. Kong, R.D. Braun, M.W. Dewhirst, Characterization of the effect of hyperthermia on nanoparticle extravasation from tumor vasculature, Cancer Res, 61 (2001) 3027-3032.

[64] D. Zhu, W. Lu, Y. Weng, H. Cui, Q. Luo, Monitoring thermal-induced changes in tumor blood flow and microvessels with laser speckle contrast imaging, Applied Optics, 46 (2007) 1911-1917.

[65] A. Shakil, J.L. Osborn, C.W. Song, Changes in oxygenation status and blood flow in a rat tumor model by mild temperature hyperthermia, Int J Radiat Oncol Biol Phys, 43 (1999) 859-865.

[66] Z. Vujaskovic, J.M. Poulson, A.A. Gaskin, D.E. Thrall, R.L. Page, H.C. Charles, J.R. MacFall, D.M. Brizel, R.E. Meyer, D.M. Prescott, T.V. Samulski, M.W. Dewhirst, Temperature-dependent changes in physiologic parameters of spontaneous canine soft tissue sarcomas after combined radiotherapy and hyperthermia treatment, Int J Radiat Oncol Biol Phys, 46 (2000) 179-185.

[67] B. Chen, M. Zhou, L.X. Xu, Study of vascular endothelial cell morphology during hyperthermia, J Therm Biol, 30 (2005) 111-117.

[68] A. Kleger, T. Seufferlein, Pharmakotherapie beim Pankreaskarzinom, Arzneimitteltherapie, 32 (2014) 274-282.

[69] Y. Zhang, K. Satoh, M. Li, Novel therapeutic modalities and drug delivery in pancreatic cancer - an ongoing search for improved efficacy, Drugs Context, 2012 (2012) 212244.

[70] H.A. Burris, 3rd, M.J. Moore, J. Andersen, M.R. Green, M.L. Rothenberg, M.R. Modiano, M.C. Cripps, R.K. Portenoy, A.M. Storniolo, P. Tarassoff, R. Nelson, F.A. Dorr, C.D. Stephens, D.D. Von Hoff, Improvements in survival and clinical benefit with gemcitabine as first-line therapy for patients with advanced pancreas cancer: a randomized trial, J Clin Oncol, 15 (1997) 2403-2413.

[71] T. Conroy, F. Desseigne, M. Ychou, O. Bouche, R. Guimbaud, Y. Becouarn, A. Adenis, J.L. Raoul, S. Gourgou-Bourgade, C. de la Fouchardiere, J. Bennouna, J.B. Bachet, F. Khemissa-Akouz, D. Pere-Verge, C. Delbaldo, E. Assenat, B. Chauffert, P. Michel, C. Montoto-Grillot, M. Ducreux, U. Groupe Tumeurs Digestives of, P. Intergroup, FOLFIRINOX versus gemcitabine for metastatic pancreatic cancer, N Engl J Med, 364 (2011) 1817-1825.

[72] E. Mini, S. Nobili, B. Caciagli, I. Landini, T. Mazzei, Cellular pharmacology of gemcitabine, Ann Oncol, 17 Suppl 5 (2006) v7-12.

[73] M.W. Ritzel, A.M. Ng, S.Y. Yao, K. Graham, S.K. Loewen, K.M. Smith, R.G. Ritzel, D.A. Mowles, P. Carpenter, X.Z. Chen, E. Karpinski, R.J. Hyde, S.A. Baldwin, C.E. Cass, J.D. Young, Molecular identification and characterization of novel human and mouse concentrative Na+-nucleoside cotransporter proteins (hCNT3 and mCNT3) broadly selective for purine and pyrimidine nucleosides (system cib), J Biol Chem, 276 (2001) 2914-2927.

[74] J.R. Mackey, R.S. Mani, M. Selner, D. Mowles, J.D. Young, J.A. Belt, C.R. Crawford, C.E. Cass, Functional nucleoside transporters are required for gemcitabine influx and manifestation of toxicity in cancer cell lines, Cancer Res, 58 (1998) 4349-4357.

[75] C. Lanz, M. Fruh, W. Thormann, T. Cerny, B.H. Lauterburg, Rapid determination of gemcitabine in plasma and serum using reversed-phase HPLC, J Sep Sci, 30 (2007) 1811-1820.

[76] V. Heinemann, L.W. Hertel, G.B. Grindey, W. Plunkett, Comparison of the Cellular Pharmacokinetics and Toxicity of 2′,2′-Difluorodeoxycytidine and 1-β-d-Arabinofuranosylcytosine, Cancer Res, 48 (1988) 4024-4031.

[77] D.Y. Bouffard, J. Laliberte, R.L. Momparler, Kinetic studies on 2',2'-difluorodeoxycytidine (Gemcitabine) with purified human deoxycytidine kinase and cytidine deaminase, Biochem Pharmacol, 45 (1993) 1857-1861.

[78] L. Wang, B. Munch-Petersen, A. Herrström Sjöberg, U. Hellman, T. Bergman, H. Jörnvall, S. Eriksson, Human thymidine kinase 2: molecular cloning and characterisation of the enzyme activity with antiviral and cytostatic nucleoside substrates, FEBS Letters, 443 (1999) 170-174.

[79] P. Huang, S. Chubb, L.W. Hertel, G.B. Grindey, W. Plunkett, Action of 2',2'-difluorodeoxycytidine on DNA synthesis, Cancer Res, 51 (1991) 6110-6117.

[80] D.D. Ross, D.P. Cuddy, Molecular effects of 2',2'-difluorodeoxycytidine (Gemcitabine) on DNA replication in intact HL-60 cells, Biochem Pharmacol, 48 (1994) 1619-1630.

[81] V. Gandhi, J. Legha, F. Chen, L.W. Hertel, W. Plunkett, Excision of 2',2'-difluorodeoxycytidine (gemcitabine) monophosphate residues from DNA, Cancer Res, 56 (1996) 4453-4459.

[82] V. Heinemann, Y.Z. Xu, S. Chubb, A. Sen, L.W. Hertel, G.B. Grindey, W. Plunkett, Cellular elimination of 2',2'-difluorodeoxycytidine 5'-triphosphate: a mechanism of self-potentiation, Cancer Res, 52 (1992) 533-539.

[83] Fachinformation Gemzar 38 mg/ml, (2015).

[84] G.G. Chabot, Clinical pharmacokinetics of irinotecan, Clin Pharmacokinet, 33 (1997) 245-259.

[85] N.F. Smith, W.D. Figg, A. Sparreboom, Pharmacogenetics of irinotecan metabolism and transport: an update, Toxicol In Vitro, 20 (2006) 163-175.

[86] M. Ramesh, P. Ahlawat, N.R. Srinivas, Irinotecan and its active metabolite, SN-38: review of bioanalytical methods and recent update from clinical pharmacology perspectives, Biomed Chromatogr, 24 (2010) 104-123.

[87] Y. Kawato, M. Aonuma, Y. Hirota, H. Kuga, K. Sato, Intracellular roles of SN-38, a metabolite of the camptothecin derivative CPT-11, in the antitumor effect of CPT-11, Cancer Res, 51 (1991) 4187-4191.

[88] A. Santos, S. Zanetta, T. Cresteil, A. Deroussent, F. Pein, E. Raymond, L. Vernillet, M.L. Risse, V. Boige, A. Gouyette, G. Vassal, Metabolism of irinotecan (CPT-11) by CYP3A4 and CYP3A5 in humans, Clin Cancer Res, 6 (2000) 2012-2020.

[89] M.C. Haaz, L. Rivory, C. Riche, L. Vernillet, J. Robert, Metabolism of irinotecan (CPT-11) by human hepatic microsomes: participation of cytochrome P-450 3A and drug interactions, Cancer Res, 58 (1998) 468-472.

[90] Irinotecan drug information, BCCA Cancer Drug Manual (2016) 1-9.

[91] D. Grapsa, K. Syrigos, M.W. Saif, Nanoliposomal irinotecan for treating pancreatic cancer, Expert Opin Orphan Drugs, 4 (2016) 541-547.

[92] A.V. Kalra, J. Kim, S.G. Klinz, N. Paz, J. Cain, D.C. Drummond, U.B. Nielsen, J.B. Fitzgerald, Preclinical activity of nanoliposomal irinotecan is governed by tumor deposition and intratumor prodrug conversion, Cancer Res, 74 (2014) 7003-7013.

[93] D.C. Drummond, C.O. Noble, Z. Guo, K. Hong, J.W. Park, D.B. Kirpotin, Development of a highly active nanoliposomal irinotecan using a novel intraliposomal stabilization strategy, Cancer Res, 66 (2006) 3271-3277.

[94] T.C. Chang, H.S. Shiah, C.H. Yang, K.H. Yeh, A.L. Cheng, B.N. Shen, Y.W. Wang, C.G. Yeh, N.J. Chiang, J.Y. Chang, L.T. Chen, Phase I study of nanoliposomal irinotecan (PEP02) in advanced solid tumor patients, Cancer Chemother Pharmacol, 75 (2015) 579-586.

[95] A. Wang-Gillam, C.P. Li, G. Bodoky, A. Dean, Y.S. Shan, G. Jameson, T. Macarulla, K.H. Lee, D. Cunningham, J.F. Blanc, R.A. Hubner, C.F. Chiu, G. Schwartsmann, J.T. Siveke, F. Braiteh, V. Moyo, B. Belanger, N. Dhindsa, E. Bayever, D.D. Von Hoff, L.T. Chen, N.-S. Group, Nanoliposomal irinotecan with fluorouracil and folinic acid in metastatic pancreatic cancer after previous gemcitabine-based therapy (NAPOLI-1): a global, randomised, open-label, phase 3 trial, Lancet, 387 (2016) 545-557.

[96] A.H. Ko, Nanomedicine developments in the treatment of metastatic pancreatic cancer: focus on nanoliposomal irinotecan, Int J Nanomedicine, 11 (2016) 1225-1235.

[97] M. Grit, D.J. Crommelin, Chemical stability of liposomes: implications for their physical stability, Chem Phys Lipids, 64 (1993) 3-18.

[98] P.T. Ingvarsson, M. Yang, H.M. Nielsen, J. Rantanen, C. Foged, Stabilization of liposomes during drying, Expert Opin Drug Deliv, 8 (2011) 375-388.

[99] K.L. Koster, M.S. Webb, G. Bryant, D.V. Lynch, Interactions between soluble sugars and POPC (1-palmitoyl-2-oleoylphosphatidylcholine) during dehydration: vitrification of sugars alters the phase behavior of the phospholipid, Biochim Biophys Acta Biomembr, 1193 (1994) 143-150.

[100] W.Q. Sun, A.C. Leopold, L.M. Crowe, J.H. Crowe, Stability of dry liposomes in sugar glasses, Biophysical Journal, 70 (1996) 1769-1776.

[101] J.H. Crowe, S.B. Leslie, L.M. Crowe, Is Vitrification Sufficient to Preserve Liposomes during Freeze-Drying?, Cryobiology, 31 (1994) 355-366.

[102] J.H. Crowe, F.A. Hoekstra, K.H.N. Nguyen, L.M. Crowe, Is vitrification involved in depression of the phase transition temperature of dry phospholipids?, Biochim Biophys Acta, 1280 (1996) 187-196.

[103] C. Chen, D. Han, C. Cai, X. Tang, An overview of liposome lyophilization and its future potential, J Control Release, 142 (2010) 299-311.

[104] L.M. Crowe, J.H. Crowe, Trehalose and dry dipalmitoylphosphatidylcholine revisited, Biochim Biophys Acta, 946 (1988) 193-201.

[105] D.J. Crommelin, E.M. van Bommel, Stability of liposomes on storage: freeze dried, frozen or as an aqueous dispersion, Pharm Res, 1 (1984) 159-163.

[106] E.M.G. Van Bommel, D.J.A. Crommelin, Stability of doxorubicin-liposomes on storage: as an aqueous dispersion, frozen or freeze-dried, Int J Pharm, 22 (1984) 299-310.

[107] E.C.A. van Winden, Freeze-Drying of Liposomes: Theory and Practice, in: Methods in Enzymology, Academic Press, 2003, pp. 99-110.

[108] E.C.A. van Winden, W. Zhang, D.J.A. Crommelin, Effect of freezing rate on the stability of liposomes during freeze-drying and rehydration, Pharm Res, 14 (1997) 1151-1160.

[109] J.C. Kasper, W. Friess, The freezing step in lyophilization: physico-chemical fundamentals, freezing methods and consequences on process performance and quality attributes of biopharmaceuticals, Eur J Pharm Biopharm, 78 (2011) 248-263.

[110] R. Geidobler, G. Winter, Controlled ice nucleation in the field of freeze-drying: fundamentals and technology review, Eur J Pharm Biopharm, 85 (2013) 214-222.

[111] X. Tang, M.J. Pikal, Design of freeze-drying processes for pharmaceuticals: practical advice, Pharm Res, 21 (2004) 191-200.

[112] M. Hossann, T. Wang, M. Wiggenhorn, R. Schmidt, A. Zengerle, G. Winter, H. Eibl, M. Peller, M. Reiser, R.D. Issels, L.H. Lindner, Size of thermosensitive liposomes influences content release, J Control Release, 147 (2010) 436-443.

[113] U. Massing, S. Cicko, V. Ziroli, Dual asymmetric centrifugation (DAC)--a new technique for liposome preparation, J Control Release, 125 (2008) 16-24.

[114] C. Bornmann, R. Graeser, N. Esser, V. Ziroli, P. Jantscheff, T. Keck, C. Unger, U.T. Hopt, U. Adam, C. Schaechtele, U. Massing, E. von Dobschuetz, A new liposomal formulation of Gemcitabine is active in an orthotopic mouse model of pancreatic cancer accessible to bioluminescence imaging, Cancer Chemother Pharmacol, 61 (2008) 395-405.

[115] L.D. Mayer, M.B. Bally, M.J. Hope, P.R. Cullis, Uptake of antineoplastic agents into large unilamellar vesicles in response to a membrane potential, Biochim Biophys Acta Biomembr, 816 (1985) 294-302.

[116] Y. Sadzuka, H. Takabe, T. Sonobe, Liposomalization of SN-38 as active metabolite of CPT-11, J Control Release, 108 (2005) 453-459.

[117] H. Eibl, W.E. Lands, A new, sensitive determination of phosphate, Anal Biochem, 30 (1969) 51-57.

[118] J.C. Dittmer, R.L. Lester, A Simple, Specific Spray for the Detection of Phospholipids on Thin-Layer Chromatograms, J Lipid Res, 5 (1964) 126-127.

[119] P. Trinder, Determination of blood glucose using 4-amino phenazone as oxygen acceptor, J Clin Pathol, 22 (1969) 246.

[120] P. Trinder, Determination of blood glucose using an oxidase-peroxidase system with a non-carcinogenic chromogen, J Clin Pathol, 22 (1969) 158-161.

[121] M. Holzer, S. Barnert, J. Momm, R. Schubert, Preparative size exclusion chromatography combined with detergent removal as a versatile tool to prepare unilamellar and spherical liposomes of highly uniform size distribution, J Chromatogr A, 1216 (2009) 5838-5848.

[122] P. Galettis, J. Boutagy, D.D. Ma, Daunorubicin pharmacokinetics and the correlation with P-glycoprotein and response in patients with acute leukaemia, Br J Cancer, 70 (1994) 324-329.

[123] L. Willerding, S. Limmer, M. Hossann, A. Zengerle, K. Wachholz, T.L. Ten Hagen, G.A. Koning, R. Sroka, L.H. Lindner, M. Peller, Method of hyperthermia and tumor size influence effectiveness of doxorubicin release from thermosensitive liposomes in experimental tumors, J Control Release, 222 (2016) 47-55.

[124] R. Geidobler, S. Mannschedel, G. Winter, A new approach to achieve controlled ice nucleation of supercooled solutions during the freezing step in freeze-drying, J Pharm Sci, 101 (2012) 4409-4413.

[125] J. van Ark-Otte, M.A. Kedde, W.J. van der Vijgh, A.M. Dingemans, W.J. Jansen, H.M. Pinedo, E. Boven, G. Giaccone, Determinants of CPT-11 and SN-38 activities in human lung cancer cells, Br J Cancer, 77 (1998) 2171-2176.

[126] Z.P. Hu, X.X. Yang, X. Chen, E. Chan, W. Duan, S.F. Zhou, Simultaneous determination of irinotecan (CPT-11) and SN-38 in tissue culture media and cancer cells by high performance liquid chromatography: application to cellular metabolism and accumulation studies, J Chromatogr B, 850 (2007) 575-580.

[127] K. Ohtsuka, S. Inoue, M. Kameyama, A. Kanetoshi, T. Fujimoto, K. Takaoka, Y. Araya, A. Shida, Intracellular conversion of irinotecan to its active form, SN-38, by native carboxylesterase in human non-small cell lung cancer, Lung Cancer, 41 (2003) 187-198.

[128] F.R. Hallett, J. Marsh, B.G. Nickel, J.M. Wood, Mechanical properties of vesicles. II. A model for osmotic swelling and lysis, Biophys J, 64 (1993) 435-442.

[129] M. Grit, D.J. Crommelin, The effect of aging on the physical stability of liposome dispersions, Chem Phys Lipids, 62 (1992) 113-122.

[130] N.J. Zuidam, H.K.M.E. Gouw, Y. Barenholz, D.J.A. Crommelin, Physical (in) stability of liposomes upon chemical hydrolysis: the role of lysophospholipids and fatty acids, Biochim Biophys Acta Biomembr, 1240 (1995) 101-110.

[131] L.F.M. van Zupthen, V. Baumans, A.C. Beynen, Grundlagen der Versuchstierkunde, Gustav Fischer Verlag, Stuttgart, 1995.

[132] L.P. Rivory, J. Robert, Reversed-phase high-performance liquid chromatographic method for the simultaneous quantitation of the carboxylate and lactone forms of the camptothecin derivative irinotecan, CPT-11, and its metabolite SN-38 in plasma, J Chromatogr B Biomed Appl, 661 (1994) 133-141.

[133] T. Xuan, J.A. Zhang, I. Ahmad, HPLC method for determination of SN-38 content and SN-38 entrapment efficiency in a novel liposome-based formulation, LE-SN38, J Pharm Biomed Anal, 41 (2006) 582-588.

[134] G.N. Chiu, S.A. Abraham, L.M. Ickenstein, R. Ng, G. Karlsson, K. Edwards, E.K. Wasan, M.B. Bally, Encapsulation of doxorubicin into thermosensitive liposomes via complexation with the transition metal manganese, J Control Release, 104 (2005) 271-288.

[135] T.H. Chou, S.C. Chen, I.M. Chu, Effect of composition on the stability of liposomal irinotecan prepared by a pH gradient method, J Biosci Bioeng, 95 (2003) 405-408.

[136] J.J. Mittag, B. Kneidl, T. Preiss, M. Hossann, G. Winter, S. Wuttke, H. Engelke, J.O. Radler, Impact of plasma protein binding on cargo release by thermosensitive liposomes probed by fluorescence correlation spectroscopy, Eur J Pharm Biopharm, 119 (2017) 215-223.

[137] A.R. Mohammed, A.G. Coombes, Y. Perrie, Amino acids as cryoprotectants for liposomal delivery systems, Eur J Pharm Sci, 30 (2007) 406-413.

[138] M. Grit, W.J. Underberg, D.J. Crommelin, Hydrolysis of saturated soybean phosphatidylcholine in aqueous liposome dispersions, J Pharm Sci, 82 (1993) 362-366.

[139] L.M. Ickenstein, M.C. Sandstrom, L.D. Mayer, K. Edwards, Effects of phospholipid hydrolysis on the aggregate structure in DPPC/DSPE-PEG2000 liposome preparations after gel to liquid crystalline phase transition, Biochim Biophys Acta, 1758 (2006) 171-180.

[140] R. Moog, M. Brandl, R. Schubert, C. Unger, U. Massing, Effect of nucleoside analogues and oligonucleotides on hydrolysis of liposomal phospholipids, Int J Pharm, 206 (2000) 43-53.

[141] Reflection paper on the data requirements for intravenous liposomal products developed with reference to an innovator liposomal product: EMA/CHMP/806058/2009/Rev. 02, European Medicines Agency, (2013) 1-13.

[142] J.B. Bassett, R.U. Anderson, J.R. Tacker, Use of Temperature-Sensitive Liposomes in the Selective Delivery of Methotrexate and Cisplatinum Analogs to Murine Bladder-Tumor, J Urol, 135 (1986) 612-615.

[143] K. Maruyama, S. Unezaki, N. Takahashi, M. Iwatsuru, Enhanced delivery of doxorubicin to tumor by long-circulating thermosensitive liposomes and local hyperthermia, Biochim Biophys Acta, 1149 (1993) 209-216.

[144] B. Banno, L.M. Ickenstein, G.N. Chiu, M.B. Bally, J. Thewalt, E. Brief, E.K. Wasan, The functional roles of poly(ethylene glycol)-lipid and lysolipid in the drug retention and release from lysolipid-containing thermosensitive liposomes in vitro and in vivo, J Pharm Sci, 99 (2010) 2295-2308.

[145] K. Affram, O. Udofot, E. Agyare, Cytotoxicity of gemcitabine-loaded thermosensitive liposomes in pancreatic cancer cell lines, Integr Cancer Sci Ther, 2 (2015) 133-142.

[146] K. Affram, O. Udofot, A. Cat, E. Agyare, In vitro and in vivo antitumor activity of gemcitabine loaded thermosensitive liposomal nanoparticles and mild hyperthermia in pancreatic cancer, Int J Adv Res 3(2015) 859-874.

[147] M. Hossann, Z. Syunyaeva, R. Schmidt, A. Zengerle, H. Eibl, R.D. Issels, L.H. Lindner, Proteins and cholesterol lipid vesicles are mediators of drug release from thermosensitive liposomes, J Control Release, 162 (2012) 400-406.

[148] J.P. May, M.J. Ernsting, E. Undzys, S.D. Li, Thermosensitive liposomes for the delivery of gemcitabine and oxaliplatin to tumors, Mol Pharm, 10 (2013) 4499-4508.

[149] H. Xu, J. Paxton, J. Lim, Y. Li, W. Zhang, L. Duxfield, Z. Wu, Development of High-Content Gemcitabine PEGylated Liposomes and Their Cytotoxicity on Drug-Resistant Pancreatic Tumour Cells, Pharm Res, (2014).

[150] W.J. Lokerse, E.C. Kneepkens, T.L. ten Hagen, A.M. Eggermont, H. Grull, G.A. Koning, In depth study on thermosensitive liposomes: Optimizing formulations for tumor specific therapy and in vitro to in vivo relations, Biomaterials, 82 (2016) 138-150.

[151] D.C. Drummond, O. Meyer, K. Hong, D.B. Kirpotin, D. Papahadjopoulos, Optimizing liposomes for delivery of chemotherapeutic agents to solid tumors, Pharmacol Rev, 51 (1999) 691-743.

[152] D.V. Devine, K. Wong, K. Serrano, A. Chonn, P.R. Cullis, Liposome-complement interactions in rat serum: implications for liposome survival studies, Biochim Biophys Acta, 1191 (1994) 43-51.

[153] H.Y. Fan, D. Das, H. Heerklotz, “Staying Out” Rather than “Cracking In”: Asymmetric Membrane Insertion of 12:0 Lysophosphocholine, Langmuir, 32 (2016) 11655-11663.

[154] R. Singh, A.K. Shakya, R. Naik, N. Shalan, Stability-indicating HPLC determination of gemcitabine in pharmaceutical formulations, Int J Anal Chem, 2015 (2015) 862592.

[155] S.K. Lim, D.H. Shin, M.H. Choi, J.S. Kim, Enhanced antitumor efficacy of gemcitabine-loaded temperature-sensitive liposome by hyperthermia in tumor-bearing mice, Drug Dev Ind Pharm, 40 (2014) 470-476.

[156] M. Celano, M.G. Calvagno, S. Bulotta, D. Paolino, F. Arturi, D. Rotiroti, S. Filetti, M. Fresta, D. Russo, Cytotoxic effects of gemcitabine-loaded liposomes in human anaplastic thyroid carcinoma cells, BMC Cancer, 4 (2004) 63.

[157] S. Limmer, Zielgerichtete Chemotherapie solider Tumoren durch thermosensitive Liposomen in Kombination mit Doxorubicin, Gemcitabine und Mitomycin C, Dissertation, (2014).

[158] A.S. Abu Lila, H. Kiwada, T. Ishida, The accelerated blood clearance (ABC) phenomenon: clinical challenge and approaches to manage, J Control Release, 172 (2013) 38-47.

[159] V. Bala, S. Rao, B.J. Boyd, C.A. Prestidge, Prodrug and nanomedicine approaches for the delivery of the camptothecin analogue SN38, J Control Release, 172 (2013) 48-61.

[160] V. Peikov, S. Ugwu, M. Parmar, A. Zhang, I. Ahmad, pH-dependent association of SN-38 with lipid bilayers of a novel liposomal formulation, Int J Pharm, 299 (2005) 92-99.

[161] R. Thakur, B. Sivakumar, M. Savva, Thermodynamic studies and loading of 7-ethyl-10-hydroxycamptothecin into mesoporous silica particles MCM-41 in strongly acidic solutions, J Phys Chem B, 114 (2010) 5903-5911.

[162] J.A. Zhang, T. Xuan, M. Parmar, L. Ma, S. Ugwu, S. Ali, I. Ahmad, Development and characterization of a novel liposome-based formulation of SN-38, Int J Pharm, 270 (2004) 93-107.

[163] F. Atyabi, A. Farkhondehfai, F. Esmaeili, R. Dinarvand, Preparation of pegylated nano-liposomal formulation containing SN-38: In vitro characterization and in vivo biodistribution in mice, Acta Pharm, 59 (2009) 133-144.

[164] M. Grit, J.H. de Smidt, A. Struijke, D.J.A. Crommelin, Hydrolysis of phosphatidylcholine in aqueous liposome dispersions, Int J Pharm, 50 (1989) 1-6.

[165] J.A. Shabbits, G.N.C. Chiu, L.D. Mayer, Development of an in vitro drug release assay that accurately predicts in vivo drug retention for liposome-based delivery systems, J Control Release, 84 (2002) 161-170.

[166] G. Xu, W. Zhang, M.K. Ma, H.L. McLeod, Human Carboxylesterase 2 Is Commonly Expressed in Tumor Tissue and Is Correlated with Activation of Irinotecan, Clin Cancer Res, 8 (2002) 2605-2611.

[167] S. Guichard, C. Terret, I. Hennebelle, I. Lochon, P. Chevreau, E. Fretigny, J. Selves, E. Chatelut, R. Bugat, P. Canal, CPT-11 converting carboxylesterase and topoisomerase activities in tumour and normal colon and liver tissues, Br J Cancer, 80 (1999) 364-370.

[168] G. Boyd, J.F. Smyth, D.I. Jodrell, J. Cummings, High-performance liquid chromatographic technique for the simultaneous determination of lactone and hydroxy acid forms of camptothecin and SN-38 in tissue culture media and cancer cells, Anal Biochem, 297 (2001) 15-24.

[169] C. Hansch, A. Leo, Exploring QSAR, American Chemical Society, Washington, 1995.

[170] M.J. Hageman, W. Morozowich, Case Study: Irinotecan (CPT-11), A Water-soluble Prodrug of SN-38, in: V.J. Stella, R.T. Borchardt, M.J. Hageman, R. Oliyai, H. Maag, J.W. Tilley (Eds.) Prodrugs: Challenges and Rewards Part 1, Springer New York, New York, NY, 2007, pp. 1269-1279.

[171] A. Casado, M.C. Giuffrida, M.L. Sagrista, F. Castelli, M. Pujol, M.A. Alsina, M. Mora, Langmuir monolayers and Differential Scanning Calorimetry for the study of the interactions between camptothecin drugs and biomembrane models, Biochim Biophys Acta, 1858 (2016) 422-433.

[172] W.J. Loos, J. Verweij, H.J. Gelderblom, M.J. de Jonge, E. Brouwer, B.K. Dallaire, A. Sparreboom, Role of erythrocytes and serum proteins in the kinetic profile of total 9-amino-20(S)-camptothecin in humans, Anticancer Drugs, 10 (1999) 705-710.

[173] J. Fassberg, V.J. Stella, A kinetic and Mechanistic Study of the Hydrolysis of Camptothecin and Some Analogues, J Pharm Sci, 81 (1992) 676-684.

[174] T.G. Burke, Z. Mi, Preferential binding of the carboxylate form of camptothecin by human serum albumin, Anal Biochem, 212 (1993) 285-287.

[175] T.G. Burke, Z. Mi, The structural basis of camptothecin interactions with human serum albumin: impact on drug stability, J Med Chem, 37 (1994) 40-46.

[176] T.G. Burke, C.B. Munshi, Z. Mi, Y. Jiang, The important role of albumin in determining the relative human blood stabilities of the camptothecin anticancer drugs, J Pharm Sci, 84 (1995) 518-519.

[177] S.A. Abraham, D.N. Waterhouse, L.D. Mayer, P.R. Cullis, T.D. Madden, M.B. Bally, The Liposomal Formulation of Doxorubicin, in: Methods in Enzymology, Academic Press, 2005, pp. 71-97.

[178] P.P. Wibroe, D. Ahmadvand, M.A. Oghabian, A. Yaghmur, S.M. Moghimi, An integrated assessment of morphology, size, and complement activation of the PEGylated liposomal doxorubicin products Doxil(R), Caelyx(R), DOXOrubicin, and SinaDoxosome, J Control Release, 221 (2016) 1-8.

[179] X. Li, D.J. Hirsh, D. Cabral-Lilly, A. Zirkel, S.M. Gruner, A.S. Janoff, W.R. Perkins, Doxorubicin physical state in solution and inside liposomes loaded via a pH gradient, Biochim Biophys Acta, 1415 (1998) 23-40.

[180] J. Kuntsche, J.C. Horst, H. Bunjes, Cryogenic transmission electron microscopy (cryo-TEM) for studying the morphology of colloidal drug delivery systems, Int J Pharm, 417 (2011) 120-137.

[181] E. Ramsay, J. Alnajim, M. Anantha, A. Taggar, A. Thomas, K. Edwards, G. Karlsson, M. Webb, M. Bally, Transition metal-mediated liposomal encapsulation of irinotecan (CPT-11) stabilizes the drug in the therapeutically active lactone conformation, Pharm Res, 23 (2006) 2799-2808.

[182] A. Gabizon, D. Tzemach, L. Mak, M. Bronstein, A.T. Horowitz, Dose dependency of pharmacokinetics and therapeutic efficacy of pegylated liposomal doxorubicin (DOXIL) in murine models, J Drug Target, 10 (2002) 539-548.

[183] A. Gabizon, H. Shmeeda, Y. Barenholz, Pharmacokinetics of pegylated liposomal Doxorubicin: review of animal and human studies, Clin Pharmacokinet, 42 (2003) 419-436.

[184] M.H. Kang, J. Wang, M.R. Makena, J.S. Lee, N. Paz, C.P. Hall, M.M. Song, R.I. Calderon, R.E. Cruz, A. Hindle, W. Ko, J.B. Fitzgerald, D.C. Drummond, T.J. Triche, C.P. Reynolds, Activity of MM-398, nanoliposomal irinotecan (nal-IRI), in Ewing's family tumor xenografts is associated with high exposure of tumor to drug and high SLFN11 expression, Clin Cancer Res, 21 (2015) 1139-1150.

[185] T.M. Allen, A. Chonn, Large unilamellar liposomes with low uptake into the reticuloendothelial system, FEBS Letters, 223 (1987) 42-46.

[186] N. Kaneda, H. Nagata, T. Furuta, T. Yokokura, Metabolism and pharmacokinetics of the camptothecin analogue CPT-11 in the mouse, Cancer Res, 50 (1990) 1715-1720.

[187] N. Kaneda, T. Yokokura, Nonlinear pharmacokinetics of CPT-11 in rats, Cancer Res, 50 (1990) 1721-1725.

[188] C.O. Noble, M.T. Krauze, D.C. Drummond, J. Forsayeth, M.E. Hayes, J. Beyer, P. Hadaczek, M.S. Berger, D.B. Kirpotin, K.S. Bankiewicz, J.W. Park, Pharmacokinetics, tumor accumulation and antitumor activity of nanoliposomal irinotecan following systemic treatment of intracranial tumors, Nanomedicine, 9 (2014) 2099-2108.

[189] C.L. Messerer, E.C. Ramsay, D. Waterhouse, R. Ng, E.M. Simms, N. Harasym, P. Tardi, L.D. Mayer, M.B. Bally, Liposomal irinotecan: formulation development and therapeutic assessment in murine xenograft models of colorectal cancer, Clin Cancer Res, 10 (2004) 6638-6649.

[190] X. Liu, A. Situ, Y. Kang, K.R. Villabroza, Y. Liao, C.H. Chang, T. Donahue, A.E. Nel, H. Meng, Irinotecan Delivery by Lipid-Coated Mesoporous Silica Nanoparticles Shows

Improved Efficacy and Safety over Liposomes for Pancreatic Cancer, ACS Nano, 10 (2016) 2702-2715.

[191] L.M. Crowe, J.H. Crowe, A. Rudolph, C. Womersley, L. Appel, Preservation of freeze-dried liposomes by trehalose, Arch Biochem Biophys, 242 (1985) 240-247.

[192] Prescribing information Doxil, (2016).

[193] G.J. Fransen, P.J.M. Salemink, D.J.A. Crommelin, Critical parameters in freezing of liposomes, Int J Pharm, 33 (1986) 27-35.

[194] E.C.A. van Winden, D.J.A. Crommelin, Long term stability of freeze-dried, lyoprotected doxorubicin liposomes, Eur J Pharm Biopharm, 43 (1997) 295-307.

## 7.2 List of abbreviations

| | |
|---|---|
| 5-FU | 5-fluorouridine |
| AUC | area under the curve |
| BN | Brown Norway rat |
| BN175 | soft tissue sarcoma cell line of Brown Norway rat |
| CF | carboxyfluorescein |
| Chol | cholesterol |
| $c_{max}$ | theoretical maximal dose |
| CN | controlled nucelation |
| CPT | camptothecin |
| CPT-11 | irinotecan |
| Cryo-TEM | cryo-transmission electron microscopy |
| DAC | dual asymmetric centrifugation |
| dFdC | gemcitabine |
| Dox | doxorubicin |
| DPPC | 1,2-dipalmitoyl-*sn*-glycero-3-phosphocholine |
| $DPPG_2$ | 1,2-dipalmitoyl-*sn*-glycero-3-phosphodiglycerol |
| DSC | differential scanning calorimetry |
| DSL-6A/C1 | pancreatic ductal cell line |
| DSPE-$PEG_{2000}$ | 1,2-distearoyl-*sn*-glycero-3-phosphoethanolamine-N-methoxy(polyethylenglycol)-2000 |
| DSPC | 1,2-distearoyl-*sn*-glycero-3-phosphocholine |
| EDTA | ethylenediaminetetraacetic acid |
| Em | emission |
| EPR-effect | enhanced permeability and retention effect |
| Ex | excitation |
| FBS | fetal bovine serum |
| FFA | free fatty acids |
| HBS | Hepes buffered saline |
| HepG2 | human liver cancer cell line |
| HPLC | high pressure liquid chromatography |
| HT | hyperthermia |
| i.v. | intravenous |
| NEFA | non-esterified fatty acids |
| NTSL | non-thermosensitive liposomes |
| PDI | polydispersity index |

| | |
|---|---|
| PK | pharmacokinetic |
| $R^2$ | coefficient of determination |
| RES | reticuloendothelial system |
| RT | room temperature |
| s.c. | subcutaneous |
| SEC | size-exclusion chromatography |
| SN-38 | 7-ethyl-10-hydroxycamptothecin |
| $t_{1/2}$ | plasma half-life |
| $T_g$` | glass transition temperature of freeze concentrated solution |
| TLC | thin layer chromatography |
| $T_m$ | phase transition temperature |
| TSL | thermosensitive liposomes |
| ζ-potential | Zeta-potential |

## 7.3 List of figures

Figure 2-1 Structure of a liposome..... 2
Figure 2-2 Principle of external active targeting approach for TSL..... 4
Figure 2-3 Principle of phase-transition of TSL..... 5
Figure 2-4 Chemical structure of DPPC, DSPC, $DPPG_2$, Lyso-PC and $DSPE\text{-}PEG_{2000}$ ..... 7
Figure 2-5 Structure of a) cytidine and b) dFdC..... 9
Figure 2-6 a) structure of camptothecin (CPT), b) pH dependent reversible structure change of lactone to carboxyl form of CPT-11 c) enzymatic reaction of CPT-11 to SN-38 by carboxylesterase enzyme family. .....11
Figure 2-7 Mechanism of water replacement during lyophilization. Adapted from [103]. .....13
Figure 3-1 Standard lyophilization cycle with controlled nucleation performed with the Epsilon 2-6D freeze-dryer .....27
Figure 3-2 Vials containing CF-liposomes wrapped in sterile bags prepared for lyophilization .....28
Figure 3-3 Standard lyophilization cycle for vials wrapped in sterile bags to avoid contaminations with cytostatic agents performed with Epsilon 2-12 D freeze-dryer.....28
Figure 4-1 Linearity of the NEFA-determination method. Values are given as mean value ± standard deviation (n=3).....35
Figure 4-2 Influence of EtOH on measured free fatty acid concentration of the commercial standard. .....36
Figure 4-3 Determination of the limit of detection of the method. The standard was diluted to concentrations between 0.05-0.5 mM with 0.9% NaCl. Values are given as mean value ± standard deviation (n=3). .....36
Figure 4-4 Osmolarity of physiological saline, HBS pH 7.4, dFdC solution and loaded TSL dispersion. Values are given as mean value ± standard deviation (n=3).....37
Figure 4-5 Wavelength scan of Gemzar® solutions titrated to higher pH with $NaHCO_3$ solution.....38
Figure 4-6 dFdC-concentration determination with HPLC of Gemzar®-solution at different pH values.....38
Figure 4-7 Steps of the passive loading strategy used for the published formulation by Limmer et al [44].....39
Figure 4-8 Steps of improved passive loading of dFdC-solution with pH 6-6.5 to preformed $DPPG_2$-based TSL with lipid composition DPPC/DSPC/$DPPG_2$ 50:20:30 (molar ratio).....39

Figure 4-9 In vitro temperature-dependent dFdC release from TSL prepared with two different preparation methods and different pH of the Gemzar®-solution. .....40
Figure 4-10 Plots of the heating phase from 20-60°C with a heating rate of 1°C/min of different dFdC-TSL formulations.....42
Figure 4-11 In vitro temperature-dependent release profile of dFdC- formulations with different phospholipid ratios.....43
Figure 4-12 In vitro temperature-dependent release profile of dFdC- formulations with different phospholipid ratios.....44
Figure 4-13 In vitro temperature-dependent release profile of dFdC-formulations with different phospholipid amounts after 1 h incubation in FBS. .....45
Figure 4-14 Free dFdC after 0-4 freezing and thawing cycles of $dFdC_6$-$TSL_{6/1/3/0}$. .....46
Figure 4-15 dFdC-TSL with different formulations and pH 3 or 6 of dFdC were prepared and stored at 2-8°C for up to 60 weeks. .....48
Figure 4-16 Temperature-dependent dFdC release after 5 min in FBS of TSL prepared with DAC (dashed lines; n=2) in comparison with TSL prepared with lipid film hydration and extrusion method (solid line; n≥4).....50
Figure 4-17 Pharmacokinetic study of $dFdC_3$-$TSL_{5/2/3/0}$ (n=2), $dFdC_6$-$TSL_{6/1/3/0}$ (n=6), $dFdC_6$-$TSL_{7/0/3/0}$ (n=6) and $dFdC_6$-$TSL_{4.5/2/3/0.5}$ (n=3). .....51
Figure 4-18 Therapeutic efficacy 6, 8 and 10 days after therapy (HT treatment at 41°C for 60 min after injection of 6 mg/kg dFdC) of improved $dFdC_6$-$TSL_{6/1/3/0}$ (n=6) and $dFdC_6$-$TSL_{7/0/3/0}$ (n=6) in comparison with non-liposomal dFdC (n=12) and published formulation $dFdC_3$-$TSL_{5/2/3/0}$ (n=6) in the BN175 soft tissue sarcoma model [44]. .....52
Figure 4-19 Therapeutic efficacy of single animals of improved $dFdC_6$-$TSL_{6/1/3/0}$ and $dFdC_6$-$TSL_{7/0/3/0}$ (n=6) in comparison with non-liposomal dFdC (n=12) and published formulation $dFdC_3$-$TSL_{5/2/3/0}$ (n=6) with HT-treatment for 60 min at 41°C after injection of 6 mg/kg dFdC in the BN175 soft tissue sarcoma model [44].....53
Figure 4-20 HPLC-profile of a solution containing CPT-11 and SN-38 with eluent 25 mM $NaH_2PO_4$ pH 3.1/ACN 50:50 (v/v) and fluorescence detection at Ex 355 nm and Em 515 nm (isocratic flow 1 ml/min). .....54
Figure 4-21 HPLC-profile of a solution containing CPT, CPT-11 and SN-38 with eluent 25 mM $NaH_2PO_4$ pH 3.1/ACN 70:30 (v/v) and fluorescence detection at Ex 355 nm and Em 515 nm (isocratic flow 1 ml/min). .....55
Figure 4-22 Linearity of the CPT-11 signal in serum measured with HPLC in the concentration range from 0.05 to 25 µg/ml. .....56
Figure 4-23 Linearity of the SN-38 signal in serum measured with HPLC in the concentration range from 0.05 to 25 µg/ml. .....56

Figure 4-24 Comparison of the determination of encapsulated CPT-11 in TSL with different drug/lipid ratios with HPLC and fluorescence spectroscopy.....57
Figure 4-25 Temperature-dependent SN-38 release of film loaded SN-38-TSL in FBS after 5 min incubation at temperatures between 37-45°C. .....59
Figure 4-26 Change of fluorescence of SN-38-TSL in presence of acceptor-vesicle liposomes DSPC/Chol 55:45 (molar ratio) in HBS pH 7.4 after 5 min incubation at different temperatures. .....60
Figure 4-27 Representative plots of the heating phase from 20-60°C with a heating rate of 1°C/min of TSL with or without SN-38 loaded with film loading.....60
Figure 4-28 Representative Cryo-TEM images of TSL prepared with film loading method a) without SN-38 and b) with SN-38. .....61
Figure 4-29 Drug/lipid ratio (mol/mol) of different liposomal batches with and without SEC after centrifugation.....63
Figure 4-30 Drug/lipid ratio (mol/mol) of CPT-11-TSL after active loading for 10, 20, 30 and 45 min at 36-37°C. .....64
Figure 4-31 Temperature-dependent release in FBS of CPT-11 from TSL with different drug/lipid ratios after 5 min incubation (left) or 1 h incubation (right) with intraliposomal a) 300 mM citrate pH 4, b) 300 mM $(NH_4)_2HPO_4$ pH 7.4 or c) 240 mM $(NH_4)_2SO_4$ pH 5.4 stored at -20°C.....65
Figure 4-32 Change in background fluorescence intensity in FBS at RT after up to 3 freezing and thawing cycles for four liposomal batches with different drug/lipid ratio.....66
Figure 4-33 Change in CPT-11 release after 1 h incubation at 37°C in FBS after up to 3 freezing and thawing cycles for four liposomal batches with different drug/lipid ratio. .....67
Figure 4-34 Z-average and PDI of CPT-11-TSL with different drug/lipid ratios after storage for up to four weeks at 2-8°C and afterwards additional storage for up to three weeks at RT (values in red box) (n=1 for each time point). .....67
Figure 4-35 Lysolipid content of CPT-11-TSL with different drug/lipid ratios after storage for up to four weeks at 2-8°C and afterwards additional storage for up to three weeks at RT (values in red box) (n=1 for each time point). .....68
Figure 4-36 Temperature-dependent CPT-11 release in FBS after 5 min of TSL with different drug/lipid ratios after storage for up to four weeks at 2-8°C and afterwards additional storage for up to three weeks at RT (blue dashed lines).....68
Figure 4-37 Temperature-dependent release in FBS of CPT-11 from TSL with different drug/lipid ratios after 5 min incubation (left) or 1 h incubation (right) with intraliposomal 240/300 mM $(NH_4)_2SO_4$ buffer pH 5.4 stored at 2-8°C. .....69

Figure 4-38 Temperature-dependent CPT-11 release in FBS after 5 min incubation at different temperatures of CPT-11-TSL (drug/lipid 0.244±0.033 (mol/mol); black line; n=9) in comparison to CPT-11-$TSL_{7/2/1}$ (drug/lipid 0.240±0.014 (mol/mol); dashed grey line; n=3). ....70
Figure 4-39 Temperature-dependent CPT-11 release in FBS after 1 h incubation at 37°C or 42°C of CPT-11-TSL (drug/lipid 0.244±0.033 (mol/mol); black bar; n=9) in comparison to CPT-11-$TSL_{7/2/1}$ (drug/lipid 0.240±0.014 (mol/mol); grey bar; n=3). ....71
Figure 4-40 Time-dependent CPT-11 release in FBS at 37-42°C for 5 min of CPT-11-TSL (drug/lipid 0.207±0.016 (mol/mol); left, solid lines) in comparison to CPT-11-$TSL_{7/2/1}$ (drug/lipid 0.240±0.014 (mol/mol); right, dashed lines). ....73
Figure 4-41 Time-dependent CPT-11 release in FBS at 37 or 42°C for 1 h of CPT-11-TSL (drug/lipid 0.194±0.035 (mol/mol); solid lines) in comparison to CPT-11-$TSL_{7/2/1}$ (drug/lipid 0.240±0.014 (mol/mol); dashed lines). ....73
Figure 4-42 Temperature-dependent CPT-11 release in FBS after 5-180 min of incubation at 37°C. ....74
Figure 4-43 Representing plots of the heating phase from 20-60°C with a heating rate of 1°C/min of $(NH_4)_2SO_4$-TSL, CPT-11+$(NH_4)_2SO_4$ (concentrations comparable to intraliposomal concentrations), Onivyde®, CPT-11-NTSL, CPT-11-TSL, CPT-11-TSL $(NH_4)_2HPO_4$, CPT-11-$TSL_{7/2/1}$. ....75
Figure 4-44 Representative Cryo-TEM images of a) unloaded TSL and b) CPT-11-TSL. ....76
Figure 4-45 Increase of fluorescence intensity of CPT-11 released from Onivyde® (solid lines) in comparison to CPT-11-NTSL (dashed line) in FBS at 37°C (grey lines) or 42°C (black lines). ....78
Figure 4-46 Pharmacokinetic study of non-liposomal CPT-11, Onivyde® or CPT-11-TSL. ....80
Figure 4-47 Top) CPT-11 concentration and bottom) SN-38 concentration in different organs (heart, liver spleen, kidney) tumor and plasma after i.v. injection of non-liposomal CPT-11, Onivyde® or CPT-11-TSL at a dose of 20 mg/kg CPT-11 in tumor bearing BN-rats (n=4) and 1 h of HT-treatment of the tumor tissue. ....82
Figure 4-48 Therapeutic efficacy of non-liposomal CPT-11, Onivyde® and CPT-11-TSL with HT-treatment for 60 min at 41° after injection of CPT-11 at dose of 20 mg/kg in the BN175 soft tissue sarcoma model (n=6 of non-liposomal CPT-11 and Onivyde®; n=7 for CPT-11-TSL). ....83
Figure 4-49 Therapeutic efficacy in single animals of non-liposomal CPT-11, Onivyde® and CPT-11-TSL with HT-treatment for 60 min at 41° after injection of CPT-11 at dose of 20 mg/kg in the BN175 soft tissue sarcoma model (n=6 of non-liposomal CPT-11 and Onivyde®; n=7 for CPT-11-TSL). ....84

Figure 4-50 Lyophilization process of CF-TSL without cryoprotectant. .....85
Figure 4-51 Liposomal dispersion lyophilization (left) and after lyophilization and reconstitution (right).....86
Figure 4-52 Osmolarity of TSL with different intra- and extraliposomal cryoprotectants and cryoprotectant concentrations (refer to Table 4-16 for exact cryoprotectant and concentration). .....87
Figure 4-53 z-average and PDI before and after lyophilization of CF-TSL with different intra- and extraliposomal cryoprotectants and cryoprotectant concentrations (refer to Table 4-16 for exact cryoprotectant and concentration). .....87
Figure 4-54 BF before and after lyophilization of CF-TSL with different intra- and extraliposomal cryoprotectants and cryoprotectant concentrations (refer to Table 4-16 for exact cryoprotectant and concentration).....88
Figure 4-55 Change in z-average and PDI after freezing either in liquid $N_2$ or with CN. .....89
Figure 4-56 Change in background CF-fluorescence after freezing either in liquid $N_2$ or with CN.....90
Figure 4-57 Lyophilization process of CF-TSL (cryoprotectant extraliposomal 5% sucrose + 0.4% NaCl) with CN at -5°C and a freezing rate of 1°C/min.....91
Figure 4-58 left) z-average and PDI before and after lyophilization of CF-TSL. right) background CF-fluorescence before and after lyophilization of CF-TSL. .....91
Figure 4-59 left) Change in z-average and PDI of lyophilized CF-TSL after 1.4 years storage at 2-8°C right) Change in background CF-fluorescence of lyophilized CF-TSL after 1.4 years storage at 2-8°C.....92
Figure 4-60 Lyophilization process of CF-TSL (cryoprotectant extraliposomal 5% sucrose + 0.4% NaCl) with CN at -5°C and a freezing rate of 1°C/min for a storage stability study at 2-8°C and RT. .....93
Figure 4-61 Change in different parameters after storage of lyophilized CF-TSL at RT or 2-8°C. .....94
Figure 4-62 Lyophilization process of CF-TSL (cryoprotectant extraliposomal 5% sucrose + 0.4% NaCl) with an annealing step at -15°C (left) or a freezing rate of 0.2°C/min (right).....95
Figure 4-63 left) Comparison of z-average and PDI of lyophilized CF-TSL after lyophilization with a freezing rate of 0.2°C/min (black) or an additional annealing step after freezing with a freezing rate of 1°C/min at -15°C for 4 h (grey) right) Comparison of background CF-fluorescence of lyophilized CF-TSL after lyophilization with a freezing rate of 0.2°C/min (black) or an additional annealing step after freezing with a freezing rate of 1°C/min at -15°C for 4 h (grey). .....96

Figure 4-64 Comparison of residual moisture of lyophilized CF-TSL after lyophilization with a freezing rate of 0.2°C/min (black) or an additional annealing step after freezing with a freezing rate of 1°C/min at -15°C for 4 h (grey). .....97
Figure 4-65 Comparison of background CF-fluorescence of lyophilized CF-TSL with a constant freezing rate of 0.2°C/min to -40°C or a freezing rate of 0.2°C/min to -25°C with a subsequent freezing rate of 1°C/min to -40°C.....98
Figure 4-66 Comparison of background CF-fluorescence after lyophilization of 1 ml or 4 ml CF-TSL in glass or plastic vials. .....99
Figure 4-67 Lyophilization process of CF-TSL, dFdC-TSL, Dox-TSL and CPT-11-TSL (cryoprotectant extraliposomal 5% sucrose + 0.4% NaCl) with a freezing rate of 0.2°C/min to -40°C. .....100
Figure 4-68 Lyophilized samples of CPT-11-TSL, dFdC-TSL, Dox-TSL and CF-TSL. .....100
Figure 4-69 CPT-11-TSL after reconstitution with ultrapure water. .....101
Figure 4-70 a) z-average before and after lyophilization for CF-TSL, Dox-TSL, CPT-11-TSL and dFdC-TSL; b) PDI before and after lyophilization for CF-TSL, Dox-TSL, CPT-11-TSL and dFdC-TSL; c) drug-leakage before and after lyophilization for CF-TSL, Dox-TSL, CPT-11-TSL and dFdC-TSL.....102
Figure 4-71 Temperature-dependent a) Dox-, b) CPT-11- or c) dFdC-release after incubation for 5 min at temperatures between 37-45°C in FBS before and after lyophilization of the TSL.....103
Figure 5-1 Comparison of relative tumor size of improved dFdC-TSL formulation ($dFdC_6$-$TSL_{6/1/3/0}$), CPT-11-TSL and the non-liposomal drugs CPT-11 and dFdC in the soft tissue sarcoma model BN175 in rats. .....125

## 7.4 List of tables

Table 2-1 Overview of distinct TSL formulations ..... 6
Table 3-1 Extra- and intraliposomal buffer systems used for active loading of Dox, CPT-11 or SN-38. ..... 19
Table 3-2 Culture medium with additional supplements and trypsin/EDTA concentration used for each cell line ..... 30
Table 4-1 Characteristics of liposomes prepared with published method with Gemzar® pH 3 (n=10) and improved method with Gemzar® pH 6-6.5 (n=4). ..... 40
Table 4-2 Characteristics of dFdC-liposomes with varying lipid concentrations of DPPC, DSPC, $DPPG_2$ and P-Lyso-PC. Values given as mean value ± standard deviation. ..... 41
Table 4-3 Overview of $T_m$ values of different dFdC-TSL formulations determined with DSC. 42
Table 4-4 Characteristics of dFdC-TSL prepared with DAC. Values given as mean value ± standard deviation. ..... 49
Table 4-5 dFdC-plasma concentration after i.v. application of 6 mg/kg different dFdC-TSL. 51
Table 4-6 Different SN-38 encapsulation methods tested and resulting encapsulation efficacy. ..... 58
Table 4-7 Overview of $T_m$ values of TSL formulations with or without SN-38 loaded with film loading determined with DSC. ..... 61
Table 4-8 Characteristics of CPT-11 NTSL (n=3). Values given as mean value ± standard deviation. ..... 62
Table 4-9 Characteristics of CPT-11-$TSL_{7/2/1}$ (n=3). Values given as mean value ± standard deviation. ..... 70
Table 4-10 Characteristics of CPT-11-TSL (n=11). Values given as mean value ± standard deviation. ..... 72
Table 4-11 Osmolarity measured for different CPT-11 liposomes and solutions used for CPT-11 encapsulation. ..... 72
Table 4-12 CPT-11 release rate constant k for CPT-11 at 37°C and 40°C for CPT-11-TSL and CPT-11-$TSL_{7/2/1}$. ..... 73
Table 4-13 Overview of $T_m$ values of the main transition peak and the pre-transition peak of $(NH_4)_2SO_4$-TSL, CPT-11-TSL, CPT-11-TSL $(NH_4)_2HPO_4$, CPT-11-$TSL_{7/2/1}$ determined with DSC. ..... 75
Table 4-14 Characterization of commercial Onivyde® (three independent measurements) in comparison to CPT-11-TSL (11 independent prepared batches). ..... 77
Table 4-15 CPT-11-plasma concentration after i.v. application of 20 mg/kg non-liposomal CPT-11, Onivyde® or CPT-11-TSL. ..... 81

Table 4-16 Overview TSL formulations with intra- and extraliposmal different cryoprotectants used for lyophilization. ....86
Table 4-17 Overview CF-TSL formulations used for evaluation of different freezing methods ....89

## 7.5 List of publications

### Publications

**Thermosensitive liposomal drug delivery systems: state of the art review**
***B. Kneidl,*** *M. Peller, G. Winter, L.H. Lindner, M. Hossann*
International journal of nanomedicine, 9 (2014), 4387-4398.

**Impact of plasma protein binding on cargo release by thermosensitive liposomes probed by fluorescence correlation spectroscopy**
*J.J. Mittag,* ***B. Kneidl,*** *T. Preiß, M. Hossann, G. Winter, S. Wuttke, H. Engelke, J.O. Rädler*
European Journal of Pharmaceutics and Biopharmaceutics, 119 (2017), 215-223.

**Liposomes for hyperthermia triggered drug release**
*W.J.M. Lokerse,* ***B. Kneidl,*** *A. Rysin, M. Petrini, L.H. Lindner*
Chapter 8 “Liposomes for hyperthermia triggered drug release” in Theranostic and Image guided drug delivery – Royal Society of Chemistry, submitted

### Oral presentations

**The iPaCT-Project (European Union Seventh Framework Programme, FP7/2007-2013)**
***B. Kneidl****, M. Hossann, M. Ries, C. Bos, S. Langereis, M. van der Bosch, C. Moonen, H. Grüll, L.H. Lindner*
Freising, 16. Wissenschaftliches Symposium der Medizinischen Klinik und Poliklinik III, July 2014

**Improvement of existing thermosensitive liposomes encapsulating gemcitabine**
***B. Kneidl****, S. Limmer, L. Pointner, M. Hossann, G. Winter, L.H. Lindner*
Zürich, 30$^{th}$ Annual Meeting European Society of Hypterthermic oncology, June 2015

**Development and optimization of $DPPG_2$-based thermosensitive liposomes**
***B. Kneidl****, S. Limmer, L. Pointner, L.H. Lindner, G. Winter, M. Hossann*
Ameland, 24th Mountain and Sea Liposome Workshop, October 2015

## Poster presentations

**Improvement of existing thermosensitive liposomes encapsulating gemcitabine**

***B. Kneidl**, S. Limmer, L. Pointner, M. Hossann, G. Winter, L.H. Lindner*

Zürich, 30th Annual Meeting European Society of Hypterthermic oncology, June 2015

Herrsching, 17. Wissenschaftliches Symposium der Medizinischen Klinik und Poliklinik III, July 2015

**Improvement of preparation method and formulation of thermosensitive liposomes encapsulating gemcitabine**

***B. Kneidl**, S. Limmer, L. Pointner, L.H. Lindner, G. Winter, M. Hossann*

Heidelberg, 4th International Symposium on Phospholipids in Pharmaceutical research and development, September 2015

**In vitro and in vivo characterization of gemcitabine loaded Phosphatidyldiglycerol-based thermosensitive liposomes**

***B. Kneidl**, S. Limmer, L. Pointner, L.H. Lindner, G. Winter, M. Hossann*

Seattle, 43rd Controlled release society annual meeting and exposition, July 2016

**Development of irinotecan loaded $DPPG_2$-based thermosensitive liposomes**

***B. Kneidl**, S. Limmer, G. Winter, L.H. Lindner, M. Hossann*

Herrsching, 19. Wissenschaftliches Symposium der Medizinischen Klinik und Poliklinik III, July 2017

# Acknowledgements

This thesis was prepared at the Department of Medicine III, University Hospital at the Ludwig-Maximilians-University in Munich under the supervision of Prof. Dr. Gerhard Winter at the Department of Pharmacy, Pharmaceutical Technology and Biopharmaceutics at the Ludwig-Maximilians-University in Munich.

First, I want to express my appreciation to my supervisor Prof. Dr. Lars Lindner at the Hospital for giving me the chance to work in this fascinating field of TSL and joining his research group. I would like to thank him for his supervision, scientific support and help when ever needed.

I would like to thank my doctoral supervisor Prof. Dr. Gerhard Winter for giving me the opportunity to prepare this thesis under his supervision. I want to thank him for his input, support and the scientific discussions during the meetings we had in the last years.

Many thanks also to Dr. Martin Hossann at the University Hospital for his scientific and personal support, for proof-reading of manuscripts during my time and especially of the thesis and for his encouragement in my work. Thank you Martin for your help also when you did not have so much time, you always found time to support me.

The EU is acknowledged for financial support of this project in framework of the iPaCT-project.

Prof. Dr. Schubert and Sabine Barnert I want to thank for performing the Cryo-TEM measurements for me.

I would like to thank also Prof. Dr. Ulrich Massing and his team for giving me the opportunity to work in his lab to perform the DAC-experiments and the help during these days.

I want to thank the AK Winter and AK Frieß for all the help and support during my experiments at the Department of Pharmacy. Special thanks to Ilona Vollrath and Julian Gitter for their help and support during all my lyophilization experiments, also in the evenings when something went wrong. Thank you very much.

Next, I want to thank the whole AG Liposomen for all the help and the wonderful time during the lab days. Anja Zengerle a big thank you for your help and teaching in my first days, weeks and months in the lab. Thank you Dr. Simone Limmer for being the person, who was the constant in the lab during my time here. Thanks for your support, for your encouraging words in tough times and the nice time together with you inside and outside of the lab. A big thank you also for performing the animal experiments for me. Many thanks to Angela Knauerhase and Lisa Pointner for your support and help in practical lab work, whenever I needed you, you helped me.

Thank you to all my friends, especially Alex for proof-reading of the thesis and Viola for her support and all the motivating words in the last years.

My deepest gratitude goes to my family, my parents and my siblings Johannes, Bernd and Evi, for their support, their encouragement, for being always there for me whenever I needed you during the last years.

Finally, I want to thank Rudi for his help, his encouragement and his love. Thank you for always being there for me.